

RELICT PLEISTOCENE DELTAS IN THE LOWER PENINSULA OF MICHIGAN

By

Michael David Luehmann

A DISSERTATION

Submitted to
Michigan State University
in partial fulfillment of the requirements
for the degree of

Geography – Doctor of Philosophy

2015

ABSTRACT

RELICT PLEISTOCENE DELTAS IN THE LOWER PENINSULA OF MICHIGAN

By

Michael David Luehmann

The purpose of this dissertation is to (1) map relict deltas that formed between ≈ 21.0 and 13.0 cal ka BP in the Lower Peninsula of Michigan, and (2) group those that have similar geomorphic, sedimentologic, and environmental components. In the past, beach ridges, wave-cut bluffs, meltwater spillways, and spits have been the primary relict landforms used to document and analyze paleolakes and coastal conditions in Michigan. This study highlights how, in addition to simply providing evidence for a paleolake, relict deltas may also be important proxies for coastal and terrestrial conditions during deglaciation.

Elevation data, stratigraphic information from well (water, oil, and gas) logs, along with surface and subsurface textural data derived from soil maps, enabled me to map 61 Pleistocene deltas in Lower Michigan. Of these, 27 had been known from previous works, whereas 34 are unique to this study. Most of the deltas are graded towards a known, ancestral, paleo-lake; however 16 deltas, many of which are kamic deltas, terminate into an unidentified and currently unknown or unstudied paleolake and/or lake stage.

Results from a numerical grouping analysis of the deltas confirm that relict late-Pleistocene deltas – at least those in Lower Michigan - have topographic and sedimentologic characteristics that facilitate placing them into unique morphologic groups. The grouping analysis suggests that there are at least five different, distinct types of relict deltas in Lower Michigan. The majority of Group 1 deltas are relatively large, sandy, and arcuate-shaped, with

sandy textured catchments. Group 2 deltas are also mostly sandy and arcuate-shaped but are relatively small; many of these deltas were sourced from a (likely) stagnant ice margin. Both Group 1 and 2 deltas are mostly located in northern Michigan. The bulk of Group 3 deltas are also sandy and arcuate-shaped, but unlike deltas in Groups 1 and 2, they have fine textured catchments and are more widely distributed. Most Group 4 deltas are relatively large, fine textured, arcuate-shaped, and have fine textured catchments; all Group 4 deltas are located in SE Michigan. The soils on these deltas are mostly fine-textured suggesting that these deltas were perhaps submerged by higher succeeding lake levels. Group 5 deltas are elongate-shaped, with multiple midchannel bars and interpreted as fluvial-dominated deltas. These deltas, all located in central Michigan, have formed at the mouths of major meltwater spillways. Arcuate-shaped deltas (Groups 1-4) are the most common type of relict delta in Lower Michigan; these deltas are interpreted as wave-dominated deltas. They are common on the eastern margins of the Lower Peninsula, in association with large lakes, where they confirm the strong, persistent and sustained winds and wave energies in the Great Lake region at this time.

Several methods have been used to record paleo-water plane elevations from relict beach ridges, wave-cut bluffs, meltwater spillways, and spits. Future studies of these relict coastal features in conjunction with relict deltas will provide a proxy for both paleocoastal and paleoterrestrial conditions.

By identifying and studying 61 relict deltas in Lower Michigan, I hope to promote further research on such systems within the Great Lakes region. Detailed and comprehensive investigations on Pleistocene deltas will advance our understanding of lake-level and landscape dynamics, along with wave and wind energies and directionalities during the late Pleistocene.

Copyright by
MICHAEL DAVID LUEHMANN
2015

ACKNOWLEDGMENTS

A countless number of people have contributed to the development and completion of this dissertation. I would like to say “thank you” many times to each of you.

I will especially always be grateful of my committee members: Dr. Randy Schaetzl, Dr. Grahame Larson, Dr. David Lusch, and Dr. Alan Arbogast. In addition, this dissertation has notably benefitted from the contributions from Dr. Kevin Kincare, Dr. Paul Delamater, Dr. Ashton Shortridge, Jay Strahan, Dr. Brad Miller, Dr. Bruce Pigozzi, Dr. Sarah Hession, and Jia Feng. However, I would like to specifically express gratitude to my major advisor Randy Schaetzl for always having his door open, listening, and helping me become a better writer, scientist, and all around person.

My parents also deserve a special word of thanks. They have supported me in many ways throughout my academic career, which began with countless after school hours spent learning the alphabet (using wooden letters) and the basics of reading. Also, thank you for never asking me “why?” and instead supporting my life decisions and providing help along the way. Lastly, I would like to express my deepest gratitude to my friend and partner, Dr. Natalie Johnson, to whom this document is dedicated; thank you for providing light at the end of the tunnel.

Funding during my PhD was provided by a scholarship from the Soil Classifiers of Michigan, a Rasmussen Graduate Fellowship from the Michigan State University Graduate School, and three separate Graduate Office Fellowships from the Department of Geography and Graduate School at Michigan State University to help support summer research.

PREFACE

This dissertation represents the first attempt to provide an inventory of the relict deltas in Lower Michigan, which formed in association with the retreat of the late Wisconsin (MIS 2) ice. Because these are relict features, I could not use contemporary processes to determine if these features formed (or are forming) as a fluvial system deposits sediment into a body of standing water. Therefore, in the dissertation I used surface and subsurface textural data, in conjunction with topographic and geomorphic information, to examine modern landforms that best represent deltaic morphology and sedimentology. I assumed that relict deltas had the following characteristics: (1) they are linked to either a modern day or prehistoric fluvial system, (2) they are fan- or broad-shaped in plan view, and (3) they are either graded towards a relict shore-zone that has previously been identified in the literature, or are located along the margins of a lake plain documented initially during this investigation. The landforms outlined in this dissertation are described to the best of my knowledge of delta formation and understanding of the glacial history of Michigan, in conjunction with the most recent digital, geospatial data available for Michigan.

Whereas most of the features discussed in this dissertation are unquestionably deltas in the traditional sense, some may actually be fan deposits that were built onto former lake plains when they were dry. Still others may be hybrid fan-delta landforms. It is not the purpose of this dissertation to determine the genetic histories for these delta-like landforms. Rather, my purpose was to record the locations of previously identified relict deltas in the Lower Peninsula of Michigan, and to identify any new, previously undocumented landforms *that may be deltas*,

given that they have similar topographic, morphologic, and textural characteristics as those landforms formerly documented in the literature as deltas.

As stated above, some of the deltas studied (and labeled as such) may have other, or polygenic, origins. Indeed, the surface profiles for some of the delta-like features, if unaccompanied by additional information, appear to suggest that they may be some type of alluvial/colluvial fan. It is possible that a few of the delta-like landforms discussed in this dissertation are fans formed largely under subaerial conditions. However, supplementary information is usually needed to definitively determine if a landform is a delta. To that end, like any investigation, the information in this document is subject to modifications, as mapping techniques and our knowledge of the glacial history of Michigan progresses. I encourage future researchers to examine the subsurface sedimentology and stratigraphy of the delta-like features I report on here, in order to definitively ascertain their genesis. Such research may involve collecting and analyzing sediment cores, and then performing particle size analysis to characterize the textural characteristics within and across each of the landforms. Additional research may also include investigating borrow pits and exposures within each of the landforms in order to determine the presence or absence of topset and foreset structures – typical of deltaic landforms and specifically Gilbert-type deltas. Subsurface stratigraphy and sedimentology perhaps could also be obtained from excavating deep soil pits, or by using either ground penetrating radar (GPR) or seismic-reflection equipment, e.g., Blewett et al. (2014).

It is my hope that this exercise in mapping and grouping relict deltas will foster subsequent research on these landforms. The data sets presented in this study may assist others in reconstructing the terrestrial, coastal, atmospheric and hydrologic conditions during

the retreat of the late Wisconsin ice. I am optimistic that the data and ideas documented in this dissertation will advance our understanding of Michigan's past and present landscapes, and help us better manage our landscapes in the future.

TABLE OF CONTENTS

| | |
|--|------------|
| LIST OF TABLES | xii |
| LIST OF FIGURES | xiv |
| Chapter 1 – Introduction to the Late Pleistocene Glacial History of Michigan and the Morphology of Deltas | 1 |
| 1. Introduction | 1 |
| 1.1 Deglaciation of the Lower Peninsula of Michigan | 4 |
| 1.1.1 Deglaciation after ≈23.0 cal ka BP | 6 |
| 1.1.2 Deglaciation after ≈17.1 cal ka BP | 8 |
| 1.1.3 Deglaciation after ≈15.1 cal ka BP | 14 |
| 1.1.4 Deglaciation after ≈13.7 cal ka BP | 18 |
| 1.1.5 Deglaciation Summary..... | 20 |
| 1.2 Delta Types and Morphologies | 21 |
| 1.2.1 Deltaic Processes | 22 |
| 1.2.2 Deltaic Components and Sediments | 24 |
| 1.2.3 Lacustrine vs. Marine Deltas | 27 |
| 1.2.4 Delta Classifications | 30 |
| 1.3 Summary | 32 |
| Chapter 2 - Relict Coastal Landforms as Paleolake-level Indicators | 33 |
| 2. Introduction | 33 |
| 2.1 Examples of Coastal Landforms used for Paleolake-level Reconstruction | 34 |
| 2.1.1 Relict Beach Ridges | 36 |
| 2.1.2 Wave-cut Bluffs | 42 |
| 2.1.3 Meltwater Spillways | 46 |
| 2.1.4 Relict Spits | 50 |
| 2.1.5 Relict Deltas | 54 |
| 2.2 Summary and Conclusions..... | 59 |
| Chapter 3 - Relict Pleistocene Deltas in the Lower Peninsula of Michigan | 62 |
| 3. Introduction | 62 |
| 3.1 Background..... | 64 |
| 3.2 Methodologies | 68 |
| 3.2.1 Data Assembly | 68 |
| 3.2.2 Identifying Additional Deltas | 70 |
| 3.2.3 Delineating Catchment Areas and Quantifying their Characteristics | 71 |
| 3.3 Results and Discussion | 74 |
| 3.3.1 Distribution of deltas | 74 |

| | |
|--|------------|
| 3.3.2 Lake Erie Basin Deltas | 81 |
| 3.3.2.1 Lake Maumee Deltas | 82 |
| 3.3.2.2 Lake Arkona Deltas..... | 83 |
| 3.3.2.3 Lake Whittlesey Deltas | 88 |
| 3.3.2.4 Lake Warren/Wayne Deltas..... | 88 |
| 3.3.2.5 Lake Grassmere/Lundy Deltas | 90 |
| 3.3.3 Lake Huron Basin Deltas | 91 |
| 3.3.3.1 Early Lake Saginaw Deltas..... | 91 |
| 3.3.3.2 Lake Saginaw Deltas..... | 94 |
| 3.3.3.3 Lake Warren Deltas..... | 95 |
| 3.3.3.4 Lake Grassmere Deltas | 98 |
| 3.3.3.5 Lake Lundy Deltas..... | 99 |
| 3.3.3.6 Other Deltas | 102 |
| 3.3.3.7 Lake Algonquin Deltas | 105 |
| 3.3.4 Lake Michigan Basin Deltas | 107 |
| 3.5 Profiles..... | 116 |
| 3.6 Review and Implications | 121 |
| 3.7 Conclusions..... | 123 |
| Chapter 4 – Natural Groupings of Relict Late-Pleistocene deltas in the Lower Peninsula of Michigan..... | 125 |
| 4. Introduction | 125 |
| 4.1 Background..... | 128 |
| 4.1.1 Delta Components and Terminology..... | 128 |
| 4.2.2 Delta Categories | 128 |
| 4.1.3 Numerical Grouping Analysis | 130 |
| 4.2 Methods | 131 |
| 4.2.1 Delineating Delta and Catchment Areas | 131 |
| 4.2.2 Quantifying Morphologic Characteristics..... | 134 |
| 4.2.3 Principal Component Analysis | 143 |
| 4.2.4 K-means Clustering Analysis..... | 149 |
| 4.3 Results and Discussion | 152 |
| 4.3.1 Delta and Catchment Sediment Characteristic | 152 |
| 4.3.2 Delta and Catchment Topographic Characteristics..... | 159 |
| 4.3.3 Delta System Extent..... | 162 |
| 4.4 Summary of Delta Group Analysis..... | 164 |
| 4.5 Conclusions..... | 165 |
| Chapter 5 – Conclusion | 174 |
| 5. Summary | 174 |
| APPENDICES..... | 180 |

| | |
|--|------------|
| APPENDIX A: Water and Oil/Gas Log Graphic Information | 181 |
| APPENDIX B: Profiles..... | 182 |
| APPENDIX C: Delta Plain Extents and Modern Catchment Areas..... | 203 |
| APPENDIX D: Raw Data - Delta and Catchment Characteristics | 226 |
| APPENDIX E: PCA Scores and K-means Group Number | 244 |
| APPENDIX F: Physical Characteristics of the Groups of Deltas | 246 |
| REFERENCES..... | 254 |

LIST OF TABLES

| | | |
|-------------------|---|-----|
| Table 1.1: | Pro- and post-glacial lakes (stages and phases in bold, outlets in italics), elevations (in meters asl), and outlets within the Erie, Huron, and Michigan basins. Compiled from Fullerton (1980), Calkin and Feenstra (1985), Eschman and Karrow (1985), Hansel et al. (1985), Colman et al. (1994), Larson and Schaetzl (2001), and Kincare and Larson (2009)..... | 7 |
| Table 2.1: | Relict coastal landforms, and a few examples of environmental indicators and proxies, used to infer paleocoastal conditions | 35 |
| Table 2.2: | A comparison of the different relict coastal landforms commonly used to record paleolake-level elevations, and the relative amount of detail that each provides | 60 |
| Table 3.1: | Pro- and post-glacial lakes (stages and phases in bold, outlets in italics), elevations (in meters asl), and outlets within the Erie, Huron, and Michigan basins. Compiled from Fullerton (1980), Calkin and Feenstra (1985), Eschman and Karrow (1985), Hansel et al. (1985), Colman et al. (1994), Larson and Schaetzl (2001), and Kincare and Larson (2009)..... | 67 |
| Table 3.2: | Values for sand, silt, and clay assigned to each SSURGO soil textural class (Miller and White, 1998) | 73 |
| Table 3.3: | Deltas mapped in Figure 3.3, along with the glacial lake their likely associated with and their inferred period of formation..... | 75 |
| Table 4.1: | Delta plain variables..... | 135 |
| Table 4.2: | Delta catchment area variables | 138 |
| Table 4.3: | Delta and catchment variables that correlate highly ($\geq \pm 0.5$) with the four principal components | 146 |
| Table 4.4: | A list of the principal components' interpreted characteristics, and their percent variance within the data set | 148 |

| | | |
|-------------------|---|-----|
| Table 4.5: | A list of the different groups of relict deltas and a comparison of the relative amount of sand content and local topographic variation within their catchment and delta areas..... | 159 |
| Table 4.6: | The common characteristics of the deltas within each of the five delta groups | 166 |
| Table D.1: | Raw Data – Delta Characteristics..... | 226 |
| Table D.2: | Raw Data - Catchment Characteristics | 235 |
| Table E.1: | Raw data - PCA Scores and K-means Group Number | 244 |

LIST OF FIGURES

| | | |
|--------------------|---|----|
| Figure 1.1: | Highlighting the extent of glacial phase limits, during the late Wisconsin, within the LP of Michigan (modified from Larson and Kincare (2009) and Larson (2011)). | 6 |
| Figure 1.2: | Approximate ice marginal position and extent of glacial lakes following the Crown Point-Port Bruce maximum (modified from Larson and Kincare (2009) and Kincare and Larson (2009)). | 9 |
| Figure 1.3: | Approximate ice margin and extent of glacial lakes following the Crown Point-Port Bruce maximum (modified from Larson and Kincare (2009) and Kincare and Larson (2009)). | 11 |
| Figure 1.4: | Approximate ice margin and extent of glacial lakes following the Crown Point-Port Bruce maximum (modified from Larson and Kincare (2009) and Kincare and Larson (2009)). | 13 |
| Figure 1.5: | Approximate ice margin position and extent of glacial lakes following the Port Huron maximum (modified from Larson and Kincare (2009) and Kincare and Larson (2009)). | 14 |
| Figure 1.6: | Approximate ice margin position and extent of glacial lakes following the Port Huron maximum (modified from Larson and Kincare (2009) and Kincare and Larson (2009)). | 17 |
| Figure 1.7: | Approximate ice margin position and extent of glacial lakes during the Two Rivers-Onaway maximum (modified from Larson and Kincare (2009) and Kincare and Larson (2009)). | 18 |
| Figure 1.8: | Approximate ice margin position and extent of glacial lakes following the Two Rivers-Onaway maximum (modified from Larson and Kincare (2009) and Kincare and Larson (2009)). | 19 |
| Figure 1.9: | Cross section of a Gilbert-type delta, with the primary delta components and facies assemblages (modified from Gilbert (1890) and Kenyon and Turcotte (1985)). | 24 |

| | | |
|---------------------|--|----|
| Figure 1.10: | Three GPR profiles along the Danaher delta - a section of the coalesced, Munising delta. GPR images illustrate the sequence stratigraphy of the Gilbert-type delta, which formed within 100 km of the dissertation study area (GPR images borrowed from Blewett et al. (2014)). | 29 |
| Figure 1.11: | Ternary classification of deltas on the basis of dominate processes and the resulting morphology (modified from Galloway (1975) and Hori and Saito (2007)). | 30 |
| Figure 2.1: | A DEM and 7.5' topographic map (5 ft contour interval) illustrating several beach ridges (i.e., a strandplain) on the northern 'thumb' of Lower Michigan, ≈10 km west of Port Austin, MI. | 36 |
| Figure 2.2: | Schematic diagram, illustrating the development of a beach ridge (modified from Baedke et al (2004). (A) During a lake-level rise the shoreline is eroded landward. (B) As the rising lake level slows and eventually stops, a topographic high (known as a 'berm') forms near the top of the swash zone. Onshore transport from shoaling waves and offshore transport from the backwash concentrate the coarsest particle-size fraction near the base of the swash zone. Eventually grasses colonize the berm crest and help trap wind-blown sediments, forming a small dune cap on top of the ridge. (C) With falling lake level, the shoreline progrades lakeward. | 37 |
| Figure 2.3: | (A) Schematic diagram of a modern wave-cut bluff during formation, showing mean water level and coarse lag deposit. (B) Diagram of the wave-cut bluff after lake recession and illustrating where to measure the former mean water plane elevation (modified from Schaetzl et al. (2002)). | 43 |
| Figure 2.4: | A DEM and 7.5' topographic map (5 m contour interval) illustrating a relict wave-cut bluff associated with Glacial Lake Algonquin, in northwestern Lower Michigan , ≈10 km southwest of Charlevoix, MI. | 44 |
| Figure 2.5: | A DEM of a large, relict spillway that includes several fluvial landforms located in the central Upper Peninsula between Au Train and Rapid River, MI. | 47 |
| Figure 2.6: | (A) An illustration of the components associated with a typical, relict glacial lake spillway (modified from Kehew and Lord (1986). (B) A section of the glacial Grand River Valley, ≈20 km east of Grand Rapids, MI, and labeling a few relict features related to the spillway. | 48 |

| | | |
|---------------------|--|----|
| Figure 2.7: | A map of the relict Delta Island spit flooded to its paleoshoreline elevation and illustrating the paleoconditions it records as shown by Jewell (2007)..... | 52 |
| Figure 2.8: | A DEM and profile of a relict spit that has subtle wave-cut bluffs near its tail end. The elevation near the base of each wave-cut bluff likely represents the former water plane elevation, implying that the lake level drop was concurrent with spit lengthening and progradation. | 53 |
| Figure 2.9: | (A) Diagram illustrating the position of the different delta sediment (sed.) sequences. (B-D) Schematic showing possible sediment sequences associated with lake level history, without labeling the separate sediments in order to simply the sketch (modified from Milligan and Chan (1998) and Gobo et al. (2014))..... | 56 |
| Figure 2.10: | A DEM and topographic profile of two relict deltas in northeastern Lower Michigan. The profile of the deltas illustrates the abrupt break in slope between the delta plain and the delta front, which marks a potential water plane elevation prior to the abandonment of the delta. | 57 |
| Figure 3.1: | Extent of the major glacial phases of the late Wisconsin ice advance, within the Great Lakes region, USA (modified from Larson and Kincare (2009) and Larson (2011))..... | 64 |
| Figure 3.2: | Statewide 10 m DEM flooded to the 225, 215, and 210 m levels of Glacial Lake Maumee, in SE Lower Michigan, illustrating bulges along relict shorelines, each showing a relict delta near the following cities: Adrian, Saline, Ypsilanti, Plymouth, and Birmingham. | 71 |
| Figure 3.3: | The locations of those 61 deltas mapped and discussed in this chapter. Labels at points refer to the delta ID and are a reference for Table 3.3. | 74 |
| Figure 3.4: | Extent of the Great Lakes drainage basins within the LP of Michigan, in relationship to the location of Pleistocene deltas..... | 79 |
| Figure 3.5: | Deltas in SE Michigan, graded to glacial Lakes Maumee (I-III) and Arkona. **note: Lake symbology within is document has no reference to water depth ** | 82 |

| | | |
|---------------------|---|----|
| Figure 3.6: | Major end moraines, heads of outwash and other uplands of glacial origin, in relationship to the relict deltas mapped in this study (modified from Blewett et al., 2009). | 85 |
| Figure 3.7: | Present day catchment areas for the deltas mapped in this study, also showing the major subsurface textural groupings associated with soil parent materials (C horizon) of the catchments..... | 86 |
| Figure 3.8: | A map of the notably dominant subsurface soil texture within each delta catchment area, and the median slope percentage within those areas..... | 87 |
| Figure 3.9: | A DEM flooded to glacial Lakes Maumee, Arkona, and Warren/Wayne shorelines, illustrating the Huron River I, II, and III deltas. | 89 |
| Figure 3.10: | A DEM flooded to several potential paleolake-level elevations to illustrate various deltas, within southeastern Lower Michigan, graded to either one of the glacial Lake Warren phases or Lake Wayne..... | 89 |
| Figure 3.11: | A) A DEM flooded to several potential paleolake-level elevations, illustrating the Huron River I-III delta complex. B) Same as (A), but for the Black River I-III delta complex..... | 90 |
| Figure 3.12: | Saginaw lowlands flooded to Early Saginaw and glacial Lake Warren stages to illustrate both Chippewa River deltas, along with the Gladwin and West Branch Rifle River deltas. | 92 |
| Figure 3.13: | DEM flooded to several potential paleolake-level elevations, illustrating the Cass River delta with its midchannel bars – characteristic of a fluvial dominated delta. | 94 |
| Figure 3.14: | DEM flooded to several potential paleolake-level elevations, illustrating Chippewa River II and Jackpines deltas. | 96 |
| Figure 3.15: | DEM flooded to several potential paleolake-level elevations, illustrating the symmetrical shape of the sequence of deltas that formed along the northern margins of Saginaw Bay. | 97 |
| Figure 3.16: | DEM flooded to a potential paleolake-level elevation for glacial Lake Grassmere, illustrating the Sevenmile Hill delta in relationship to the Jackpines delta..... | 99 |

| | | |
|---------------------|--|-----|
| Figure 3.17: | DEM flooded to a likely glacial Lake Lundy shoreline elevation, illustrating the Flint River delta. | 100 |
| Figure 3.18: | DEM flooded to likely glacial Lake Lundy shoreline elevations in northeastern Lower Michigan..... | 101 |
| Figure 3.19: | DEM flooded to possible lake-level elevations within the Houghton Lake Sandy Fats and Ridges region, illustrating the Beaver Creek I and II and Coy Ridge deltas..... | 102 |
| Figure 3.20: | Illustrating the Elk Hill, Kneeland, and Bull Gap deltas and how they stand above the modern day Au Sable River. | 103 |
| Figure 3.21: | Highlighting the Indian Creek I and II, Turtle Lake, and Brush Creek deltas in NE Michigan and the low relief lake plain areas the deltas stand above. | 104 |
| Figure 3.22: | DEM flooded to a likely Lake Algonquin shoreline elevation, illustrating the Black River, Sturgeon-Pigeon, and McPhee Creek deltas. | 105 |
| Figure 3.23: | Maple River delta in relationship to the Imlay channel. | 107 |
| Figure 3.24: | DEM flooded to the Calumet and Glenwood II lake-level elevations, illustrating the Allendale and Zeeland deltas and their midchannel bars – characteristic of fluvial dominated deltas. | 109 |
| Figure 3.25: | The Sanborn Creek Fan, Slagle Fan, and Cole Creek Fan deltas in relationship to the Manistee River..... | 110 |
| Figure 3.26: | DEM flooded to several potential paleolake-level elevations, illustrating the Houghton and Higgins Lake Ridge delta and how they grade southward from the E-W trending heads of outwash that encompass the Houghton Lake Sandy Fats and Ridges region..... | 112 |
| Figure 3.27: | DEM flooded to the Calumet phase of glacial Lake Chicago, illustrating the Fair Plain delta. | 113 |
| Figure 3.28: | (A-D) DEM flooded to one or more Lake Algonquin paleolake-level elevations, illustrating the well defined, symmetrical shape of these deltas, all of which | |

| | | |
|---------------------|--|-----|
| | formed in NW Lower Michigan. Note: Lake symbology has no reference to water depth..... | 114 |
| Figure 3.29: | Topographic profiles of the 39 deltas that have a Gilbert-type surface profile. Many of these landforms have a well developed, generally flat delta plain, and a steep delta front. | 117 |
| Figure 3.30: | Topographic profiles of the 22 deltas that have a nearly linear profile from the apex to the toe of the delta. | 118 |
| Figure 3.31: | An illustration of an idealized topographic profile for each of the two main profile groups mapped in this study. | 119 |
| Figure 4.1: | The frequently used ternary categorization of deltas based on the dominate processes influencing their morphology (modified from Galloway (1975) and Hori and Saito (2007))..... | 129 |
| Figure 4.2: | Three maps illustrating (a) 10 m NED DEM and hillshade, (B) subsurface soil texture – yellow are sandy soils, and (C) soil wetness – orange and green are well drained soils, along with the delta plain boundaries associated with five deltas mapped in Lower Michigan. | 133 |
| Figure 4.3: | Illustrating examples of outputs from the Minimum Bounding Geometry tool and how the diameter of the circular envelop was used to estimate either the length or width of the delta, as well as how the length and width measurements of the rectangular envelope were used to estimate either the length or width of the delta. | 142 |
| Figure 4.4: | Variable loadings associated with PC1. | 144 |
| Figure 4.5: | Variable loadings associated with PC2. | 144 |
| Figure 4.6: | Variable loadings associated with PC3. | 145 |
| Figure 4.7: | Variable loadings associated with PC4. | 145 |
| Figure 4.8: | The goodness of “fit” for each number of clusters specified. Local peaks in the graph suggest potential numbers of clusters. | 151 |

| | | |
|---------------------|---|-----|
| Figure 4.9: | The distribution of the five groups of deltas, as identified by the K-means clustering analysis. | 153 |
| Figure 4.10: | The frequency and distribution of PCA scores associated with each of the four components extracted from the PCA. | 154 |
| Figure 4.11: | The distribution of the five groups of deltas and the extent of each delta's catchment area (outlined in blue), overlain onto a map of soil subsurface (C horizon) texture. Red and green colors represent fine textured soils and orange and yellow colors represent sandy textured soils. | 155 |
| Figure 4.12: | A graduated circle map illustrating sand content (%) in the subsurface horizon (C horizon) of soils within the delta catchment areas. | 156 |
| Figure 4.13: | A graduated circle map illustrating clay content (%) in the subsurface horizon (C horizon) of soils within the delta plain extent. | 157 |
| Figure 4.14: | A graduated circle map illustrating the median percent slope within a 3 x 3 cell neighborhood, using a DEM, measured for delta catchment. | 160 |
| Figure 4.15: | A graph that compares each delta's perimeter length (excluding those deltas in Group 5) to its measured catchment area. | 163 |
| Figure 4.16: | A map of the Black River delta and its catchment in northern Michigan, illustrating the typical sediment characteristics of a Group 1 delta and its catchment. | 167 |
| Figure 4.17: | A map of the Higgins Lake Ridge and Coy Ridge deltas, along with their modern catchments, that illustrates the typical sediment characteristics Group 2 deltas. These are examples of kame deltas and thus the modern catchment area is much smaller than what would have been present while the deltas were forming... | 169 |
| Figure 4.18: | A map of the Big Creek and Cedar Creek I deltas, along with their catchments, and illustrating the typical sediment characteristics Group 3 deltas. | 170 |
| Figure 4.19: | A map illustrating the North Branch Clinton River delta and its catchment, and illustrating the typical sediment characteristics of a Group 4 delta. | 171 |

| | | |
|---------------------|---|-----|
| Figure 4.20: | A map illustrating the Cass River delta and its catchment, and illustrating the typical sediment characteristics of a Group 5 delta. | 172 |
| Figure A.1: | Graphic display of well log information for a few wells located on a delta plain (delta plain shaded in black) | 181 |
| Figure B.1: | Raisin River delta profile | 182 |
| Figure B.2: | Saline River delta profile | 182 |
| Figure B.3: | Huron River I delta profile | 183 |
| Figure B.4: | Huron River II delta profile | 183 |
| Figure B.5: | Huron River III delta profile | 183 |
| Figure B.6: | Middle Rouge River delta profile | 184 |
| Figure B.7: | Tarabusi Creek delta profile..... | 184 |
| Figure B.8: | Rochester delta profile | 184 |
| Figure B.9: | Clinton River delta profile | 185 |
| Figure B.10: | North Branch Clinton River delta profile | 185 |
| Figure B.11: | Belle River delta profile..... | 185 |
| Figure B.12: | Smiths Creek delta profile..... | 186 |
| Figure B.13: | South Pine River delta profile | 186 |
| Figure B.14: | Black River I delta profile | 186 |
| Figure B.15: | Black River II delta profile | 187 |
| Figure B.16: | Black River III delta profile | 187 |

| | | |
|---------------------|---------------------------------------|-----|
| Figure B.17: | Pine River delta profile..... | 187 |
| Figure B.18: | Flint River delta profile | 188 |
| Figure B.19: | Cass River delta profile | 188 |
| Figure B.20: | Chippewa River I delta profile..... | 188 |
| Figure B.21: | Chippewa River II delta profile..... | 189 |
| Figure B.22: | Gladwin delta profile | 189 |
| Figure B.23: | Rifle River I delta profile | 189 |
| Figure B.24: | Rifle River II delta profile | 190 |
| Figure B.25: | Big Creek delta profile..... | 190 |
| Figure B.26: | Cedar Creek I delta profile | 190 |
| Figure B.27: | Cedar Creek II delta profile | 191 |
| Figure B.28: | Johnson Creek delta profile | 191 |
| Figure B.29: | Au Gres River I delta profile | 191 |
| Figure B.30: | Au Gres River II delta profile..... | 192 |
| Figure B.31: | West Branch Rifle delta profile | 192 |
| Figure B.32: | Jackpines delta profile | 192 |
| Figure B.33: | Sevenmile Hill delta profile | 193 |
| Figure B.34: | Coy Ridge delta profile..... | 193 |
| Figure B.35: | Beaver Creek I delta profile | 193 |

| | | |
|---------------------|--|-----|
| Figure B.36: | Beaver Creek II delta profile | 194 |
| Figure B.37: | Bull Gap delta profile | 194 |
| Figure B.38: | Kneeland delta profile..... | 194 |
| Figure B.39: | Elk Hill delta profile | 195 |
| Figure B.40: | Indian Creek I delta profile | 195 |
| Figure B.41: | Indian Creek II delta profile | 195 |
| Figure B.42: | Turtle Lake delta profile..... | 196 |
| Figure B.43: | Brush Creek delta profile | 196 |
| Figure B.44: | Sturgeon-Pigeon River delta profile..... | 196 |
| Figure B.45: | Black River delta profile | 197 |
| Figure B.46: | McPhee Creek delta profile | 197 |
| Figure B.47: | Fair Plain delta profile..... | 197 |
| Figure B.48: | Zeeland delta profile | 198 |
| Figure B.49: | Allendale delta profile..... | 198 |
| Figure B.50: | Maple River delta profile | 198 |
| Figure B.51: | Sanborn Creek Fan delta profile | 199 |
| Figure B.52: | Lake City, Harrison Ridge delta profile..... | 199 |
| Figure B.53: | Slagle Fan delta profile..... | 199 |
| Figure B.54: | Cole Creek Fan delta profile..... | 200 |

| | | |
|---------------------|--|-----|
| Figure B.55: | Houghton Lake Ridge delta profile | 200 |
| Figure B.56: | Higgins Lake Ridge delta profile..... | 200 |
| Figure B.57: | Platte River delta profile | 201 |
| Figure B.58: | Boardman River delta profile..... | 201 |
| Figure B.59: | Rapid River delta profile | 201 |
| Figure B.60: | Deer Creek delta profile..... | 202 |
| Figure B.61: | Brown Creek delta profile | 202 |
| Figure C.1: | Color symbology used to label the subsurface textural class's within each delta's catchment area. | 203 |
| Figure C.2: | Raisin River delta..... | 203 |
| Figure C.3: | Saline River delta | 204 |
| Figure C.4: | Huron River I, II, and III deltas..... | 204 |
| Figure C.5: | Middle Rouge and Tarabusi Creek deltas | 205 |
| Figure C.6: | Rochester delta | 205 |
| Figure C.7: | Clinton River and North Branch Clinton River deltas..... | 206 |
| Figure C.8: | Belle River delta | 206 |
| Figure C.9: | Smith's Creek, South Pine River, and Pine River deltas | 207 |
| Figure C.10: | Black River (B.R.) I, Black River II, and Black River III deltas | 207 |
| Figure C.11: | Flint River delta | 208 |
| Figure C.12: | Cass River delta | 208 |

| | | |
|---------------------|---|-----|
| Figure C.13: | Chippewa River I and Chippewa River II deltas | 209 |
| Figure C.14: | Gladwin delta | 209 |
| Figure C.15: | Rifle River I and Rifle River II deltas | 210 |
| Figure C.16: | Big Creek and Cedar Creek I and Cedar Creek II deltas | 210 |
| Figure C.17: | Johnson Creek delta..... | 211 |
| Figure C.18: | Au Gres River I and Au Gres River II deltas | 211 |
| Figure C.19: | West Branch Rifle River delta | 212 |
| Figure C.20: | Jackpines and Sevenmile Hill deltas..... | 212 |
| Figure C.21: | Coy Ridge delta | 213 |
| Figure C.22: | Beaver Creek I and Beaver Creek II deltas | 213 |
| Figure C.23: | Bull Gap delta..... | 214 |
| Figure C.24: | Kneeland delta | 214 |
| Figure C.25: | Elk Hill delta..... | 215 |
| Figure C.26: | Indian Creek I and Indian Creek II deltas | 215 |
| Figure C.27: | Turtle Lake delta | 216 |
| Figure C.28: | Brush Creek delta..... | 216 |
| Figure C.29: | Sturgeon-Pigeon River delta | 217 |
| Figure C.30: | Black River delta..... | 218 |
| Figure C.31: | McPhee Creek delta..... | 218 |
| Figure C.32: | Fair Plain delta | 219 |

| | | |
|---------------------|--|-----|
| Figure C.33: | Allendale and Zeeland deltas..... | 220 |
| Figure C.34: | Maple River delta (?). Leverett and Taylor (1915, pg. 256 and 257) emphatically states this feature is not a delta but “seems more like a kame”. | 220 |
| Figure C.35: | Sanborn Creek delta..... | 221 |
| Figure C.36: | Lake City, Harrison Ridge delta | 221 |
| Figure C.37: | Slagle Fan delta | 222 |
| Figure C.38: | Cole Creek delta | 222 |
| Figure C.39: | Houghton Lake Ridge delta..... | 223 |
| Figure C.40: | Coy Ridge delta | 223 |
| Figure C.41: | Platte River delta..... | 223 |
| Figure C.42: | Boardman River delta | 224 |
| Figure C.43: | Rapid River delta | 224 |
| Figure C.44: | Deer Creek and Brown Creek deltas | 225 |
| Figure F.1: | A graduated circle map illustrating clay content (%) in the subsurface horizon (C horizon) of soils within the delta catchments. | 246 |
| Figure F.2: | A graduated circle map illustrating silt content (%) in the surface mineral horizon of soils within the delta catchments..... | 247 |
| Figure F.3: | A graduated circle map illustrating sand content (%) in the subsurface horizon (C horizon) of soils within the delta plains..... | 248 |
| Figure F.4: | A graduated circle map illustrating silt content (%) in the surface mineral horizon of soils within the delta plains. | 249 |
| Figure F.5: | A graduated circle map illustrating the percentage of gravelly soil parent materials within the delta plains. | 250 |

| | | |
|--------------------|---|-----|
| Figure F.6: | A graduated circle map illustrating the different delta catchment areal extents. | 251 |
| Figure F.7: | A graduated circle map illustrating the different delta plain length-width ratios. Larger values indicate more elongate deltas whereas smaller values indicate wider, more fan-shaped deltas..... | 252 |
| Figure F.8: | A graduated circle map illustrating the different delta plain perimeter lengths. | 253 |

Chapter 1 – Introduction to the Late Pleistocene Glacial History of Michigan and the Morphology of Deltas

1. Introduction

Deltas form at the junction between a river and a standing body of water, when the amount of alluvium being delivered to the mouth of the river is greater than the rate at which coastal processes are able to redistribute the newly deposited sediment away from the river mouth (Lyell, 1832). Furthermore, deltas may form if either the rate of sediment supply is greater than the *increase* rate in accommodation space (i.e., the space available for potential sediment accumulation) - perhaps due to sea-level rise, or if the constant sediment supply is greater than the *decrease* rate in accommodation space - perhaps due to sea-level fall (Jervey, 1998). Although deltas are often found along of the coasts of large continents where sizeable rivers meet an ocean, arguably the most influential delta study was undertaken in the arid western part of the United States. Here is where Grove Karl Gilbert developed the classic model for the morphology and progradation of a coarse-grained or “Gilbert” type delta. In the pair of papers put forward by Gilbert (1885, 1890), he mapped and described the topographic features along the Pleistocene-aged, Lake Bonneville lakeshore and inferred how rivers had shaped the shorelines. Following these works, numerous studies have used the Lake Bonneville deltas and various shoreline features to help better understand the glacial chronology, paleoclimate, paleolimnology, and paleohydrology within the Basin and Range physiographic province of the western United States (e.g., Atwood, 1909; Hunt, et al., 1953; Bissell, 1963; Scott et al., 1983; Currey and Oviatte, 1985; Smith and Jol, 1992; Lemons et al., 1999; Oviatt et al., 2003; Nelson et al., 2005; Nishizawa et al., 2013). Similar relict-delta research has also been employed within

alpine lake basins in the interior of south-central British Columbia (e.g., Clague et al., 1991; Margold et al., 2013), the shores of Lake General Carrera, in southern Chile (e.g., Bells, 2009) and various high altitude lakes in Switzerland (e.g., Adams et al., 2001), and even on Mars, along the margins of an impact crater (e.g., Mangold and Ansan, 2006; Di Achille and Hynek, 2010).

However, very few studies have focused on deltas that formed during the Pleistocene within the Lower Peninsula of Michigan (LP). Instead, much of the research on glacial and postglacial lakes in Michigan has focused on relict shorelines in the form of beach ridges, meltwater spillways, alluvial terraces, and wave-cut cliffs, all of which could have formed in a relatively short period of time, and often vary in morphology and elevation over short distances (e.g., Spencer, 1891; Goldthwait, 1908; Leverett and Taylor, 1915; Bay, 1937; Bretz, 1951, 1953, 1964; Dreimanis, A. 1966; Karrow, 1986; Thompson, 1992; Kehew, 1993; Thompson and Baedke, 1995; Krist and Schaetzl, 2001; Schaetzl et al., 2002). Conversely, Pleistocene deltas not only record generally long term, paleoshoreline conditions, such as lake-level elevation, wave energy, wind and longshore drift direction, but also provide evidence for paleoterrestrial conditions within the delta's catchment area upstream. In this dissertation I intend to rectify this literature gap by focusing on the distribution and characteristics of Pleistocene deltas, forming mainly between ≈ 21.0 and 13.0 cal ka BP, in the Lower Peninsula of Michigan.

Opportunities to study Pleistocene coastal features associated with pro- and post-glacial lakes have always existed in Michigan (Spencer, 1891; Taylor, 1892; Goldthwait, 1908; Leverett and Taylor, 1915; Bretz, 1951; Hough, 1958; Karrow, 1986, 1988; Thompson, 1992; Thompson and Baedke, 1995; Krist and Schaetzl, 2001; Schaetzl et al., 2002; Vader et al., 2012). However,

recent technological advances in digital spatial data and field data collection methods have led to the reassessment and often reclassification of previously studied glacial landforms and regions within the Lower Peninsula (LP) of Michigan (e.g., Schaetzl, 2001; Kehew et al., 2012; Dryzga et al., 2012; Schaetzl et al., 2013a; Blewett et al., 2014). For example, Geographic Information Systems (GIS) have created an effective means to collect and analyze statewide datasets, such as elevation and county-level soils data, and have prompted mapping of similar and/or related geologic features, even across state boundaries (Gao and Liu, 2001; Asselen and Seijmonsbergen, 2006; Arrell et al., 2007; Saha et al., 2011). Detailed, comprehensive investigations of Michigan's relatively unstudied glacial landscape will help researchers better understand the manner of deglaciation in the LP of Michigan, and the Great Lakes region as a whole.

Three major chapters are provided in this dissertation. Each chapter, listed below, has three major *research questions* or *guiding principals*:

Chapter 2 –

- 1) What approaches have been used to record the paleo-water plane elevation(s) from relict beach ridges, wave-cut bluffs, meltwater spillways, spits, and deltas, particularly within the Great Lakes region (although also including Glacial Lake Agassiz), as well as the Lake Bonneville area in the western United States?
- 2) What are the inherent constraints or limitations of these approaches for examining these types of relict coastal landforms, especially with regard to their utility for inferring paleolake-level(s)?

Chapter 3 -

- 1) Where are major Pleistocene deltas that have formed in the Lower Peninsula of Michigan and what are their special characteristics?
- 2) What lake phase/stage are they graded towards?
- 3) What are the textural and topographic characteristics of their catchment areas?

Chapter 4 -

- 1) Can the physical characteristics of relict deltas be used to numerically group deltas into like-groups?
- 2) What are the major differences in physical characteristics between the delta groups?

In short, the purpose of this dissertation is to map, characterize, and interpret the spatial characteristics of the deltas that formed during the Pleistocene in the Lower Peninsula of Michigan. My main objectives are to emphasize the importance of studying Pleistocene deltas, map known and previously unknown deltas, group different types of relict deltas, and lastly, provide additional knowledge on the paleoenvironmental conditions under which the deltas formed during the Pleistocene.

1.1 Deglaciation of the Lower Peninsula of Michigan

Late Pleistocene deglaciation of the LP of Michigan did not proceed as a steady retreat, but instead was irregular and punctuated by a series of glacial retreats and readvances (Leverett and Taylor, 1915; Hough, 1958; Mickelson et al., 1982; Larson and Schaetzl, 2001). The complicated series of stadial and interstadial glacial events that occurred here led to large fluxes of glacial meltwater and consequently the development of numerous meltwater rivers, coupled with pro- and post-glacial lakes within the Great Lake basins and on interior uplands (Spencer, 1891; Coleman, 1901; Goldthwait, 1908; Leverett and Taylor, 1915; Deane, 1950;

Eschman and Karrow, 1985; Colman et al., 1994; Larson and Schaetzl, 2001). The following discussion focuses on the timing of the major glacial advances and retreats that occurred between ≈ 21.0 and 13.0 cal ka BP, in the Lower Peninsula of Michigan. (Throughout this document “cal” refers to calibrated, “ka” to thousand, and “BP” to years before present). Also included are the pro- and post-glacial lakes that formed in the Erie, Huron, and Michigan basins, during the late Pleistocene. Knowledge of the timing and geographic extent of the various ice-marginal positions and the associated glacial lakes is one of the few ways to assist researchers in assigning ages to the coastal features (e.g., shorelines, beach ridges, deltas, etc.). Many of the moraines and outwash surfaces associated with the ice-marginal positions in Lower Michigan lack datable organic material (Winters et al., 1986) that could potentially be employed to estimate the ages of these landforms using the Accelerator Mass Spectrometry (AMS) radiocarbon dating method. Thus, shoreline elevations determined to be associated with a certain time period is often mapped and interpreted across multiple states within Great Lakes region. However, this mapping effort is complicated even more by the fact that former coastal features are upwarped towards the north-northeast in the direction of thicker and longer-lasting ice sheets that existed during the late Wisconsin (Spencer, 1891; Taylor, 1892; Larsen, 1994; Lewis et al., 2005). These deformed shorelines are the result of isostatic rebound which relates to isostatic adjustment of Earth’s crust due to the removal of a former ice sheet load (Lewis et al., 2005). This differential rebound proceeded throughout the period of ice retreat and continues today. Chapter 3 will use isobase maps and published shoreline positions to link the various deltas that were mapped in this dissertation to a specific lake phase and relative period of formation.

1.1.1 Deglaciation after ≈ 23.0 cal ka BP

When the Laurentide ice sheet (LIS) reached its maximum extent during the late Wisconsin Substage (≈ 21.8 cal ka BP¹) the entire state of Michigan, including the Huron, Erie, and Michigan basins² were covered by glacial ice (Farrand and Eschman, 1974; Mickelson et al., 1982; Curry and Petras, 2011; Figure 1.1; Table 1.1). The three sublobes of the LIS that advanced and later retreated from the LP of Michigan, during the latter part of the Wisconsin included the Huron-Erie, Michigan, and Saginaw lobes (Leverett and Taylor, 1915; Eschman and

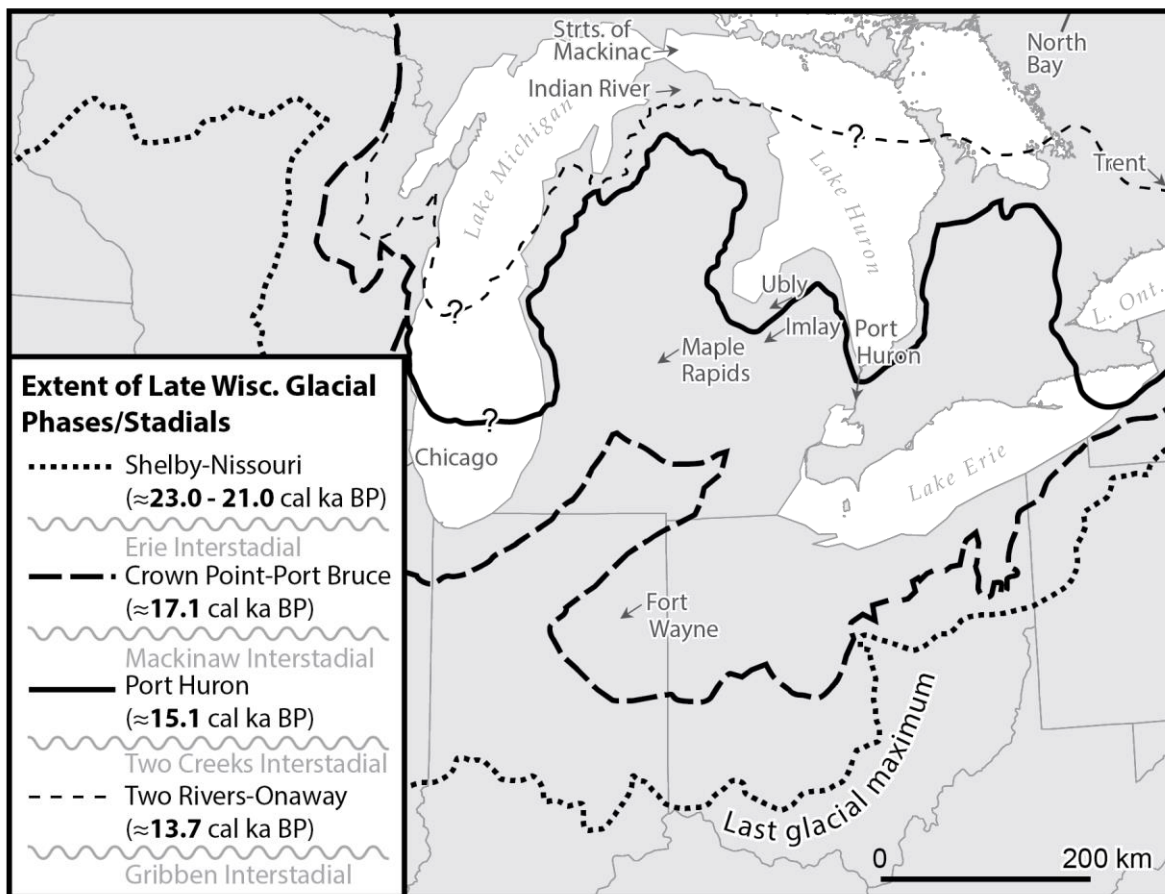


Figure 1.1: Highlighting the extent of glacial phase limits, during the late Wisconsin, within the LP of Michigan (modified from Larson and Kincare (2009) and Larson (2011)).

¹ Herein, previously reported radiocarbon ages were converted to calendar dates using the calibration curve of Fairbanks et al. (2005).

² The term “Erie basin”, “Huron basin, and “Michigan basin” throughout this paper is referred to the basin in which the waters of Lake Erie, Huron, and Michigan reside.

Table 1.1: Pro- and post-glacial lakes (stages and phases in bold, outlets in italics), elevations (in meters asl), and outlets within the Erie, Huron, and Michigan basins. Compiled from Fullerton (1980), Calkin and Feenstra (1985), Eschman and Karrow (1985), Hansel et al. (1985), Colman et al. (1994), Larson and Schaetzl (2001), and Kincare and Larson (2009)

| Erie basin | Huron basin | Lake Michigan basin |
|---|--|---|
| Shelby-Nissouri Phase/Stadial $\approx 23.0 - 21.0$ cal ka BP | | |
| Erie Interstade | | |
| Leverett <i>(Niagara Escarpment)</i> | ? <i>(Erie basin)</i> | Milwaukee <i>(Mississippi River)</i> |
| Crown Point-Port Bruce Phase/Stadial ≈ 17.1 cal ka BP | | |
| Mackinaw Interstadial | | |
| Maumee I (244) <i>(Wabash River/Fort Wayne)</i> | Ice | Ice |
| Maumee II (232) III (237) <i>(II - ? /III - Imlay Channel and Fort Wayne)</i> | Early Lake Saginaw (225) <i>(Glacial Grand Valley)</i> | Lake Chicago Glenwood I (195) <i>(Chicago Outlet)</i> |
| Arkona (216-212) <i>(Glacial Grand Valley)</i> | Arkona (216-212) <i>(Glacial Grand Valley)</i> | |
| Ypsilanti (<166) <i>(Niagara River)</i> | Post-Arkona Low ? <i>(Trent Lowlands)</i> | Mackinaw Low (<170) <i>(Straits of Mackinac and Indian River Lowlands)</i> |
| Port Huron Phase/Stadial ≈ 15.1 cal ka BP | | |
| Whittlesey (225) <i>(Uby Channel)</i> | Saginaw (212) <i>(Glacial Grand Valley)</i> | Lake Chicago Glenwood II (195) <i>(Chicago Outlet)</i> |
| Two Creeks Interstadial | | |
| Warren I & II (210-199) <i>(Glacial Grand Valley)</i> | Warren I & II (210-199) <i>(Glacial Grand Valley)</i> | Lake Chicago Glenwood II (195) <i>(Chicago Outlet)</i> |
| Wayne (210-199) <i>(Mohawk Valley)</i> | Wayne (210-199) <i>(Mohawk Valley)</i> | |
| Warren III (206-203) <i>(Buffalo, NY/Mohawk Valley)</i> | Warren III (206-203) <i>(Buffalo, NY/Mohawk Valley)</i> | |
| Grassmere (195-189) <i>(Mohawk Valley)</i> | Grassmere (195-189) <i>(Mohawk Valley)</i> | |
| Lundy (195-189) <i>(Mohawk Valley)</i> | Lundy (195-189) <i>(Mohawk Valley)</i> | |
| Early Lake Erie (<159) <i>(Niagara River)</i> | Kirkfield (173) <i>(Kirkfield Outlet/Trent Lowlands)</i> | Two Creeks (170) <i>(Straits of Mackinac)</i> |
| Two Rivers-Onaway Phase/Stadial ≈ 13.7 cal ka BP | | |
| Gribben Interstadial | | |
| Early Lake Erie (<159) <i>(Niagara River)</i> | Huron-Algonquin (184) <i>(Trent Lowlands and Port Huron Outlet(?))</i> | Calumet (189) <i>(?)</i> |
| | | Toleston (184) <i>(?)</i> |
| | Main Lake Algonquin (184) <i>(Port Huron Outlet)</i> | Main Lake Algonquin (184) <i>(Straits of Mackinac, Indian River Lowlands, and Chicago Outlet)</i> |
| | Algonquin (184) <i>(Trent Lowlands and Port Huron Outlet(?))</i> | Algonquin (184) <i>(Straits of Mackinac, Indian River Lowlands, and Chicago Outlet)</i> |

Karrow, 1985; Grimley, 2000). In the LP of Michigan there are generally three glacial phases or stadials that mark the retreat from the last glacial maximum, or the Shelby-Nissouri ($\approx 23.0 - 21.0$ cal ka BP) stadial: (1) Crown Point-Port Bruce (≈ 17.1 cal ka BP), (2) Port Huron (≈ 15.1 cal ka BP), and (3) Two Rivers-Onaway (≈ 13.7 cal ka BP) (Larson, 2011; Figure 1.1; Table 1.1). Separating these glacial stadials are three interstadials: (1) Erie, (2) Mackinaw, and (3) Two Creeks, respectively (Karrow et al., 2000; Figure 1.1; Table 1.1).

The first lakes to form during the Erie interstadial included glacial Lake Leverett which occupied the Erie basin and presumably drained easterly toward and over the Niagara Escarpment and into the Atlantic Ocean (Mörner and Dreimanis, 1973; Karrow, 1984; Fullerton 1980; Barnett, 1992). During the same period, glacial Lake Milwaukee occupied the southern part of the Lake Michigan basin and presumably drained south into the Mississippi drainage system (Schneider and Need, 1985; Table 1.1). Continued northward retreat of the Huron-Erie lobe likely resulted in an unnamed lake in the Lake Huron basin, which would have drained into the Lake Erie basin (Leverett and Taylor, 1915; Eschman and Karrow, 1985; Kincare and Larson, 2009; Table 1.1).

1.1.2 Deglaciation after ≈ 17.1 cal ka BP

The Erie interstadial was followed by the Crown Point-Port Bruce stadial (≈ 17.1 cal ka BP) (Fullerton, 1980; Karrow et al., 2000; Figure 1.1; Table 1.1). After this readvance, during the Mackinaw interstadial, large glacial lakes once again formed in the Great Lakes' basins. Glacial Lake Maumee (Figure 1.2), in the Lake Erie basin, was the first to develop and initially discharged southwest into the Wabash River valley via an outlet near Fort Wayne, Indiana and eventually into the Ohio River valley (Leverett and Taylor, 1915; Calkin and Feenstra, 1985;

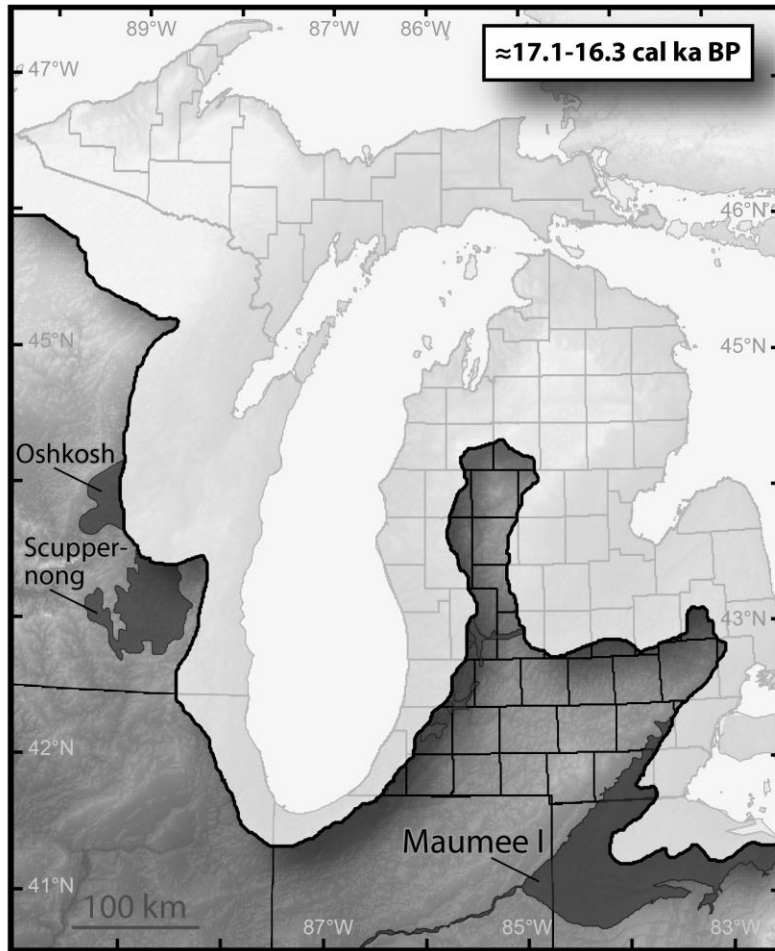


Figure 1.2: Approximate ice marginal position and extent of glacial lakes following the Crown Point-Port Bruce maximum (modified from Larson and Kincare (2009) and Kincare and Larson (2009)).

Figure 1.2). As the Huron-Erie Lobe continued to retreat northward during this interstadial, glacial Lake Maumee expanded north and eventually drained north and then west across the “thumb” of the LP of Michigan via an unknown outlet (Leverett and Taylor, 1915; Calkin and Feenstra, 1985; Larson and Schaetzl, 2001; Figure 1.1; Table 1.1). At roughly the same time, northward retreat of the Michigan lobe allowed glacial Lake Chicago to develop in the Lake Michigan basin, with drainage flowing south and into the Mississippi River drainage system via the Des Plaines River outlet near Chicago (Leverett and Taylor, 1915; Hansel et al., 1985; Table

1.1). Glacial Lake Chicago persisted throughout all subsequent stadial and interstadial conditions; however, presumably at times its drainage was temporarily diverted from an outlet near Chicago to northern outlet(s) near the Straits of Mackinaw (Hough, 1963; 1966; Bretz, 1964; Hansel et al., 1985; Colman et al., 1994). These drainage shifts resulted in multiple phases or lake levels for glacial Lake Chicago (Leverett and Taylor, 1915; Hough, 1963; 1966; Bretz, 1964; Hansel et al., 1985; Colman et al., 1994).

There was a minor readvance of the Huron-Erie lobe during the Mackinaw interstadial, and subsequently glacial Lake Maumee drained via the Imlay Channel on the “thumb” of Lower Michigan (Leverett and Taylor, 1915; Eschman and Karrow, 1985; Figure 1.1; Table 1.1). Once drainage from glacial Lake Maumee was directed across the “thumb” and westward down the glacial Grand River Valley and into glacial Lake Chicago, multiple glacial Lake Maumee phases became established (Larson and Schaetzl, 2001). Some researchers have suggested that at least two phases of glacial Lake Maumee drained southwesterly through the outlet near Fort Wayne (e.g., Bleuer and Moore, 1972) whereas others suggested that the later phases of glacial Lake Maumee drained to the north via the Imlay channel (Leverett and Taylor, 1915; Hough, 1958, 1966; Table 1.1). Nonetheless, all agree that prolonged northward retreat of the Huron-Erie Lobe eventually resulted in glacial Lake Maumee draining into Early Lake Saginaw (Figure 1.3), which developed in the Saginaw lowlands during the Mackinaw interstadial (Leverett and Taylor, 1915; Eschman and Karrow, 1985; Figures 1.1 and 1.3; Table 1.1). Early Lake Saginaw drained west into the glacial Grand River Valley via an outlet near Maple Rapids, Michigan (Leverett and Taylor, 1915; Bretz, 1951; Eschman and Karrow, 1985; Kehew, 1993; Figure 1.3). Ongoing retreat of the Huron-Erie lobe eventually exposed enough of the “thumb” to allow the



Figure 1.3: Approximate ice margin and extent of glacial lakes following the Crown Point-Port Bruce maximum (modified from Larson and Kincare (2009) and Kincare and Larson (2009)).

merging of waters in the Huron and Erie basins with that in the Saginaw lowlands. The joining of Early Lake Saginaw and glacial Lake Maumee resulted in the formation of glacial Lake Arkona (Figure 1.4). The latter also drained into the glacial Grand River Valley via the outlet near Maple Rapids, Michigan (Leverett and Taylor, 1915; Eschman and Karrow, 1985; Larson and Schaetzl, 2001). Eventually, due to continued ice retreat, an even lower outlet opened; drainage from glacial Lake Arkona was then directed eastward, towards an outlet near the Trent lowlands, Ontario (Eschman and Karrow, 1985; Barnett, 1985, 1992). Glacial Lake Arkona was subsequently replaced by two eastward-draining, lower-level lakes: glacial Lake Ypsilanti in the Lake Erie basin, which drained via the Niagara River (Kunkle, 1963; Barnett, 1985, 1992) and an unnamed lake in the Lake Huron basin, which drained via the Trent lowlands (Dreimanis, 1977; Fullerton, 1980; Table 1.1). At roughly the same time, the Indian River lowlands and the Straits of Mackinac presumably become ice free, resulting in a significant drop in the level of glacial Lake Chicago and the development of a low-level lake (i.e., the intra-Glenwood low phase, or the Mackinaw Low). Drainage from this lake was directed to the east and into the Lake Huron basin via the Straits (Hough, 1958; Hansel et al., 1985; Monaghan and Hansel, 1990; Lewis et al., 2008; Figure 1.1; Table 1.1).



Figure 1.4: Approximate ice margin and extent of glacial lakes following the Crown Point-Port Bruce maximum (modified from Larson and Kincare (2009) and Kincare and Larson (2009)).

1.1.3 Deglaciation after ≈ 15.1 cal ka BP

Following the Mackinaw Interstadial was an ice advance referred to as the Port Huron stadial (≈ 15.1 cal ka BP) (Leverett and Taylor, 1915; Blewett, 1991; Figures 1.1 and 1.5; Table 1.1). As the ice-margin advanced to the Port Huron moraine position, the more northern lake outlets were eventually covered by ice and subsequently, the low-level lakes in the central Great Lakes region were replaced by higher-level lakes. Glacial Lake Whittlesey was one of these high-level lakes which formed in the Lake Erie basin at this time (Calkin and Feenstra, 1985; Figure 1.5). Drainage was once more directed to the north and then west across the



Figure 1.5: Approximate ice margin position and extent of glacial lakes following the Port Huron maximum (modified from Larson and Kincare (2009) and Kincare and Larson (2009)).

“thumb” of Michigan, albeit now via the Ubly channel - just north of the Imlay channel and near the city of Ubly, Michigan (Leverett and Taylor, 1915; Fullerton, 1980; Calkin and Feenstra, 1985). Drainage from the Ubly channel flowed into glacial Lake Saginaw, within the Lake Huron basin, and from here drainage was to the west, as previously, into the glacial Grand River Valley via Maple Rapids (Leverett and Taylor, 1915; Eschman and Karrow, 1985). At this time, glacial Lake Chicago, within the Lake Michigan basin, was reestablished due to the Straits of Mackinac and Indian River lowlands being covered by ice (Leverett and Taylor, 1915; Figure 1.1). The Glenwood II phase of glacial Lake Chicago, which stabilized at the same elevation as the Glenwood I phase (195 m asl), presumably draining through the Chicago outlet and was fed by the glacial Grand River (Leverett and Taylor, 1915; Hansel et al., 1985; Kehew, 1993). Note, ice did not cover the entire Erie and Michigan basins, nor the Saginaw lowlands, during the maximum extent of the Port Huron readvance, and thus, lakes were able to occupy portions of these areas throughout this stadial (Figures 1.1 and 1.5).

Eventually, during the Two Creeks interstadial, as the ice margin began its northward retreat from the Port Huron moraine, the lakes that occupied the Erie, Michigan, and Saginaw basins began expanding toward the north (Figures 1.1 and 1.5). The northward expansion of these lakes resulted in the coalescence of glacial Lakes Saginaw and Whittlesey, to form glacial Lake Warren; this lake initially drained via the glacial Grand River Valley (Dreimanis, 1966; Kehew, 1993). As the Huron-Erie lobe continued to retreat, a lower outlet became exposed near Buffalo, New York and drainage from glacial Lake Warren was directed to the east and into the Mohawk River valley (Calkin and Feenstra, 1985). Some believe a short-lived, lower-level lake, known as glacial Lake Wayne, developed shortly after the opening of the eastern outlet,

and subsequently a third glacial Lake Warren phase formed after lake-level rose slightly (Leverett and Taylor, 1915; Fullerton, 1980; Muller and Prest, 1985; Table 1.1). Short stints of lake-level raise were perhaps due to isostatic uplift of the eastern outlet, fluctuations in the size of the lake basin as well as precipitation and meltwater additions, or a combination of these factors (Lewis et al., 2005). Eventually the new outlet near Buffalo led to drainage of glacial Lake Warren and the establishment of glacial Lake Grassmere, and later glacial Lake Lundy in the Huron and Erie basins (Hough, 1966; Calkin, 1970; Fullerton, 1980; Calkin and Feenstra, 1985; Lewis et al., 1994; Table 1.1). These lakes are also thought to have drained eastwardly into the Mohawk River valley, however the exact locations of their outlets are unknown (Calkin and Feenstra, 1985). While glacial Lakes Warren, Wayne (?), Grassmere, and Lundy occupied the Erie basin, the Glenwood II phase of glacial Lake Chicago persisted in the Lake Michigan basin and continued to drain via the Chicago outlet (Hansel et al., 1985). Continued northward retreat of the Huron-Erie lobe during the Two Creeks interstadial eventually exposed an even lower outlet, north of Buffalo, New York. As a result, water levels in the Lake Erie basin fell to the Early Lake Erie level. Early Lake Erie drained north via the Niagara River and then into the Lake Ontario basin (Calkin and Feenstra, 1985). The Lake Erie basin at this time was receiving water from the early stages of glacial Lake Algonquin, which had formed in the Huron basin, via an outlet at Port Huron, Michigan (Hough, 1958; Lewis et al., 2008). However, eventually an outlet (Fenelon Falls) near the head of the Trent River valley became ice-free and as a result, the water level in the Lake Huron basin fell to a low (Kirkfield) phase, as water was redirected to the Kirkfield outlet and into the Lake Ontario basin (Hough, 1966; Fullerton, 1980; Eschmand and Karrow, 1985; Lewis et al., 2008; Figure 1.6). Deglaciation of the Straits of Mackinac at



Figure 1.6: Approximate ice margin position and extent of glacial lakes following the Port Huron maximum (modified from Larson and Kincare (2009) and Kincare and Larson (2009)).

roughly the same time also caused the Glenwood II phase of glacial Lake Chicago to fall in the Lake Michigan basin, forming the Two Creeks low phase (Hansel et al., 1985; Kaiser, 1994; Larson et al., 1994; Figure 1.6). With these northern outlets ice-free, low-water phases persisted in the Lake Huron, Lake Michigan, and Lake Erie basins until the Two Rivers-Onaway stadial (Lewis et al., 2008; Figures 1.1 and 1.6).

1.1.4 Deglaciation after ≈ 13.7 cal ka BP

Ice associated with the Two Rivers-Onaway stadial (≈ 13.7 cal ka BP) blocked the Straits of Mackinac, reestablishing glacial Lake Chicago and forming the Calumet and Toleston phases within the Lake Michigan basin (Hansel et al., 1985; Colman et al., 1994; Figures 1.1 and 1.7; Table 1.1). The actual outlets, however for the Calumet and Toleston phases are unknown (Kincare and Larson, 2009); perhaps these lakes had a closed lake basin or drainage via the Chicago outlet. The closing of the northern outlets also caused water levels to rise within the Huron basin, leading to the establishment of early glacial Lake Algonquin (or glacial lake Huron-

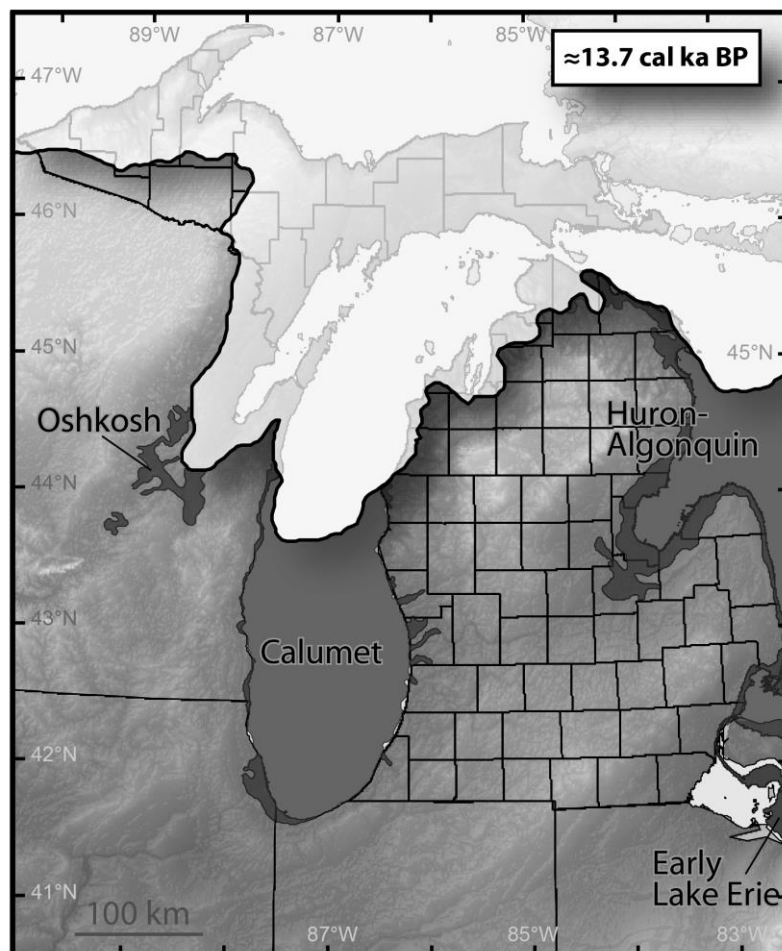


Figure 1.7: Approximate ice margin position and extent of glacial lakes during the Two Rivers-Onaway maximum (modified from Larson and Kincare (2009) and Kincare and Larson (2009)).

Algonquin; Kincaid and Larson, 2009) (Leverett and Taylor, 1915; Karrow et al., 1975; Larson, 1987; Drzyzga et al., 2011; Figure 1.7). Soon thereafter, during the Gribben interstadial, as the southern margin of the LIS retreated, for the last time, off of the LP of Michigan, lakes within the Lake Michigan and Lake Huron basins merged to form the main stage of glacial Lake Algonquin (Leverett and Taylor, 1915; Karrow et al., 1975; Figure 1.8). Continued northward retreat of the ice margin caused glacial Lake Algonquin to slowly transgress northward (Eschman and Karrow, 1985; Figure 1.8), and eventually drainage was directed to the south and

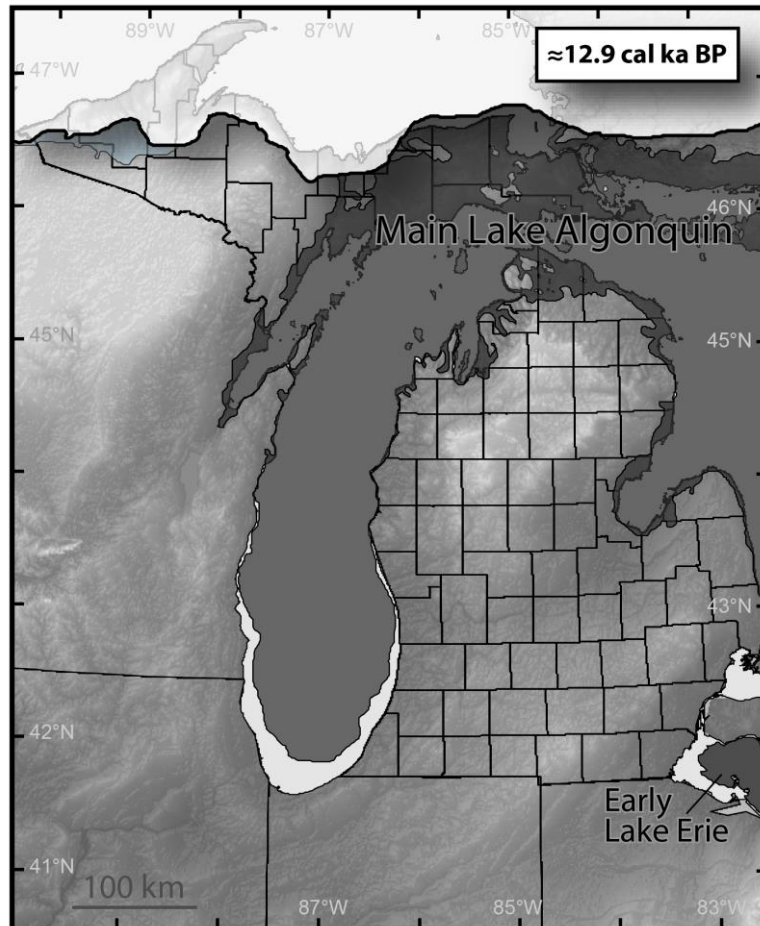


Figure 1.8: Approximate ice margin position and extent of glacial lakes following the Two Rivers-Onaway maximum (modified from Larson and Kincaid (2009) and Kincaid and Larson (2009)).

east via the Trent lowlands. Whether glacial Lake Algonquin drained through the Port Huron outlet continues to be debated (Eschman and Karrow, 1985; Larsen, 1987; Lewis and Anderson, 1992; Larson and Schaetzl, 2001). However, all agree that the northward retreat of the ice margin, during this time, eventually uncovered a succession of northern lower outlets, near the head of the Ottawa River near North Bay, Ontario. Thus, the level of glacial Lake Algonquin fell incrementally to form a series of short-lived, low-level, post Algonquin lakes (Lewis and Anderson, 1992; Schaetzl et al., 2002; Drzyzga, 2007; Lewis et al., 2008; Drzyzga et al., 2012). Coastal features associated with these subsequent lake stages are not the focus or discussed in this dissertation, and thus, the history of those lake phases are not outlined here.

1.1.5 Deglaciation Summary

Many of the surficial deposits and landforms that blanket the Lower Peninsula of Michigan are late Pleistocene in age, and were deposited during successive advances and retreats of the LIS. The ice sheet covered all of the Great Lakes' basins when it reached its maximum extent, around 21.8 cal ka BP. During subsequent maxima, at about 17.1, 15.1, and 13.7 cal ka BP, the LP of Michigan was affected by three distinct glacial lobes: Huron-Erie, Michigan, and Saginaw. These three ice lobes formed the lobate pattern of the moraines that surround the modern day Great Lakes. The various proglacial lakes that developed along the margins of the Huron-Erie, Michigan, and Saginaw lobes fluctuated in size and shape as their ice margins advanced and retreated over the course of the late Pleistocene.

Between approximately 23.0 and 11.5 cal yrs BP, roughly 15 different, named glacial lakes are known to have formed in both the Erie and Huron basins, and roughly 10 formed in the Michigan basin (Table 1.1). Within the Erie basin, drainage shifted between five different

outlets, whereas in the Huron and Michigan basins, drainage moved between four and three, respectively (Table 1.1). With each outlet adjustment, lake-level elevation shifted, and thence base level for the fluvial systems that were active during the late Pleistocene. Within the LP of Michigan, several changes in base level, over a relatively short period of time, presumably promoted massive fluxes of sediment towards the mouths of the meltwater systems. Under these conditions, delta formation would seemly have been ideal, and thus deltas should have commonly formed during the late Pleistocene. Delta formation should have been promoted in areas where wave energies along the shores of proglacial lakes were lacking the strength to keep pace with redistributing newly deposited alluvial sediment away from the river mouths. These paleofluvial conditions, during the late Pleistocene, were the impetus for scanning the entire LP of Michigan for relict deltas, and thus the motivation for this dissertation.

1.2 Delta Types and Morphologies

The term *delta* is usually applied to a depositional plain formed by a river at its mouth, where sediment accumulation results in an irregular progradation of the shoreline (Coleman and Wright, 1975). The feature was first named more than 2500 years ago by the historian Herodotus, who noted that the land created at the mouth of the Nile River resembled the Greek letter Δ (delta) (Miall, 1984). Historically, sedimentologists and geologists have been more interested in the internal structure and sediments of a delta, and particularly the portions of the delta that are continuously submerged. Hence, there is an extensive amount of literature relating to deltaic processes and subaqueous sediments (e.g., Shirley and Ragsdale, 1966; LeBlanc, 1976a; 1976b; Coleman, 1981; Coleman et al., 1998). However, geomorphologists have traditionally been more interested in the fluvial processes that produce deltas and hence, are

usually concerned with the subaerial portions of deltas (e.g., Gilbert, 1890; Smith and Jol, 1997; Blewett et al., 2014). While a delta is active, this area of the delta is perhaps the most noticeable feature on the landscape, and it continues to be so for several millennia after the delta becomes abandoned. This dissertation aligns with the geomorphologists' interests and focuses mostly on mapping and quantifying the characteristics of the subaerial portions of the Pleistocene deltas in Lower Michigan (i.e., the delta plain).

In order to clarify how deltas form, the following discussion highlights (1) the processes involved in delta formation, (2) the major components and typical sediments of deltas, and (3) the main morphologic differences between lacustrine and marine deltas. The closing discussion in this chapter emphasizes deltaic classification and is later applied in Chapter 4, which largely focuses on mapping, describing, and classifying the different types of deltas that were studied in this dissertation.

1.2.1 Deltaic Processes

Deltas result from the rapid and/or continued supply of sediment by a river or rivers to a stagnant body of water (Gilbert, 1885). Initially the deltaic system originates underwater. Subsequently, the landform becomes visible as a subaerial landmass, once the deltaic sediment aggrades to the elevation of the water plain (Ritter et al., 2006).

Deltas exhibit a wide range of configurations and are associated with a variety of depositional landforms. The surface topography, geometry, and sedimentary sequences of a delta largely depend on (1) the discharge regime and sediment load of the associated river, (2) the geometry of the river mouth, (3) the relative magnitudes of coastal forces (e.g., longshore currents and waves), (4) deformation of the deltaic sediments, and (5) more long-term

processes, such as changes in river course, catchment area, local climate, and slope and size of the receiving basin (Barrell, 1912; Coleman and Wright, 1975).

Where deltas are experiencing significant coastal disturbances in the form of waves and longshore currents, their sediments are often redistributed and remolded into features and shapes that are more in equilibrium with the coastal system. Komar (1973), Wright and Coleman (1973), Wright (1977), and Caldwell and Edmonds (2014) documented the theoretical and actual deltaic configurations resulting from various riverine sediment contributions and wave disruptions. These studies found that nearshore, wave energy values tend to be lowest along delta coasts with a relatively low gradient, littoral profile. In addition, river-dominated regimes with relatively high-discharges are often associated with the flattest delta profiles and have irregular distal margins, whereas wave-dominated regimes are often associated with steep delta profiles and have smooth, arcuate distal margins (Wright and Coleman, 1973). In the river-dominated regimes, the flattening of the delta profile occurs at a greater rate than the rate at which longshore currents and waves are capable of molding the deltaic sediments (Wright and Coleman, 1973; Galloway, 1975). Conversely, in wave-dominated regimes, the river is unable to deposit enough sediment near the river mouth to overcome wave effects, resulting in a cusped-shaped delta plain that grades smoothly with the adjoining shorelines (Wright and Coleman, 1973; Galloway, 1975).

Many of the late-Pleistocene deltas on Lake Bonneville (Utah), which formed in a lacustrine setting, are cusped-shaped, with relatively smooth outer margins, as viewed from above, or as shown on a topographic map (Gilbert, 1885, 1890). These patterns indicate that during delta construction, there was ample wave action to remove sediment by longshore

currents, so as to maintain a stable and smooth outer margin (Gilbert, 1885; Russel, 1967).

Gilbert (1885, 1890) defined many of these fan-shaped, relict-lacustrine deltas as Gilbert-type deltas. These types of deltas are often divided into three components and sedimentary facies.

The following discussion focuses on the major parts of a delta and their associated facies.

1.2.2 Deltaic Components and Sediments

Deltas are composed of both subaqueous and subaerial components, which are often separated into three physiographic parts called the delta plain, the delta front, and the prodelta (Coleman, 1981; Hori and Saito, 2007; Figure 1.9). The delta plain begins where its alluvial plain is no longer confined laterally by valley walls (Ritter et al., 2006). When this constraint ends, the river system often widens and splits into two or more distributary channels. Each of the alluvial

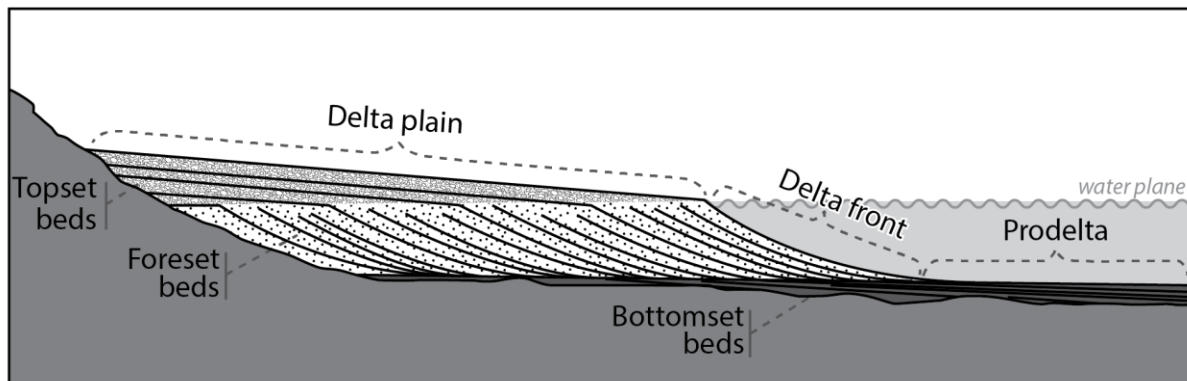


Figure 1.9: Cross section of a Gilbert-type delta, with the primary delta components and facies assemblages (modified from Gilbert (1890) and Kenyon and Turcotte (1985)).

plains associated with these distributaries merges to form a series of subaerial plains known as the delta plain. The delta plain is fronted by a steeper slope, known as the delta front. On the delta front, sediment is deposited most actively and is often transported downslope by creep and periodic, subaqueous avalanching or landslides (Wright and Coleman, 1974). Sediment is also deposited here by density currents when denser water - due to a higher concentration of

sediment - sinks below less dense water within the basin (i.e., hyperpycnal flow). The prodelta region lies lakeward of the delta front and is the distal part of the depositional sequence. Here, sediment is mostly transported in subaqueous suspension under hypopycnal flows, which is when the density of the suspended sediment flow is less than the water in the basin (Bates, 1953; Wright and Coleman, 1974; Kenyon and Turcotte, 1985; Hori and Saito, 2007).

Gilbert-type deltas are common in deep, freshwater lakes and reservoirs where the density of the discharged water is relatively equal or somewhat greater than that of the receiving water body (Gilbert, 1885; Barrell, 1912; Postma, 1990; Coleman and Wright, 1981; Chidsey, 2002; Gobo et al., 2014). These conditions are typical of sandy, high bed-load rivers entering freshwater lakes. Thus, Gilbert-type deltas are arguably less common in marine settings where freshwater rivers are entering salt water which is denser than freshwater in the absence of a sediment load. Gilbert-type deltas are often used to describe and illustrate deltaic processes, as shown above in Figure 1.9, because their deltaic components and sediment facies are relatively straightforward. Two papers by G.K. Gilbert (1885, 1890) defined the sequences of sediments found within the different deltaic components of a Gilbert-type delta and labeled them as topset, foreset, and bottomset beds (Figure 1.9). The topset beds are a complex of lithologic units deposited in the various subaerial environments of the delta plain. Layers in the topset unit are mostly horizontal and shift between fine and coarse textured sediments (Gilbert, 1890; Figure 1.9). As the delta builds lakeward either due to a stable water plain elevation or a regression phase, coarser grained deltaic sediments are deposited on top of finer-grained prodelta muds. This results in a coarsening upward vertical succession of facies. However, a transgressive phase followed by a regression phase will result in a wedge of

sediments in which deeper-water sediments (i.e., finer-grained sediments) are deposited on top of shallower-water sediments (i.e., coarser-grained sediment) in the *basal* part of the wedge, and finer-grained sediments are deposited on top of coarser sediments near the top of the wedge (Gobo et al., 2014).

Foreset deposits accumulate in portions of the subaqueous delta front (Figure 1.9). These deposits are usually coarser near the mouth of the major feeder channels that are supplying sediment to the delta and become finer lakeward (Gilbert, 1890). Strata in the foreset unit are often inclined lakeward, at an angle reflecting that of the delta front slope (Gilbert, 1890; Scruton, 1960). Foreset units are also often oblique near the inflection point at the delta front, where the delta plain surface meets the top of the foreset slope (Figure 1.9). Foreset beds grade gradually lakeward into bottomset beds and become finer grained (Figure 1.9). Bottomset deposits are often composed of the finest grain sediments within the deltaic depositional system, because of flow velocities significantly diminishing lakeward towards the receiving basin floor (Gilbert, 1890; Scruton, 1960). These beds usually dip at very low angles that are consistent with the bottom topography of the lake (Scruton, 1960; Ritter et al., 2006).

To summarize, the classic morphology of a prograding Gilbert-type delta, as described by Gilbert (1885, 1890) and Kenyon and Turcotte (1985), is as follows: (1) fine-grained, suspended-load sediments settle to the floor of the receiving basin in front of the advancing delta front to form gently inclined bottomset beds, (2) individual particles of coarse-grained, bed load material are dropped near the river mouth and are transported down the front of the delta to form foreset beds lying at the angle of repose, and (3) the top of all the foreset beds except the youngest are eroded and truncated by the overlying topset bed. However, the

sediment sequences associated with a Gilbert-type delta are not common, since they form mostly in freshwater lakes where coarse sediment is deposited immediately upon entering a basin, forming relatively steep foreset beds (Coleman and Wright, 1981; Chidsey, 2002).

Nonetheless, the Gilbert-type delta is widely described in introductory texts as one of the most common types of deltas (Chorley et al., 1964; LeBlanc, 1975; Friedman and Sanders, 1978; Coleman and Wright, 1981; Ritter et al., 2006; Haslett, 2000).

1.2.3 Lacustrine vs. Marine Deltas

Freshwater and marine deltaic environments are distinguishable by examining various morphologies and processes within the delta system (Smith, 1991). There are generally three major differences between the development of freshwater or lacustrine deltas, as compared to marine deltas. Marine deltas are formed in association with: (1) tidal effects, (2) stronger wave energies, and (3) contrasts in water salinity. For example, in the classic Gilbert-type delta, prograding into fresh water, the absence of a density contrast between the river water and that of the receiving basin favors three-dimensional mixing and rapid deposition of sediment close to the river mouth, and thus the development of steep delta foresets (Postma, 1990; Bowman, 1990; Bell, 2009). In particular, colder-water rivers that have a large load (i.e., either bed load or suspended load) and flow into deep, warmer-water basins result in rapid deposition and steep delta foresets. Freshwater deltas often form under these hyperpycnal and homopycnal flow conditions, in which the density of the discharged water is greater than, or relatively equal to, that of the receiving water body. Alternatively, in the marine environment the density contrast between the lower-density freshwater and the higher-density seawater (i.e., hypopycnal flow) often results in plumes of suspended sediment that are carried far out to sea. Generally, foreset

beds dipping at a relatively low angles (<15 degrees), suggest deltaic deposition from a buoyant jet (i.e., hypopycnal flow), and thus, under a marine setting. Alternatively, steep angle foreset beds suggest deltaic deposition by homopycnal flows and thus, a lacustrine depositional setting (Bates, 1953). As a result, Gilbert-type deltas are relatively less common in marine settings.

Knowledge of the subsurface structure of the deltas studied in this dissertation is absent. However, Blewett et al. (2014) provide roughly 30 km of ground-penetrating radar (GPR) imagery in the eastern Upper Peninsula (UP) of Michigan that illustrates clear evidence of topset and forest beds (Figure 1.10). Results from their study found that the high-standing outwash aprons that flank the southern margins of the Munising moraine, in the eastern UP, grade into large coalescing-deltas. The elevations of the deltas, along with their foreset beds, suggest that the deltas were graded to Main Lake Algonquin (between ≈ 13.0 -12.5 cal ka BP), and likely formed as the ice margin stabilized at the Munising moraine. These relict, lacustrine deltas occupy a region that is less than 100 km from this dissertations' study area (Figure 1.10). Furthermore, the delta foreset beds dip at an average angle between 13 and 16° (Figure 1.10), suggesting Gilbert-type deltas, which often have foreset beds that dip around 15° (Bates, 1953). These data emphasize the likelihood that many of the deltas mapped as part of this dissertation also have Gilbert-type origins and sediment structures.

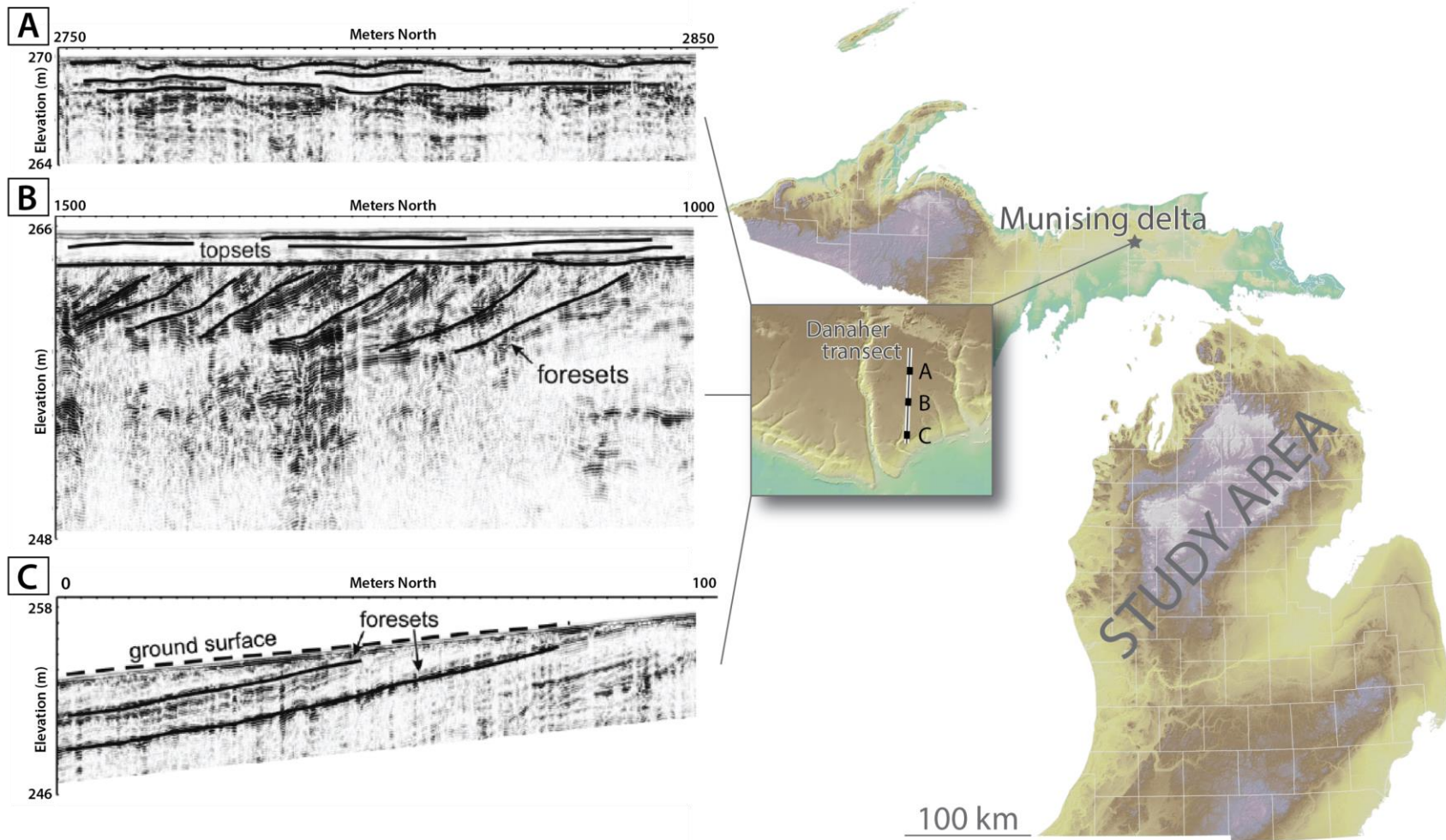


Figure 1.10: Three GPR profiles along the Danaher delta - a section of the coalesced, Munising delta. GPR images illustrate the sequence stratigraphy of the Gilbert-type delta, which formed within 100 km of the dissertation study area (GPR images borrowed from Blewett et al. (2014)).

1.2.4 Delta Classifications

There are generally two major ways to classifying deltas. One considers the influences that created the landform (i.e., wave, fluvial, tide, and Gilbert type deltas), while the other considers its shape (i.e., cusped, lobate, elongate, and estuarine). The most well-known classification system for deltas was originally proposed by Galloway (1975) and is illustrated in a ternary diagram (Figure 1.11). This classification scheme followed that of Fisher (1969), who subdivided deltas into two major types: (1) high-constructive and (2) high-destructive deltas. Galloway's (1975) classification system incorporates the relative intensities of fluvial and marine processes (i.e., tides and waves) operating along the margins of a delta, and classifies deltas into three groups: (1) fluvial-dominated, (2) wave-dominated, and (3) tide-dominated

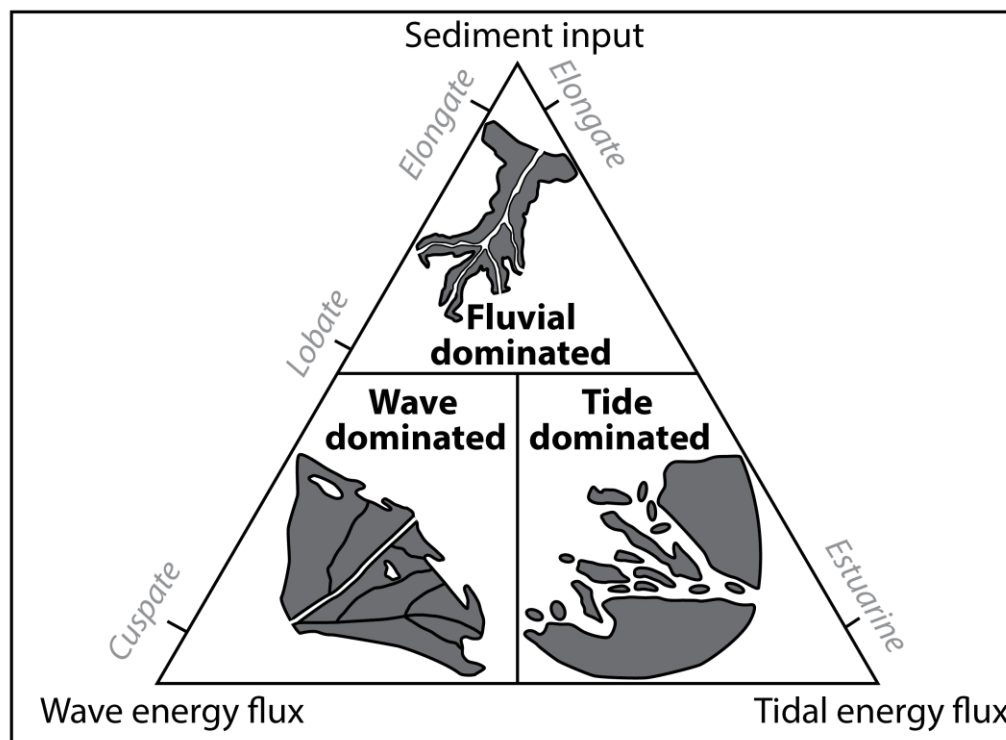


Figure 1.11: Ternary classification of deltas on the basis of dominate processes and the resulting morphology (modified from Galloway (1975) and Hori and Saito (2007)).

(Figure 1.11). Fluvial or river-dominated deltas are typically elongated, whereas wave-dominated deltas have cusped shorelines, and tide-dominated deltas have an estuary-like geometry to their distributary mouths (Figure 1.11). Orton and Reading (1993) proposed a new classification system similar to that of Galloway (1975), but which also considered sediment grain size of the delta deposits. Orton and Reading (1993) believed it important to differentiate between gravelly and muddy deltas. More recently, Bhattacharya and Giosan (2003) proposed using quantitative data to classify the coastal disturbance along the margins of a delta. Their classification system applies Orton and Reading's (1993) system and Galloway's (1975) ternary diagram to generate an asymmetry index A , to express the degree of dominance of marine versus fluvial forces. The A index is defined as the ratio between the net longshore transport rate at the river mouth ($\text{m}^3 \text{ year}^{-1}$) and river discharge ($10^6 \text{ m}^3 \text{ month}^{-1}$). A low index value favors symmetrical deltas, whereas deltas with a high index are more asymmetrical. These classification systems are useful because they help researchers better understand the major processes acting on a delta, by recording the dominant fluvial, coastal, and depositional processes in subsequent geometries and sediment facies of the delta (Hori and Saito, 2007). More importantly, in this dissertation, these classification systems can be variously employed in interpreting the paleoenvironments of relict deltas.

In the past, delta classification systems, as discussed above, have largely focused on modern deltas, and on present or relatively short term fluvial and/or coastal conditions, as opposed to paleoconditions. Pleistocene deltas are composite systems that record depositional processes through a range of phases (e.g., catchment area, climate, sediment supply, base-level, basin area, etc.) (Galloway, 1975; Coleman and Wright, 1975; McPherson et al., 1987;

Postma, 1990; Orton and Reading, 1993). Therefore, in this dissertation, Pleistocene or relict deltas are classified according to their overall shape and number of paleodistributary channels, which is thought to more likely be a product of long term conditions, as opposed to grain size and thickness patterns, which could have changed over relatively short periods of time. Since Galloway's (1975) classification largely differentiates deltas based delta shape and is not designed to capture sedimentary processes and sediment preservation, this study proposes Galloway's (1975) ternary classification as the most fitting for classifying relict deltas.

1.3 Summary

In summary, rivers contribute both sediment and water to coastal environments; a delta forms if sediment additions are greater than the rate of sediment relocation at the river mouth. Numerous meltwater-rivers and pro- and post-glacial lakes formed during the Pleistocene in the Lower Peninsula of Michigan, and thus, deltas were common features that formed during that epoch.

Various terrestrial and coastal factors influence delta morphology. The forces that influence the growth of the delta are often recorded in the geometry and sediment characteristics of the delta. Because of the link between deltaic form and process, mapping and describing the characteristics of Pleistocene deltas can provide an important step in advancing our knowledge of the paleoenvironmental conditions during that time. After the locations and types of deltas are identified, paleoshoreline conditions, such as lake level elevation, wave energy, wind and longshore drift direction can be inferred during the formation period of the delta, as well as paleoterrestrial conditions, such as stable vs. unstable landscapes.

Chapter 2 - Relict Coastal Landforms as Paleolake-level Indicators

2. Introduction

For more than a century, researchers have been studying relict coastal landforms in the Great Lakes region that are associated with pro- and post-glacial lakes related to the last glaciation (e.g., Spencer, 1891; Taylor, 1892; Chamberlin, 1909; Goldthwait, 1908; Leverett and Taylor, 1915; Bretz, 1951; Hough, 1958). These relict coastal landforms have commonly served as evidence for (1) the presence of a paleolake, (2) the chronologic progression (phases) of a lake, and (3) the extent of a paleolake (Leverett and Taylor, 1915; Evenson, 1973; Dott and Mickelson, 1995; Breckenridge, 2013). In addition, relict beach ridges, wave-cut bluffs, meltwater spillways, spits, and deltas have also been used to estimate the water plane elevations (cf. Schaetzl et al., 2002; Baedke et al., 2004; Fisher 2005, 2007; Drzyzga, 2007). However, many studies that have studied these relict coastal features have varied in their methods and assumptions when recording water plane elevations (e.g., Olson, 1958a,b; Evenson, 1973; Thompson, 1988a; Thompson, 1992; Larsen, 1994; Chrzastowski and Thompson, 1992, 1994; Lichter, 1995, 1997; Dott and Mickelson, 1995; Johnston et al., 2007, 2014; Breckenridge, 2013; Teller and Leverington, 2004; Teller et al., 2005; Kozlowski et al., 2005). Each mapping approach, arguably, has advantages and disadvantages, as well as limitations, when employed to interpret paleolake-level history. This chapter seeks to shed light on a few of the various techniques (and inconsistencies) in recording paleolake-level elevations from relict coastal landforms; I also discuss a few additional environmental proxies that they may provide. For the sake of brevity, this chapter mostly focuses on research conducted in the Great Lakes region (although also including Glacial Lake Agassiz) and those within the Lake

Bonneville area in the western United States. The topics and matters considered in this chapter will hopefully further promote studying the utility of relict deltas everywhere.

2.1 Examples of Coastal Landforms used for Paleolake-level Reconstruction

Several researchers have observed that the precise elevation of relict coastal landforms and the water plane under which they formed, along with their age, provide critical information for reconstructing the outlet locations, water budgets, and mid-continental meltwater routings during the late Pleistocene (Broecker et al., 1989; Clark et al., 2001; Fisher et al., 2002; Teller et al., 2002; Fisher, 2007; Lewis et al., 2010; Johnston et al., 2014). Early work by Lawson (1891), however, cautioned that a researcher's ability to delimit the true paleo-water plane elevation during which the relict coastal feature formed is particularly difficult, given the varying modes of their formation and the erosional processes that often follow their construction (Drzyzga, 2007). Lawson (1981) contended that the elevation measured along the base of any coastal feature does not specifically represent the water level(s) that existed when the feature formed, but instead is the elevation of the shore feature - from which the actual water level may only be *inferred*.

A list of the relict coastal landforms that have commonly been employed by researchers to infer paleolake-level and to mark the boundaries of Pleistocene glacial lakes is provided in Table 2.1. Adjacent to each relict landform is a list of several other indicators and/or proxies that these landforms provide. Table 2.1 also lists a few studies that have used a particular relict coastal landform in order to infer one or more paleocoastal conditions.

Table 2.1: Relict coastal landforms, and a few examples of environmental indicators and proxies, used to infer paleocoastal conditions

| Relict coastal landforms | Potential Indicators and Proxies | References |
|---------------------------------|--|--|
| Beach ridges | Margin of a water body; rate of isostatic rebound; water plane elevation; high lake stand; sediment supply; wave energy and climate; lake-level fluctuations | Leverett and Taylor (1915), Olson (1958a,b), Evenson (1973), Thompson (1988a), Thompson (1992), Larsen (1994), Lichter (1995, 1997), Dott and Mickelson, (1995), Thompson and Baedke (1995, 1997), Petty et al. (1996); Lichter (1998), Baedke et al. (2004), Argyilan et al. (2005), Johnston et al. (2007, 2014), Argyilan et al. (2010) |
| Wave-cut bluffs | Margin of a water body; rate of isostatic rebound; water plane elevation; wave energy and climate; lake-level fluctuations | Leverett and Taylor (1915), Miller (1939), Futyma (1981), Rovey and Borucki (1994), Schaetzel et al. (2002), Fisher (2005, 2007), Drzyzga (2007), Janecke and Oaks (2011), Kor et al. (2012), Drzyzga et al. (2012), Breckenridge (2013) |
| Meltwater spillways | Margin of a water body; rate of isostatic rebound; sediment supply | Leverett and Taylor (1915), Kehew and Lord (1986, 1987), Teller (1987), Lord (1991), Kehew (1993), Baker (1996), Fisher (2003, 2005, 2007), Teller and Leverington (2004), Teller et al. (2005), Kozlowski et al. (2005) |
| Spits | Margin of a water body; dominant wind and longshore current direction; wave energy and climate | Taylor (1892), Leverett (1897), Leverett and Taylor (1915), Chrzastowski and Thompson (1992, 1994), Blair (1999), Krist and Schaetzel (2001), Holcombe et al. (2003), Schofield et al. (2004), Jewell (2007), Schaetzel et al. (under review) |
| Delta morphology | Margin of a water body; rate of isostatic rebound; water plane elevation; high and low lake stand; sediment supply; wave energy and climate; lake-level fluctuations; stability and sediment supply within the catchment | Gilbert (1885, 1890), Leverett and Taylor (1915), Feth (1955) Bissell (1963), Burgis (1977), Milligan and Chan (1998), Milligan and Lemons (1998), Lemons and Chan (1999), Janecke and Oaks (2011), Vader et al. (2012), Gobo et al. (2014) |

2.1.1 Relict Beach Ridges

Beach ridges have long been used as a shoreline indicator and as a proxy for lake-level variability (Leverett and Taylor, 1915; Olson, 1958a,b; Table 1). Beach ridges are small linear and curvilinear ridges, often between 0.5 and 3 m high, parallel to the shoreline, and deposited by wave and/or wind action along the beach (Olson, 1958a; Thompson and Baedke, 1995; Baedke et al., 2004, Johnston et al., 2014). Beach ridges are often deposited in embayments of lakes where there is a positive sediment supply, strong longshore drift, and large amounts of wave and wind energy (Thompson, 1992; Thompson and Baedke, 1995; Baedke et al., 2004). If several beach ridges occur in the same embayment, they form what is known as a ‘strandplain’ (Figure 2.1). The main elements of a beach ridge are the foreshore, upper shoreface, and dune backshore (Figure 2.2; Baedke et al., 2004).

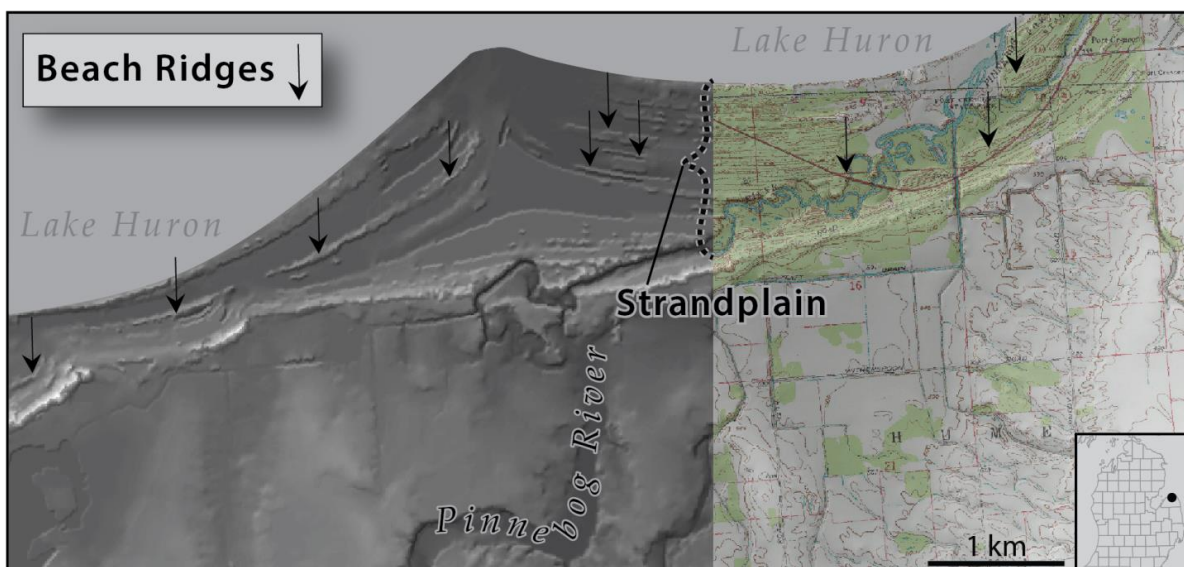


Figure 2.1: A DEM and 7.5' topographic map (5 ft contour interval) illustrating several beach ridges (i.e., a strandplain) on the northern 'thumb' of Lower Michigan, ~10 km west of Port Austin, MI.

A beach ridge initially forms during the *final* stages of a lake-level *rise* (Figure 2.2). The ridge may originally develop as the water plane approaches its highest elevation and as the shoreline undergoes a period of aggradation (Figure 2.2). This aggradation creates a water-lain berm at the crest of the swash zone (Figure 2.2). The berm and associated nearshore sediments form the core of a beach ridge. However, soon after the berm forms, grasses often colonize it and trap wind-blown sediment, producing a dune cap of varying thickness, atop the ridge and

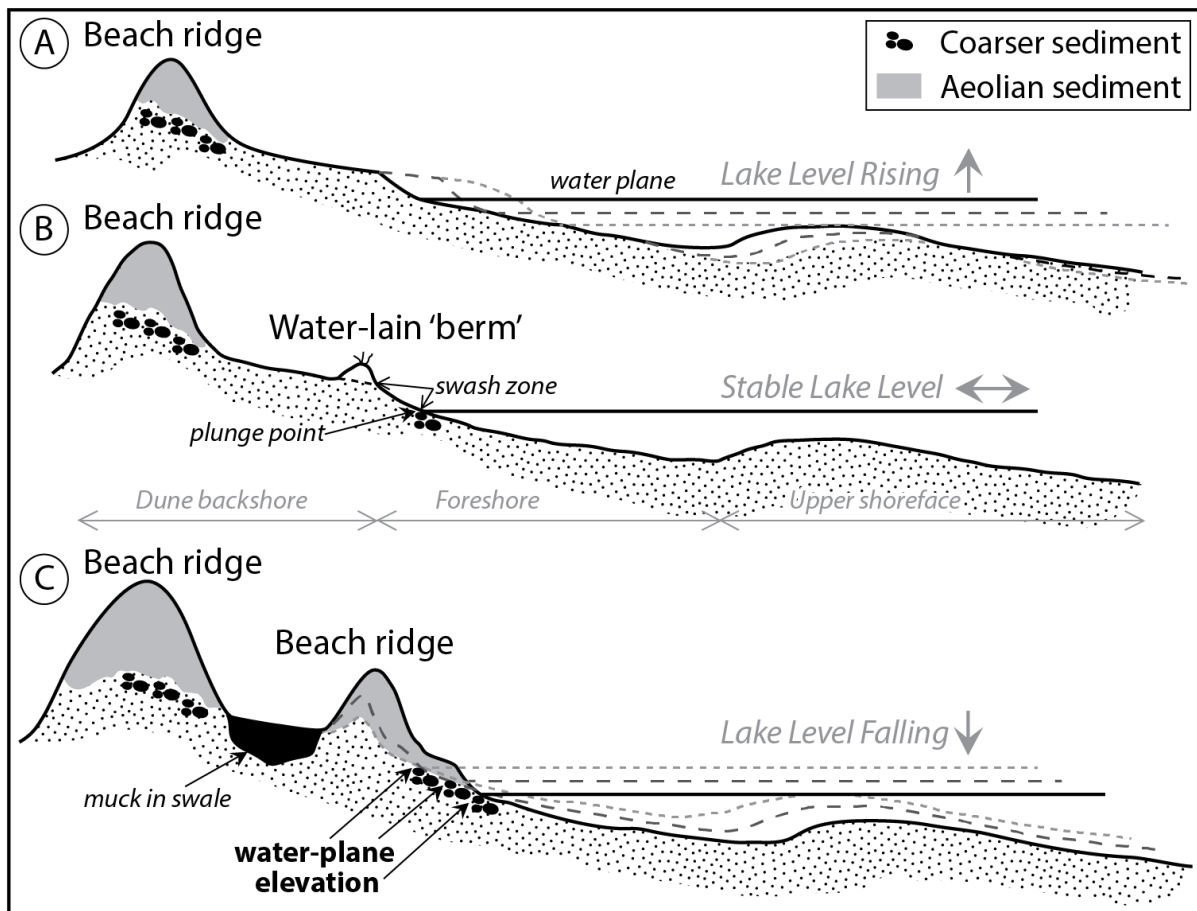


Figure 2.2: Schematic diagram, illustrating the development of a beach ridge (modified from Baedke et al (2004)). (A) During a lake-level rise the shoreline is eroded landward. (B) As the rising lake level slows and eventually stops, a topographic high (known as a 'berm') forms near the top of the swash zone. Onshore transport from shoaling waves and offshore transport from the backwash concentrate the coarsest particle-size fraction near the base of the swash zone. Eventually grasses colonize the berm crest and help trap wind-blown sediments, forming a small dune cap on top of the ridge. (C) With falling lake level, the shoreline progrades lakeward.

parallel to the active shoreline (Thompson, 1992; Baedke et al., 2004). The dune cap grows over time, usually as the water plane elevation lowers and the shoreline progrades lakeward (Figure 2.2; Thompson, 1992).

The foreshore environment incorporates the swash zone area. Here, waves break and force water up (swash) the shoreface (Figure 2.2). The foreshore, or swash zone, sediments are often the coarsest and commonly the most poorly sorted part of the coastal system (Fraser et al., 1991). The swash zone sediment often consists of medium-grained sand to granular sand with pebbles and cobbles, depending on the source of sediment (Baedke et al., 2004).

Backwash from shoaling waves often concentrates the largest particle-size fractions near the base of the swash zone (Figure 2.2). This coarse-grained deposit, near the plunge-point, is often interpreted to mark the still-water elevation of the water body when the beach ridge formed (Figure 2.2; Fraser et al., 1991; Thompson, 1992; Thompson and Baedke, 1995; Schaetzl et al., 2002; Baedke et al., 2004; Drzyzga, 2007; Drzyzga et al., 2012; Johnston et al., 2014).

To summarize, a beach ridge is a depositional feature that consists of both beach and berm sediments, which can eventually become capped with eolian sand as the lake-level elevation lowers and as the shoreline progrades (Olson, 1958a; Thompson, 1992; Figure 2.2). Although the surface expression of beach ridges is often the ridge or dune, many researchers (see Table 2.1) use the water-lain sediment near the core of a beach ridge to serve as the best proxy for the water plane elevation when the ridge formed (Thompson, 1992). Thompson (1988a, 1992) cored the dune caps of beach ridges to penetrate to the underlying foreshore deposits; the elevation of the coarse-grained foreshore sediment below was used to determine the lake-level from which the elevation of the lake prior to shore progradation (Lichter, 1994).

Foreshore sediments in beach ridges can be identified by particle size analysis; they exhibit decreased sorting, when compared to the overlying eolian facies, as well as by mm- to cm-scale lakeward-dipping laminae (Thompson, 1992; Thompson and Baedke, 1997; Baedke et al., 2004; Argyilan et al., 2005). This approach has been applied by others in the upper Great Lakes region for reconstructing lake-level histories (e.g., Dott and Mickelson, 1995; Thompson and Baedke, 1995, 1997; Lichter, 1998; Baedke et al., 2004; Argyilan et al., 2005; Johnston et al., 2007; Argyilan et al., 2010; Johnston et al., 2014).

In addition to interpreting lake-level elevation, both the organic materials that accumulate in low, wet areas between the beach ridges (Figure 2.2) and the (usually) sandy sediments that form the ridges may be dated, by radiocarbon and luminescence methods, respectively (see below), in order to determine the approximate age of the ridge (Thompson, 1992; Thompson and Baedke, 1995; 1997; Lichter, 1995; 1998; Baedke and Thompson, 2000; Argyilan et al., 2005). As such, Beach ridges are thought to provide one of the best geomorphic records of paleo lake level (Thompson, 1992; Thompson and Baedke, 1995, 1997; Lichter, 1998; Baedke et al., 2004; Argyilan et al., 2005; Johnston et al., 2007; Argyilan et al., 2010; Johnston et al., 2014).

The original approach to estimating the age of a beach ridge was to date the base of organic deposits and wood in the swales between ridges using radiocarbon dating methods. The radiocarbon ages provide a minimum limiting age for the ridge that formed immediately lakeward of the corresponding inter-ridge swale or wetland. A relatively recent approach to dating beach ridges is to date the eolian sands (if present) on top of the ridge. This technique, optically-stimulated luminescence (OSL), is an advantageous approach because it provides

discrete, absolute ages for quartz sand grains from littoral and eolian depositional sequences within the ridge. Recent advance in OSL dating approaches (i.e., single-aliquot regeneration (SAR)) yields ages in agreement with ^{14}C control spanning the past 5000 years (Argyilan et al., 2005). Argyilan et al. (2005) contended that samples analyzed by luminescence dating from the foreshore facies of individual beach ridges can also provide accurate ages for strandline sequences that span the past ≈ 4500 years.

There are, however, a few limitations when employing beach ridges for recording the paleolake-level history. For example, beach ridges provide evidence for lake-level lowering from a high stand (Olson, 1958). And unless the shoreline receives a substantial amount of sediment from longshore drift, or the lake level drops, the beach ridge will be eroded during succeeding higher lake levels (Baedke et al., 2004). Beach ridges are therefore mostly limited to recording a consistently lowering lake-level during the late Holocene (ca 4500 yrs) (Argyilan et al., 2005; Johnston et al., 2014). Additionally, when using radiocarbon to estimate the age of a beach ridge, an assumption must be made that the wetland was established and began accumulating organic material immediately after the lakeward beach ridge formed. Consequently, Lichter (1997) concluded that there may be considerable uncertainty in the timing between beach ridge establishment and the accumulation of organic matter in swales or wetland environments between them. Moreover, Lichter (1995) discussed how there is a large potential for organics of *various ages* to accumulate within the swales between beach ridges. Larsen (1994) highlighted this issue when illustrating how some strandplains adjacent to Lake Michigan show an unclear relationship between the age of basal peats and ridge distance from the present shoreline. Lastly, Larsen (1994) discussed how radiocarbon ages from beach ridge organics often cluster,

indicating that peat deposits mainly formed during a particular interval after the development of a strandplain, rather than immediately after a swale developed between two beach ridges. In this situation, the synchronous formation of peat within a strandplain perhaps reflects changes in local hydrology instead of fluctuations in lake level.

There are also a few inconsistencies within the literature regarding the methods used in estimating the paleo-water plane elevation from a beach ridge. For example, Evenson (1973) interpreted the shoreline elevation using the highest contour elevation along the beach ridge. Conversely, Larsen (1994) estimated the water plane elevation from beach ridges by recording the contour elevation where he thought the largest break in slope occurred between the upper foreshore zone and the overlying dune sediment. Thompson (1992) argued that, in order to infer an accurate water plane elevation from a beach ridge, the elevation of the basal foreshore sediments must be identified (Figure 2.2). The base of the foreshore is thought to occur at the position where waves break (plunge point), forcing water up the beach face, thereby separating the upper shoreface (finer sediment) from the exposed foreshore (coarser sediment) (Thompson, 1992; Thompson and Baedke, 1997; Baedke et al., 2004; Argyilan et al., 2005; Johnston et al., 2007). Thompson (1992) contended that because foreshore sediments form *at* lake-level, they create a stratigraphic marker for the elevation of the lake at the time of deposition (Figure 2.2). Use of coarse foreshore sediments as a proxy for lake level has been the prevailing method in recording detailed estimates of paleolake-level elevation within the Great Lakes region (Schaetzl et al., 2002). The papers discussed above illustrate a few of the different techniques and inconsistencies in reconstructing the lake-level history using relict beach ridges,

which should be considered when combining paleolake-level measurements from different studies.

2.1.2 Wave-cut Bluffs

Unlike a beach ridge, a wave-cut bluff is largely an erosional feature. Miller (1939) contended that wave-cut bluffs are one of the best proxy indicators of former sea levels. A wave-cut bluff begins to form due to headward erosion of the land surface by shoaling waves (Dietz and Menard, 1951). Rovey and Borucki (1994) modeled erosion rates of wave-cut bluffs along the western shores of Lake Michigan. They concluded that wave-cut bluffs form near the original shoreline elevation as wave scour erodes a near-horizontal plane into the sloping land surface (Figure 2.3). As this erosional surface or bench widens, a notch is cut into the land surface (Figure 2.3). If the eroding materials are cohesive, this notch eventually grows inland and forms a hollow area with an opening, near the base of the bluff. Any overhanging part of the bluff eventually can collapse into the shoreline, leaving a relatively steep bluff behind (Figure 2.3; Dietz and Menard, 1951). Therefore, the best proxy for the original shoreline position is the inflection point where the bottom abruptly steepens (Dietz and Menard, 1951; Rovey and Borucki, 1994; Figure 2.4).

Several studies within the Great Lakes region have used what appear to be wave-cut bluffs as evidence of paleoshoreline locations (e.g., Spencer, 1891; Goldthwait, 1908; Leverett and Tylor, 1915; Karrow et al., 1975; Fullerton, 1980; Futyma, 1981; Schaetzl et al., 2002; Drzyzga, 2007; Drzyzga et al., 2012; Figure 2.4). However, very few studies have exclusively used wave-cut bluffs to record the water plane *elevation* of a paleolake (cf. Breckenridge, 2013). Although Fisher (2005) did not solely use wave-cut bluffs or escarpments, he did discuss

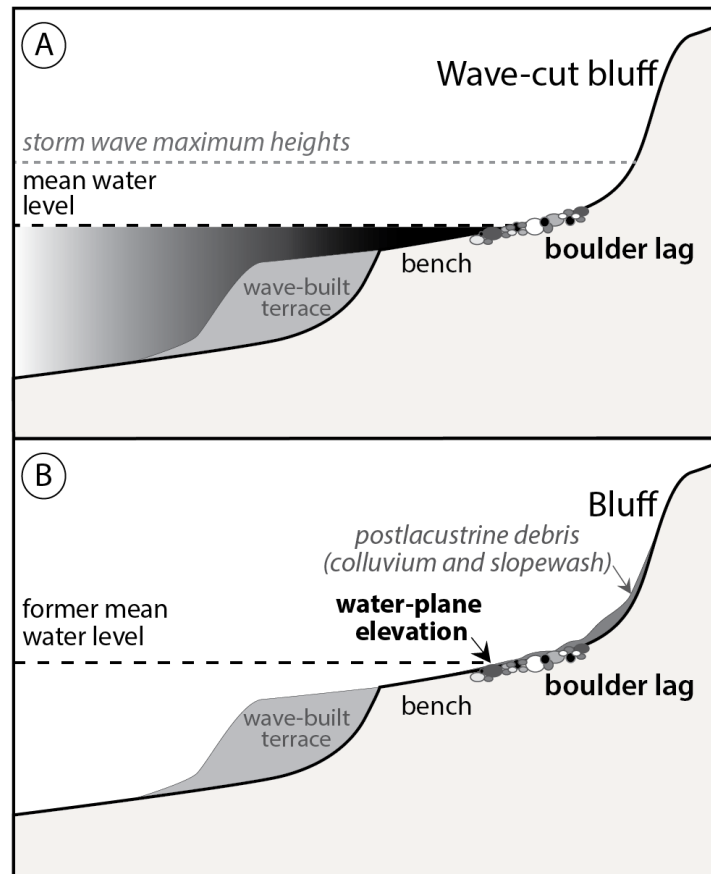


Figure 2.3: (A) Schematic diagram of a modern wave-cut bluff during formation, showing mean water level and coarse lag deposit. (B) Diagram of the wave-cut bluff after lake recession and illustrating where to measure the former mean water plane elevation (modified from Schaetzl et al. (2002)).

the methods used to estimate paleo-water planes from these features. He noted how Thompson (1992) used foreshore gravels from vibracores in the proximal edge of beach ridges in order to identify late Holocene water plane elevations near Lake Michigan. Because Thompson (1992) found that foreshore gravel was overlain by as much as 6 m of washover and eolian sand, Fisher (2005) suggested using the lowest contour elevation along the base of escarpments, spits, and beach ridges (break in slope, or point of maximal slope inflection) for

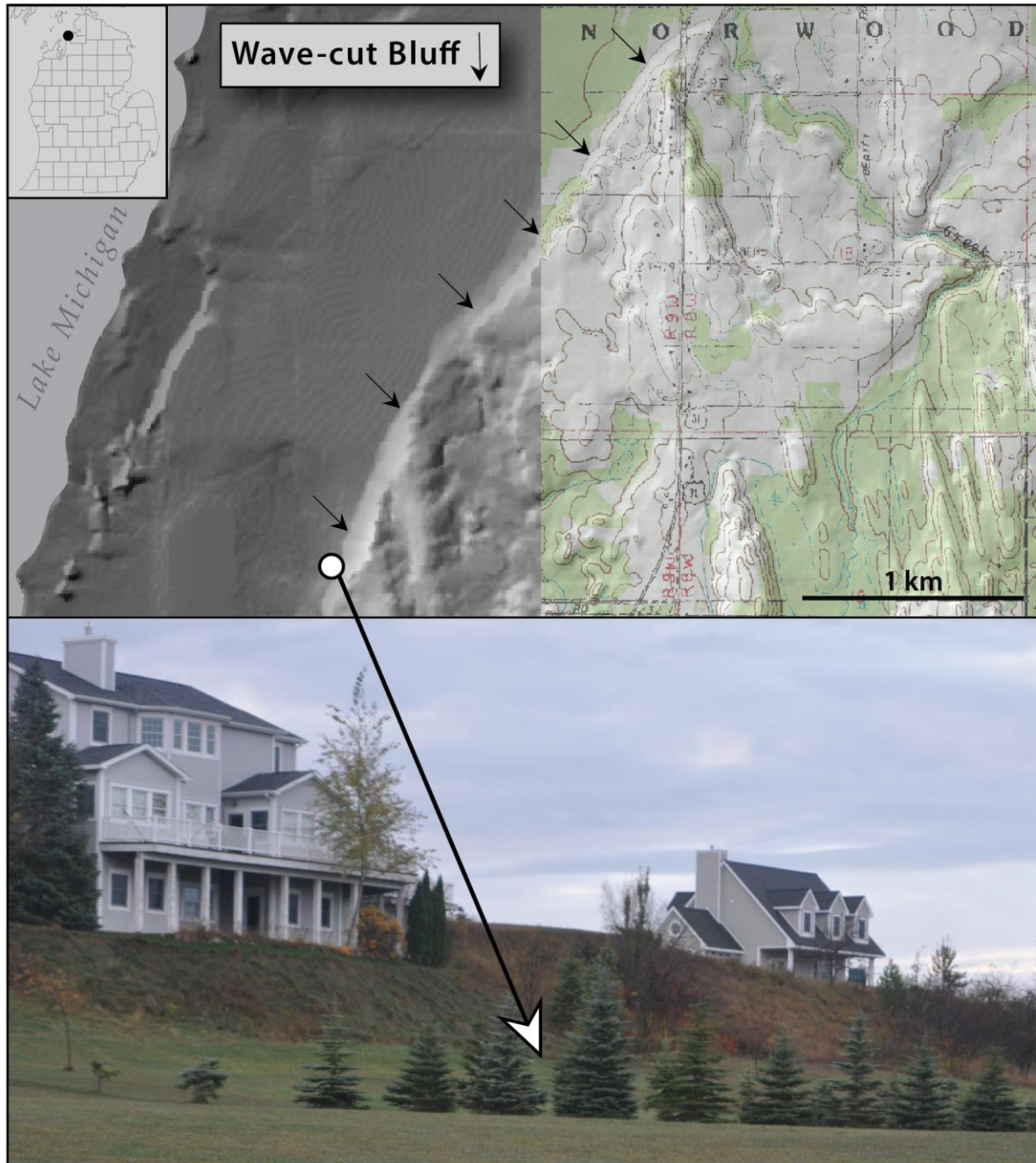


Figure 2.4: A DEM and 7.5' topographic map (5 m contour interval) illustrating a relict wave-cut bluff associated with Glacial Lake Algonquin, in northwestern Lower Michigan , ≈10 km southwest of Charlevoix, MI.

estimating paleo–water planes, rather than the contour elevation near the crest of escarpments.

Schaetzl et al. (2002) developed a relatively robust approach to identifying the water plane elevation from wave-cut bluffs. Schaetzl et al. (2002) and Drzyzga et al. (2012) found that a boulder/gravelly lag often occurs near the surface of wave-built terraces or benches that regularly form just below the base of wave-cut bluffs in northern Michigan. These particular wave-cut bluffs are associated with the late Pleistocene, Glacial Lake Algonquin shoreline. Schaetzl et al. (2002) noted that several of the Lake Algonquin, wave-cut bluffs have accumulated up to 2+ m of detritus (i.e., slopewash and colluvium) at their base. Therefore, they suggest coring to the coarse lag deposit, near the bluff inflection point, and measuring the depth to the lag deposit, in order to best estimate the level of the former water plane. Furthermore, a GPS unit with sub meter accuracy is necessary, in order to obtain an accurate elevation reading for the base of the bluff. Schaetzl et al. (2002) argued that the most creditable *mean* water plane elevation, interpreted from a wave-cut bluff, is the depth of the boulder lag, minus the elevation at the surface near the base of the bluff (Figure 2.3; Drzyzga et al., 2012).

One source of error that may arise when applying the methods discussed by Schaetzl et al. (2002) for estimating former water planes involves interpreting the inflection point of a lag deposit that is several meters wide and buried by colluvium. Schaetzl et al. (2002) noted that although the location of the lag deposit may not be as accurate as one from a relatively undisturbed wave-cut bluff (i.e., absent of colluvial fill), the error associated with each colluvial fill estimate is often not more than ± 2 m. This amount of error is arguably more accurate than

interpreting the water plane elevation exclusively from a topographic map or digital elevation model (DEM). The amount of error suggested by Schaetzl et al. (2002) is also less than many *depositional* landforms proxies, such as spits and bars, which Thompson et al. (1988b) suggested may permit as much as ± 5 m of variation in estimates of the water plane elevation.

2.1.3 Meltwater Spillways

All of the proglacial lakes that developed in front of the Laurentide ice sheet drained through one or more spillways (Kehew and Lord, 1986; Teller, 1987; Lord, 1991; Kehew, 1993; Fisher, 2007; Teller, 2002; Teller et al., 2005; Kozlowski et al., 2005). Meltwater spillways often display the morphologic characteristics of fluvial channels and generally consist of deeply incised inner channels that are flanked by broad, scoured outer zones and terraces (Kehew and Lord, 1986; Figure 2.5). Kehew and Lord (1986) contended that the origins of many of the meltwater spillways in North America are attributed to one or more catastrophic, high-discharge, outburst floods. After geomorphic analysis of several spillways in the northern Great Plains of North America, Kehew and Lord (1986) developed a generalized model for the development of mid-continent glacial lake spillways (Figure 2.6). In this model there are two basic spillway levels: the inner channel and the outer zone (Figure 2.6). The inner channel has the characteristic, trench-like-shape and often meanders. However, the sinuosity is commonly low (Kehew and Lord, 1986; Figure 2.6).

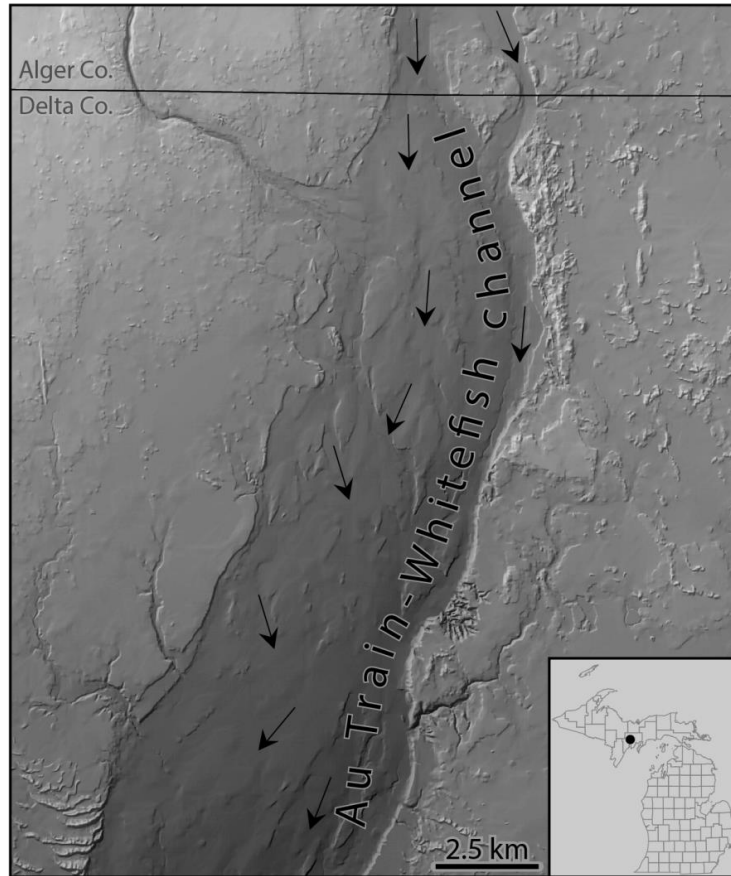


Figure 2.5: A DEM of a large, relict spillway that includes several fluvial landforms located in the central Upper Peninsula between Au Train and Rapid River, MI.

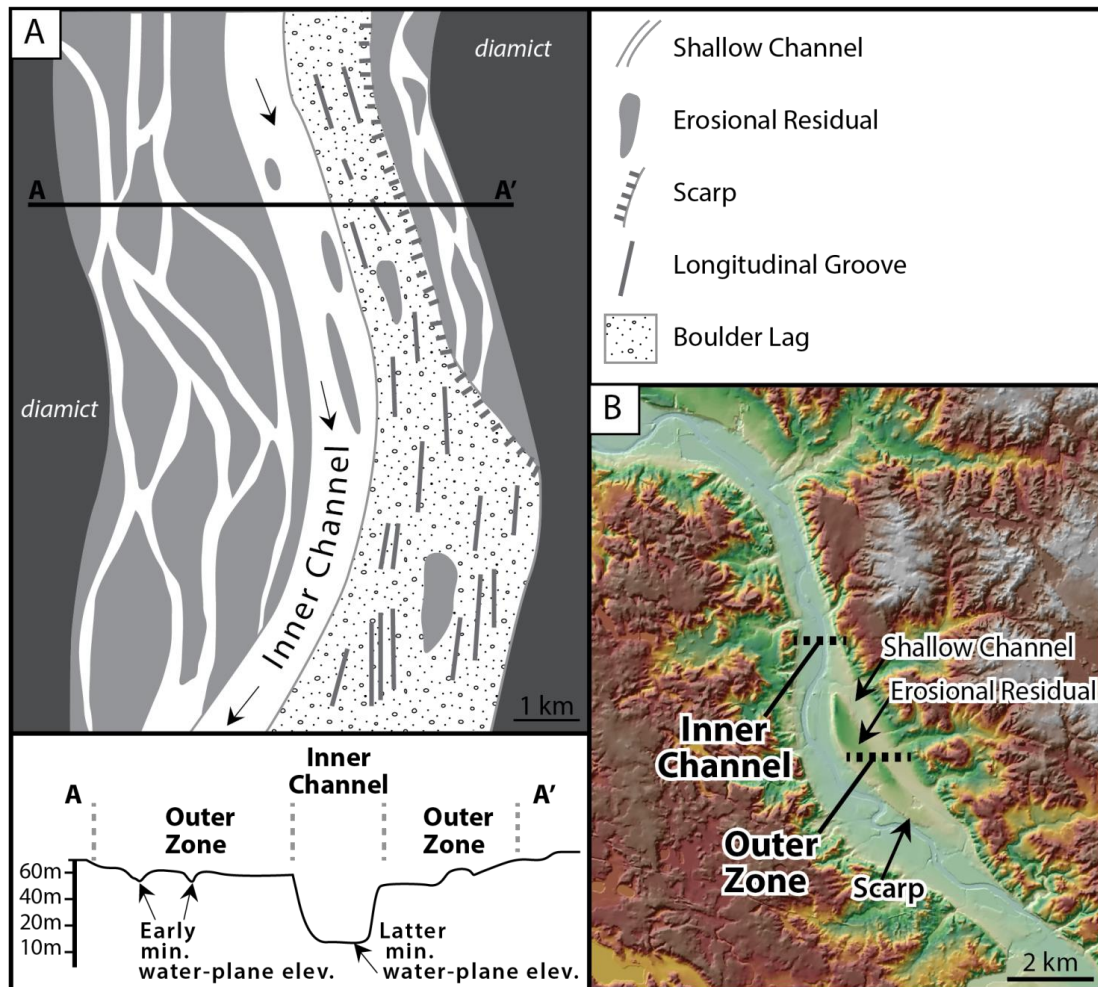


Figure 2.6: (A) An illustration of the components associated with a typical, relict glacial lake spillway (modified from Kehew and Lord (1986)). (B) A section of the glacial Grand River Valley, ≈20 km east of Grand Rapids, MI, and labeling a few relict features related to the spillway.

Conversely, the spillway's outer zones often consist of broad surfaces that flank the inner channel(s) and include a variety of erosional features produced by flood waters. Spillways that lack an outer zone suggest that the existing valleys were able to convey large discharges of water, or that stagnant ice bounded the inner channel during maximum discharge. Kehew and Lord (1986) subdivided the outer zone into two transitional types of topography: (1) slightly scoured areas where shallow, anastomosing channels predominate and (2) deeply scoured areas where longitudinal grooves and well-developed boulder-lag deposits predominate (Figure 2.6). In some places, a scarp that may be several meters high creates two subdivisions of the outer zone (Figure 2.6). Kehew (1982) postulated that the outer zone represents the initial channel scoured by floodwater draining from a glacial lake, where a valley was unable to contain the flow of water. Eventually the broad, shallow, outer-zone channels became ineffective drainageways due to the relatively large wetted perimeter associated with the channels. Thus, conversion to a small wetted perimeter is induced by the widening and deepening of one of the centrally located, longitudinal grooves (Figure 2.6). To summarize, the initial stages of meltwater flow produces shallow, anastomosing channels and continued erosion produces longitudinal grooves, streamline erosional residuals, and surficial boulder-lag deposits. Subsequently, an inner channel develops by the enlargement of one or more centrally located, longitudinal grooves.

J.T. Teller and T.G. Fisher have published several studies regarding outlets and spillways associated Lake Agassiz during the late-Pleistocene (e.g., Teller, 1987; Fisher, 2003, 2005, 2007; Teller and Leverington, 2004; Teller et al., 2005). These studies often focus on when certain spillways were active/open. Their methods generally include coring the outer zones and inner

channels of spillways to obtain basal organics from the floor of the channels, as well as elevation readings near the base of the spillway (e.g., Fisher, 2005; Teller, 2005). The basal organics in the cores are a minimum-limiting age for the time when water stopped flowing through the spillway. These studies also assume that the contact between organic and inorganic sediments marks the elevation of the channel floor, which would provide a minimum water plane elevation for the spillway (Figure 2.6). Therefore, spillways may be analyzed in conjunction with other shoreline features (i.e., spits, escarpments, and beach ridges) in order to estimate the water plane elevation when the spillway was active (e.g., Fisher, 2005; Teller, 2005). In brief, the elevation near the floor of a spillway, which is often the contact between organic and inorganic sediments, is a minimum water plane elevation for the paleolake, and should primarily be used to mark the elevation where that lake level could have potentially 'spilled-over'. Furthermore, an elevation reading from a channel floor in the outer zone of a spillway likely reflects an earlier 'spill-over' elevation, whereas an elevation at the bottom of an inner channel imitates an elevation after an extended period of time from when the spillway was initially active (Figure 2.6).

2.1.4 Relict Spits

The term 'spit' has been formally defined as "a ridge or embankment of sediment attached at one end and terminating in open water at the other" (Evans, 1942; Schofield et al., 2004). Spits form as a result of longshore sediment transport from waves obliquely approaching a shoreline (Gilbert, 1890; Evans, 1942; Schofield et al., 2004; Jewell, 2007). Within my study area, spits are common and range in size (between < 1 to > 20 km). They are mostly composed of well-sorted, stratified, sand and gravel (Chrzastowski and Thompson, 1992; Krist and

Schaetzl, 2001; Schofield et al., 2004; Jewell, 2007; Vader et al., 2012). In the past, relict spits have served as a shoreline indicator and as evidence for a particular lake stage/phase within a region (e.g., Taylor, 1892; Leverett, 1897; Leverett and Taylor, 1915; Chrzastowski and Thompson, 1992; 1994, Krist and Schaetzl, 2001; Schaetzl et al., under review; Table 2.1). Similar to relict meltwater spillways, relict spits have seldom been used to record a relatively precise paleo-water plane elevation. Instead, lake level elevations are often indirectly applied to spits by measuring their overall range in elevation and then assigned a lake level elevation that relates to the lake stage/phase that falls within the spits elevation range. For example, Chrzastowski and Thompson (1992, 1994) used USGS 7.5' topographic maps to analyze several relict spits along the southern shores of Lake Michigan. These authors used the *crest* elevation of the spits to assign certain spits to a specific lake phase and then lake level elevation during the late Pleistocene within the Lake Michigan basin.

More commonly, orientations of relict spits have been used as a proxy for paleo-wind and -longshore drift direction in a region (e.g., Krist and Schaetzl, 2001; Holcombe et al., 2003; Schofield et al., 2004; Jewell, 2007; Vader et al., 2012; Schaetzl et al., under review). Spits are predominantly formed under strong and/or persistent wave action, and because wind duration and intensity are equal to the amplitude and energy of waves (CERC, 1984) they are one of the best sources of paleowind direction (Schofield et al., 2004; Jewell, 2007). For example, Figure 2.7 is a map of a > 20 km long relic spit in the Upper Peninsula of Michigan. The orientations of the topographic and sedimentologic features that are associated with the spit provide evidence for predominantly north-northeasterly winds when the spit formed (Figure 2.7). Furthermore, the elevation of the geomorphic features associated with the spit suggests that the spit formed

in glacial Lake Algonquin, which was present between ca. 13.2 and 11.5 cal ka BP (Drzyzga, 2007; Drzyzga et al., 2012; Blewett et al., 2014)(Figure 2.7). Note that several wave-cut bluffs that decrease in elevation lakeward often form near the tail end of the spit (e.g., Figure 2.8). In this instance, the elevation near the base of each wave-cut bluff likely represents an estimate of lake level change as the spit formed (Figure 2.8). This is arguably a more precise method to infer a paleo-water plane elevation from a spit, rather than measuring the elevation from the crest of geomorphic features associated with the spit.

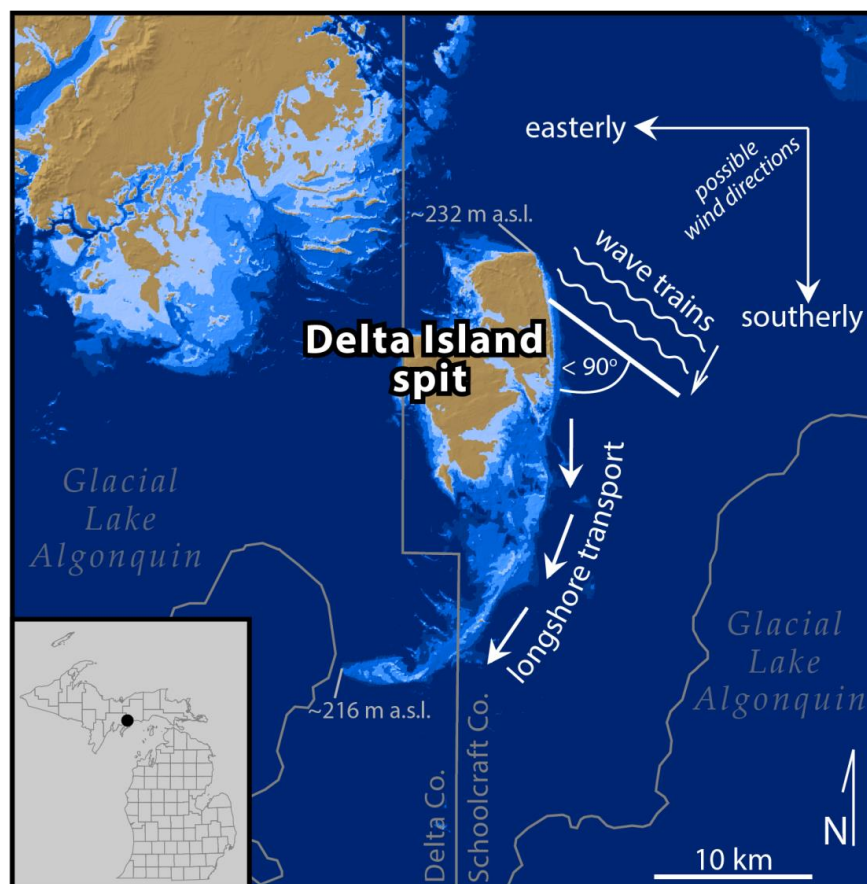


Figure 2.7: A map of the relict Delta Island spit flooded to its paleoshoreline elevation and illustrating the paleoconditions it records as shown by Jewell (2007).

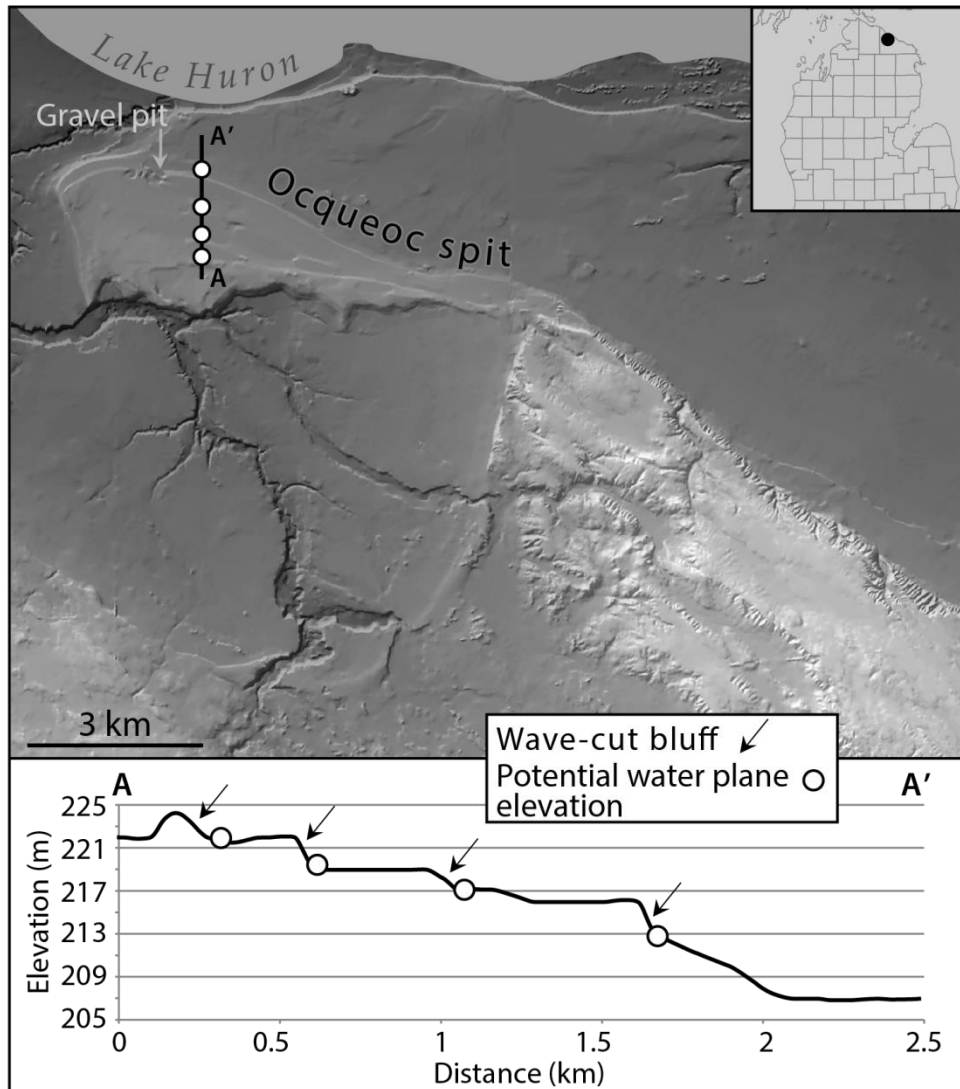


Figure 2.8: A DEM and profile of a relict spit that has subtle wave-cut bluffs near its tail end. The elevation near the base of each wave-cut bluff likely represents the former water plane elevation, implying that the lake level drop was concurrent with spit lengthening and progradation.

To summarize, spits were not used within the study area to assign a relatively precise water plane during the late Pleistocene. However, if wave-cut bluffs appear on the hooked end of a spit, elevations near the bases of the bluffs could be used to record the water plane elevation when that portion of the spit formed (Figure 2.8). Chrzastowski and Thompson (1992, 1994) also suggested that the linearity of certain parts of relict spits may provide evidence for sediment deposition below water. These data may be used to assign certain sections of a spit to high and low lake-level stages, or to establish a minimum-limiting water plane elevation. Nevertheless, relict spits are excellent proxies for paleowind directions and the range in elevations of the components linked to the relict spit enable them to be assigned to certain lake phases. Arguably the size of the relict spit and the sediment characteristics may also provide evidence for the duration and persistence of the wind direction, as well as wind and longshore drift strength.

2.1.5 Relict Deltas

Deltas represent a combination of aerial and subaerial deposits emplaced at the junction between a river and a standing body of water. Deltas form when the amount of sediment being delivered to the mouth of the river is greater than the accommodation space of the nearshore basin. In addition, the rate of deposition at the mouth of the river must exceed the rate at which the newly deposited sediment is transported away from the river mouth by coastal processes (Lyell, 1832; Gilbert, 1885). With time, the continued supply of sediment by a network of fluvial systems results in the progradation of a shoreline and the protuberance of a delta into a body of water.

Similar to relict spits, relict deltas have been employed to mark boundaries of glacial lakes and provide evidence for certain lake phases within the Great Lakes region (e.g., Leverett and Taylor, 1915; Burgis, 1977; Kehew, 1993; Vader et al., 2012; Blewett et al., 2014). Also, like spits, large deltas perhaps point to a relatively long-standing lake stage, given that deltas often form over a longer period of time compared to beach ridges. However, like beach ridges, relict deltas also have the potential to provide a detailed record of the water plane elevation(s) associated with a lake. Coarse-grained (gravelly and sandy) Gilbert-type deltas, which were perhaps most common in Michigan during the Pleistocene (cf. Blewett et al., 2014), are especially known as being good proxies of lake-level elevations (Gilbert, 1890; Milligan and Chan, 1998; Janecke and Oaks; Gobo et al., 2014). Their classic tripartite architecture, which includes a horizontal topset unit of fluvial delta-plain deposits and a steeply inclined foreset unit of subaqueous delta-slope deposits, passing down-dip into a subhorizontal bottomset unit of prodelta deposits, can provide detailed evidence of past lake levels (Gilbert, 1885; Barrell, 1912; Smith and Jol, 1997; Gobo et al., 2014; Figure 2.9). The water plane elevation is often assumed to be near the elevation where topset units intersect with foreset units, often near the brink point, where sediment cascades down the slope of the delta front into deeper water (Bell, 2009; Figure 2.9).

Many studies have examined relict, coarse-grained, Gilbert-type deltas with ground penetrating radar (GPR), in order to construct a three dimensional image of the delta sedimentology (Smith and Jol, 1992; 1997; Milligan and Chan, 1998; Eilertsen et al., 2011). A three dimensional image of a Gilbert-type delta helps to identify its internal structure and mark textural and slope contrasts between sediment sequences. Near horizontal units of sediment

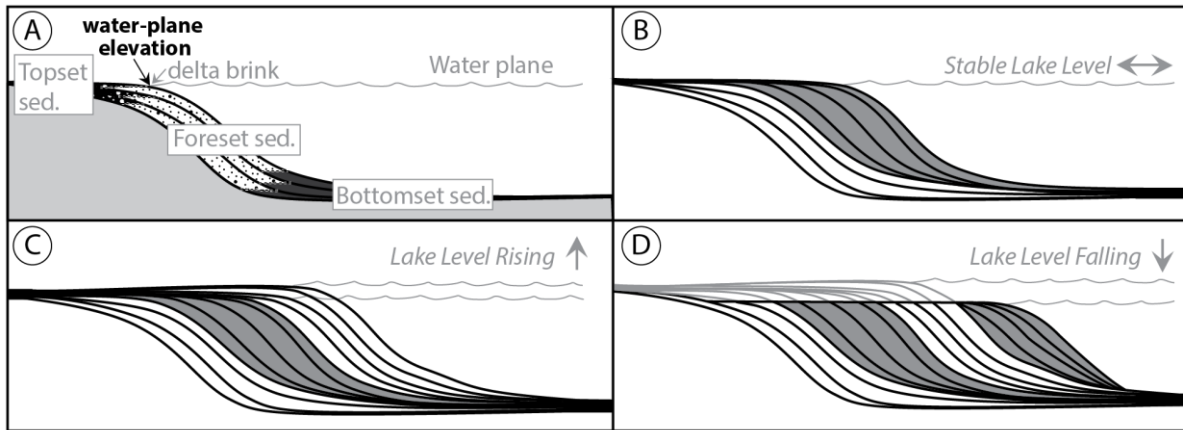


Figure 2.9: (A) Diagram illustrating the position of the different delta sediment (sed.) sequences. (B-D) Schematic showing possible sediment sequences associated with lake level history, without labeling the separate sediments in order to simply the sketch (modified from Milligan and Chan (1998) and Gobo et al. (2014)).

are interpreted to represent topsets beds, deposited under subaerially conditions, whereas relatively steeply dipping units of sediment are interpreted to represent foreset beds, deposited under subaqueous conditions. Hence, the contact between these two units of sediment represents a water plane elevation.

Using those assumptions, a few studies have used two dimensional elevation models (e.g., topographic maps and digital elevation models) to interpret the water plane elevation from a Gilbert type delta (cf. Mangold and Ansan, 2006; Janecke and Oaks, 2011) (Figure 2.10). Those studies that employ digital elevation models and laser illuminated detection and ranging (LIDAR) data simply rely on changes in slope of deposits at the *surface* of the delta, as opposed to changes at *depth*, in order to differentiate between topset and foreset deposits (Figures 2.9 and 2.10). It is important to note that the water plane elevation interpreted from relict deltas using a two dimensional elevation model is solely an estimate of the water plane elevation prior to abandonment of the delta (Figure 2.10). Therefore one must be cognisant that the water

plane may have existed sometime in the past at an elevation above or below the elevation at the current position between the relict delta plain and the relict delta front (Figure 2.10).

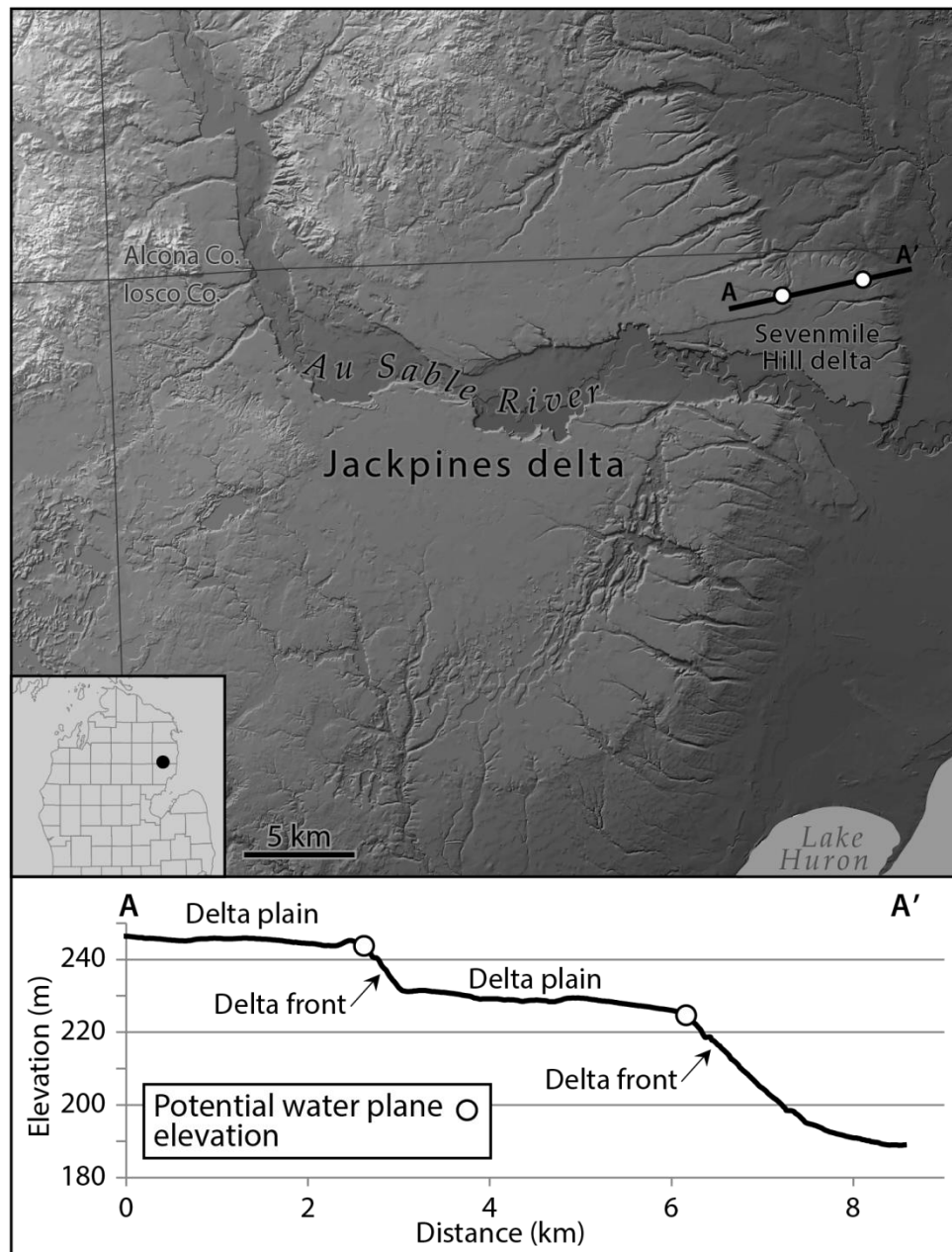


Figure 2.10: A DEM and topographic profile of two relict deltas in northeastern Lower Michigan. The profile of the deltas illustrates the abrupt break in slope between the delta plain and the delta front, which marks a potential water plane elevation prior to the abandonment of the delta.

Currently, the preferred technique for acquiring the most robust subsurface information from a relict delta, in order to record paleo-water plane elevations, is through GPR. However, GPR is relatively expensive and requires considerable time to process the data (Smith and Jol, 1992; 1997; Milligan and Chan, 1998; Eilertsen et al., 2011). Therefore, identifying the transition from topset to bottomset deposits in relict deltas is also sometimes obtained from exposures such as road cuts, or from data obtained from well logs, and the use of open pits from mining operations (Sohn et al., 1997; Breda et al., 2007; 2009; Gobo et al., 2014). Although subsurface information is absent from the most detailed surface elevation models, as more extensive sub-meter elevation models are made available, researchers can focus on studying alternative ways to identify multiple water plane elevations from relict deltas.

Future research within the Great Lakes region should also be expanded beyond simply using relict deltas as a shoreline indicator, but rather to also record paleo-water plane elevations (e.g., Evans and Clark, 2011). For instance, because deltas are the product of a terrestrial system which ultimately flows into a lacustrine/marine system, relict deltas are unique in their ability to help infer both paleoshoreline and paleoterrestrial conditions (Lemons and Chan, 1999; Milligan and Chan, 1998; Janecke and Oaks, 2011; Gobo, 2014). In some instances, a relict delta may record evidence of the paleocoastal environment (e.g., lake-level elevation, wave energy, wind direction, river mouth dynamics, basin subsidence, direction and intensity of longshore currents) as well as paleoenvironmental conditions within the catchment area (e.g., climate, discharge, sediment load, and landscape stability) (Coleman and Wright, 1973; Orton and Reading, 1993; Suter, 1994; Milligan and Chan, 1998; Bhattacharya and Giosan, 2003). An example of using a relict delta to provide both paleoterrestrial and coastal

conditions would be to infer a relatively wet and unstable landscape, with strong and persistent winds/waves along a coastline, from an arcuate-shaped delta. This inference could be made because there must have been enough flowing water in the river to transport sediment to the shoreline, because large amounts of sediment were transported to the river mouth. Further analysis may reconcile that the landscape within the delta catchment area was unstable as a result of being minimally vegetated due to, perhaps, expanses of permafrost. Additionally, during the same period of time, wind and wave energies were perhaps strong and persistent, being that an arcuate-shaped delta is characteristic of a wave-dominated/influenced delta system. Using the geomorphic and sedimentologic characteristics of relict deltas in the Lower Peninsula of Michigan to provide evidence for different paleoenvironmental conditions is highlighted in Chapter 4 of this dissertation. I encourage future studies on the glacial history of the Great Lakes region to examine deltas as proxies, to record the water plane elevations in which they formed and to infer certain terrestrial and coastal conditions during their formative periods.

2.2 Summary and Conclusions

Relict beach ridges, wave-cut bluffs, meltwater spillways, spits, and deltas represent relict coastal landforms that have commonly been used to reconstruct lake-level histories. Several methods exist for estimating paleo-water plane elevation(s) to a moderate to high degree of detail, e.g., relict beach ridges, wave-cut bluff, and deltas, especially if the contact between subaerial and subaqueous components can be identified (Table 2.2). However, to date, methods for identifying the boundary between subaerial and subaqueous constituents of relict meltwater spillways and spits have been minimal. Only the range in elevations linked to

relict meltwater spillways and spits are measured, and therefore, they provide a relatively low amount of detail regarding paleolake-level elevation (Table 2.2).

Table 2.2: A comparison of the different relict coastal landforms commonly used to record paleolake-level elevations, and the relative amount of detail that each provides

| Relict coastal landforms | Detailed record of paleolake-level elevation |
|--------------------------|--|
| Beach ridges | High |
| Wave-cut bluffs | Moderate to High |
| Meltwater spillways | Low |
| Spits | Low to Moderate |
| Deltas | Moderate to High |

Although resource and technological availability are some of the factors that determine which of the above mapping techniques are employed and minimal data are better than none, the precision and accuracy of lake-level estimates (e.g., topo maps with a 10 ft contour interval vs. a GPS unit with sub-meter accuracy) should be considered when estimating paleolake-levels. The literature review that comprises this chapter suggests that relict beach ridges, wave-cut bluffs and deltas may provide highly accurate and detailed records of lake-level elevations during their formative periods (Table 2.2). However in any case, three dimensional maps (i.e., subsurface data) are needed to infer paleo-water plane elevations from relict beach ridges, wave-cut bluffs, meltwater spillways, spits, and deltas. Two dimensional maps of relict deltas merely provide a potential water plane elevation prior to the abandonment of the delta. Because high resolution elevation maps, as well as digital geologic maps, are becoming more readily available, they should be further utilized to determine alternative ways to interpret water plane elevations from beach ridges, wave-cut bluffs, meltwater spillways, spits, and deltas. To conclude, researchers must be aware that paleolake-level reconstructions may differ

depending on both the methods employed and relict coastal feature(s) used to interpret the elevation of the water plane.

Chapter 3 - Relict Pleistocene Deltas in the Lower Peninsula of Michigan

3. Introduction

Deltas form at the junction between a river and a standing body of water when the amount of sediment being delivered to the mouth of the river is greater than the rate at which coastal processes are able to transport the newly deposited sediment away from the river mouth (Lyell, 1832; Galloway, 1975). With time, the continued supply of sediment by one or more fluvial systems results in the formation of a delta and the progradation of a shoreline. The various formation mechanisms and scenarios for deltas have been discussed in Chapter 1.

During the deglaciation of the Great Lakes region, throughout Marine Isotope Stage (MIS) 2, the massive flux of glacial meltwater (cf. Kehew and Lord, 1987; Kehew, 1993; Fisher, 2003; Kozlowski et al., 2005, Kehew et al., 2012) and associated sediment from the ice and ice-free landscapes (cf. Schaetzl et al., 2013a), coupled with the large numbers of pro- and post-glacial lakes that existed across the region, would have led to seemingly ideal conditions for delta formation. However, to date, only a few Quaternary maps of Michigan have identified any such features (Leverett and Taylor, 1915; Martin, 1955), and detailed studies of Michigan's Pleistocene deltas are sparse (Burgis, 1977; Vader et al., 2012). Alternatively, much of the research regarding Michigan's coastal landforms and conditions during pro- and post-glacial lakes stages have focused on relict shorelines features such as beach ridges, meltwater spillways, and wave-cut bluffs. All of these landforms could have formed in a relatively short period of time, and often vary in morphology and elevation over short distances. The few relict Pleistocene deltas that have been mapped (e.g., Leverett and Taylor, 1915; Scherzer, 1916; Bay, 1937, 1938; Martin, 1955; Kunkle, 1963; Burgis, 1977; Vader et al., 2012) were active following

the last glacial maximum and formed in those higher-than-present lake levels. These deltas are now abandoned and left high and dry on the landscape, and often are located several kilometers from the modern day Great Lakes' shorelines. Relict deltas not only record paleoshoreline conditions, such as lake-level elevation, wave energy, wind and longshore drift direction (Coleman and Wright, 1973; Orton and Reading, 1993; Suter, 1994; Bhattacharya and Giosan, 2003; Woodroffe and Saito, 2011), but they also provide evidence for paleoterrestrial conditions within the contributing drainage basins, e.g., runoff, sediment load, and landscape stability (Oldale et al., 1983; Shipp et al., 1991; Barnhardt et al. 1995, 1997; Walker, 1998; Mangold and Ansan, 2006; Bell, 2009; Vader et al., 2012).

The purpose of this study is to inventory and map the relict Pleistocene deltas that formed during the last deglaciation in the Lower Peninsula of Michigan. For each delta identified, I will estimate or correlate the delta's associated lake stage(s); a goal is to assign an age range to its interval of formation. The specific study objectives are to (1) report on the previously studied or mapped Pleistocene deltas in the LP of Michigan, and (2) identify, name, and map any previously unidentified deltas. I then will describe the general distribution of the deltas, as well as their textural and topographic characteristics, and that of their catchment areas. The resulting map of Pleistocene deltas in Southern Michigan will hopefully encourage researchers to implement more thorough and focused studies of these deltas, e.g., via the use of ground penetrating radar, particle size analysis, and/or optically stimulated luminescence dating. Detailed analyses and better knowledge of deltaic processes across the region will aid in our understanding of ice-marginal positions, lake-level history, and terrestrial and coastal conditions during the late Pleistocene.

3.1 Background

When the Laurentide ice sheet (LIS) reached its maximum extent during the late Wisconsin Substage (≈ 21.8 cal ka BP) the entire state of Michigan including the Huron, Erie, and Michigan basins were covered by glacial ice (Farrand and Eschman, 1974; Mickelson et al., 1983; Curry and Petras, 2011). Within the LP, three glacial phases or stadials mark the retreat from the last glacial maximum: the Crown Point-Port Bruce, Port Huron, and Two Rivers-Onaway (Larson, 2011; Figure 3.1). Separating these glacial stadials are three corresponding interstadials: the Erie, Mackinaw, and Two Creeks (Karrow et al., 2000). During the Erie

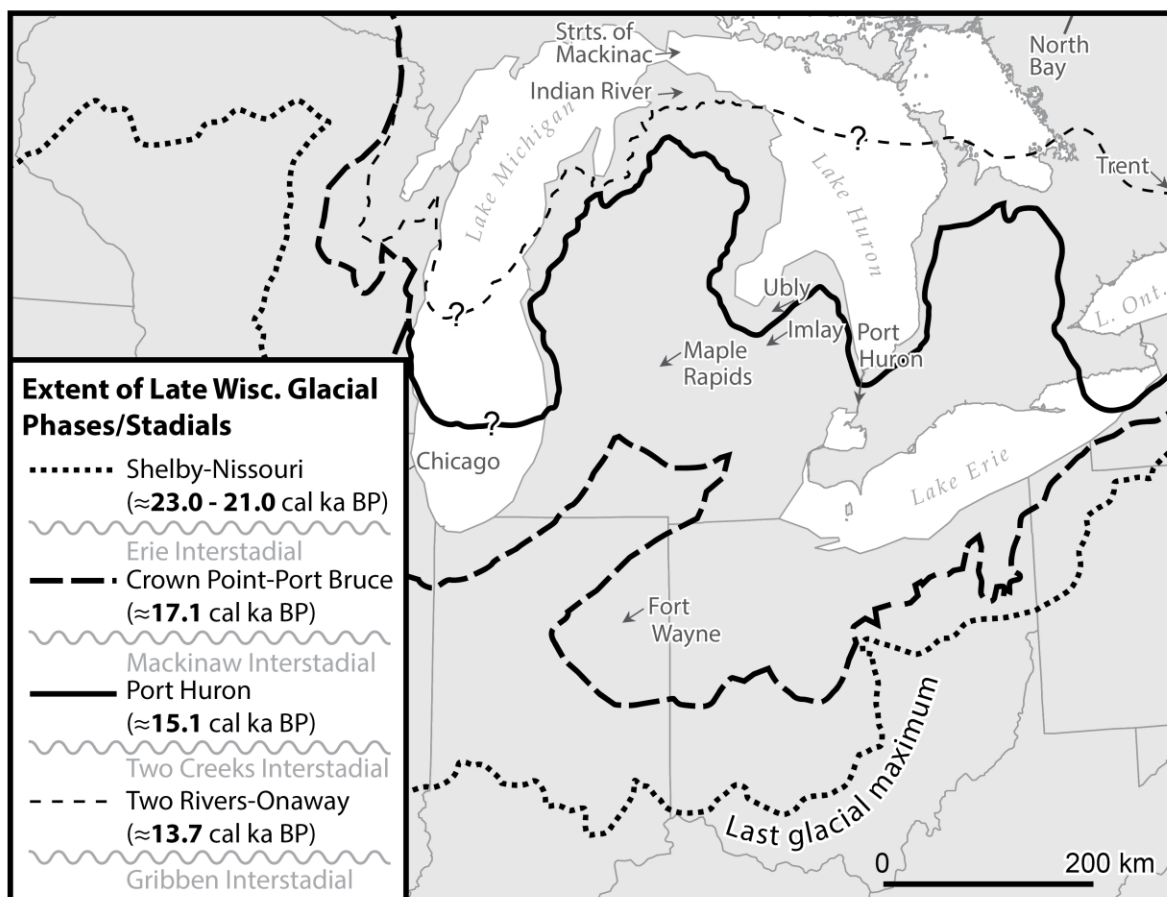


Figure 3.1: Extent of the major glacial phases of the late Wisconsin ice advance, within the Great Lakes region, USA (modified from Larson and Kincade (2009) and Larson (2011)).

interstadial, as the southern margin of the LIS receded from the Shelby-Nissouri Phase limit – the last glacial maximum (Figure 3.1), several proglacial lakes began to form within the Huron, Erie, and Michigan basins between the distal high topography and the retreating ice margin (Leverett and Taylor, 1915; Eschman and Karrow, 1985; Calkin and Feenstra, 1985). After each successive interstadial, the re-advancing ice margin fell short of its previous extent, exposing more of the landmass and the surrounding lake basins for potential delta formation (Figure 3.1). Furthermore, the likely occurrence of permafrost in the region (Johnson, 1990; Clayton et al., 2001; Schaetzl, 2008; Lusch et al., 2009) would have hindered the growth of vegetation and thus, promoted runoff and erosion of the subaerial uplands. Therefore, sediment transport by fluvial systems would have been prevalent, resulting in ideal conditions for delta formation in the many proglacial lakes (Vader et al., 2012).

The waxing and waning of the ice margin also resulted in (1) the opening and closing of different lake outlets, each at a unique elevation (Karrow, 1984), (2) changing rates and patterns of isostatic uplift (Dreimanis, 1977; Baedke and Thompson, 2000; Lewis et al., 2005; Scott et al., 2011), (3) periodic cutting and filling of meltwater spillways (Bretz, 1951, 1955; Kehew, 1993), and (4) fluctuations in the net input of glacial meltwater and precipitation entering the lake basins (Hansel and Mickelson, 1988; Holcombe et al., 2003). This dynamism led to the formation of a number of late Wisconsin lakes in the Great Lakes basins (Leverett and Taylor, 1915; Larson and Schaetzl, 2001). Evidence for these various lakes is generally marked by coastal features, such as bars, spits, wave-cut bluffs or strandlines, beach ridges, and deltas, all of which formed across a range of elevations (e.g., Spencer, 1891; Goldthwait, 1908; Leverett and Taylor, 1915; Bay, 1937; Bretz, 1951, 1953, 1964; Dreimanis, A. 1966; Karrow,

1986; Thompson, 1992; Kehew, 1993; Thompson and Baedke, 1995; Schaetzl et al., 2002; Kincare and Larson, 2009). In the past, researchers have used the elevations of these coastal features to inform about spillways, isostatic rebound, shoreline position, and extent of the pro- and postglacial lakes (and lake stages) that formed in and near the Great Lakes' basins (Gilbert, 1898; Clark et al., 1994; Lewis et al., 2005). Although the majority of the late Wisconsin, or pre-glacial Lake Algonquin, shorelines have been identified and their elevations interpreted across large extents of the *southern* Great Lakes region (i.e., northern Ohio, Indiana, Illinois, Pennsylvania), only a few studies have identified shorelines north of latitude $\approx 42^\circ$ N (Suess, 1954; Goldthwait, 1958; Forsyth, 1959; Totten, 1985; Barnett, 1985).

The complexity and abundance of Pleistocene lakes forced early researchers to assign different lake *phases* to many of the individual lake *stages* (e.g., the Glenwood I and II *phase* of the glacial Lake Chicago *stage*), depending on shoreline elevation and outlet characteristics (Table 3.1). Lake stages that formed within the Erie, Huron, and Michigan basins during the late Wisconsin are listed in chronologic order in Table 3.1 along with their commonly accepted water plain elevation, and their outlet(s).

Table 3.1: Pro- and post-glacial lakes (stages and phases in bold, outlets in italics), elevations (in meters asl), and outlets within the Erie, Huron, and Michigan basins. Compiled from Fullerton (1980), Calkin and Feenstra (1985), Eschman and Karrow (1985), Hansel et al. (1985), Colman et al. (1994), Larson and Schaetzl (2001), and Kincare and Larson (2009)

| Erie basin | Huron basin | Lake Michigan basin |
|---|--|--|
| Shelby-Nissouri Phase/Stadial $\approx 23.0 - 21.0$ cal ka BP | | |
| Erie Interstade | | |
| Leverett (<i>Niagara Escarpment</i>) | ? (<i>Erie basin</i>) | Milwaukee (<i>Mississippi River</i>) |
| Crown Point-Port Bruce Phase/Stadial ≈ 17.1 cal ka BP | | |
| Mackinaw Interstadial | | |
| Maumee I (244) (<i>Wabash River/Fort Wayne</i>) | Ice | Ice |
| Maumee II (232) III (237) (<i>II - ? /III - Imlay Channel and Fort Wayne</i>) | Early Lake Saginaw (225) (<i>Glacial Grand Valley</i>) | Lake Chicago Glenwood I (195) (<i>Chicago Outlet</i>) |
| Arkona (216-212) (<i>Glacial Grand Valley</i>) | Arkona (216-212) (<i>Glacial Grand Valley</i>) | |
| Ypsilanti (<166) (<i>Niagara River</i>) | Post-Arkona Low ? (<i>Trent Lowlands</i>) | Mackinaw Low (<170) (<i>Straits of Mackinac and Indian River Lowlands</i>) |
| Port Huron Phase/Stadial ≈ 15.1 cal ka BP | | |
| Whittlesey (225) (<i>Uby Channel</i>) | Saginaw (212) (<i>Glacial Grand Valley</i>) | Lake Chicago Glenwood II (195) (<i>Chicago Outlet</i>) |
| Two Creeks Interstadial | | |
| Warren I & II (210-199) (<i>Glacial Grand Valley</i>) | Warren I & II (210-199) (<i>Glacial Grand Valley</i>) | Lake Chicago Glenwood II (195) (<i>Chicago Outlet</i>) |
| Wayne (210-199) (<i>Mohawk Valley</i>) | Wayne (210-199) (<i>Mohawk Valley</i>) | |
| Warren III (206-203) (<i>Buffalo, NY/Mohawk Valley</i>) | Warren III (206-203) (<i>Buffalo, NY/Mohawk Valley</i>) | |
| Grassmere (195-189) (<i>Mohawk Valley</i>) | Grassmere (195-189) (<i>Mohawk Valley</i>) | |
| Lundy (195-189) (<i>Mohawk Valley</i>) | Lundy (195-189) (<i>Mohawk Valley</i>) | |
| Early Lake Erie (<159) (<i>Niagara River</i>) | Kirkfield (173) (<i>Kirkfield Outlet/Trent Lowlands</i>) | Two Creeks (170) (<i>Straits of Mackinac</i>) |
| Two Rivers-Onaway Phase/Stadial ≈ 13.7 cal ka BP | | |
| Gribben Interstadial | | |
| Early Lake Erie (<159) (<i>Niagara River</i>) | Huron-Algonquin (184) (<i>Trent Lowlands and Port Huron Outlet(?)</i>) | Calumet (189) (?) |
| | | Toleston (184) (?) |
| | Main Lake Algonquin (184) (<i>Port Huron Outlet</i>) | Main Lake Algonquin (184) (<i>Straits of Mackinac, Indian River Lowlands, and Chicago Outet</i>) |
| | Algonquin (184) (<i>Trent Lowlands and Port Huron Outlet(?)</i>) | Algonquin (184) (<i>Straits of Mackinac, Indian River Lowlands, and Chicago Outet</i>) |

3.2 Methodologies

3.2.1 Data Assembly

Mapping Pleistocene deltas in the LP began by reviewing the literature on the origin and evolution of the Great Lakes (e.g., Leverett and Taylor, 1915; Farrand and Eschman, 1974; Karrow and Calkin, 1985; Larson and Schaetzl, 2001). Each delta mentioned in this literature was marked with a point feature in an ArcMap 10.1 project (© ESRI, Redlands, CA). Martin's (1955) and Farrand and Bell's (1972) Quaternary geology maps were georeferenced and the locations of the Pleistocene deltas and shorelines on those maps digitized within a geographic information system (GIS). In addition, the water well and oil/gas log data for each county in the LP of Michigan, downloaded from the Michigan Geographic Data Library (<http://www.mcgi.state.mi.us/mgdl/?action=meta>), were added to the GIS project. Well data were formatted as point-features, whereas the attribute data were saved in Microsoft Excel. The well log attributes were joined to the well-log locations, to aid in identifying the primary lithology, depth, thickness, and color of the strata for each well. However, in order to more efficiently interpret and describe the subsurface sediments, a graphical depth plot (Appendix A) was created for each well log using the R software package (version 3.1.2 - <http://www.r-project.org/>). An R script, coded specifically for this study (see here: https://www.msu.edu/~luehmann/files_data.html), was used to read in the well-log information for each county and construct a depth plot for every well. The individual depth plots were saved as PDFs. The original point-feature shapefile, developed on a county-by-county basis, was then converted to a peninsula-wide geodatabase and the depth plot images

were joined to the associated well-log point using the “add attachments” tool in ArcGIS. The “HTML Popup” tool in ArcGIS could then be employed to select multiple well points in a region and graphically display the stratigraphy and textural characteristics to depths exceeding 500 ft in some cases (Appendix A).

In addition to the data sets listed above, several of the geographic data layers listed in Schaetzl et al. (2013) were also added to this study’s GIS project. In particular, the Michigan statewide USGS 7.5’ topographic map, the seamless 10 m National Elevation Dataset (NED), digital elevation model (DEM) and hillshade DEM (Gesch, et al., 2002), and the surface and subsurface (C horizon) soils data, derived from the Natural Resource Conservation Service (NRCS) Soil Survey Geographic Database (SSURGO), were added to the layer scheme. In addition to helping identify the locations of the deltas discussed in previous maps and studies, digital GIS data layers on the soil parent material, upper and lower profile soil texture, gravelly soils, and natural soil drainage index layers (Schaetzl et al., 2009; Schaetzl et al., 2013) assisted in recognizing the full extent the deltaic landforms/deposits and in characterizing their drainage basins. The majority of the deltas mentioned in the literature were portrayed using the geospatial data layers mentioned above; I searched for landforms that formed a bulge along a relict shoreline, often with a fan-shaped outline, cf. Vader et al. (2012). Furthermore, many of the deltaic landforms consisted mainly of sandy, well-drained sediments, included one or more paleochannels, had a graded longitudinal profile (i.e., a consistent and predictable profile) down-delta, and were located within (or above) a relatively low relief and poorly drained landscape (i.e., a lake plain). Therefore, in this study, these geospatial characteristics were identified as typical relict delta attributes.

3.2.2 Identifying Additional Deltas

After reviewing > 240 references listed in the “Origin and Evolution of the Great Lakes” by Larson and Schaetzl (2001), in addition to several more recent articles, the deltas discussed in those references were coded into a GIS. Each county in the LP was then carefully scanned for any additional relict deltaic landforms. Previously identified deltas held their original name, whereas each newly found delta was named after the current river/creek, or previously named geologic feature that connects to it, and which was likely associated with the delta during its formation. A Roman numeral was added to the delta name for situations in which multiple deltas had formed from a single fluvial system, as a result of changing lake level elevations. Deltas assigned a Roman numeral were labeled from oldest to youngest (Luehmann et al., 2013). In order to assist in this mapping effort, the statewide 10 m DEM was used to “flood” the landscape at the appropriate elevation where there appeared to be a bulge along a presumably relict shoreline (Figure 3.2). This exercise allowed for a more accurate description of the overall shape and area of a particular delta, and the identification of any additional deltas or subdeltas (Luehmann et al., 2013).

A topographic profile was created for each delta (Appendix B) using a statewide 10 m DEM and the Profile tool in ArcMap. Each profile began near the apex of the delta and ended beyond the delta front, approximately at the start of the prodelta position. Helen Martin’s (1955) “Map of the Surface Formations of the Southern Peninsula of Michigan”, which again was georeferenced within an ArcMap project, was used in combination with the profile information (Appendix B) in order to determine the late Wisconsin shoreline (shown on Martin (1955)) that each delta was graded towards.

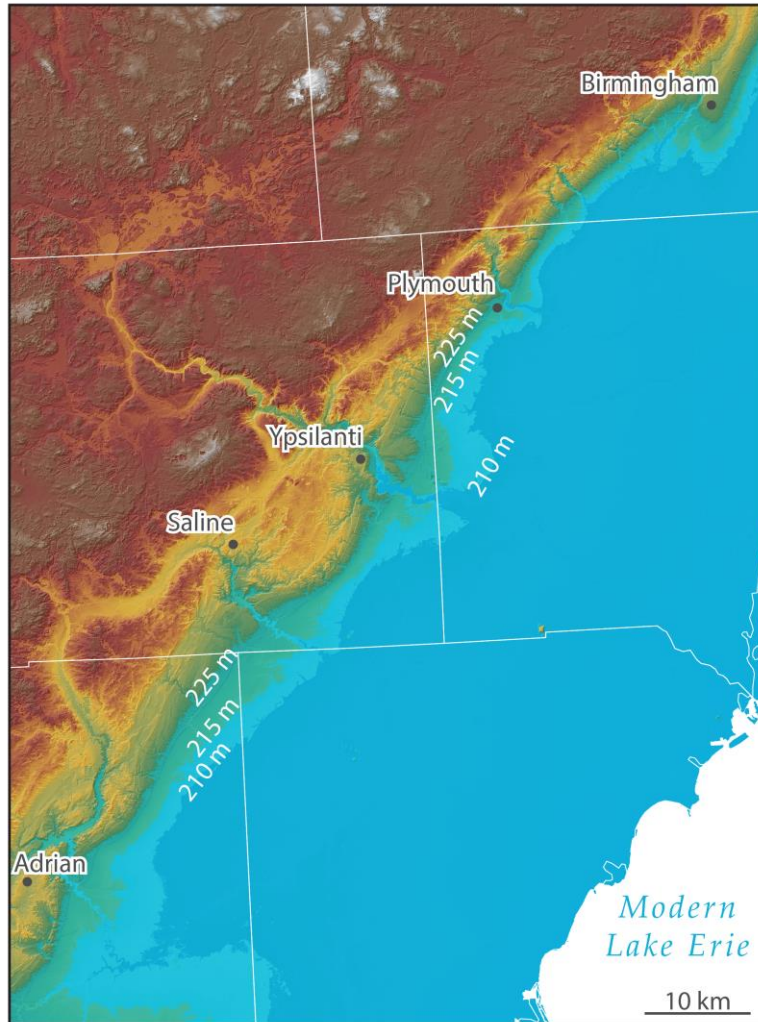


Figure 3.2: Statewide 10 m DEM flooded to the 225, 215, and 210 m levels of Glacial Lake Maumee, in SE Lower Michigan, illustrating bulges along relict shorelines, each showing a relict delta near the following cities: Adrian, Saline, Ypsilanti, Plymouth, and Birmingham.

3.2.3 Delineating Catchment Areas and Quantifying their Characteristics

After the locations of the known and previously unidentified deltas were recorded in the GIS, the catchment area associated with each delta was delineated using the watershed tool within the hydrology tool set in ArcToolbox (© ESRI, Redlands, CA). The estimated catchment area for each delta was conceptualized as the landscape extent that could have potentially contributed sediment to the delta during its formation period. The Michigan statewide, 10 m

NED DEM was employed for calculating the catchment area in ArcGIS. Each delta's "pour point" or "pour line", which is the reference for the Watershed tool to calculate areas that presently drain to them, was digitized into the DEM at the junction between the relict shoreline and the apex of the delta. The same 10 m DEM was then also used to determine the mean and median slope gradient (in %), within a 3 x 3 cell neighborhood, throughout each catchment. These slope values were used as a quantitative measure of the degree of topographic variation, slope steepness, and relief within each of the catchments.

After the extent of each catchment was determined, two methods were adapted to quantify their soil-textural character. The first approach quantifies the dominant upper-profile and subsurface (lowest described horizon) soil textural class identified from the NRCS SSURGO, county-level soil maps, which were converted from digital vector files to a statewide 30 m raster grid (Schaetzl et al., 2013). The second method, which also uses the SSURGO data, assigns the percentage of sand, silt, and clay in each of the soils mapped in the catchments, depending on their upper and subsoil textural classes (Table 3.2). The latter method follows Miller and White's (1998) approach; it determines the amount of the various grain-size fractions by taking the values of sand, silt, and clay at the midpoint of each polygon that delimits a textural class on the United States Department of Agriculture (USDA) soil textural triangle (Table 3.2). The SSURGO textural classes are a combination of the standard 12 USDA textural classes. Those textural classes with a textural modifier (e.g., stony, cobbly, gravelly, coarse, fine, very fine, etc. were assigned to the textural class without consideration of the modifier (Table 3.2).

Table 3.2: Values for sand, silt, and clay assigned to each SSURGO soil textural class (Miller and White, 1998)

| SSURGO Soil Textural Class | USDA Textural Triangle Class | % Sand | % Silt | % Clay |
|-------------------------------|---------------------------------|--------|--------|--------|
| Clay | Clay | 22 | 20 | 58 |
| Silty clay | Silty clay | 6 | 47 | 47 |
| Clay loam | Clay loam | 32 | 34 | 34 |
| Silty clay loam | Silty clay loam | 10 | 56 | 34 |
| Sandy clay loam | Sandy clay loam | 58 | 15 | 27 |
| Loam | Loam | 43 | 39 | 18 |
| Silt loam | Silt loam | 17 | 70 | 13 |
| Stony silt loam | Silt loam | 17 | 70 | 13 |
| Cobbly silt loam | Silt loam | 17 | 70 | 13 |
| Very fine sandy loam | Sandy loam | 58 | 32 | 10 |
| Fine sandy loam | Sandy loam | 58 | 32 | 10 |
| Sandy loam | Sandy loam | 58 | 32 | 10 |
| Loamy very fine sand | Loamy sand | 82 | 12 | 6 |
| Loamy fine sand | Loamy sand | 82 | 12 | 6 |
| Loamy sand | Loamy sand | 82 | 12 | 6 |
| Loamy coarse sand | Loamy sand | 82 | 12 | 6 |
| Coarse loamy sand | Loamy sand | 82 | 12 | 6 |
| Silt | Silt | 10 | 85 | 5 |
| Very fine sand | Sand | 92 | 5 | 3 |
| Sand | Sand | 92 | 5 | 3 |
| Fine sand | Sand | 92 | 5 | 3 |
| Coarse sand | Sand | 92 | 5 | 3 |
| Gravelly sand | Sand | 92 | 5 | 3 |
| Marl | NA | 0 | 0 | 0 |
| Muck | NA | 0 | 0 | 0 |

3.3 Results and Discussion

3.3.1 Distribution of deltas

This mapping exercise identified 61 relict Pleistocene deltas in Lower Michigan (Figure 3.3; Table 3.3). Of these, 27 had been acknowledged in previous works, whereas 34 deltas are

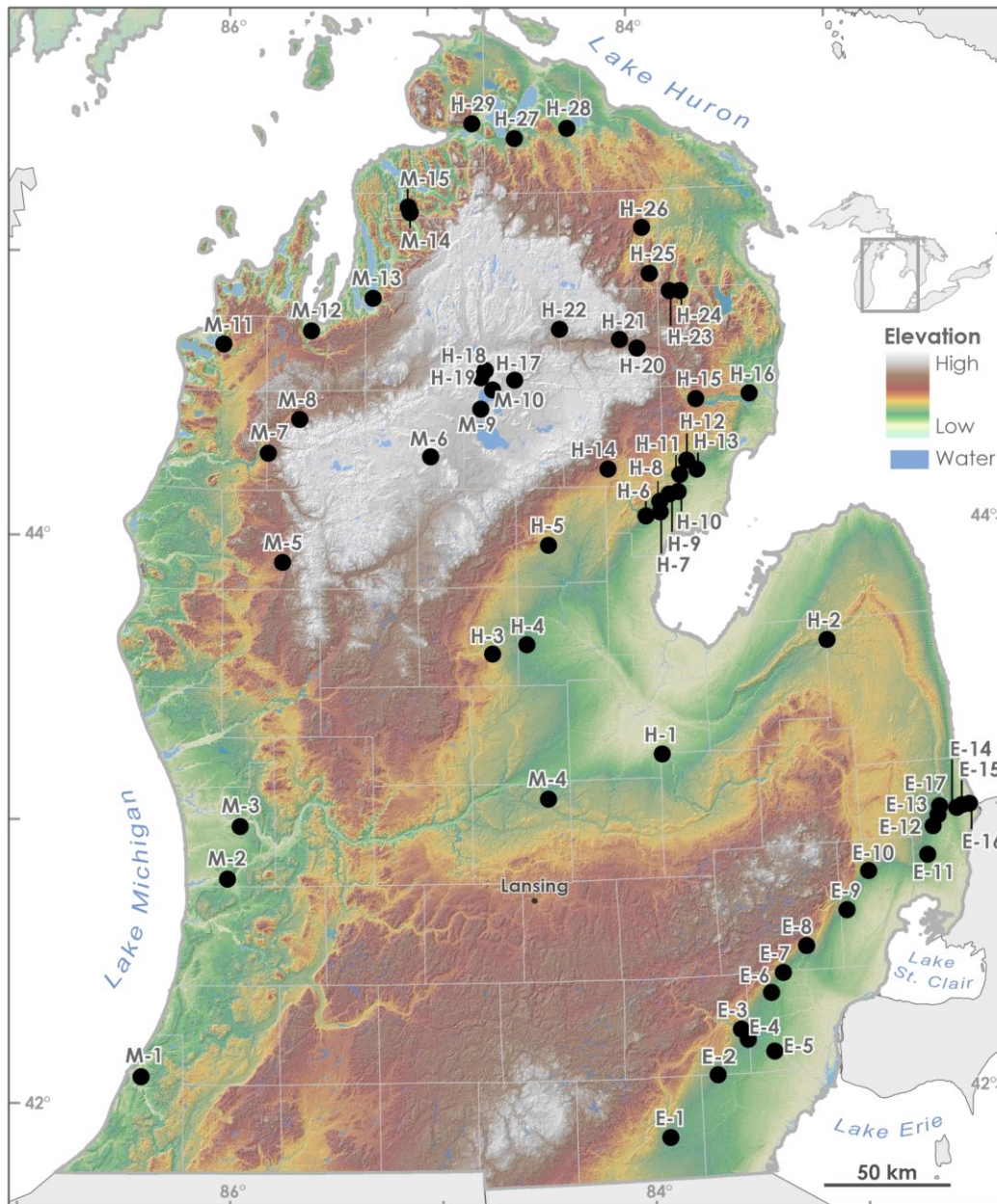


Figure 3.3: The locations of those 61 deltas mapped and discussed in this chapter. Labels at points refer to the delta ID and are a reference for Table 3.3.

Table 3.3: Deltas mapped in Figure 3.3, along with the glacial lake their likely associated with and their inferred period of formation

| Map ID | Delta name | Latitude/Longitude of delta center | Delta Plain Elevation (m asl) | Glacial Lake (Phase) | Estimated Age Range (cal ka BP) | Reference(s) |
|--------|----------------------------|------------------------------------|-------------------------------|---------------------------------------|---------------------------------|--|
| E-1 | Raisin River | N41° 52' 1" / W83° 55' 50" | 221-212 | Arkona (I-III) | 16.0-15.5 | Leverett and Taylor, 1915; Martin, 1955 |
| E-2 | Saline River | N42° 5' 32" / W83° 43' 54" | 221-217 | Arkona (I-III) | 16.0-15.5 | Leverett and Taylor, 1915 |
| E-3 | Huron River I | N42° 14' 43" / W83° 35' 9" | 233-230 | Maumee (I-III) | 17.1-16.3 | Leverett and Taylor, 1915; Scherzer, 1916; Bay, 1937,1938; Martin, 1955 |
| E-4 | Huron River II | N42° 13' 4" / W83° 33' 34" | 220-213 | Arkona (I-III) | 16.0-15.5 | Leverett and Taylor, 1915; Scherzer, 1916; Bay, 1937,1938 |
| E-5 | Huron River III | N42° 9' 34" / W83° 26' 2" | 199-197 | Warren (I-II), Wayne | 15.1-14.7 | Leverett and Taylor, 1915; Scherzer, 1916; Bay, 1937,1938 |
| E-6 | Middle River Rouge | N42° 22' 3" / W83° 26' 24" | 220-211 | Arkona (I-III) | 16.0-15.5 | Leverett and Taylor, 1915; Scherzer, 1916; Bay, 1937,1938 |
| E-7 | Tarabusi Creek | N42° 26' 15" / W83° 22' 50" | 220-215 | Arkona (I-III) | 16.0-15.5 | Leverett and Taylor, 1915 |
| E-8 | Rochester | N42° 30' 21" / W83° 15' 0" | 219-212 | Maumee (I-III) | 17.1-16.3 | Leverett and Taylor, 1915; Scherzer, 1916; Bay, 1937, 1938; Howard, 2010 |
| E-9 | Clinton River | N42° 39' 1" / W83° 4' 12" | 220-210 | Maumee (I-III), Arkona, Warren, Wayne | 17.1-14.7 | Leverett and Taylor, 1915; Martin, 1955 |
| E-10 | North Branch Clinton River | N42° 47' 27" / W82° 57' 11" | 225-215 | Arkona (I-III) | 16.0-15.5 | Leverett and Taylor, 1915 |
| E-11 | Belle River | N42° 50' 4" / W82° 39' 60" | 206-203 | Warren (I-III) | 15.1-14.7 | Leverett and Taylor, 1915 |
| E-12 | Smiths Creek | N42° 56' 10" / W82° 38' 24" | 208-206 | Warren (I-III) | 15.1-14.7 | Leverett and Taylor, 1915 |
| E-13 | South Pine River | N42° 58' 21" / W82° 36' 53" | 208-203 | Warren (I-III) | 15.1-14.7 | Leverett and Taylor, 1915 |

Table 3.3 (cont'd)

| Map ID | Delta name | Latitude/Longitude of delta center | Delta Plain Elevation (m asl) | Glacial Lake (Phase) | Estimated Age Range (cal ka BP) | Reference(s) |
|--------|-------------------------|------------------------------------|-------------------------------|----------------------|---------------------------------|---|
| E-14 | Black River I | N42° 59' 30" / W82° 31' 57" | 206-198 | Warren (I-III) | 15.1-14.7 | Leverett and Taylor, 1915 |
| E-15 | Black River II | N43° 0' 27" / W82° 29' 56" | 196-192 | Warren (I-III) | 15.1-14.7 | Leverett and Taylor, 1915 |
| E-16 | Black River III | N43° 0' 47" / W82° 27' 57" | 190-188 | Grassmere, Lundy | 14.7-14.3 | Leverett and Taylor, 1915 |
| E-17 | Pine River | N43° 0' 9" / W82° 36' 16" | 210-206 | Warren (I-III) | 15.1-14.7 | Leverett and Taylor, 1915 |
| H-1 | Flint River | N43° 13' 11" / W83° 56' 2" | 197-191 | Lundy | 14.7-14.3 | This study |
| H-2 | Cass River | N43° 35' 47" / W83° 7' 40" | 238-225 | Saginaw | 15.1 | Leverett and Taylor, 1915; Martin, 1955; Larson and Kincare, 2009 |
| H-3 | Chippewa River I | N43° 36' 54" / W84° 44' 1" | 232-226 | Early Saginaw | 16.3-16.0 | Martin, 1955 |
| H-4 | Chippewa River II | N43° 36' 36" / W84° 34' 41" | 219-212 | Warren (I-III) | 15.1-14.7 | This study |
| H-5 | Gladwin | N43° 59' 0" / W84° 26' 56" | 241-230 | Early Saginaw | 16.3-16.0 | This study |
| H-6 | Rifle River I | N44° 3' 19" / W83° 58' 47" | 227-220 | Warren (I-III) | 15.1-14.7 | This study |
| H-7 | Rifle River II | N44° 4' 5" / W83° 54' 2" | 207-200 | Grassmere | 14.7-14.3 | This study |
| H-8 | Big Creek | N44° 6' 26" / W83° 54' 26" | 227-220 | Warren (I-III) | 15.1-14.7 | This study |
| H-9 | Cedar Creek I | N44° 7' 50" / W83° 51' 47" | 227-225 | Warren (I-III) | 15.1-14.7 | This study |
| H-10 | Cedar Creek II | N44° 8' 18" / W83° 49' 7" | 207-200 | Grassmere | 14.7-14.3 | This study |
| H-11 | Johnson Creek | N44° 11' 43" / W83° 47' 3" | 208-205 | Lundy | 14.7-14.3 | This study |
| H-12 | Au Gres River I | N44° 14' 0" / W83° 45' 56" | 218-210 | Grassmere | 14.7-14.3 | This study |
| H-13 | Au Gres River II | N44° 13' 10" / W83° 45' 13" | 208-206 | Lundy | 14.7-14.3 | This study |
| H-14 | West Branch Rifle River | N44° 13' 42" / W84° 10' 15" | 265-255 | Early Saginaw | 16.3-16.0 | This study |
| H-15 | Jackpines | N44° 26' 8" / W83° 37' 32" | 260-245 | Warren (I-III) | 15.1-14.7 | Leverett and Taylor, 1915; Martin, 1955; Burgis, 1977, 1981 |

Table 3.3 (cont'd)

| Map ID | Delta name | Latitude/Longitude of delta center | Delta Plain Elevation (m asl) | Glacial Lake (Phase) | Estimated Age Range (cal ka BP) | Reference(s) |
|--------|-----------------------|------------------------------------|-------------------------------|-----------------------|---------------------------------|--|
| H-16 | Sevenmile Hill | N44° 27' 35" / W83° 29' 21" | 235-220 | Grassmere | 14.7-14.3 | Leverett and Taylor, 1915; Martin, 1955; Burgis, 1977, 1981 |
| H-17 | Coy Ridge | N44° 32' 44" / W84° 36' 15" | 375-368 | ? | < 17.1 | This study |
| H-18 | Beaver Creek I | N44° 35' 35" / W84° 45' 45" | 402-393 | ? | < 17.1 | This study |
| H-19 | Beaver Creek II | N44° 33' 46" / W84° 46' 27" | 386-371 | ? | < 17.1 | This study |
| H-20 | Bull Gap | N44° 38' 40" / W84° 1' 5" | 310-295 | ? | < 15.1 | This study |
| H-21 | Kneeland | N44° 40' 26" / W84° 4' 3" | 326-317 | ? | < 15.1 | Burgis, 1977, 1981 |
| H-22 | Elk Hill | N44° 43' 34" / W84° 22' 23" | 389-380 | ? | < 15.1 | This study |
| H-23 | Indian Creek I | N44° 49' 34" / W83° 48' 38" | 262-259 | ? | < 15.1 | This study |
| H-24 | Indian Creek II | N44° 50' 40" / W83° 47' 10" | 249-241 | ? | < 15.1 | This study |
| H-25 | Turtle Lake | N44° 54' 22" / W83° 56' 6" | 245-238 | ? | < 15.1 | This study |
| H-26 | Brush Creek | N45° 4' 11" / W83° 58' 10" | 260-255 | ? | < 15.1 | Burgis, 1977, 1981 |
| H-27 | Sturgeon-Pigeon River | N45° 23' 7" / W84° 35' 40" | 219-205 | Algonquin | 13.2-11.5 | This study |
| H-28 | Black River | N45° 25' 45" / W84° 19' 49" | 214-207 | Algonquin | 13.2-11.5 | Vader et al., 2012 |
| H-29 | McPhee Creek | N45° 26' 46" / W84° 47' 60" | 219-210 | Algonquin | 13.2-11.5 | This study |
| M-1 | Fair Plain | N42° 5' 42" / W86° 25' 34" | 195-189 | Chicago (Calumet) | 13.7-12.9 | Leverett and Taylor, 1915; Martin, 1955; Kincare, 2007 |
| M-2 | Zeeland | N42° 47' 55" / W86° 1' 28" | 204-198 | Chicago (Glenwood II) | 15.1-14.7 | Leverett and Taylor, 1915; Martin, 1955; Evenson, 1973 |
| M-3 | Allendale | N42° 58' 28" / W85° 57' 46" | 201-198 | Chicago (Glenwood II) | 15.1-14.7 | Leverett and Taylor, 1915; Bretz, 1953, 1966; Martin, 1955; Hough, 1958, 1963; Muller, 1977; Kehew, 1993 |

Table 3.3 (cont'd)

| Map ID | Delta name | Latitude/Longitude of delta center | Delta Plain Elevation (m asl) | Glacial Lake (Phase) | Estimated Age Range (cal ka BP) | Reference(s) |
|--------|---------------------------|------------------------------------|-------------------------------|----------------------|---------------------------------|--|
| M-4 | Maple River | N43° 2' 28" / W84° 29' 17" | 224-222 | Chicago (Glenwood I) | 17.1-16.3 | This study |
| M-5 | Sanborn Creek Fan | N43° 54' 23" / W85° 44' 46" | 280-276 | ? | < 17.1 | This study; K. Kincare, personal |
| M-6 | Lake City, Harrison Ridge | N44° 16' 31" / W85° 1' 12" | 372-370 | ? | < 17.1 | This study |
| M-7 | Slagle Fan | N44° 17' 33" / W85° 48' 58" | 311-252 | ? | < 17.1 | This study; K. Kincare, personal communication |
| M-8 | Cole Creek Fan | N44° 24' 45" / W85° 39' 43" | 310-295 | ? | < 17.1 | This study; K. Kincare, personal |
| M-9 | Houghton Lake Ridge | N44° 26' 57" / W84° 46' 38" | 385-375 | ? | < 17.1 | This study |
| M-10 | Higgins Lake Ridge | N44° 30' 30" / W84° 42' 54" | 384-381 | ? | < 17.1 | This study |
| M-11 | Platte River | N44° 40' 8" / W86° 1' 50" | 220-210 | Algonquin | 13.2-11.5 | This study |
| M-12 | Boardman River | N44° 43' 51" / W85° 37' 11" | 220-210 | Algonquin | 13.2-11.5 | This study |
| M-13 | Rapid River | N44° 50' 17" / W85° 17' 45" | 206-190 | Algonquin | 13.2-11.5 | This study |
| M-14 | Deer Creek | N45° 8' 6" / W85° 6' 22" | 191-190 | Algonquin | 13.2-11.5 | This study |
| M-15 | Brown Creek | N45° 9' 24" / W85° 7' 11" | 198-195 | Algonquin | 13.2-11.5 | This study |

unique to this study (Table 3.3). Each delta presumably formed sometime between ≈ 17.0 and 11.0 cal ka BP, i.e., between the Mackinaw and Gribben Interstadials (Figure 3.1; Tables 3.1 and 3.3). Within Lower Michigan, 17 deltas were mapped in the Lake Erie drainage basin ($\approx 15,016$ km²; 1 delta per ≈ 883 km²), 29 in the Lake Huron drainage basin ($\approx 38,250$ km²; 1 delta per ≈ 1319 km²) and 15 in the Lake Michigan drainage basin ($\approx 53,195$ km²; 1 delta per ≈ 3546 km²) (Figure 3.4). Deltas are incrementally labeled from south to north within each lake basin, albeit all of the deltas in a delta complex were labeled first before assigning the next northern delta an ID (e.g. Figures 3.3 and 3.4). Therefore, deltas are not entirely listed in order by latitude as a

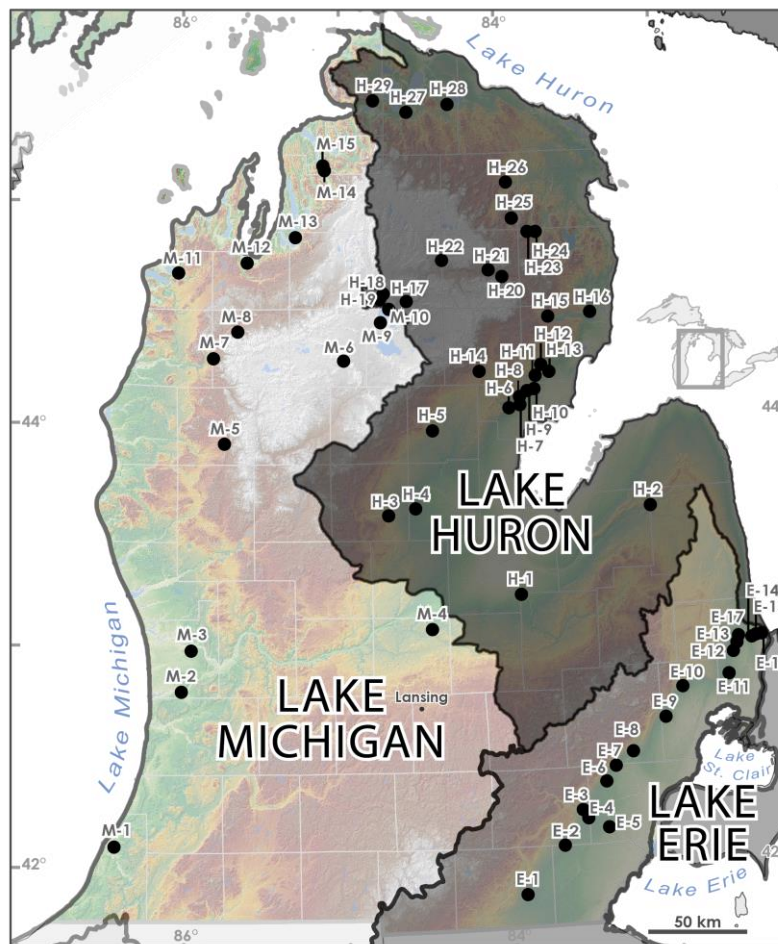


Figure 3.4: Extent of the Great Lakes drainage basins within the LP of Michigan, in relationship to the location of Pleistocene deltas.

result of seven delta complexes in the Lake Erie and Michigan basins (Table 3.3).

The relatively higher concentration of deltas on the eastern margins of Lower Michigan compared to the western margins may relate to the fact that lake level elevations varied more within the Lake Erie and Huron basins (12 and 11 different elevations, respectively), as compared to the Lake Michigan basin (mainly 2 different elevations) between the Crown Point-Port Bruce and Two Rivers-Onaway Phases (Figure 3.1; Table 3.1). The higher density of deltas and greater variation in lake-level elevations within the Lake Erie and Huron basins, as opposed to the Lake Michigan basin, implies that the fluvial systems draining to the east coast of the LP had to make more long-profile adjustments as their base levels changed. Thus, more deltas had the potential to have formed within the Lake Huron and Erie basins. Figures 3.3 and 3.4 also illustrate how there are often multiple closely spaced or stacked deltas (i.e., a delta complex), each associated with only one fluvial system, within the Lake Erie and Huron drainage basins. However, I found no evidence of multiple deltas forming from a single fluvial system, linked with different lake-level elevations, within the Lake Michigan drainage basin (Figures 3.3 and 3.4).

Another possible reason for the higher concentrations of deltas on the eastern margins of the LP and fewer deltas on the western margins, perhaps relates to the strength of the longshore currents during certain periods of time within the individual lake basins. For instance, longshore currents may have been strong enough to carry away most of the stream load that entered the shorelines that developed along the western margins of the LP and thus preventing deltas from forming on the western margins of the LP (Larson, G.J., personal communication). Alternatively, deltas may have formed on the west side of Lower Michigan but were

subsequently destroyed by coastal erosion from strong, longshore currents that developed during succeeding lake stages/phases (Larson, G.J., personal communication). In both cases the strength and persistence of the longshore drift direction would have been governed by the dominant wind direction.

As a follow-up to this discussion, the succeeding sections aim to (1) provide an inventory of the deltas that formed during the late Wisconsin in Lower Michigan and (2) describe the main meltwater and sediment sources for the deltas, along with the topographic and textural characteristics of their catchments. These data, regarding the timing and types of the fluvial systems that contributed to delta construction, will aid in our understanding of the environmental attributes that influenced delta formation during the late Wisconsin.

3.3.2 Lake Erie Basin Deltas

The Lake Erie drainage basin (Figure 3.4) was occupied by glacial Lakes (from oldest to youngest) Maumee (I-III), Arkona (I-III), Ypsilanti, Whittlesey, Warren (I-III), Wayne, Grassmere, Lundy, and Early Lake Erie between ≈ 17.1 and 13.7 cal ka BP, during the period of final ice retreat (Figure 3.5 and Section 1.1: Figures 1.2-1.8).

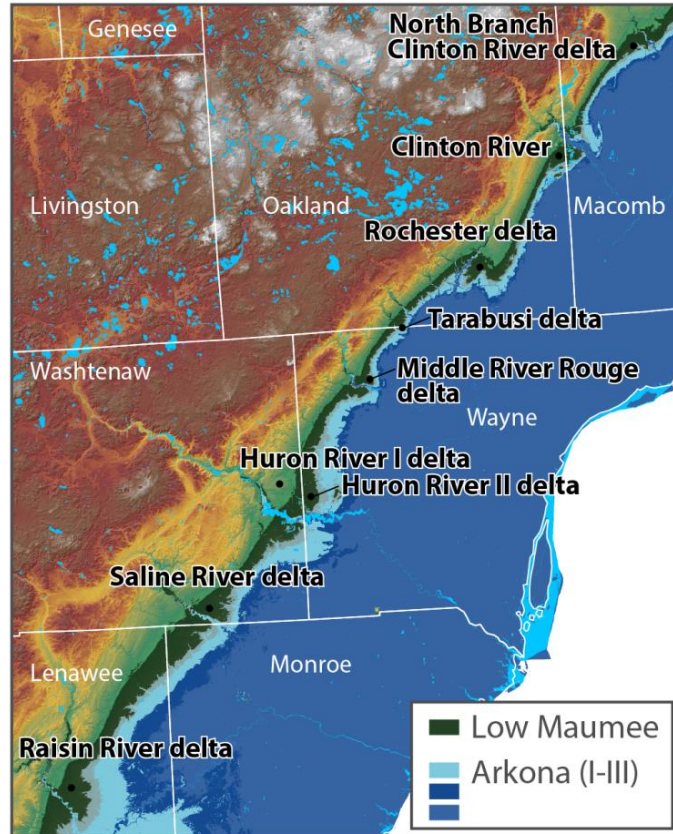


Figure 3.5: Deltas in SE Michigan, graded to glacial Lakes Maumee (I-III) and Arkona. **note: Lake symbology within is document has no reference to water depth **

3.3.2.1 Lake Maumee Deltas

Leverett and Taylor (1915, pg. 383) stated that several rivers built deltas into glacial Lake Maumee (mainly to its lowest stage), including the Huron, Rouge, and Clinton Rivers.

Topographic and sediment characteristics presented in this study support Leverett and Taylor (1915) and suggest that the Huron River built two deltas, located in eastern Washtenaw and western Wayne Counties, and are graded towards separate lake levels. The Huron River I delta has a longitudinal profile graded towards glacial Lake Maumee, whereas the Huron River II delta is graded towards Lake Arkona (Table 3.3; Figure 3.5; Appendix B and C).

The Rochester delta, located in SE Oakland County, just south of the city of Birmingham, is also graded to glacial Lake Maumee (I-III) and hence presumably formed sometime between ≈ 17.1 and 16.3 cal ka BP (Table 3.3; Figure 3.5; Appendix C). The delta was originally discussed by Leverett and Taylor (1915), Scherzer (1916), Bay (1937, 1938) and Howard (2010). This delta is associated with the Rochester meltwater channel which was active while the Birmingham moraine was being deposited by the Huron-Erie lobe in SE Michigan (Howard et al., 2010; Figures 3.5 and 3.6).

The Clinton River delta, located ≈ 3 km SE of Rochester, MI, is topographically muted; it was likely inundated and wave-worked in certain parts by waters from Lake Whittlesey (Leverett and Taylor, 1915; Hough, 1958). As a result, I could not determine if the Clinton River delta had formed mainly during glacial Lake Maumee, Arkona, Warren, or Wayne (Table 3.3), but agree with Leverett and Taylor (1915, pg. 383) that the Clinton River delta has “old distributaries which belong to Lake Maumee and are too high to have served at the time of Lake Whittlesey” and that “... the Whittlesey beach skirts along the front of the Maumee deltas ...” which suggests that the Clinton River delta was built into glacial Lake Maumee (Table 3.3; Figure 3.5; Appendix C).

3.3.2.2 Lake Arkona Deltas

The following seven deltas have longitudinal profiles that are graded to glacial Lake Arkona: (1) Raisin River, (2) Saline River, (3) Huron River II, (4) Middle River Rouge, (5) Tarabusi Creek, (6) Clinton River, and (7) North Branch Clinton River (Table 3.3; Figure 3.5; Appendix B and C). These seven deltas form a SW-NE trending group in southeastern Lower Michigan, spanning from eastern Lenawee and Washtenaw Counties, north-west Wayne County, and

west-central Macomb County (Figure 3.5; Appendix C). These deltas were likely active sometime between ≈ 16.0 and 15.0 cal ka BP and are associated with the ancestral fluvial systems of those rivers that presently incise the now perched deltas. The series of fluvial systems that deposited these deltas were the major drainageways for the SE Michigan interlobate region during the Mackinaw Interstadial when the Huron-Erie and Saginaw lobes retreated northward (Leverett and Taylor, 1915; Figure 3.6). The catchment areas for these deltas consist of moderately sloping landscapes and are dominantly composed of loamy textured deposits (Figures 3.6 -3.8).

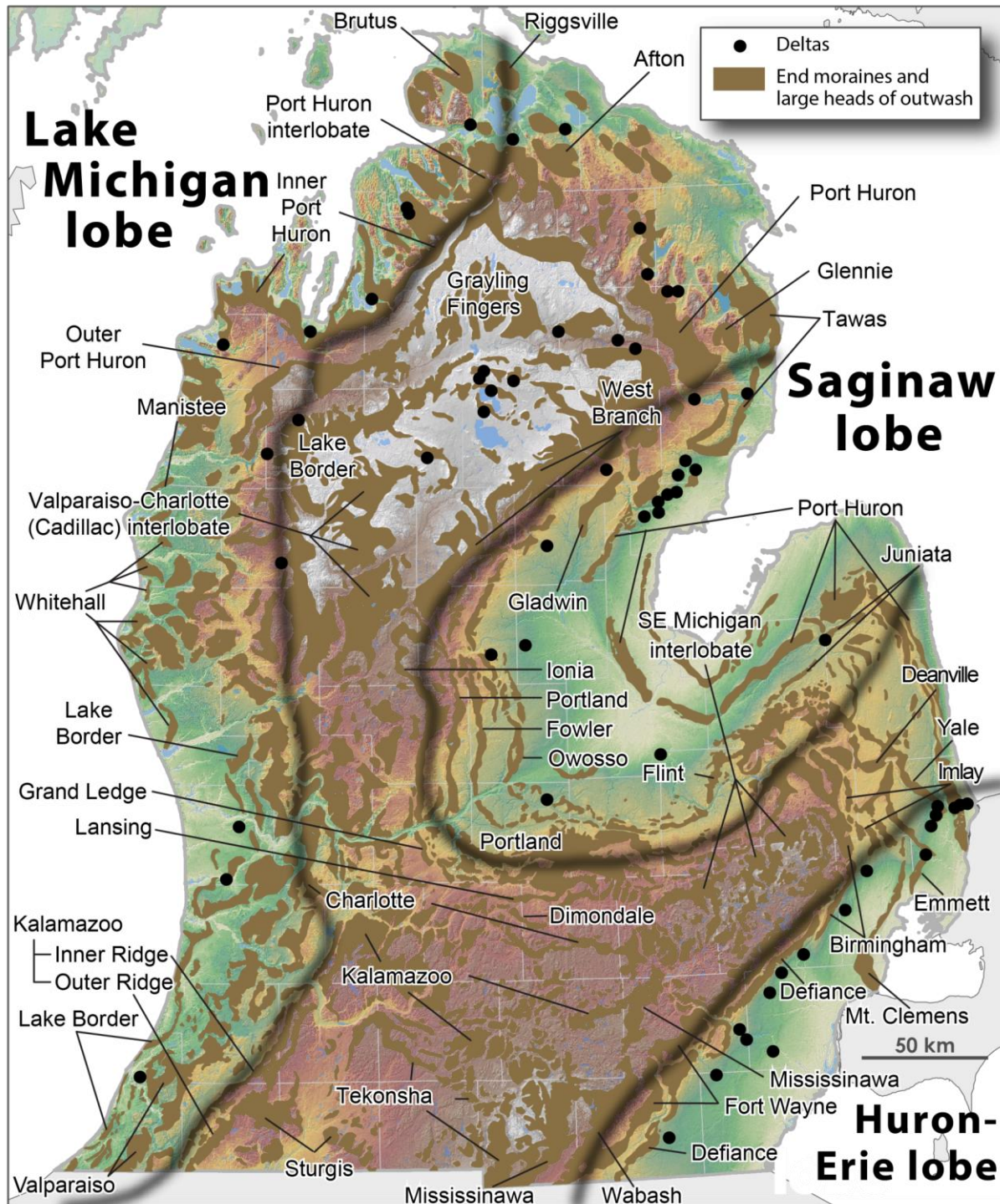


Figure 3.6: Major end moraines, heads of outwash and other uplands of glacial origin, in relationship to the relict deltas mapped in this study (modified from Blewett et al., 2009).

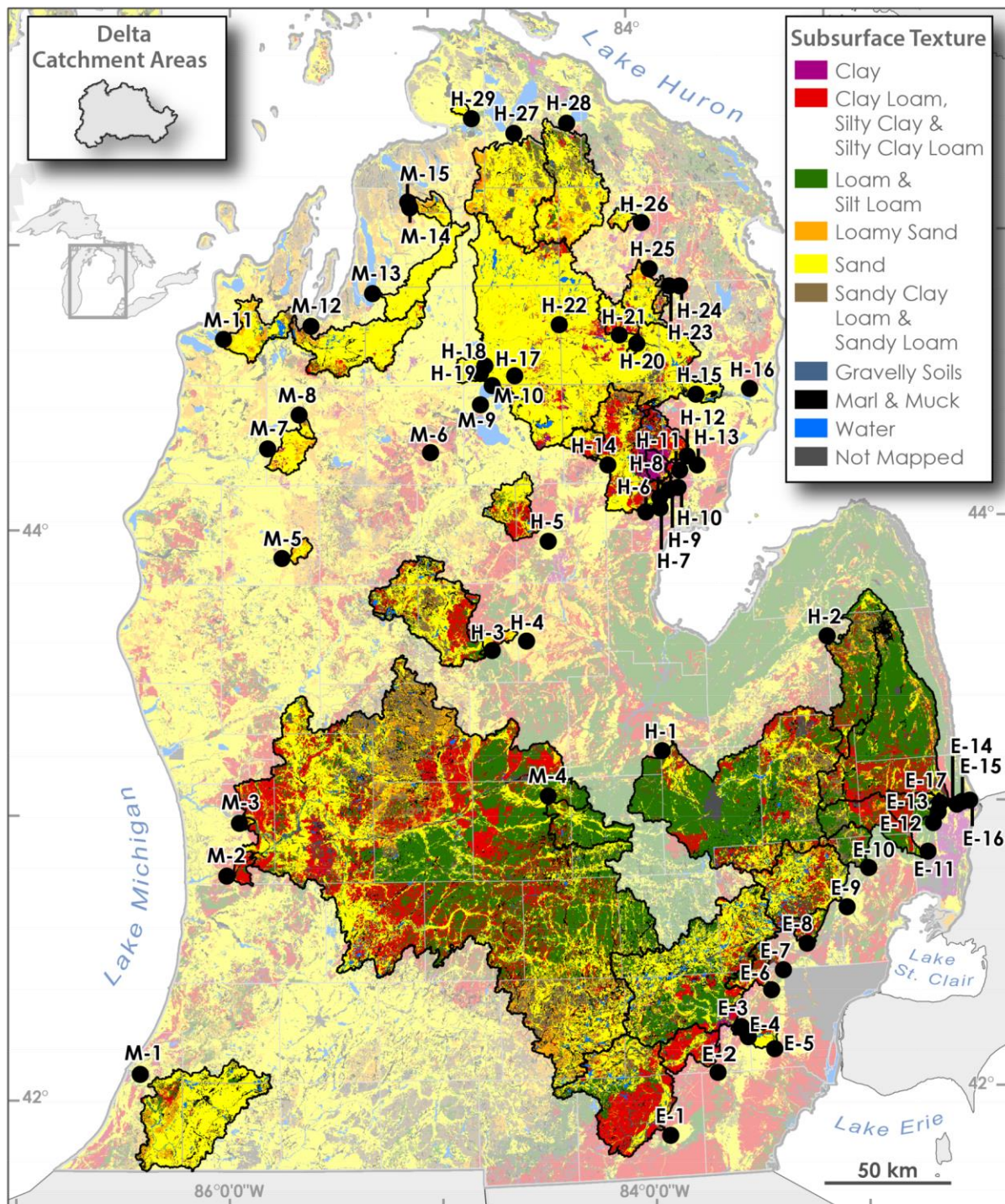


Figure 3.7: Present day catchment areas for the deltas mapped in this study, also showing the major subsurface textural groupings associated with soil parent materials (C horizon) of the catchments.

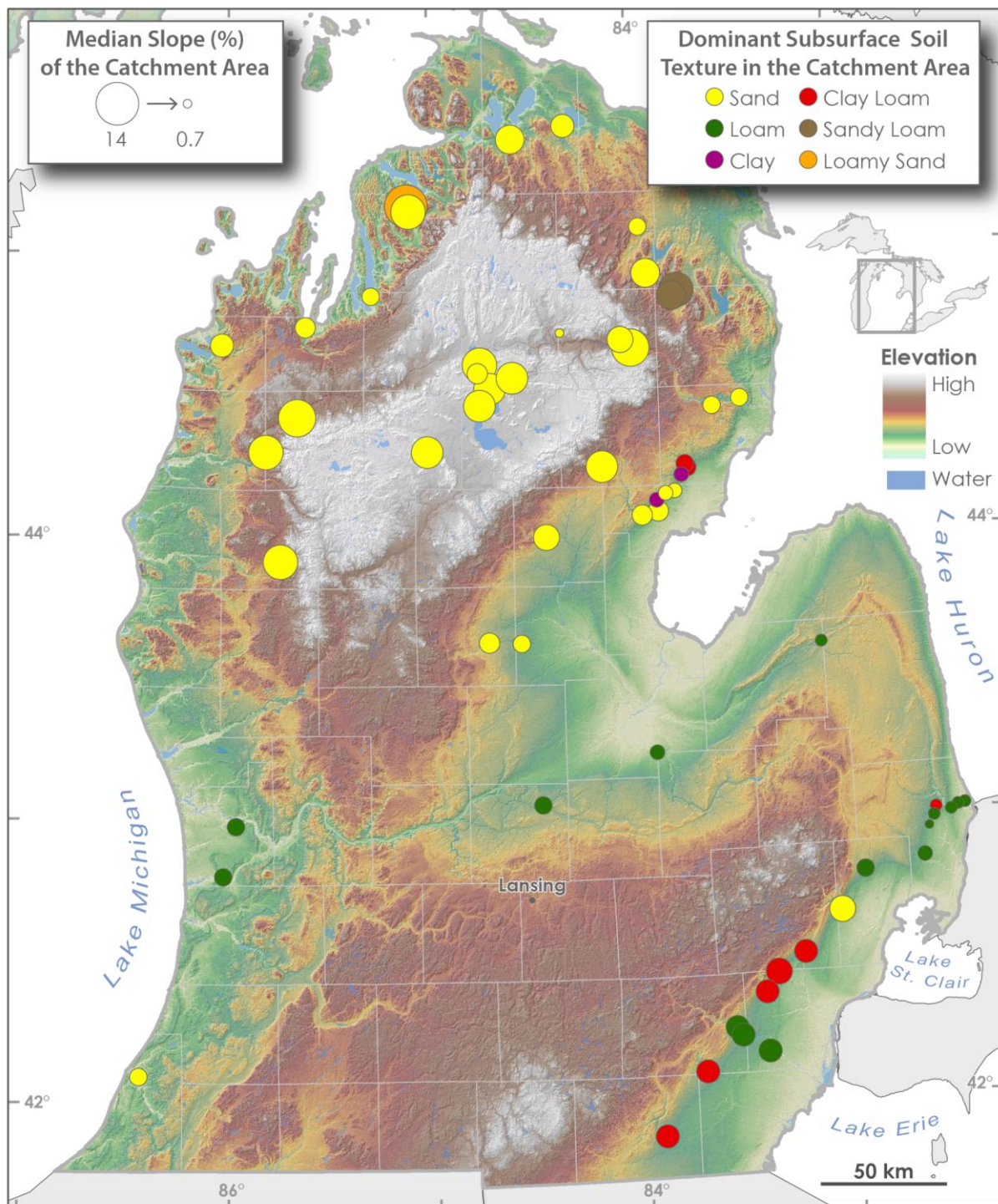


Figure 3.8: A map of the notably dominant subsurface soil texture within each delta catchment area, and the median slope percentage within those areas.

No deltas mapped in this study are apparently graded to glacial Lake Ypsilanti (Table 3.3; Appendix B). Glacial Lake Ypsilanti was an extremely low lake-level phase, <166 m above sea level (asl), within the Lake Erie basin, and lasted for a brief period of time around 15.5 cal ka BP (Calkin and Feenstra, 1985). Given that this study did not pursue mapping relict deltas via the use of the modern day Great Lakes bathymetry, no deltas were mapped below \approx 175 m asl.

3.3.2.3 Lake Whittlesey Deltas

No deltas were found graded towards glacial Lake Whittlesey (Table 3.3). Leverett and Taylor (1915, pg. 383) stated that “one of the exceptional characteristics of the shores of Lake Whittlesey is their general lack of deltas of the ordinary type” and “... the streams that entered this lake must have carried on substantially the same work of erosion and deposition as in the preceding and succeeding lake stages, but the Whittlesey shores show almost no suggestion of the delta deposits that predominate all along the shores of Lake Maumee and Arkona”.

3.3.2.4 Lake Warren/Wayne Deltas

In southeastern Lower Michigan, the following seven deltas are graded towards either one of the three glacial Lake Warren phases or the glacial Lake Wayne stage: (1) Huron River III (Figure 3.9), (2) Belle River, (3) Smiths Creek, (4) South Pine River, (5) Black River I, (6) Black River II, and (7) Pine River (Figure 3.10; Appendix B and C). These deltas formed when the lake-levels in the Lake Erie basin, steadily lowered, between \approx 15.1 and 14.7 cal ka BP, as the Huron-Erie and Saginaw lobes retreated northward from the Port Huron maximum (Table 3.3). Akin to those deltas that formed earlier during glacial Lakes Maumee and Arkona, and are also present in the southeast LP, the catchment areas for the above seven deltas mainly consist of moderately sloping landscapes and loamy textured deposits. In regards to the Huron River III

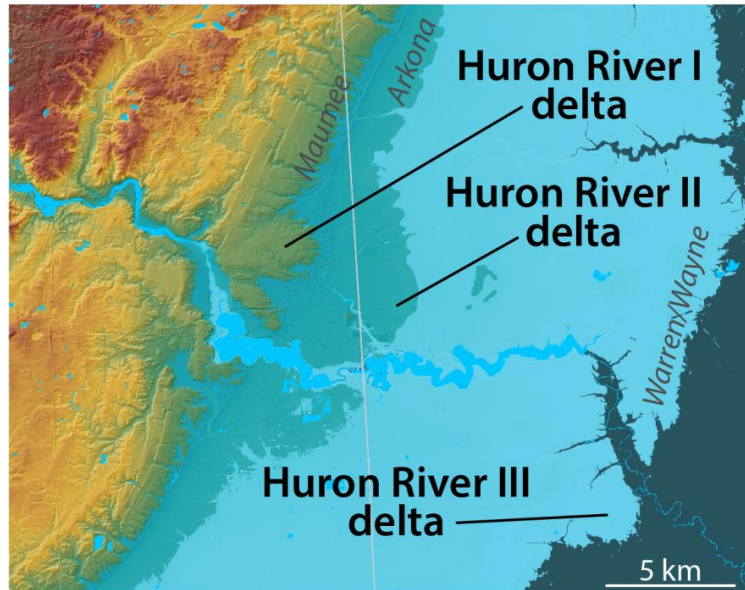


Figure 3.9: A DEM flooded to glacial Lakes Maumee, Arkona, and Warren/Wayne shorelines, illustrating the Huron River I, II, and III deltas.

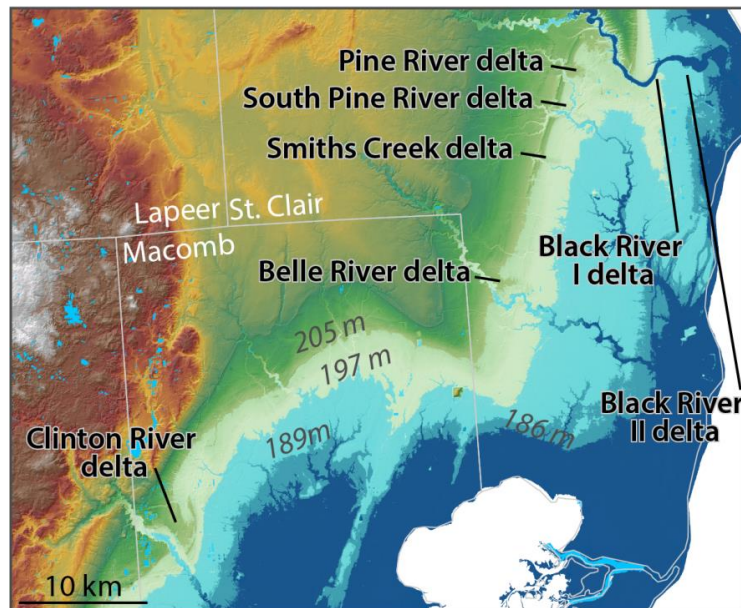


Figure 3.10: A DEM flooded to several potential paleolake-level elevations to illustrate various deltas, within southeastern Lower Michigan, graded to either one of the glacial Lake Warren phases or Lake Wayne.

delta (Figure 3.9), the Huron River perhaps built a delta during glacial Lakes Maumee, Arkona and Whittlesey as a result of the extensive area (presently >2000 km²) that it drained within the SE Michigan interlobate region. The Huron River watershed is largely composed of moderately sloping landscapes with a variety of soil textural characteristics, typical of interlobate regions in southern Lower Michigan (Figures 3.6 – 3.8).

3.3.2.5 Lake Grassmere/Lundy Deltas

The Black River III delta, located in west-central St. Clair County (Figure 3.11), has a longitudinal profile that intersects with the glacial Lake Grassmere and/or Lundy shorelines (Appendix B and C). As such, the Black River III delta is the youngest delta (between ≈14.7 and 14.3 cal ka BP) mapped in this study, within the Lake Erie basin (Table 3.3). The Black River III delta is located ≈6 km east of the Port Huron maximum in SE Michigan, near the city of Port Huron. Analogous to the Huron River, the Black River presently has a particularly large drainage area (>1800 km²) and the catchment area is dominated by loam textured deposits (Figures 3.7 and 3.8; Appendix C). Furthermore, similar to the Huron River, the Black River built a stacked

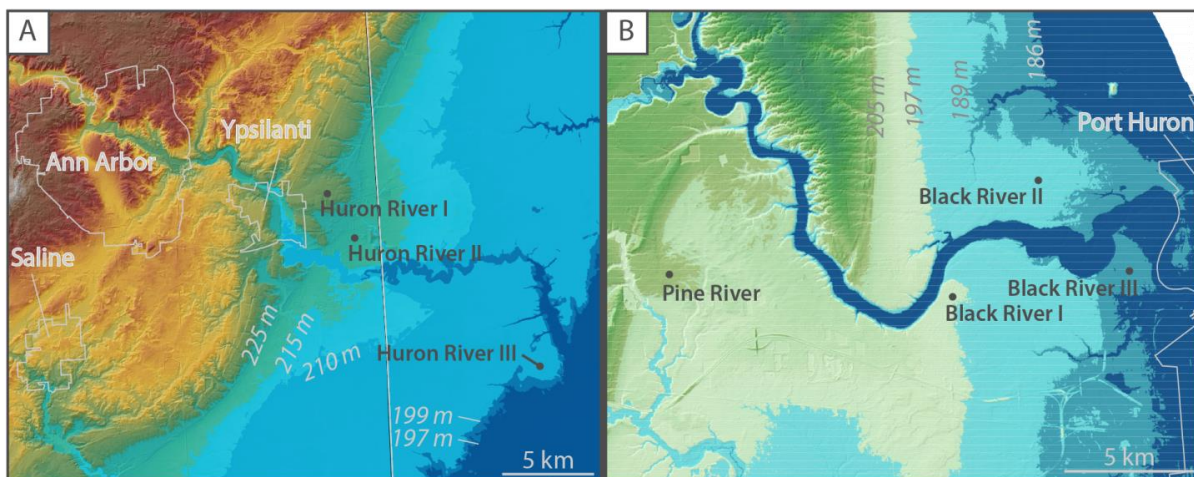


Figure 3.11: A) A DEM flooded to several potential paleolake-level elevations, illustrating the Huron River I-III delta complex. B) Same as (A), but for the Black River I-III delta

series of deltas that are associated with different lake-level elevations (i.e., a delta complex; Figure 3.11). Both the Black River and Huron Rivers drained much of the SE interlobate region and “thumb” of Lower Michigan during the Two Creeks interstadial (Figures 3.6 and 3.7). As ice retreated from the Port Huron maximum, an abundant amount of meltwater would have been funneled towards the mouth of the Black River, aiding the formation of the Black River III delta.

3.3.3 Lake Huron Basin Deltas

The Lake Huron basin was occupied by several glacial Lakes. From oldest to youngest they are Early Lake Saginaw, Arkona (I-III), Post-Arkona low phase, Saginaw, Warren (I-III), Wayne, Grassmere, Lundy, Kirkfield, and Algonquin. All of these lakes were present between ≈ 17.1 and 13.7 cal ka BP during the retreat from the LGM in Lower Michigan. Early Lake Saginaw and Lake Saginaw were confined to the Saginaw lowlands (Schaetzl et al., 2013b), whereas the remaining lake stages occupied parts of both the Saginaw basin and the Lake Huron basin (Section 1.1 Figures 1.2 – 1.8).

3.3.3.1 Early Lake Saginaw Deltas

The Chippewa River I, Gladwin, and West Branch Rifle River deltas are located within the Saginaw lowlands, in Isabella, Gladwin and Ogemaw County (Figure 3.12; Schaetzl et al., 2013b). These three deltas are graded to the Early Saginaw shoreline elevation (> 225 m asl) and presumably formed sometime between ≈ 16.3 and 16.0 cal ka BP during the Mackinaw interstadial (Table 3.3; Appendix B and C). These deltas stand east of a series of N-S trending glacial margins, i.e., from west to east they are the West Branch, Ionia, Portland, Fowler, and Owosso moraines (Figure 3.6). The Chippewa River I, Gladwin, and West Branch Rifle River deltas likely formed soon after the Saginaw lobe retreated from the easternmost margin – at

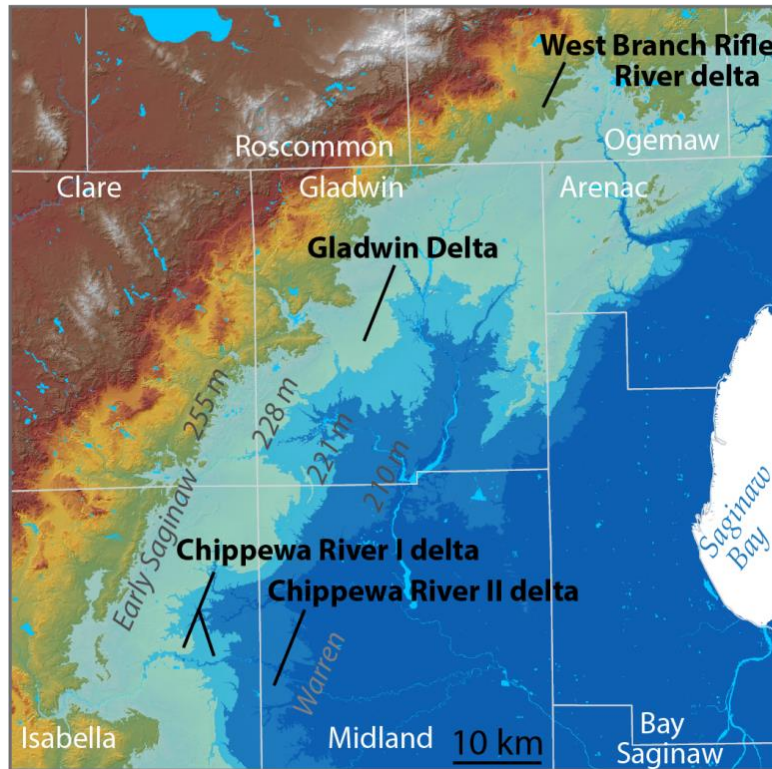


Figure 3.12: Saginaw lowlands flooded to Early Saginaw and glacial Lake Warren stages to illustrate both Chippewa River deltas, along with the Gladwin and West Branch Rifle River deltas.

the Owosso moraine - as the Michigan-Saginaw interlobate region of Lower Michigan slowly became subaerially exposed (Figure 3.6). These deltas represent a shift from meltwater predominantly draining subaerially towards the southwest, forming outwash plains, to waters draining mainly to the east and southeast, towards the Saginaw lowlands, forming deltas when the Saginaw lowlands were still ice covered (Figure 3.6). Given that the Saginaw lobe ice margin was retreating eastward and northward in both the high plains interlobate region and the Saginaw lowlands, and the western ice margin was oriented SW-NE, these deltas were likely activated in the following order: (1) Chippewa River I, (2) Gladwin, and (3) West Branch Rifle River (Figure 3.12). Note that the West Branch Rifle River delta currently stands several meters

(between $\approx 10\text{-}20$ m) above the Chippewa and Gladwin deltas (Figure 3.12). This is likely a result of isostatic rebound where the land surface has rebounded to a higher elevation over time in more northern regions of Lower Michigan (Gilbert, 1898, Clark et al. 1994; Lewis et al., 2005). The modern day catchment areas associated with these deltas encompass the southernmost regions of the Cadillac Morainic Uplands, the Houghton Lake Sandy Flats and Ridges, and the West Branch Moraine (Schaetzl et al., 2013b). These physiographic regions are dominated by moderate to high relief landscapes and mainly composed of sandy textured deposits (Figures 3.7 and 3.8).

No deltas were found that grade to glacial Lake Arkona (216-212 m asl) in the Lake Huron basin, even though several such deltas had formed during this period within the Lake Erie basin (Appendix B and C). It is possible that stream flows diminished within this region due to the limited source of water following the drainage of those lakes that likely occupied the Central High Plains region/Houghton Lake Sandy Flats and Ridges. However, the author is not convinced that deltaic emplacement ceased during glacial Lake Arkona, within the Lake Huron basin. Rather, the Chippewa River I, Gladwin, and West Branch Rifle River deltas (Figure 3.12) were likely also active at some point during this time. Apart from the Chippewa River I delta, the Gladwin and West Branch Rifle River deltas have a concave upwards profile, suggesting that these deltas were influenced by a lowering lake level (Appendix B). Therefore the Chippewa River I delta, Gladwin, and West Branch Rifle River deltas were likely active while lake levels lowered from Early Lake Saginaw to Arkona.

Around the same time that glacial Lake Ypsilanti (low lake-level stage) occupied the Lake Erie basin (≈ 15.5 cal ka BP; Table 3.1), a post-Arkona low lake-level stage existed within the

Lake Huron basin (Eschman and Karrow, 1985; Lewis et al., 2008). However, given that this study did not employ bathymetric data, I could not identify deltas relating to the post-Arkona low.

3.3.3.2 Lake Saginaw Deltas

The Cass River delta (Figure 3.13) merges with the glacial Lake Saginaw shoreline and as such, was likely active during the Port Huron advance around 15.1 cal ka BP (Table 3.3; Appendix B and C). This delta is tucked between the Port Huron and Juniata ice marginal positions (Figures 3.3 and 3.6). The Cass River delta was active during the Port Huron advance when the Cass River functioned as a spillway between glacial Lake Whittlesey (within the Lake Erie basin) and glacial Lake Saginaw (within the Huron basin, especially the lowlands flanking Saginaw Bay). Meltwater from Lake Whittlesey was funneled through the Ubly channel to the mouth of the Cass River into glacial Lake Saginaw (Leverett and Taylor, 1915). The majority of

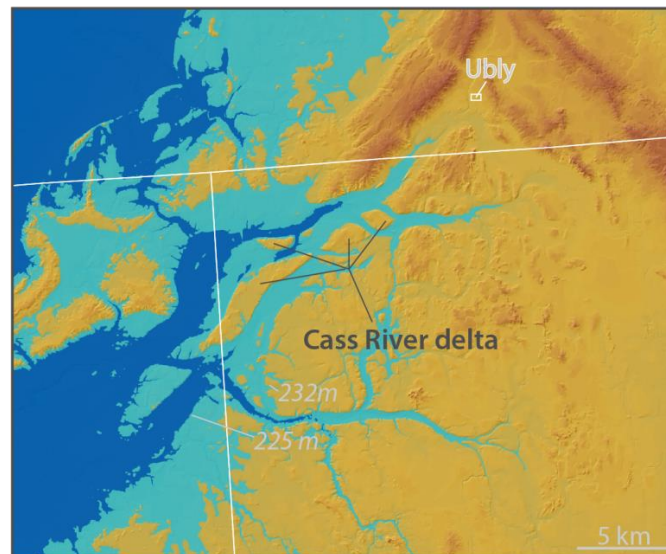


Figure 3.13: DEM flooded to several potential paleolake-level elevations, illustrating the Cass River delta with its midchannel bars – characteristic of a fluvial dominated delta.

the sediments composing this delta were derived from downcutting of the Uby channel, given that the spillover from Lake Whittlesey would have been low in suspended sediments since these would have settle out in the glacial lake. Although the spillover from glacial Lake Whittlesey fed the majority of Cass River delta system, the present day Cass River does drain parts of the “thumb” of Lower Michigan. The modern Cass River catchment area is dominated by loam textured deposits (Figures 3.7 and 3.8). Topographically, the perched Cass River delta displays several midchannel bars that may have formed as a result of the predominantly fluvial characteristics of the delta (Figure 3.13).

3.3.3.3 Lake Warren Deltas

The following five deltas have longitudinal profiles that are graded to glacial Lake Warren (I-III): (1) Chippewa River II, (2) Rifle River I, (3) Big Creek, (4) Cedar Creek I, and (5) Jackpines (Table 3.3; Figures 3.5 and 3.14; Appendix B and C). Thus, these deltas were presumably active sometime between ≈ 15.1 -14.7 cal ka BP (Table 3.3; Figure 3.3). The Chippewa River II delta stands near the southwestern margins of the Saginaw lowlands, in Isabella and Midland County (Figure 3.14). The Chippewa River II delta is a continuation of the Chippewa River I delta, although a lower, second-tier formation within the delta complex (Appendix C). The majority of the water and sediment feeding the Chippewa River II delta was presumably sourced from the Cadillac Morainic Uplands and Houghton Lake Sand Flats and Ridges. These regions are mostly composed of moderate to high relief landscapes and sandy textured deposits (Figures 3.7 and 3.8; Schaetzl et al., 2013b).

The Rifle River I, Big Creek, and Cedar Creek I deltas formed along the eastern margins of the PHM, in Arenac County (Figure 3.15). These deltas were built during a regression phase

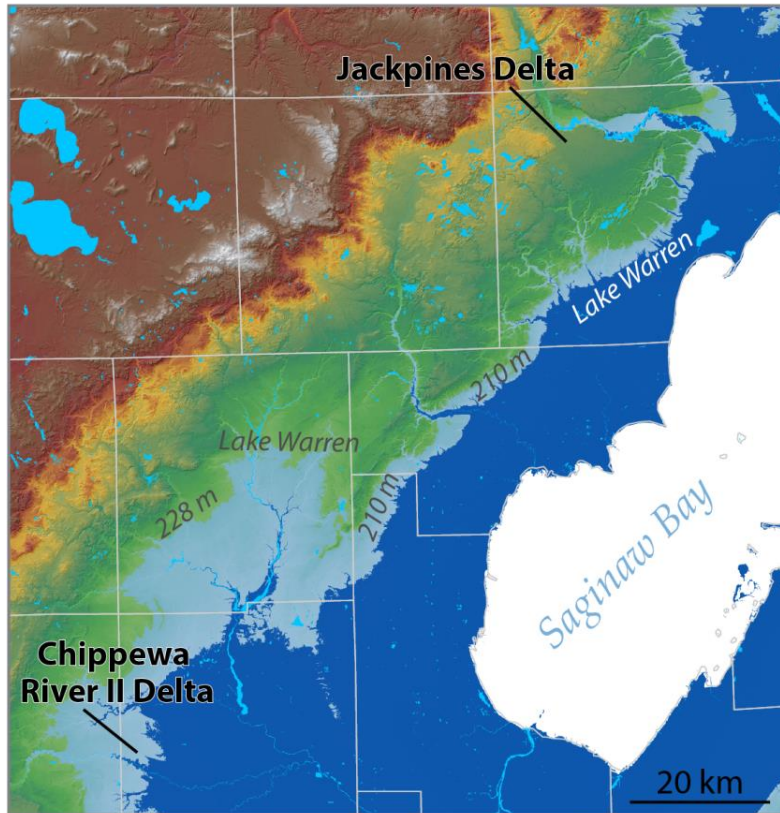


Figure 3.14: DEM flooded to several potential paleolake-level elevations, illustrating Chippewa River II and Jackpines deltas.

within the Lake Huron basin. During this time, lake levels dropped between ≈ 6 and 9 m from glacial Lake Saginaw to Warren. This ensured further subaerial exposure of those landscapes in northeastern Lower Michigan, when compared to the formation interval during glacial Lake Saginaw time. The lower lake level also presumably decreased the accommodation space in the basin and perhaps promoted the growth of deltas within the Saginaw Bay region of northern Lower Michigan. Their catchment areas head within the Port Huron Moraine – NW and Ogemaw Pitted Plain physiographic regions, which encompass moderate to high relief landscapes that are dominated by both fine and coarse textured deposits (Figures 3.7 and 3.8;

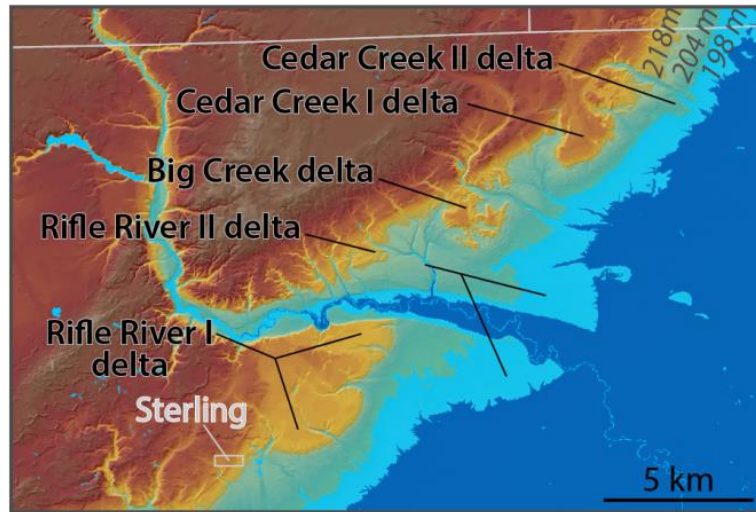


Figure 3.15: DEM flooded to several potential paleolake-level elevations, illustrating the symmetrical shape of the sequence of deltas that formed along the northern margins of Saginaw Bay.

Schaetzl et al., 2013b). These deltas are highly symmetrical (Figure 3.15; Appendix C), and have relatively sandy, high relief catchment areas (Figures 3.7 and 3.8).

The Jackpines delta is located just north of the northern limits of the Saginaw lowlands (Figures 3.14 and 3.15). The Jackpines delta, located along the distal margins of the Port Huron moraine (Figures 3.3 and 3.6), is graded to a higher shoreline elevation than the Chippewa River II delta, even though both deltas were presumably deposited during the glacial Lake Warren phase (Figure 3.14; Appendix C). These deltas perhaps formed during different Lake Warren phases (e.g., Warren I vs. Warren III) and were influenced by different rates of isostatic rebound (Figure 3.14; Table 3.3). This issue, again, designates the need for future studies to construct a ‘rebound corrected DEM’ for this area.

The Jackpines delta was deposited soon after the Port Huron readvance (Burgis, 1977). Burgis (1977) contends that the delta was initially active when water was ponded in the lower

reaches of the glacial Au Sable Valley. Burgis did not name this lake, and simply suggests that for a short period of time drainage was blocked by Port Huron ice that was slow to retreat in the northern Saginaw Bay region. The Jackpines delta continued to grow eastward as the Saginaw lobe retreated east and northward, largely when glacial Lake Warren extended into Saginaw Bay. During this time, the western margin of the Huron lobe remained at the Port Huron moraine (PHM) (Leverett and Taylor, 1915; Burgis, 1977; Blewett, 1991). Meltwater from the PHM in northeastern Lower Michigan fed a series of N-S trending outwash plains and channels that flowed into the glacial Au Sable River. Copious amounts of meltwater and sediment were then transported east towards the shoreline of glacial Lake Warren (Burgis, 1977). The present day Au Sable River watershed covers >4000 km² and mostly includes the Houghton Lake Sandy Flats and Ridges, Outer Port Huron Plains, and Graying Fingers physiographic regions. These regions are dominated by sandy and moderate to high relief landscapes (Figures 3.7 and 3.8; Schaetzl et al., 2013b). The fortuitous set of circumstances which included an extensive catchment area that would have presumably had large areas of sandy, frozen ground (Schaetzl, 2008), in combination with a meltwater source from a regional-scale ice-margin, led to the formation of the massive Jackpines delta. Also, note that there are no Huron Basin deltas associated with glacial Lake Wayne, probably because (1) it was short lived and (2) it was submerged beneath Warren III.

3.3.3.4 Lake Grassmere Deltas

The following deltas have longitudinal profiles that are graded to glacial Lake Grassmere in the Saginaw Basin, and presumably formed sometime between ≈14.7-14.3 cal ka BP: (1) Rifle

River II, (2) Cedar Creek II, (3) Au Gres River I, and (4) Sevenmile Hill (Figure 3.3; Table 3.3; Appendix B and C).

The Sevenmile Hill delta protrudes outwards at an elevation roughly 10 m below the central-outer margins of the Jackpines delta (Figure 3.16). The catchment area of the Sevenmile Hill delta is akin to the Jackpines delta (Figure 3.7; Appendix C). Unlike the Jackpines delta, the Sevenmile Hill delta did not have an extensive ice-marginal meltwater source (Figure 3.16). When the Sevenmile Hill delta was active the Port Huron (PH) ice margin had retreated northward to a position where meltwater from the ice margin was directed northwards, rather than to the south feeding the Au Sable River (Burgis, 1977).

3.3.3.5 Lake Lundy Deltas

Three additional deltas formed within the Saginaw basin after the Grassmere stage, probably during glacial Lake Lundy, ca. ≈ 15.1 -14.7 cal ka BP. They are the (1) Flint River, (2)

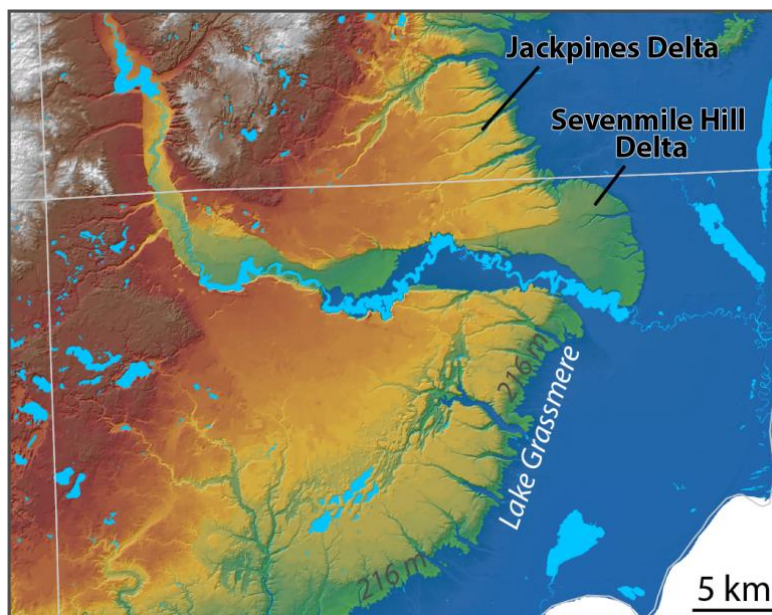


Figure 3.16: DEM flooded to a potential paleolake-level elevation for glacial Lake Grassmere, illustrating the Sevenmile Hill delta in relationship to the Jackpines delta.

Johnson Creek, and (3) Au Gres River II deltas (Figure 3.3; Table 3.3; Appendix C). Glacial Lakes Grassmere and Lundy were both relatively short-lived lake stages that had similar minimum and maximum lake-level elevations (Table 3.1) within the southern Great Lakes region where they have mainly been studied, making it difficult for researchers to determine the difference in ages between these two stages (Eschman and Karrow, 1985). Deltas that had a longitudinal profile graded to either glacial Lake Grassmere or Lundy were assigned to glacial Lake Grassmere if the delta was slightly higher in elevation (Table 3.3; Appendix C).

The Flint River delta is located distal to the Port Huron ice-marginal position, along the southern margins of the Saginaw basin (Figure 3.17). It lies between the Flint and Port Huron moraines (Figures 3.6 and 3.17; Appendix C). It has an extensive catchment area (presently > 3000 km²) that heads within the SE Michigan interlobate region (Figures 3.6 and 3.7). Presently, the Flint River catchment includes mostly moderately sloping landforms and loam textured sediments (Figures 3.7 and 3.8), but this area continued to supply enough sediment to the mouth of the Flint River to build a delta during glacial Lake Lundy.

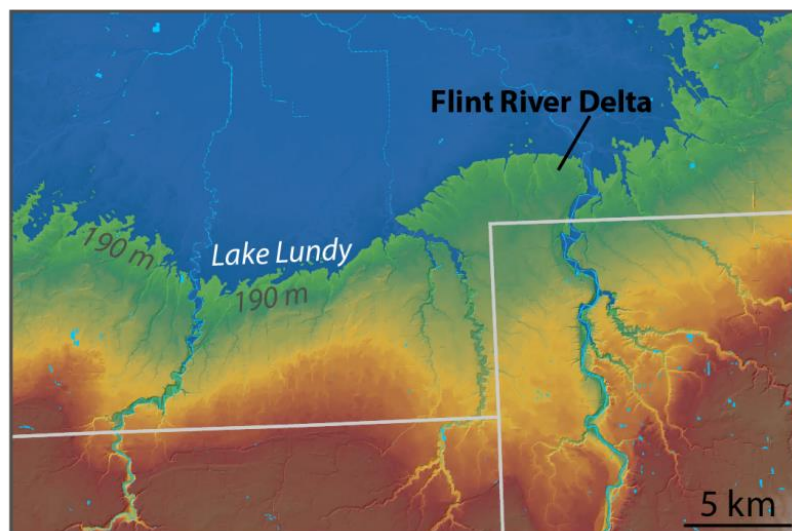


Figure 3.17: DEM flooded to a likely glacial Lake Lundy shoreline elevation, illustrating the Flint River delta.

Analogous to the Rifle River, Big Creek, Cedar Creek and Au Gres River deltas, the Johnson Creek delta is located along the eastern margins of the Port Huron ice-marginal position, in northeastern Lower Michigan (Figure 3.18). It has similar catchment area characteristics as those deltas (Figures 3.7 and 3.8). The Johnson Creek and Au Gres River II deltas were presumably built contemporaneously and merged in some areas, but later were incised and separated by Mongo Creek (Figure 3.18; Appendix C). The Au Gres River II delta is

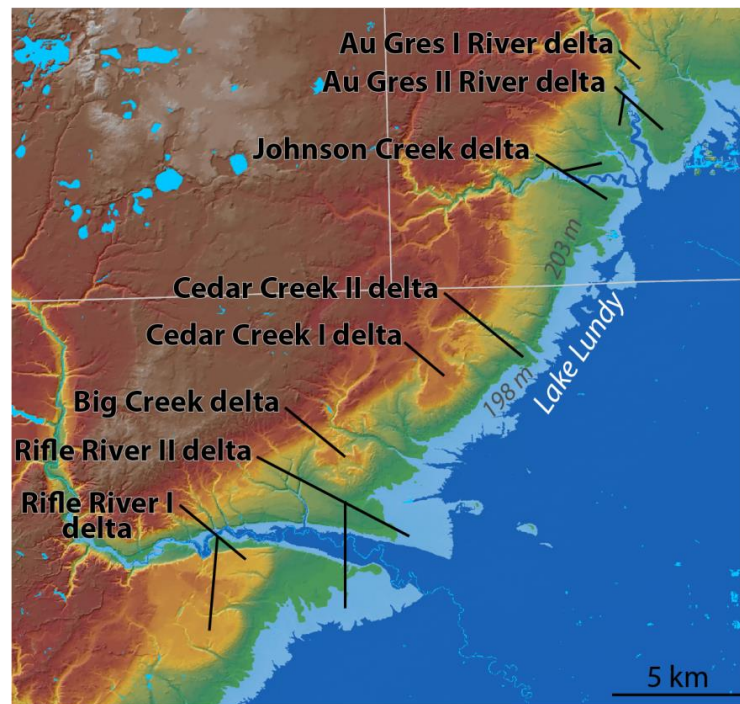


Figure 3.18: DEM flooded to likely glacial Lake Lundy shoreline elevations in northeastern Lower Michigan.

part of a delta complex and likely formed due to continued delta growth after glacial Lake Grassmere had transitioned into Lundy.

3.3.3.6 Other Deltas

This study identified ten deltas (H-17-26; Table 3.3) within the Lake Huron basin that have deltaic deposits graded to a shoreline elevation that is *not* identified and named within the literature on the glacial history of Lower Michigan. The Coy Ridge and Beaver Creek I and II deltas stand along the southern edge of the Coy and Eldorado ridges, located near the northern extent of the Houghton Lake Sandy Fats and Ridges region (Burgis, 1977; Schaetzl et al., 2013b). These three deltas have longitudinal profiles that grade smoothly northward into the E-W trending heads of outwash (Figure 3.19; Appendix B and C). For an unknown amount of time, meltwater presumably occupied the low areas between the sandy ridges (Tardy, 2005; Arbogast et al., 2015). The catchment areas associated with the Coy Ridge and Beaver Creek I and II deltas are composed of sandy deposits, but given the local depositional settings of these ice-marginal deltas, i.e., associated with heads of outwash, they presently have no catchment area (between $< 0.1\text{-}4\text{ km}^2$) (Figures 3.7 and 3.8). They stand above the St. Helen outwash plain (Burgis, 1977), which was likely periodically inundated with water during the deposition of the



Figure 3.19: DEM flooded to possible lake-level elevations within the Houghton Lake Sandy Fats and Ridges region, illustrating the Beaver Creek I and II and Coy Ridge deltas.

E-W trending heads of outwash that dissect this region (Figure 3.19; Appendix C). The diminutive size of the delta catchment areas suggests that the deltas were directly sourced from the ice margins that deposited the heads of outwash; therefore, I contend that the Coy Ridge and Beaver Creek I and II deltas are kame deltas. Because the heads of outwash were presumably deposited while the ice margin retreated northward during the Mackinaw interstadial, and ice did not advance again over this region, these deltas are assumed to have been deposited soon after ≈ 17.1 cal ka BP.

The Bull Gap, Kneeland, and Elk Hill deltas, also linked to an unnamed lake(s) (Table 3.3; Figure 3.3), were deposited north of the Houghton Lake Sandy Fats and Ridges province, and are associated with the glacial Au Sable meltwater channel (Figure 3.20). These deltas were presumably active when meltwater was ponded in northeastern LM, within the reentrant of the Port Huron moraine, when the Port Huron ice-margin blocked the Au Sable River from draining to the east (Figure 3.6) (Burgis, 1977). The Bull Gap delta has a relatively small, sandy, and high relief catchment area (Figures 3.7 and 3.8; Appendix C) and was aided by the steep terrain that

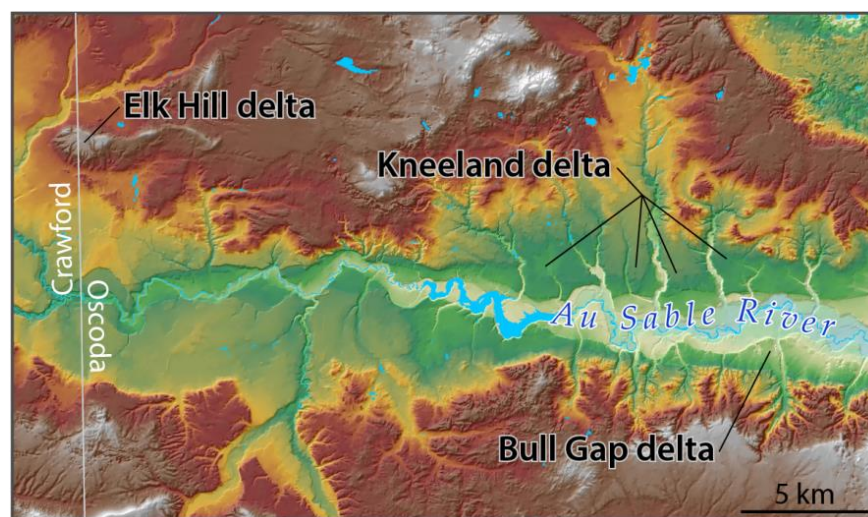


Figure 3.20: Illustrating the Elk Hill, Kneeland, and Bull Gap deltas and how they stand above the modern day Au Sable River.

dominates the catchment. The Kneeland delta also has a sandy, high relief catchment area (Figures 3.7, 3.8 and 3.20; Appendix C), however it has somewhat of a larger catchment area and for a given period of time the Port Huron ice margin likely also contributed meltwater to the delta. The Elk Hill delta, like the Coy Ridge and Beaver Creek I and II deltas, presently has an extremely small catchment area and was likely sourced directly from an ice margin, making it a kamic feature. All three of the deltas (i.e., the Bull Gap, Kneeland, and Elk Hill deltas) were deposited during and soon after the Port Huron advance. Because the ice margin did not again advance over this region, these deltas probably formed sometime after ≈ 15.1 cal ka BP.

The Indian Creek I and II, Turtle Lake, and Brush Creek deltas are located in NE Lower Michigan, along the proximal side of the ice-contact slope of the Port Huron moraine (Figures 3.3, 3.6 and 3.21; Appendix C). As the Port Huron ice-margin retreated northward from its southernmost position, standing water must have occupied the low areas in NE Michigan; drainage was blocked by the high topography to the south (i.e., Port Huron moraine) and the

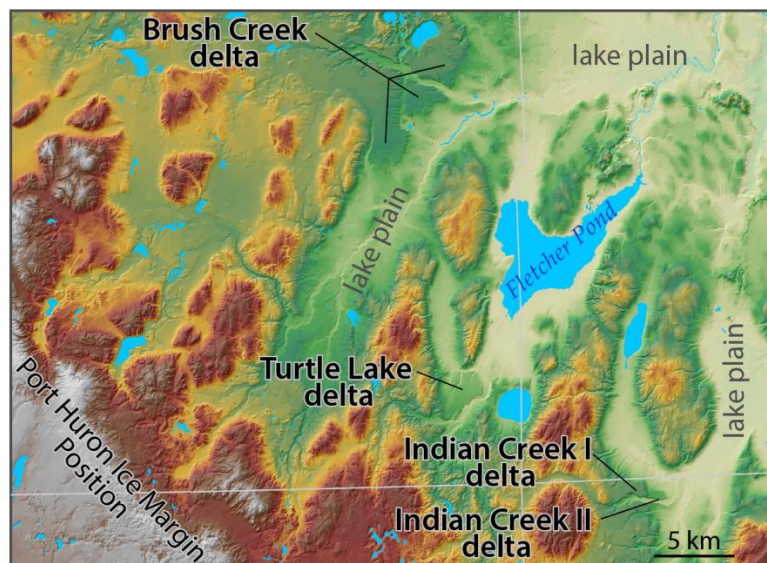


Figure 3.21: Highlighting the Indian Creek I and II, Turtle Lake, and Brush Creek deltas in NE Michigan and the low relief lake plain areas the deltas stand above.

ice-margin to the north (Figure 3.21). These deltas presently have moderately sized catchment areas and they are not interpreted as kamic features but perhaps were sourced from runoff, opposed to direct glacial meltwater. The catchment areas are dominated by sandy and loamy sediments and moderate to high relief landscapes (Figures 3.7 and 3.8). The Indian Creek I and II, Turtle Lake, and Brush Creek deltas are seemingly associated with one or more unnamed lakes that intertwine within the broad uplands of NE Michigan, but which are now broad, low relief areas that are also low in elevation (Figure 3.21). The deltas were likely deposited very shortly after the Port Huron advance (≈ 15.1 cal ka BP).

3.3.3.7 Lake Algonquin Deltas

The Black River, Sturgeon-Pigeon River, and McPhee Creek deltas have longitudinal profiles that are graded towards the glacial Lake Algonquin shoreline within northern Lower Michigan (Table 3.3; Figures 3.3 and 3.22; Appendix B and C). As such, these deltas were seemingly active sometime between ≈ 13.2 and 11.5 cal ka BP (Drzyzga et al., 2012; Vader et al.,

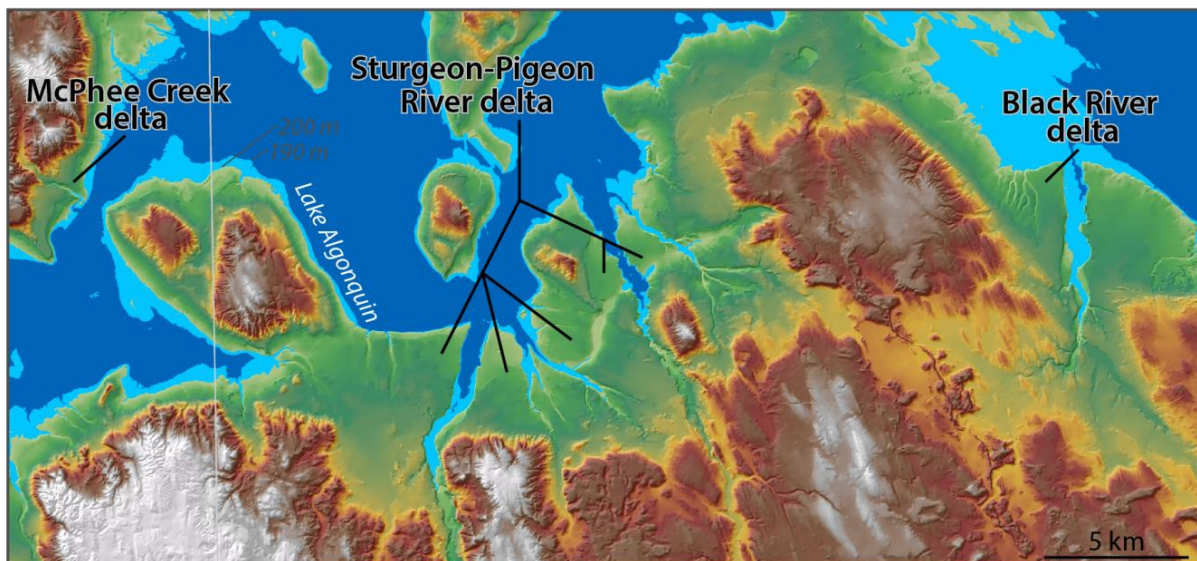


Figure 3.22: DEM flooded to a likely Lake Algonquin shoreline elevation, illustrating the Black River, Sturgeon-Pigeon, and McPhee Creek deltas.

2012). Vader et al. (2012) documented the topographic and textural characteristics of the Black River delta. In their study, they illustrate several particle-size distribution maps of sediments near the delta surface that suggest a westward longshore drift direction during its formative period. These data support strong easterly winds for a given period of time during Lake Algonquin in NE Lower Michigan (Krist and Schaetzl, 2001). The study by Vader et al. (2012) exemplifies how mapping the morphologic and textural characteristics of a relict delta can help interpret the paleoclimate of the late Pleistocene.

The Black River, Sturgeon-Pigeon River, and McPhee Creek deltas presumably formed penecontemporaneously. The Black River and Sturgeon-Pigeon River presently have large catchment areas that are dominated by sandy, high relief landscapes (Figures 3.7 and 3.8; Appendix C). Similar to the Indian Creek I and II, Turtle Lake, and Brush Creek deltas, the Black River and Sturgeon-Pigeon River deltas are located along the proximal side of the ice-contact slopes of the Port Huron moraine in northern Michigan (Figures 3.6 and 3.22). The Sturgeon-Pigeon River delta was presumably deposited by both the Sturgeon and Pigeon Rivers and formed as their deltaic deposits merged (Figure 3.22). Roughly 12 km northwest of the Sturgeon-Pigeon River delta, the McPhee Creek delta stands near the southern edge of Brutus-Levering Island (Schaetzl et al., 2013b), and was likely sourced by meteoric water (i.e., runoff). This island was molded by Port Huron and Greatlakean ice and is part of a sandy, moderate to high relief, archipelago within glacial Lake Algonquin (Figures 3.6, 3.7).

3.3.4 Lake Michigan Basin Deltas

The Lake Michigan basin was occupied by glacial Lakes (from oldest to youngest) Chicago – Glenwood I, Mackinaw Low, Chicago – Glenwood II, Two Creeks, Calumet, Toleston, and Algonquin between ≈ 17.1 and 13.7 cal ka BP during the retreat from the LGM (Table 3.1). This study mapped 15 deltas graded to two lake stages (i.e., Chicago and Algonquin) within the Lake Michigan basin.

The Maple River delta, the oldest delta mapped in this study within the Lake Michigan basin, is located near the southeastern corner of the Saginaw lowlands in Clinton County (Figures 3.3 and 3.23; Appendix C). The Maple River delta is graded to the Imlay channel. The delta was deposited east of the Portland moraine, near the Flint and Owosso moraines (Figures 3.3, 3.6 and 3.23). Presently the Maple River has a relatively small catchment area that is dominated by low relief landforms and loamy deposits. The Maple River delta would have been active while the Imlay channel was directing meltwater from the Lake Erie basin to the Saginaw basin. Leverette and Taylor (1915) discussion of the Maple River delta (?) begins on the bottom of page 256 of Monograph 53: "At that time [referring to when the Imlay outlet river first began

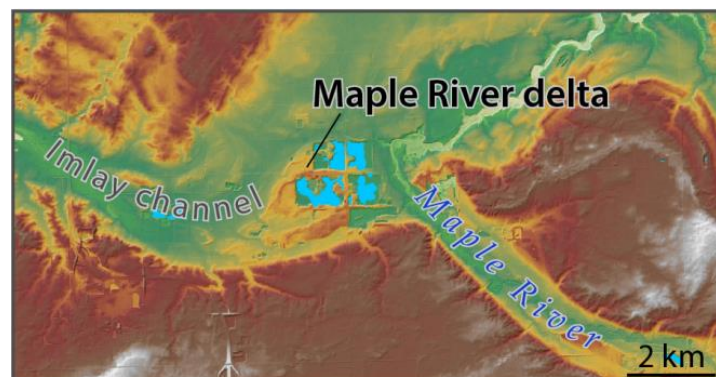


Figure 3.23: Maple River delta in relationship to the Imlay channel.

to flow when the Saginaw Lobe margin was at the Flint Moraine] the outlet river had a small lake-like expansion just west of Duplain. In the east side of this a large gravel deposit occupies the position of a delta, but seems rather to have been an island-like obstacle in the flow of the river ..." Leverett and Taylor continue their discussion of this feature on page 257, "This deposit seems more like a kame than any other type - a kame deposited in a small reentrant of the ice front and shaped partly by the ice with which it was in contact and perhaps partly by the later river current. It seems impossible to explain its peculiarities on the supposition that it is simply a delta." Today there are a series of active gravel pits occupying the Maple River delta, providing evidence of sands and gravels, however making it difficult to acquire a representative profile for this feature (Appendix C). The morphology and soils data alone suggests that this feature is a delta, although further analysis of subsurface data is needed in order to clarify that this feature is indeed a deltaic feature.

The Mackinaw Low lake stage occurred within the Lake Michigan basin during roughly the same time (between ≈ 15.5 and 15.1 cal ka BP) that Lake Ypsilanti occupied the Lake Erie basin and the Post-Arkona Low existed in the Lake Huron basin (Table 3.1; Eschman and Karrow, 1985; Hansel and Mickelson, 1988). Similar to the Lake Ypsilanti and Post-Arkona Low, the Mackinaw Low was presumably fixed at an elevation below 175 m asl, perhaps around 170 m asl (Table 3.1), and thus no deltas were mapped in this study associated with the Mackinaw Low stage.

The Zeeland and Allendale deltas stand nearly 10 km inland from the present-day mouths of the Grand and Macatawa Rivers, in Ottawa County (Figure 3.24). Both deltas are grade toward glacial Lake Chicago – Glenwood II phase (Figure 3.3; Table 3.3; Appendix B and C)

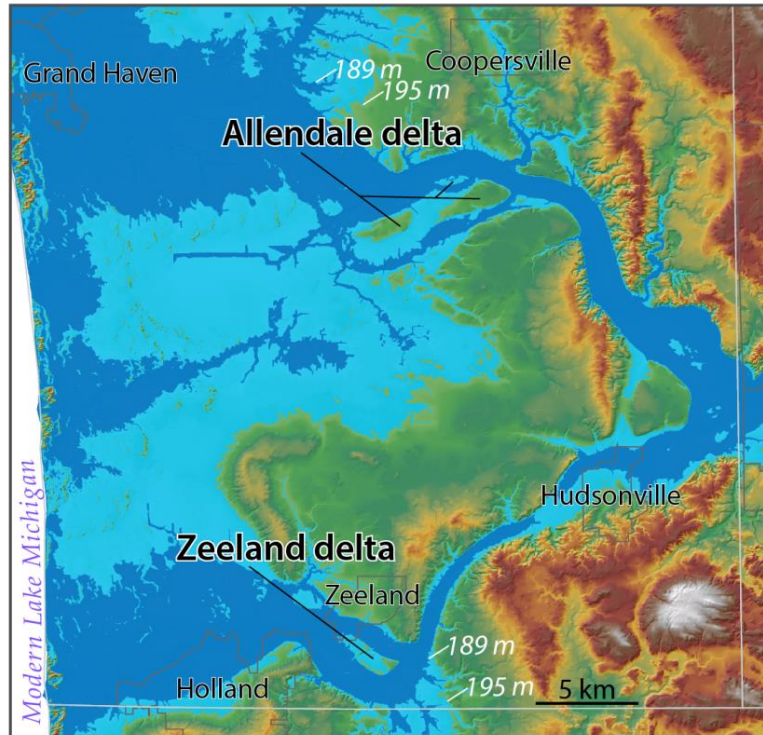


Figure 3.24: DEM flooded to the Calumet and Glenwood II lake-level elevations, illustrating the Allendale and Zeeland deltas and their midchannel bars – characteristic of fluvial dominated deltas.

and were probably active sometime between ≈ 15.1 and 14.7 cal ka BP (Leverett and Taylor, 1915; Bretz, 1953, 1966; Martin, 1955; Hough, 1958, 1963; Evenson, 1973; Muller, 1977; Kehew, 1993). The Zeeland and Allendale deltas are presently part of the Grand River watershed which includes an extensive amount ($> 13,500 \text{ km}^2$) of central Lower Michigan (Figure 3.7; Appendix C). The modern day catchment area is dominated by low to moderately sloping landscapes that are mainly loam textured (Figure 3.7). Like the Cass River delta in the “thumb” of Michigan, the Zeeland and Allendale deltas are located at the mouth of a spillway that joined two vast glacial lakes; they display several midchannel bars (Figure 3.24). These deltas were deposited contemporaneously for some period of time, while the glacial Grand

Valley drained the retreating Saginaw lobe, and while it directed proglacially ponded meltwater from the Lake Huron and Erie basins into the Lake Michigan basin (Kehew, 1993).

Within the Lake Michigan basin, the following six deltas have longitudinal profiles that are graded towards a shoreline elevation that is not identified and named within the literature:

(1) Sanborn Creek Fan, (2) Lake City-Harrison Ridge, (3) Slagle Fan, (4) Cole Creek Fan, (5) Houghton Lake Ridge, and (6) Higgins Lake Ridge (Table 3.3; Figure 3.3; Appendix B and C). The Sanborn Creek Fan, Slagle Fan, and Cole Creek Fan deltas are located in Lake and Wexford Counties in northwestern Lower Michigan (Figure 3.25). The deltas stand on the west side of the Lake Border moraine, at the base of the steep ice-contact slopes that are associated with the moraine (Figures 3.6 and 3.25). Similar to those deltas that formed in northeastern Michigan, in association with the ice-contact slopes of the Port Huron moraine and the retreating ice-margin, the Sanborn Creek Fan, Slagle Fan, and Cole Creek Fan deltas likely

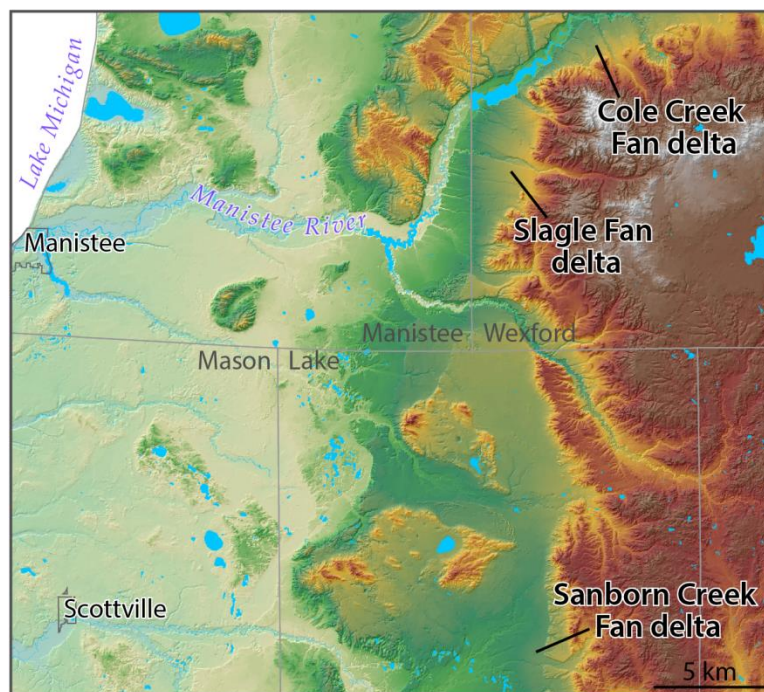


Figure 3.25: The Sanborn Creek Fan, Slagle Fan, and Cole Creek Fan deltas in relationship to the Manistee River.

initially formed as ice pulled back from a topographic high and ponded water between the ice margin and the surrounding higher landscape. Here, during the Mackinaw interstadial, the Michigan lobe would have retreated west and north from the Lake Border moraine, possibly allowing water to pool (Figure 3.6).

The deltaic deposits from the Slagle Creek Fan delta, located ≈ 5 km southwest of Mesick, are exposed in cutbanks as much as 30 m above the modern river, because of fluvial incision by the Manistee River, as its base level lowered over time (Luehmann et al., 2013). The deltaic sediments are horizontally laminated fine to medium sands, with clay and silt in thin rhythmites, often illustrating penecontemporaneous loading and dewatering deformation structures (Kincare, K.A. pers. comm.). After the Slagle Creek fan/delta was predominantly emplaced by fluvial processes, it was likely buried by colluvial fan sediments that were eroding out of the sandy, high-relief moraine that borders the southern margins of the Manistee River, hiding the delta's original geomorphology.

The Sanborn Creek Fan and Cole Creek Fan deltas have topographic and sedimentologic characteristics comparable to the Slagle Creek Fan delta and thus are interpreted to have evolved via similar geomorphic processes (Figure 3.25). All three fan deltas presently have small to moderately size catchment areas, but are dominated by highly sloping landscapes that are mostly composed of sand-textured sediments (Figures 3.7 and 3.8; Appendix C).

Like the Coy Ridge and Beaver Creek I and II deltas, the Lake City-Harrison Ridge, Houghton Lake Ridge, and Higgins Lake Ridge deltas are kame deltas that protrude from the heads of outwash that encompass the Houghton Lake Sandy Fats and Ridges region (Figure 3.26). The Houghton Lake Ridge and Higgins Lake Ridge deltas are located in northern

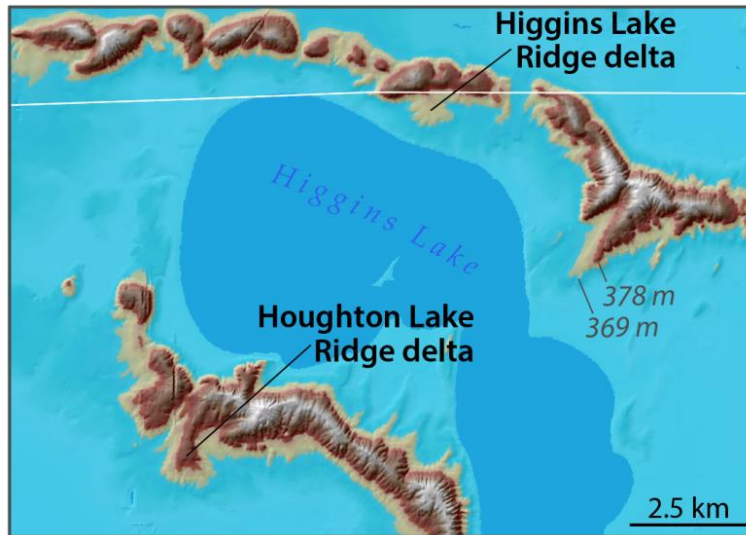


Figure 3.26: DEM flooded to several potential paleolake-level elevations, illustrating the Houghton and Higgins Lake Ridge delta and how they grade southward from the E-W trending heads of outwash that encompass the Houghton Lake Sandy Fats and Ridges region.

Roscommon County (Figure 3.26), whereas the Lake City-Harrison Ridge stands roughly 25 km south in Missaukee County. The catchment areas associated these deltas are mostly composed of sandy deposits, but given the narrow structure of the heads of outwash, the deltas presently have extremely small catchment areas (between $< 0.2\text{--}6\text{ km}^2$) (Figures 3.7 and 3.8; Appendix C). The small to nonexistent catchment areas for these deltas suggests that the deltas were directly sourced from the ice margins associated with the heads of outwash, making them kames. Furthermore, because the ice margin made an incremental northward retreat during the Mackinaw interstade, these deltas are assumed to have been deposited time-transgressively sometime after $\approx 17.1\text{ cal ka BP}$ (Figures 3.1, 3.3 and 3.6).

The Fair Plain delta stands in the southwest corner of Lower Michigan, in Berrien County (Figure 3.27). The delta is roughly 2 km inland from the mouth of the St. Joseph River. The Fair Plain delta has deltaic deposits that merge with the shoreline of the Calumet phase of glacial

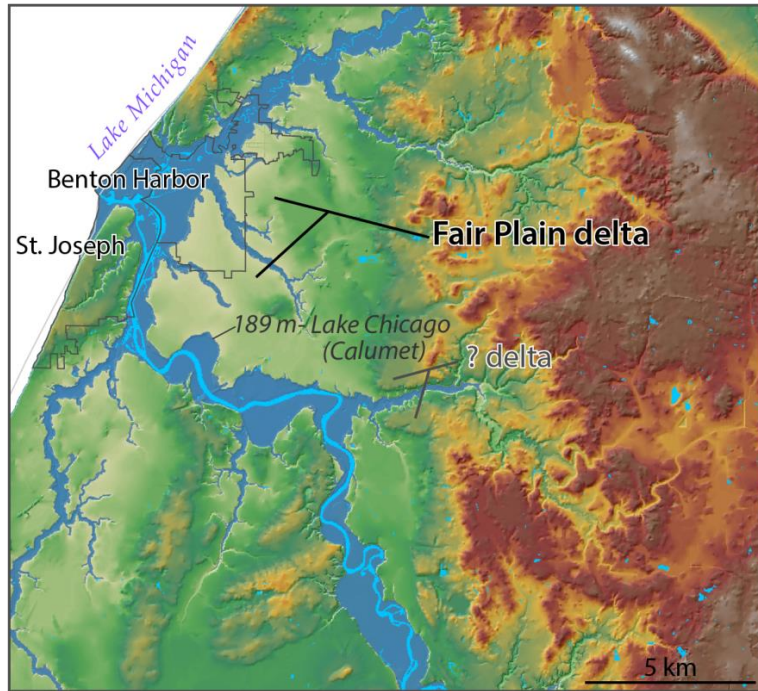


Figure 3.27: DEM flooded to the Calumet phase of glacial Lake Chicago, illustrating the Fair Plain delta.

Lake Chicago, implying that the delta formed sometime between ≈ 13.7 and 12.9 cal ka BP (Table 3.3; Figure 3.3; Appendix B and C). The delta presently has a moderately sized catchment area ($> 1300 \text{ km}^2$) that is mainly composed of low sloping landscapes that mostly consist of sandy deposits (Figures 3.7 and 3.8; Appendix C). The Fair Plain delta abuts the Valparaíso ice-marginal position on the west side, and conceivably formed soon after the St. Joseph River redirected its drainage from a southern direction (into the Kankakee Torrent) to mainly a northerly direction, into glacial Lake Calumet (Figure 3.6; Kincare, 2007).

The Platte River, Boardman River, Rapid River, Deer Creek, and Brown Creek deltas are all located in northwestern Lower Michigan, within Benzie, Grand Traverse, Kalkaska, and Charlevoix Counties (Figure 3.28; Appendix C). The deltas stand just north of the Greatlakean ice-marginal position, i.e., the extent of the Two Rivers-Onaway phase limit (Figures 3.1). These

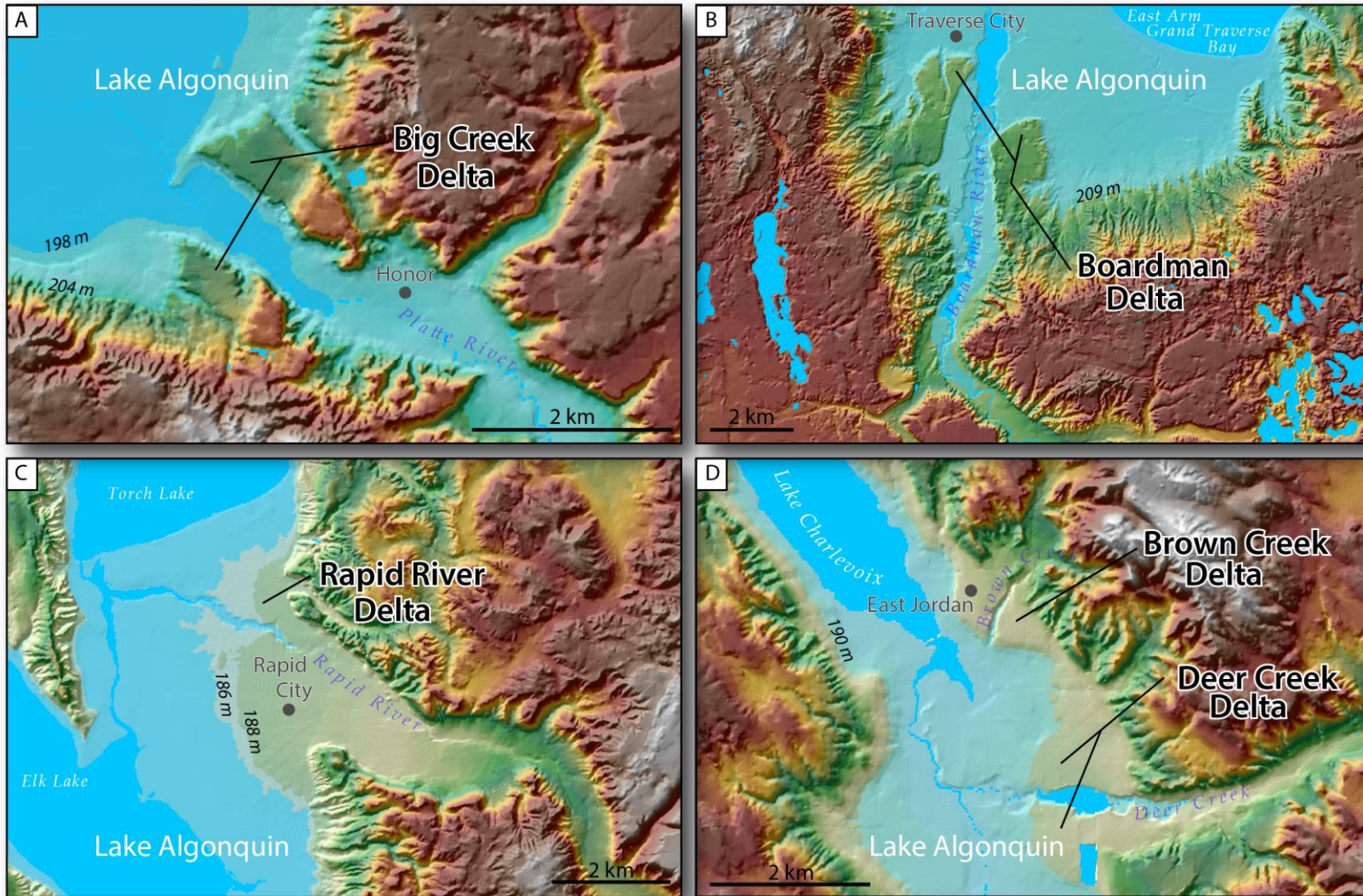


Figure 3.28: (A-D) DEM flooded to one or more Lake Algonquin paleolake-level elevations, illustrating the well defined, symmetrical shape of these deltas, all of which formed in NW Lower Michigan. Note: Lake symbology has no reference to water depth.

deltas have longitudinal profiles that are graded towards the glacial Lake Algonquin shoreline and as such, the deltas presumably formed sometime between ≈ 13.2 and 11.5 cal ka BP (Table 3.3). The five deltas presently have small to moderately size catchment areas (ave. $< 300 \text{ km}^2$) that are largely composed of moderate to highly sloping landscapes and mostly consist of sandy and sandy loam-textured deposits (Figures 3.7 and 3.8; Appendix C). These catchments mainly include ice-contact landforms and meltwater channels associated with the Greatlakean readvance; they incorporate the Northern Lower Peninsula Tunneled Uplands physiographic region (Schaetzl et al., 2013b). This physiographic region is a high relief landscape that is dominated by large, steep-sided uplands that are often gullied and/or hummocky (Schaetzl et al., 2013b).

3.5 Profiles

The surface, longitudinal profiles of the 61 landforms identified as deltas in this dissertation are illustrated below in Figures 3.29 and 3.30, as well as in Appendix B. These data were obtained by plotting the land surface elevation at ≈ 10 m increments along a transect drawn near the center axis of the landform, starting approximately at the junction between the valley mouth and relict shoreline, and ending at the basin floor. In the profile diagrams, both the Y and X axes are normalized, in order to better compare the topographic characteristics of each profile (Figures 3.29 and 3.30).

To better categorize the various delta forms, I have divided them into groups based on their surface-profile shape, leading to two different profile shapes: (1) Gilbert-type delta profiles ($n = 39$) and (2) generally linear profiles ($n = 22$) (Figures 3.29 and 3.30). Figure 3.31 shows an idealized example of each of the profile groups.

Many of the Gilbert-type delta profiles resemble traditional, sandy, lacustrine deltas (Milligan and Chan, 1998; Vader et al., 2012; Gobo et al., 2014; Blewett et al., 2015). These profiles show both flat and/or gently sloping delta plains, and have a clear and often relatively steep delta front. The gradually sloping delta plain is likely linked to the source river's ability to supply sandy, coarse grained sediments to the delta. The relatively steeply sloping delta plain develops in order to efficiently transport sandy sediments from the apex of the delta to its margins. Conversely, the relatively flat delta plain may develop because a lower gradient or a slower water velocity is necessary to transport fine material, such as clay, silt, and fine sand, to the delta front. Moreover, note that several of the Gilbert-type delta profiles in Figure 3.29

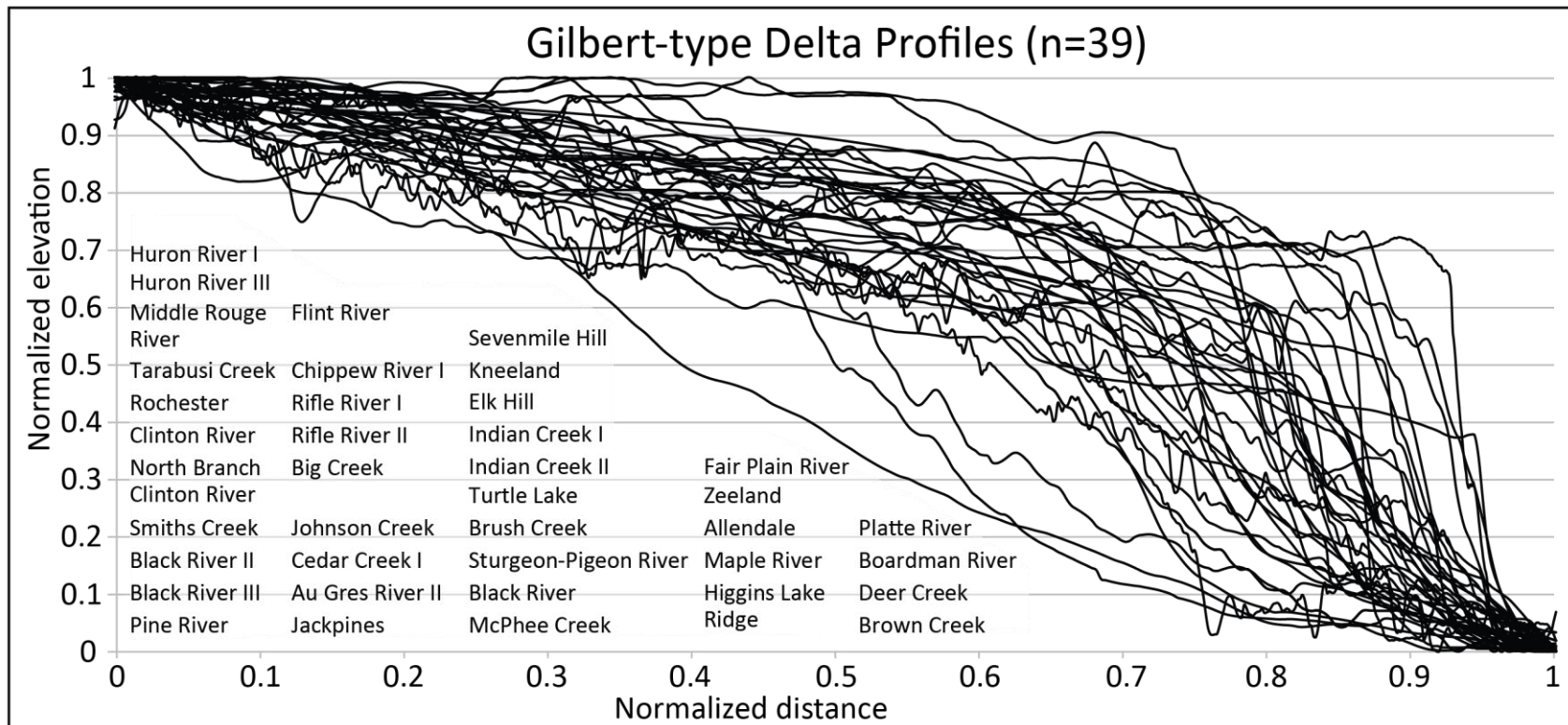


Figure 3.29: Topographic profiles of the 39 deltas that have a Gilbert-type surface profile. Many of these landforms have a well developed, generally flat delta plain, and a steep delta front.

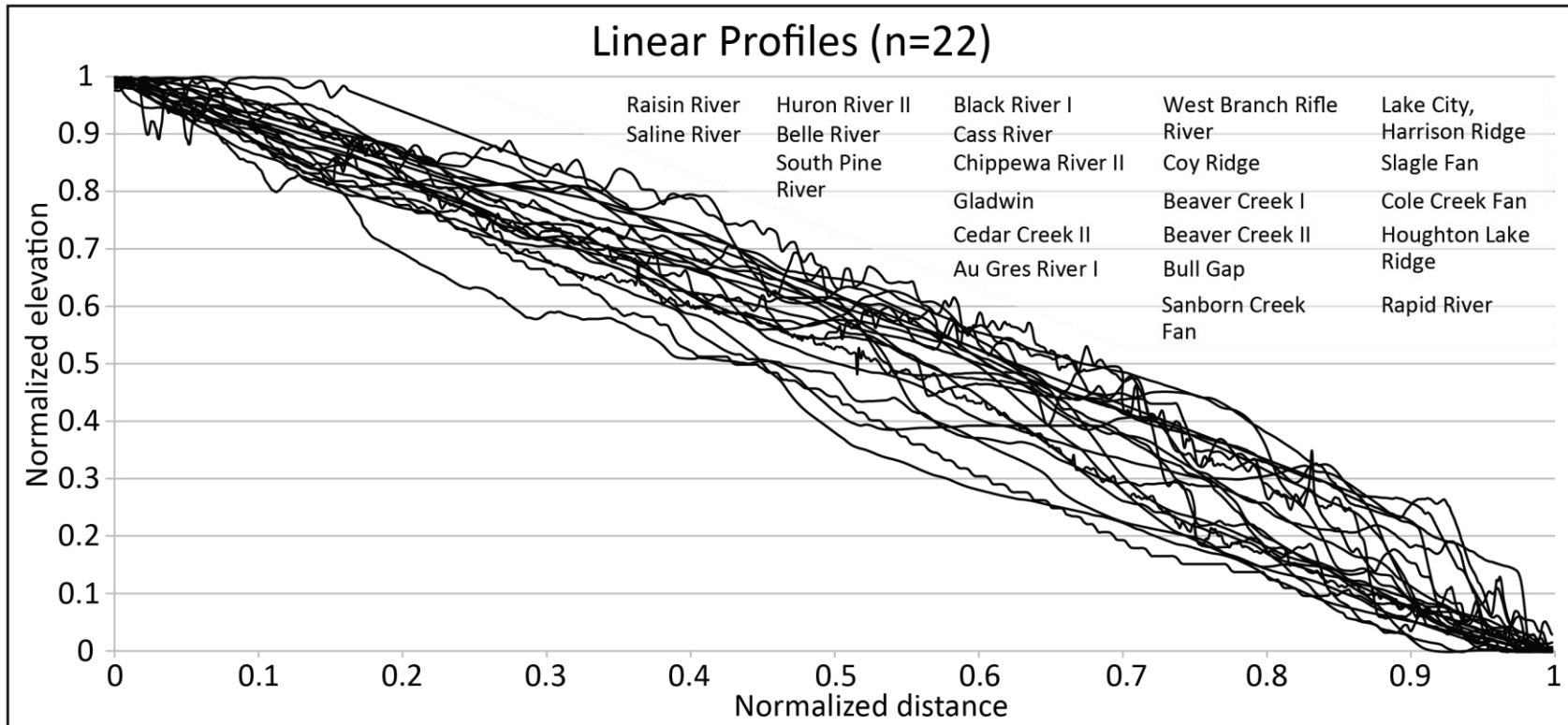


Figure 3.30: Topographic profiles of the 22 deltas that have a nearly linear profile from the apex to the toe of the delta.

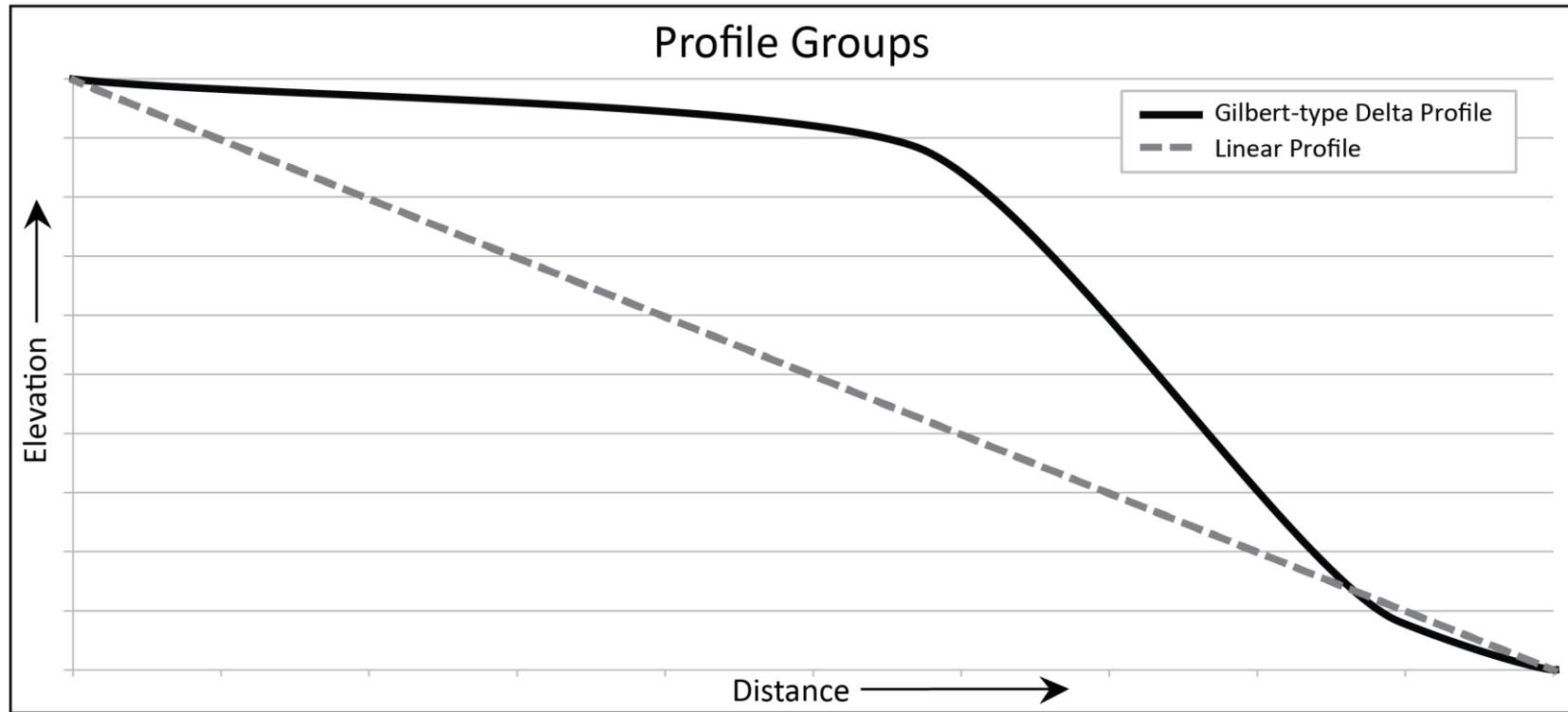


Figure 3.31: An illustration of an idealized topographic profile for each of the two main profile groups mapped in this study.

have a concave-upward slope that extends basinward, beyond the linear portion (i.e., delta plain) of the profile (Appendix B). These Gilbert-type delta profiles may illustrate deltas that have been eroded by waves from lower, succeeding lake levels. Gilbert-type delta profiles that show a relatively short delta plain and a long/broad, concave-upward slope likely represent deltas that have been influenced to a larger degree by post-deposition, erosion processes. Conversely, profiles with a short, concave-upward slope and a large delta plain may symbolize deltas that were minimally shaped by post-depositional, erosion processes.

Unlike the Gilbert-type delta profiles, 22 others show a generally linear form along the representative transect (Figure 3.30; Appendix B). In many cases, these profiles are particularly steep and lack the two definitive slope segments of the Gilbert-type deltas, i.e., a generally linear, low gradient slope that grades into a relatively steep, distal slope. Because the generally linear delta profiles do not illustrate a distinct delta plain and delta front, some may actually represent fan-like features that were built onto lake plains after the lakes had lowered, or no longer existed in the basin. Such landforms may not be *true* deltas, but are categorized as such in this dissertation because they are linked to either a modern or prehistoric fluvial system, are fan- or broad-shaped in plan view, and are graded towards a relict shore-zone.

Deltas and fans which form in different depositional situations - a delta is built largely under subaqueous conditions whereas a fan forms mostly under subaerial conditions - may acquire the same form and slope, making it difficult to differentiate between the two when they become relict. However, it is not the purpose of this research to differentiate between deltas, pseudo deltas, alluvial and colluvial fans. Rather, this dissertation is an exploratory study that presents an inventory of delta-like landforms in southern Michigan.

In summary, the deltas mapped in this study have generally two types of longitudinal profiles. Gilbert-type delta profiles are thought to represent traditional, sandy lacustrine deltas, whereas other deltas or fans have more linear profiles; additional data are needed to differentiate between the genesis of the landforms with these two types of profiles. Subsequent investigations of these landforms should incorporate a sedimentological approach, as opposed to using mainly geomorphic and topographic methods for their identification and interpretation. The various maps, figures, and data presented in this dissertation pinpoint many delta-like features and provide a strong foundation for additional research on these landforms.

3.6 Review and Implications

This study presents an extensive map of Pleistocene deltas in the Lower Peninsula of Michigan. Elevation data (10 m NED DEM), used in conjunction with surface and subsurface textural data (NRCS SSURGO county-level soils maps and water and oil/gas log data), enabled the mapping of 61 Pleistocene deltas - 27 of these have been acknowledged in previous works, whereas 34 deltas are unique to this study and are thus, newly documented. Most of the relict deltas are associated with one or more fluvial systems presently within the region that acted as major meltwater conduits during the late Wisconsin (MIS 2) and likely transported copious amounts of sediment. The majority of the deltas that were mapped are graded towards an ancestral Great Lakes' shoreline; however 16 deltas, several of which are kame deltas, terminate into an unidentified and currently unknown or unstudied paleolake (most likely small, ice marginal lakes). Furthermore, many of the deltaic systems and landforms mentioned in previous works consist of multiple deltas (i.e., a delta complex) and formed during several lake stages.

During deglaciation, many regions in Lower Michigan would have presumably had an abundance of freshly exposed sediment, with thawing ground and remnant glacial ice, and likely had minimal vegetation. These periglacial conditions would have promoted an unstable landscape and encouraged a massive amount of sediment to be transported to the lake basins, promoting delta formation. The catchments areas associated with the relict deltas in southern Lower Michigan are dominated by low to moderate relief landscapes and the soils have relatively low percent sand contents in their subsoil horizons. Conversely, the catchments in northern Lower Michigan are dominated by relatively high relief landscapes and sandy soils. The relatively slow infiltration rates associated with the loamy textured sediments would have favored surface runoff in the southern delta catchment areas. Surface runoff perhaps invoked sizable amounts of sediment directed towards the mouths' of those catchments. Hence, the textural characteristics of the delta catchments in southern Michigan may have contributed to delta formation. Alternatively, the relatively steep terrain and sandy landscapes associated with the northern delta catchments may have promoted delta construction there.

This research has a number of implications: (1) natural or statistically derived groupings of the various delta regions could reveal the different atmospheric, hydrologic, and/or terrestrial conditions that influence delta formation , (2) the numerous unidentified deltas indicates that there existed several pro- and postglacial lakes, or lake phases, that were overlooked or unidentified in previous works, (3) because so many (>30) deltas formed in sandy landscapes, with sandy catchments, this suggests that many areas in northern Michigan were likely impermeable and thus often frozen during the period of delta formation, (3) relict deltas may record more persistent lake level elevations, as compared to elevations inferred from

beach ridges, shoreline berms, or escarpments, and lastly (4) maps of relict deltaic landscapes could serve as references for potential borrow pit operations (namely sand) and agricultural land, or used to guide land-use decisions.

The map of Pleistocene deltas in Lower Michigan, illustrated in this study, will hopefully encourage researchers to study some of these relict deltaic systems within the Great Lakes region. Additional studies on relict deltas in Michigan and the surrounding Great Lake states will ultimately advance our knowledge in ice margin locations, landscape and lake-level instabilities, wave energy, and wind direction during the Pleistocene.

3.7 Conclusions

This study has shown that far more deltas exist in Lower Michigan than had been previously reported in the literature. During the late Wisconsin, massive amounts of sediment were transported and deposited within the Great Lakes basins, to form these deltas and fans. The sheer size of the features illustrates that the deglacial landscapes of southern Michigan were unstable for several hundreds to even thousands of years following deglaciation, as in Wisconsin (Clayton et al., 2001; 2008).

The deltas chronicled in this research occur where a valley mouth joins an abandoned shoreline. These deltaic deposits may be important proxies for paleo-terrestrial, -shoreline, -atmospheric and -hydrologic conditions during their formative periods, and if so, such information may be useful to reconstruct the evolution of those landscapes. Moreover, the deltaic deposits can serve as a resource for aggregate or fill materials, and the low relief landscapes provide excellent conditions for agriculture and forestry.

Based on their *surface* topography, morphology, and soil characteristics, I identified 61 landforms in Lower Michigan that presumably may have had deltaic origins. It goes without saying that additional analyses of the *subsurface* topography and sedimentology are necessary to confirm whether each feature has specific deltaic lineages, particularly topset and foreset bedding, and basin-ward textural fining trends. Landforms in the delta "list" that lack these subsurface structures and/or textural trends may indicate that they formed mainly under subaerial conditions and are thus alluvial/colluvial fans. It is not the purpose of this research, however, to discriminate between these genetic histories. Rather, this is an exploratory study that develops a sweeping inventory of delta-like landforms. This list is provided in Table 3.3.

Chapter 4 – Natural Groupings of Relict Late-Pleistocene deltas in the Lower Peninsula of Michigan

4. Introduction

Deltas represent a river's ability to deposit more sediment at its mouth than can be accommodated by the nearshore water body and removed by longshore drift (Barrell, 1912; Miall, 1976). Leverett and Taylor (1915) identified over 20 relict deltas in the Lower Peninsula of Michigan in their classic USGS Monograph 53 (Luehmann, 2015). Following Monograph 53, Scherzer (1916) and Bay (1937; 1938) published several Quaternary geology maps for the Detroit area that highlight many of the same deltas. Several years later, Martin (1955) published a "Map of the Surface Formations of the Southern Peninsula of Michigan" which then labeled the majority of those deltas previously documented in Monograph 53. More than 20 years later, Burgis (1977) reported on the glacial landforms and meltwater patterns in northeastern Lower Michigan in her PhD dissertation. Burgis highlighted the evolution of several of the deltas mentioned in Monograph 53, and also identified a few additional deltas in northern Lower Michigan. Excluding Burgis (1977) and a few more recent studies that discussed relict deltas in Michigan (i.e., Kehew, 1993; Vader et al., 2012; Blewett et al., 2014), research involving the mapping and description of relict deltas in Michigan has been minimal since Leverett and Taylor's (1915) seminal work. Indeed, beach ridges, as well as shoreline features such as berms and escarpments, have continued to be the foci of studies of paleolakes, and it is these features, not deltas, that have generally served as the indicators of paleoshoreline location and paleolake elevation within the Laurentian Great Lakes (e.g., Forsyth, 1959; Thompson, 1992; Thompson and Baedke, 1995; Holcombe et al., 2003; Schaetzl et al., 2002;

Baedke et al., 2004; Drzyzga, 2007; Drzyzga et al., 2012). Even though, as Milligan and Chan (1998) and Gobo et al. (2014) clearly documented, ancient deltas such as coarse textured Gilbert-type deltas can provide an excellent record of water plain fluctuations within a basin.

Burgis (1977) published one of the first studies in Michigan to document the utility of relict deltas, beyond simply as a proxy for shoreline *position*. Her dissertation illustrated how glacial meltwater patterns and sediment sources can be inferred from mapping the topographic characteristics of relict deltas in northern Michigan. Kehew (1993) also documented that glacial lake outbursts and episodic valley incision can be interpreted from relict deltas. That study employed the topographic, sedimentologic, and geographic relationships between several shoreline features, including a relict delta located at the mouth of a major meltwater spillway, in order to discern flooding events. More recently, Vader et al. (2012) demonstrated that relict deltas can provide clues to wind and longshore drift direction, as well as wave energies. Additionally, in the Upper Peninsula of Michigan, Blewett et al. (2014) asserted that the surface and subsurface characteristics of several relict deltas can indeed provide evidence of past ice marginal positions and lake levels.

Numerous studies in the western United States have mapped the geomorphic components of late Pleistocene deltas, e.g., within Lake Bonneville, as well as other shoreline features, in order to aid in the reconstruction of past glacial chronologies, paleoclimate, limnology, and hydrology (e.g., Atwood, 1909; Hunt, et al., 1953; Bissell, 1963; Scott et al., 1983; Currey and Oviatt, 1985; Smith and Jol, 1992; Milligan and Chan, 1998; Lemons et al., 1999; Oviatt et al., 2003; Nelson et al., 2005; Nishizawa et al., 2013). These relict delta studies, and the few conducted in Lower Michigan, have demonstrated that further analysis of the

geomorphic components associated with relict deltas may indeed help us understand the environmental conditions during their formative periods. Mapping the morphologies of relict Pleistocene deltas will also help recognize the morphologic variation in the types of deltas that formed during deglaciation. The different groupings of deltas can then perhaps be linked to distinct morphologic processes and act as proxies for various paleo-climate, -terrestrial and -coastal conditions during their emplacement.

This study provides examples of the utility of mapping relict Pleistocene deltas. I provide quantitative descriptions of many of the relict deltas identified in previous work, as well as contributing data on several additional (newly discovered) relict deltas in Lower Michigan. The purpose of this chapter is to numerically group the 61 deltas listed in Chapter 3 of this dissertation and to categorize the deltas based on their unique characteristics. Categorizing the relict late-Pleistocene deltas will shed light on the different morphologic processes that were contributing to delta formation in different regions of Michigan, which may provide insight to the different paleocoastal and terrestrial conditions during that time period.

Deltas will be grouped mainly according to their topography, size, fluvial and sediment characteristics, wetness, and glacial history, with the goal of highlighting the different types of deltas and determining if these types have distinct geographies. The methods used to delineate relict delta boundaries and their present-day catchment areas are a focus of this chapter; they may be useful for mapping relict deltas elsewhere. Furthermore, the statistical grouping procedure presented here is sufficiently flexible so to be applicable to a wider range of geologic features.

4.1 Background

4.1.1 Delta Components and Terminology

The major geomorphic components of a delta generally include the feeder and distributary channels, delta plain, delta front, and prodelta (Gilbert, 1890; Wright and Coleman, 1973; Coleman and Wright, 1975; Orton and Reading, 1993). The feeder channel normally is the primary river that is contributing sediment to the delta, whereas the distributary channel(s) typically refer to the ephemeral streams or rivers that branch off from it and distribute sediment across the delta (Collela and Prior, 1990). The delta plain is the relatively smooth and horizontal plain that includes all alluvial subaerial regions of the delta. Distributary channels flow across the delta plain, on their way to the lake or sea. The delta front is the portion of the delta that slopes into the deeper water offshore, whereas the prodelta region lies lakeward of the delta front and is the distal “toeslope” part of the depositional sequence (Scruton, 1960; Wright and Coleman, 1973; Galloway, 1975).

4.2.2 Delta Categories

Deltas are frequently categorized and modelled on the basis of their shape (i.e., cusperate, lobate, elongate, and estuarine) and the environmental variables influencing their construction (i.e., wave-influenced, river-influenced, and/or tide-influenced) (Figure 4.1; Holmes, 1965; McPherson et al., 1987; Bhattacharya and Giosan, 2003), in addition to thickness distribution patterns (Coleman and Wright, 1975; Wright, 1985) and dominant grain size (Orton, 1988; Orton and Reading, 1993). Some classification schemes use a combination of these factors (Postma, 1990). For instance, Galloway’s (1975) tripartite delta classification system focuses exclusively on the shape of the delta in order to infer wave, tide, and river influences; it is

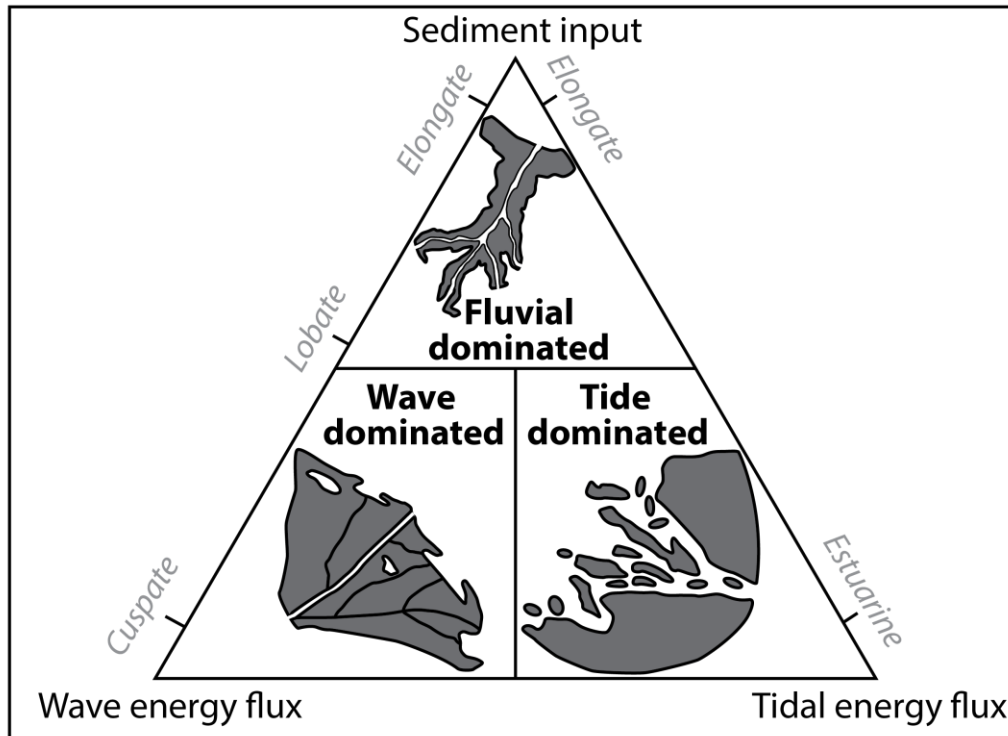


Figure 4.1: The frequently used ternary categorization of deltas based on the dominate processes influencing their morphology (modified from Galloway (1975) and Hori and Saito (2007)).

regularly used to model and categorize modern deltaic depositional systems (Orton and Reading, 1993; Galloway and Hobday, 1996).

Using similar models and data to those listed above, the paleoenvironments of abandoned (relict) deltas may also be inferred (Bhattacharya and Giosan, 2003; Gobo et al., 2014, Vader et al., 2012). However, note that the paleoenvironments of many relict deltas changed over time, and that these deltas often represent composite systems that record a range of depositional phases. Therefore, fitting a particular relict delta into a single category may not always be the best option, and may in fact, be difficult and controversial (Galloway and Hobday, 1996; Bhattacharya and Giosan, 2003). Nevertheless, this study seeks to capture overall depositional environments by grouping the relict deltas of Lower Michigan using a

number of variables. In addition to shape, which was discerned from the length-width ratio of the delta, the relict deltas are also grouped according to their location, size, slope, fluvial and sediment characteristics, wetness, and glacial history, as well as their catchment size, topographic variation, and sediment characteristics.

4.1.3 Numerical Grouping Analysis

In this analysis, I used principal components analysis (PCA) and a K-means clustering approach to group relict deltas with similar geomorphic and environmental components, and with comparable sediment and morphologic characteristics. PCA is a data mining method that groups the variables within a multivariate dataset, which helps to mitigate redundant, irrelevant, or correlated variables within the matrix of data (Abdi and Williams, 2010; Shlens, 2014). The K-means clustering analysis however, is an algorithm that seeks to assign individual observations into natural groups or clusters (Jain, 2010). Within the geosciences, PCA has been employed to transform bulky datasets into linear, independent and, arguably, more powerful variables (Morgan, 1971; Jolliffe, 2002; Antisari et al., 2010). The independent groups of variables can then serve as the noteworthy “components” for a particular dataset. For example, Scull and Schaetzl (2011) used PCA to characterize loess deposits in Wisconsin. In their study, >800 loess samples were analyzed throughout the state of Wisconsin. Out of the 42 particle size *variables* that were obtained from each loess sample, Scull and Schaetzl were able to separate the loess samples into 4 textural components (or variables) using PCA. Similarly, albeit more related to grouping relict deltas, Phillips and Desloges (2014) performed a PCA on alluvial floodplains in southern Ontario, Canada that had been recently deglaciated. Their study included 109 field site locations (i.e., observations) and a combination of 20 fluvial process and

floodplain variables. By employing PCA, Phillips and Desloges were able to suggest that the different types of rivers in the study are largely characterized by two principal components: (1) stream power-resistance and (2) floodplain sedimentology. They then used the results from their PCA and applied a K-means clustering analysis. The results from the K-means clustering analysis suggested there were four primary floodplain types, which were based on the morphological, stratigraphical, and sedimentological characteristics of their contributing rivers. This study illustrates that a PCA, used in combination with a K-means clustering analysis, can help identify different, major, types of fluvial and depositional landforms and processes within recently deglaciated regions.

The methods discussed in this section of the dissertation, regarding the numerical grouping of relict deltas in Lower Michigan, will largely follow the methodologies outlined in Phillips and Desloges (2014). I will apply a PCA to *isolate* the major physical characteristics that may exist between relict deltas. The results from the PCA will then be analyzed within a K-means clustering algorithm in order to group relict deltas with similar geomorphic components.

4.2 Methods

4.2.1 Delineating Delta and Catchment Areas

In order to operationalize this procedure, each delta mentioned in Chapter 3 of this dissertation was first coded within a GIS. Within this data set, 27 were previously identified relict deltas; 34 relict deltas are unique to this dissertation. Previously recognized relict deltas were identified from the following references: Leverett and Taylor (1915), Scherzer (1916), Bay (1937, 1938), Bretz (1951, 1953), Hough (1958, 1963), Martin (1955), Evenson (1973), Burgis (1977), Kehew (1993), and Vader et al. (2012).

The next step was to outline the delta plain (i.e., the subaerial portion of the delta) associated with each of the previously identified deltas (Figure 4.2). Using the original hard copy maps of those deltas helped to calibrate the digital mapping effort. The delta plains were digitized in ArcMap 10.1 (© ESRI, Redlands, CA) using those geospatial data layers listed in Chapter 3 of this dissertation. In brief, those datasets included the following: graphical representations of water well and oil/gas log data, downloaded from the Michigan Geographic Data Library, a statewide mosaic of USGS 7.5' topographic maps, seamless 10 m NED DEM and hillshade layers, slope gradient and relief layers derived from the statewide DEM, and surface (first mineral horizon) and subsurface (usually the C horizon) information obtained from NRCS SSURGO soils data. The soils data were employed to construct maps of soil parent material, upper and subsurface soil texture, gravelly/cobbly soils, and soil wetness as indicated by the Drainage Index (Schaetzl et al., 2009). The DI considers natural soil drainage class, texture, percent slope of the landscape, and other variables in its calculation.

A total of 61 delta plains were mapped using the data layers mentioned above. Note, all pertinent geospatial data layers were considered when delineating delta plain boundaries, and thus, each delta boundary represents a combination of geologic characteristics; it was never determined based on a single data set (e.g., see Figure 4.2). In some instances, the soils data would suggest a larger extent of the delta, when compared to, for example, topographic data. However, because this study was focused on mapping primarily the delta plain area, topographic characteristics were given priority over textural characteristics. That is, in many cases, the delta boundary was marked by a steep slope, downstream from the apex of the delta. This slope was interpreted as the delta front, which could not have been determined

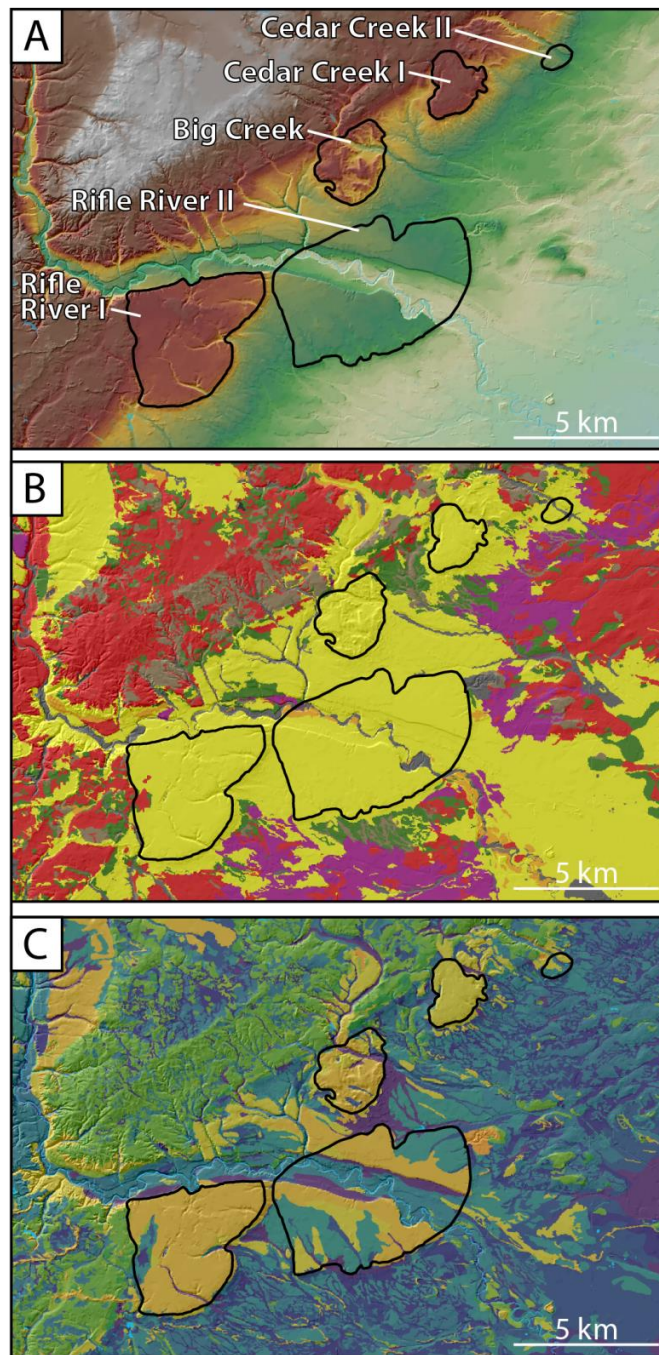


Figure 4.2: Three maps illustrating (a) 10 m NED DEM and hillshade, (B) subsurface soil texture – yellow are sandy soils, and (C) soil wetness – orange and green are well drained soils, along with the delta plain boundaries associated with five deltas mapped in Lower Michigan.

primarily by soils data. This approach represented a relatively conservative method for determining the outlining of the deltas. Furthermore, the majority of the delta plains have been variously incised by one or more ancestral and/or modern fluvial systems. Interpretation of the delta plain between these eroded areas was avoided by focusing on areas that were less incised, which were thought to better reflect the original delta surface.

Next, the catchment area associated with each of the 61 deltas was mapped using the watershed tool within the hydrology tool set in ArcToolbox (© ESRI, Redlands, CA). As outlined in Chapter 3 of the dissertation, the estimated catchment area for each delta was conceptualized as the landscape extent that could have potentially contributed sediment to the delta during its formative period. Each delta's "pour point", which is the reference for the Watershed tool to calculate areas that presently drain to them, was digitized using the DEM. It was usually located near the apex of the delta plain. A "pour line(s)," rather than a point, was used for deltas that were notably wide, or broad, and/or which had multiple feeder channels graded to the delta plain. The pour line followed the majority of the upstream regions of the delta plain (i.e., the delta head or apex), in order to incorporate additional areas that likely contributed to the growth of the delta.

4.2.2 Quantifying Morphologic Characteristics

After each delta plain and catchment area extent was saved into a shapefile as a polygon, a copy of each polygon was converted to a raster file. A 10 m grid was created for each delta and catchment extent in order to quantify the elevation information within those areas. An additional 30 m grid was developed for each delta and catchment in order to quantify the NRCS SSURGO soils data within each area. Nineteen delta plain characteristics and twelve

catchment area characteristics were then measured for each delta-catchment pairing. Each characteristic (i.e., variable) is listed in Table 4.1, along with a general description of each variable. Generally, the delta plain characteristics can be separated in to seven categories: (1) locational data, (2) topographic data, (3) areal extent data, (4) fluvial characteristics, (5) sediment characteristics, (6) wetness characteristics, and (7) glacial history (i.e., whether or not the delta is located at the outlet of a major glacial lake or connected to a former meltwater spillway) (Table 4.1). Delta catchment area characteristics could generally be separated into three categories: (1) areal extent data, (2) topographic data, and (3) sediment characteristics (Table 4.2). Soil textural characteristics follow those methods outlined in Chapter 3 of this dissertation, where the most areally extensive upper-profile and subsurface soil textural class (which was of the first mineral and the lowest described horizon) were identified from the NRCS SSURGO soil data, and the amount of the various grain-size fractions was estimated by taking the values of sand, silt, and clay at the midpoint of each polygon that delimits a textural class on a standard USDA soil textural triangle (Miller and White, 1998).

Table 4.1: Delta plain variables

| Categories | Abbreviations | Delta Plain Characteristics | Comments |
|-------------------------|---------------|------------------------------|--|
| Locational data | LAT | Latitude (m) | Located at the centroid of the delta plain |
| | LONG | Longitude (m) | Located at the centroid of the delta plain |
| Topographic data | DESDP | Slope of the delta plain (%) | Transect drawn near the center axis of the delta plain, from the head to the downstream distal margins of the delta. An elevation reading was taken every 500 m (minimum of 4), avoiding irregularities (i.e., depressions, sand dunes, paleochannels, etc.) on the delta plain surface. |

Table 4.1 (cont'd)

| | | | |
|---------------------------------|--------|--|--|
| Topographic data | DMMDP | Max. elev. - Min. elev. (m) | Measured at the head of the delta plain and at its most distal margin |
| Areal extent data | DPL | Perimeter length (km) | Length of polygon drawn in ArcGIS to delimit the delta outline |
| | DLWR | Length/Width (m) | Used the Minimum Bounding Geometry tool in ArcMap to apply a circular and rectangular envelope around the outside of the delta plain. The diameter of each circle and maximum width and length of each rectangle were then exported from ArcMap and used to estimate the maximum width and length for each delta. The maximum length of each delta was divided by its maximum width to determine the length-width ratio. In some instances the delta length-width ratio had to be manually measured. |
| Fluvial Characteristics | DAMFC | Abundance of major feeder channels | Assigned a "1" to deltas that had a single feeder channel and a "2" to deltas that had more than one feeder channel |
| Fluvial Characteristics | DAPDC | Abundance of paleodistributary channels | Assigned a "1" to deltas that had a single paleodistributary channel and a "2" to deltas that had more than one paleodistributary channel. Paleodistributary channels were defined as sinuous channels (dry or wet) and/or deposits of sediment that bifurcated from the main feeder channel, and were perhaps remnants of streams that contributed to dispersing sediment across the delta plain and to the margins of the delta. |
| Sediment Characteristics | DDUPST | Most areally extensive upper soil textural class | Used the NRCS SSURGO soil data to determine the most commonly mapped upper soil (first mineral horizon) textural class within the delta plain extent |

Table 4.1 (cont'd)

| | | | |
|-------------------------------------|---------|---|---|
| Sediment Characteristics | DDSUBST | Most areally extensive subsurface textural class | Used the NRCS SSURGO soil data to determine the most commonly mapped subsurface soil (lowest described horizon) textural class within the delta plain extent |
| | DPCUPS | Clay content in upper soil (%) | Areally weighted percentage of clay, based on dividing the number of cells within an area by the sum of each cell count multiplied by the percentage of clay associated with a specific soil textural class - determined by midpoints of polygons in a standard NRCS Textural Triangle (see Miller and White (1998)). |
| | DPSUPS | Sand content in upper soil (%) | Areally weighted percentage of sand, based on dividing the number of cells within an area by the sum of each cell count multiplied by the percentage of sand associated with a specific soil textural class - determined by midpoints of polygons in a standard NRCS Textural Triangle (see Miller and White (1998)). |
| | DPTUPS | Silt content in upper soil (%) | Areally weighted percentage of silt, based on dividing the number of cells within an area by the sum of each cell count multiplied by the percentage of silt associated with a specific soil textural class - determined by midpoints of polygons in a standard NRCS Textural Triangle (see Miller and White (1998)). |
| | DPCSUBS | Clay content in soil subsurface (%) | Areally weighted percentage of clay, based on dividing the number of cells within an area by the sum of each cell count multiplied by the percentage of clay associated with a specific soil textural class - determined by midpoints of polygons in a standard NRCS Textural Triangle (see Miller and White (1998)). |

Table 4.1 (cont'd)

| | | | |
|---------------------------------|---------|---|---|
| Sediment Characteristics | DPSSUBS | Sand content in soil subsurface (%) | Areally weighted percentage of sand, based on dividing the number of cells within an area by the sum of each cell count multiplied by the percentage of sand associated with a specific soil textural class - determined by midpoints of polygons in a standard NRCS Textural Triangle (see Miller and White (1998)). |
| | DPTSUBS | Silt content in soil subsurface (%) | Areally weighted percentage of silt, based on dividing the number of cells within an area by the sum of each cell count multiplied by the percentage of silt associated with a specific soil textural class - determined by midpoints of polygons in a standard NRCS Textural Triangle (see Miller and White (1998)). |
| | DGA | Extent of gravelly soils across the delta (%) | Areally weighted percentage of soils with coarse fragments at depth, based on multiplying by 100 the total number of cells within an area divided by the number of cells with soils that have either a gravelly or cobbly modifier associated with their standard soil textural class (see Schaetzl et al. (2013b)). |
| Wetness | DDDC | Most areally extensive Drainage Index value | Defined by the most common Drainage Index value (0-99) within an area. Lower values represent drier or better drainage soils and larger values represent wetter or poorly drained soils (see Schaetzl et al. (2009)). |
| Glacial History | GLC | Glacial lake contributions | Assigned a "0" if no known major glacial lake contribution and "1" if one or more glacial lakes were known to have spilled through the delta system |

Table 4.2: Delta catchment area variables

| Categories | Abbreviations | Catchment Area Characteristics | Comments |
|------------|---------------|--------------------------------|-----------------|
| Size | CA | Area | km ² |

Table 4.2 (cont'd)

| | | | |
|---------------------------------|----------------|---|---|
| Topography | CMNS | Mean slope (%) | Based on the mean percent slope within a 3 x 3 cell neighborhood, calculated through the catchment, from the DEM |
| | CMDS | Median slope (%) | Based on the median percent slope within a 3 x 3 cell neighborhood, calculated through the catchment, from the DEM |
| | CMRN | Melton basin ruggedness number (MRN) | Basin relief divided by the square root of the basin area ($Z_{max} - Z_{min} / \text{basin area}^2$) (Melton, 1965). Larger MRNs imply greater relief. |
| Sediment Characteristics | CDUPST | Most areally extensive upper soil textural class | Used the NRCS SSURGO soil data to determine the most commonly mapped upper soil (first mineral horizon) textural class within the catchment extent |
| | CDSUBST | Most areally extensive subsurface soil textural class | Used the NRCS SSURGO soil data to determine the most commonly mapped subsurface soil (lowest described horizon) textural class within the delta catchment extent |
| | CPCUPS | Clay content in upper soil (%) | Areally weighted percentage of clay, based on dividing the number of cells within an area by the sum of each cell count multiplied by the percentage of clay associated with a specific soil textural class - determined by midpoints of polygons in a standard NRCS Textural Triangle (see Miller and White (1998)). |
| | CPSUPS | Sand content in upper soil (%) | Areally weighted percentage of sand, based on dividing the number of cells within an area by the sum of each cell count multiplied by the percentage of sand associated with a specific soil textural class - determined by midpoints of polygons in a standard NRCS Textural Triangle (see Miller and White (1998)). |

Table 4.2 (cont'd)

| | | | |
|-------------------------------------|----------------|---|--|
| Sediment Characteristics | CPTUPS | Silt content in upper soil (%) | Areally weighted percentage of silt, based on dividing the number of cells within an area by the sum of each cell count multiplied by the percentage of silt associated with a specific soil textural class - determined by midpoints of polygons in a standard NRCS Textural Triangle (see Miller and White (1998)). |
| | CPCSUBS | Clay content in soil subsurface (%) | Areally weighted percentage of clay, based on dividing the number of cells within an area by the sum of each cell count multiplied by the percentage of clay associated with a specific soil textural class - determined by midpoints of polygons in a standard NRCS Textural Triangle (see Miller and White (1998)). |
| | CPSSUBS | Sand content in soil subsurface (%) | Areally weighted percentage of sand, based on dividing the number of cells within an area by the sum of each cell count multiplied by the percentage of sand associated with a specific soil textural class - determined by midpoints of polygons in a standard NRCS Textural Triangle (see Miller and White (1998)). |
| | CPTSUBS | Silt content in soil subsurface (%) | Areally weighted percentage of silt, based on dividing the number of cells within an area by the sum of each cell count multiplied by the percentage of silt associated with a specific soil textural class - determined by midpoints of polygons in a standard NRCS Textural Triangle (see Miller and White (1998)). |

The following section continues to describe the measurements used to quantify the physical characteristic of the delta and catchment areas. The relative amount of topographic

variation within a catchment area was measured by calculating the mean and median percent slope, within 3 x 3 cell neighborhood, throughout the extend of catchment area. The slope measurements were determined using a 10 m DEM. The Melton Ruggedness Number was also employed as an indicator of terrain roughness within the delta catchment (Melton, 1965). This value was calculated by dividing the basin relief (max. elev. – min. elev.) by the square root of the basin area (Melton, 1965). The slope of the delta plain was estimated along a transect line, using the profile tool in ArcMap. The line was drawn along the central axis of the delta plain, from its apex to the distal margins of the delta plain. An elevation reading was taken every 500 m, with a minimum of four elevation readings, and avoiding surface irregularities (i.e., depressions, sand dunes, paleochannels, etc.). The absolute elevation range of the delta plain was estimated by determining the mathematical difference between the maximum and minimum elevations near the apex and the distal margins of the delta plain, respectively. The length-width ratio of the delta was determined using the Minimum Bounding Geometry tool in ArcMap. First a circular envelope was applied to each delta plain and the diameter of the circle was used to measure either the width or length of the delta, depending on its shape (Figure 4.3). The Minimum Bounding Geometry tool was applied a second time using the rectangular envelope and either the maximum width or length of the rectangle was employed for either the width or length of the delta, depending on its shape (Figure 4.3). The maximum length measurement - calculated by either the circular or rectangular envelope - was then divided by the maximum width value – again, calculated by either the circular or rectangular envelope - to arrive at a length-width ratio (Figure 4.3). In some instances, such as where deltas had several sub-lobes, it was more accurate to manually measure the maximum length and width of the

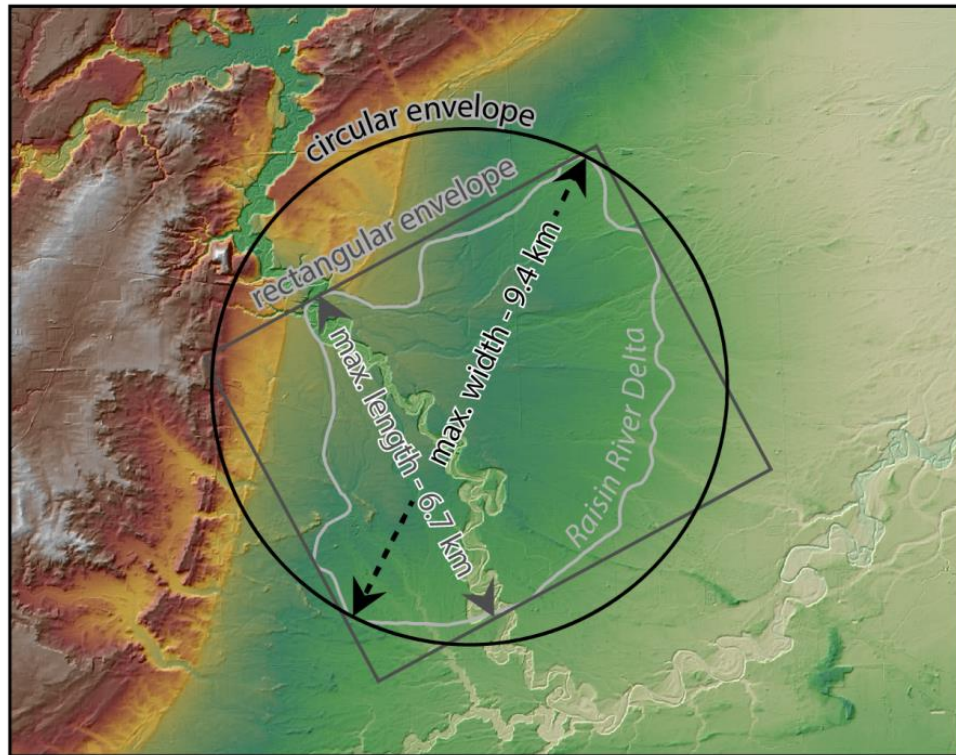


Figure 4.3: Illustrating examples of outputs from the Minimum Bounding Geometry tool and how the diameter of the circular envelop was used to estimate either the length or width of the delta, as well as how the length and width measurements of the rectangular envelope were used to estimate either the length or width of the delta.

delta, instead of using the Minimum Bounding Geometry tool. The most areally extensive surface textural class (first mineral horizon) and the subsurface textural class (usually the C horizon) within each delta and catchment extent were recorded as the soil textural class with the largest cell count within the individual areas. Lastly, the areally weighted percentages of sand, silt, and clay within the catchment and delta areas were determined by dividing the number of cells within a particular area by the sum of each cell count multiplied by the percentage of either sand, silt, or clay associated with a specific soil textural class - determined by midpoints of polygons in a standard NRCS Textural Triangle (see Miller and White (1998).

The entire list of raw data measurements for the nineteen delta plain characteristics and twelve catchment characteristics are provided in Appendix D.

4.2.3 Principal Component Analysis

The 31 variables listed in Tables 4.1 and 4.2 were entered into a Principal Component Analysis using the “*princomp ()*” function in the R software package (version 3.1.2 - <http://www.r-project.org/>). A correlation matrix was extracted in the PCA and the minimum eigenvalue was set to 1. Four factors were extracted, determined by identifying the number of factors with a total variance \geq to 5% (Kagan and Shepp, 1998). A second PCA was then run using the “*principal ()*” function in R, but after applying a varimax rotation to the four components that were extracted from the original dataset. The varimax rotation helps align the axes of the coordinate system in which the components are plotted, in order to maximize the sum of variances of the squared loadings within each component (Kaiser, 1958). The variable loadings for each component are reported in Figures 4.4-4.7. The loading plots are a summary of the relationships between the variables. The loading value assigned to each variable represents the relationship between the variables with a particular component; hence, it is also known as the correlation between the variables. Therefore whether the loading is negative or positive is not as important as the correlation between the variables. The most highly correlated variables for each component - both negative and positive - are reported in Table 4.3.

The four most positively correlated variables in the first component (PC1) include (1) catchment most areally extensive subsoil texture (CDSUBST), (2) catchment silt content in the upper soil (CPTUPS), (3) catchment silt content in the subsoil (CPTSUBS), and (4) catchment clay content in the upper soil (CPCUPS) (Figure 4.4; Table 4.3). These four positively correlated

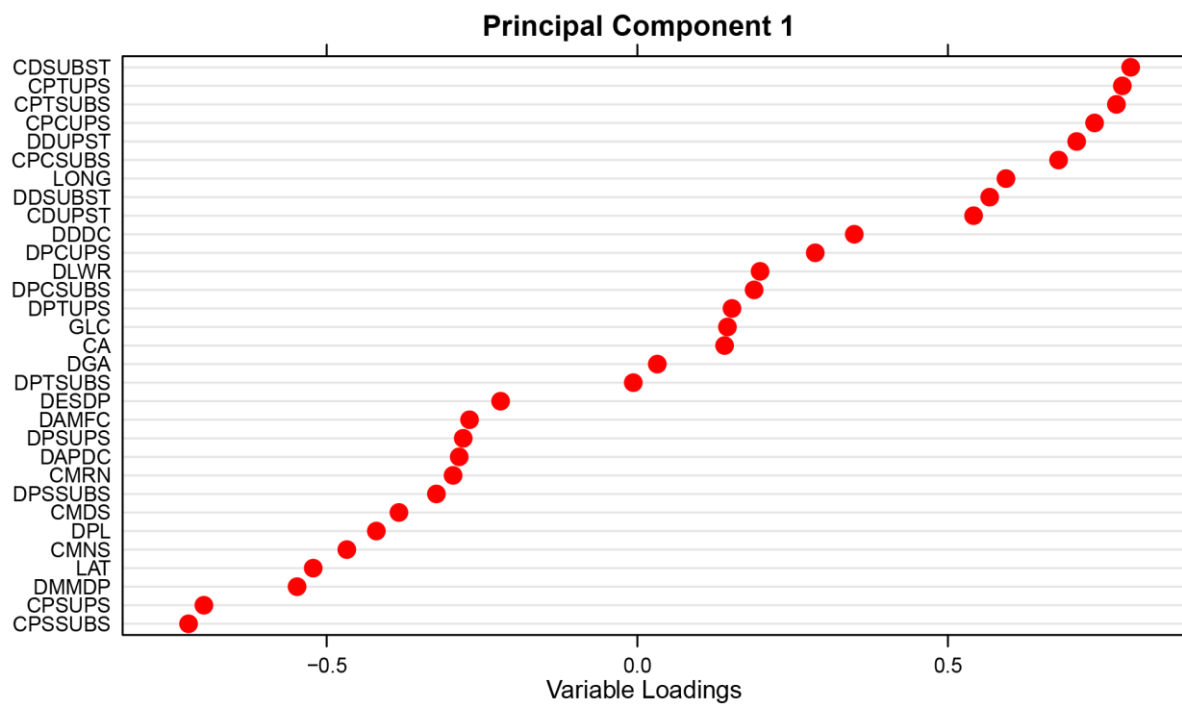


Figure 4.4: Variable loadings associated with PC1.

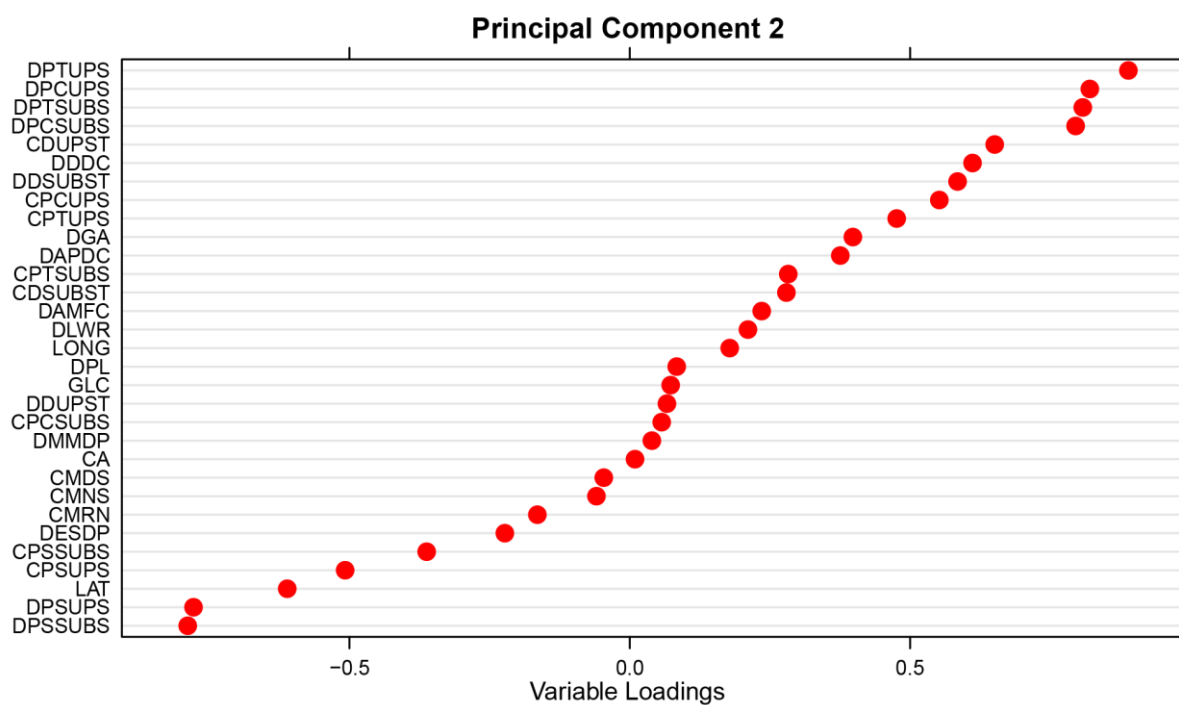


Figure 4.5: Variable loadings associated with PC2.

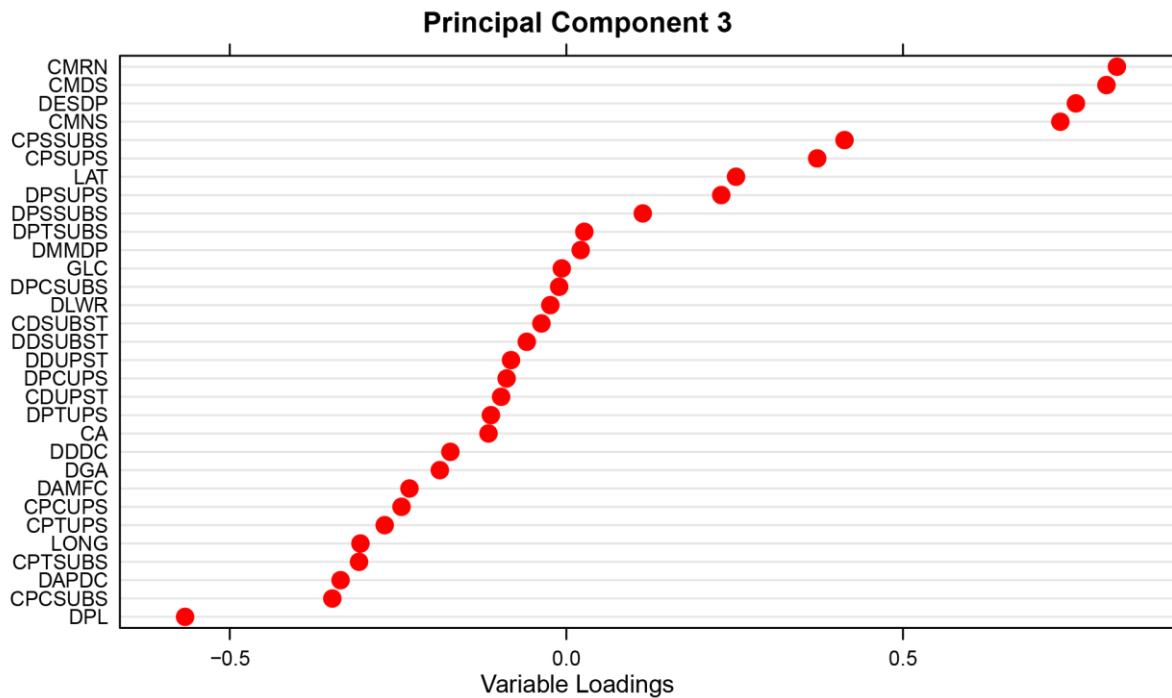


Figure 4.6: Variable loadings associated with PC3.

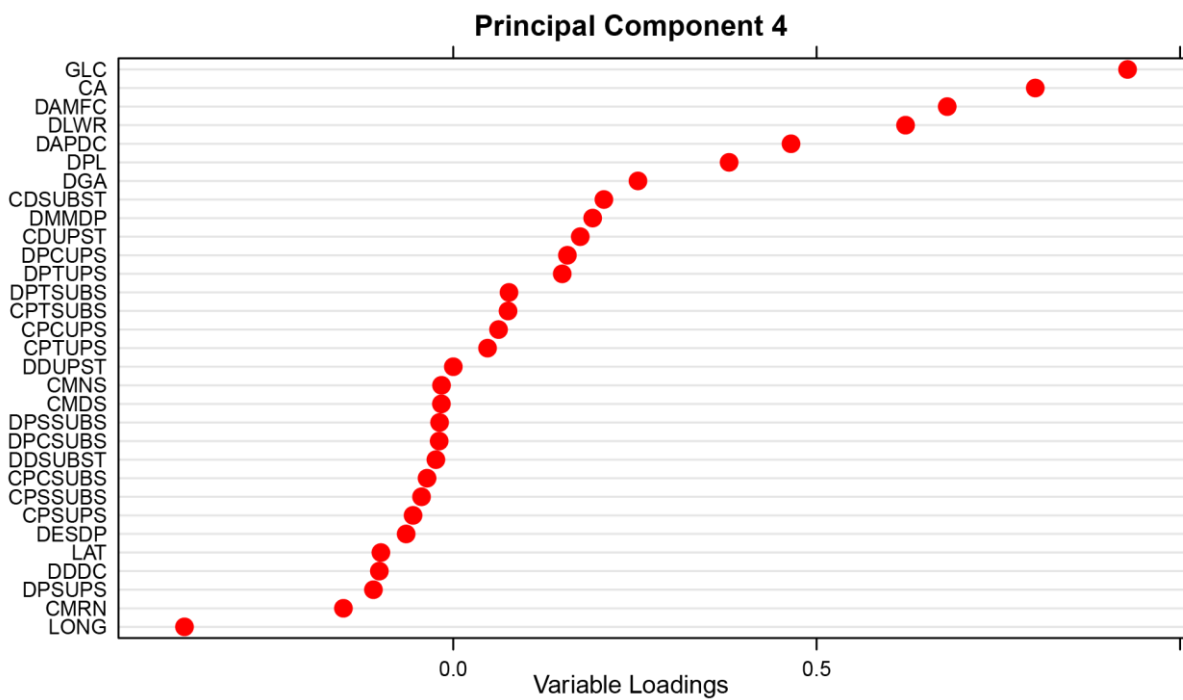


Figure 4.7: Variable loadings associated with PC4.

Table 4.3: Delta and catchment variables that correlate highly ($\geq \pm 0.5$) with the four principal components

| <u>PC1 - positively correlated</u> | <u>Correlation/Loadings</u> |
|---|------------------------------------|
| <i>Catchment:</i> most areally extensive subsurface soil textural class | 0.79 |
| <i>Catchment:</i> silt content in upper soil | 0.78 |
| <i>Catchment:</i> silt content in soil subsurface | 0.77 |
| <i>Catchment:</i> clay content in upper soil | 0.74 |
| <i>Delta:</i> most areally extensive upper soil textural class | 0.71 |
| <i>Catchment:</i> clay content in soil subsurface | 0.68 |
| <i>Delta:</i> longitude | 0.59 |
| <i>Delta:</i> most areally extensive subsurface textural class | 0.57 |
| <i>Catchment:</i> most areally extensive upper soil textural class | 0.54 |
| <u>PC1 - negatively correlated</u> | <u>Correlation/Loadings</u> |
| <i>Catchment:</i> sand content in soil subsurface | -0.72 |
| <i>Catchment:</i> sand content in upper soil | -0.70 |
| <i>Delta:</i> max-min elevation difference of the delta plain | -0.55 |
| <i>Delta:</i> latitude | -0.52 |
| <u>PC2 - positively correlated</u> | <u>Correlation/Loadings</u> |
| <i>Delta:</i> silt content in upper soil | 0.89 |
| <i>Delta:</i> clay content in upper soil | 0.82 |
| <i>Delta:</i> silt content in soil subsurface | 0.81 |
| <i>Delta:</i> clay content in soil subsurface | 0.80 |
| <i>Catchment:</i> most areally extensive upper soil textural class | 0.65 |
| <i>Delta:</i> most areally extensive drain index value | 0.61 |
| <i>Delta:</i> most areally extensive subsurface textural class | 0.58 |
| <i>Catchment:</i> clay content in upper soil | 0.55 |
| <u>PC2 - negatively correlated</u> | <u>Correlation/Loadings</u> |
| <i>Delta:</i> sand content in soil subsurface | -0.79 |
| <i>Delta:</i> sand content in upper soil | -0.78 |

Table 4.3 (cont'd)

| | |
|---|-------|
| <i>Delta</i> : latitude | -0.61 |
| <i>Catchment</i> : sand content in upper soil | -0.51 |

| | |
|---|------------------------------------|
| <u>PC3 - positively correlated</u> | <u>Correlation/Loadings</u> |
| <i>Catchment</i> : Melton basin ruggedness number | 0.82 |
| <i>Catchment</i> : median percent slope | 0.80 |
| <i>Delta</i> : slope of the delta plain | 0.76 |
| <i>Catchment</i> : mean percent slope | 0.73 |

| | |
|---|------------------------------------|
| <u>PC3 - negatively correlated</u> | <u>Correlation/Loadings</u> |
| <i>Delta</i> : perimeter length | -0.57 |

| | |
|---|------------------------------------|
| <u>PC4 - positively correlated</u> | <u>Correlation/Loadings</u> |
| <i>Delta</i> : glacial Lake contributions | 0.93 |
| <i>Catchment</i> : area | 0.80 |
| <i>Delta</i> : abundance of major feeder channels | 0.68 |
| <i>Delta</i> : length-width ratio | 0.62 |

| | |
|---|------------------------------------|
| <u>PC4 - negatively correlated</u> | <u>Correlation/Loadings</u> |
| NA | NA |

variables in PC1 are related to fine sediment textures (i.e., silt and clay contents). Likewise, PC1 correlates most negatively with (1) catchment sand content in the subsoil (CPSSUBS), (2) catchment sand content in the upper soil (CPSUPS), (3) the difference between the maximum and minimum elevation on the delta plain (DMMDP), and (4) delta latitude (LAT) (Figure 4.4; Table 4.3). The most negatively correlated variables in PC1 relate to sand content within the catchment. PC1 is therefore interpreted to represent the sediment characteristics (particle size) of the catchment areas. The latitude of the delta is also highly correlated in PC1, presumably because sandy landscapes dominate the northern regions (higher latitudes) of the study area, whereas southern regions (lower latitudes) in Michigan have landscapes with less sandy deposits.

The most positive loadings within the second component (PC2) include (1) delta silt content in the upper soil (DPTUPS), (2) delta clay content in the upper soil (DPCUPS), (3) delta silt content in the subsoil (DPTSUBS), and (4) delta clay content in the subsoil (DPCSUBS) (Figure 4.4; Table 4.3). Similar to PC1, the most positively correlated variables in PC2 relate to fine textures and the most negatively correlated variables relate to sand content in the upper and subsurface soils within the delta (Figures 4.4 and 4.5; Table 4.3). Therefore, PC2 is interpreted to represent the sediment characteristics (particle size) of the delta plain. PC1 and PC2 each represent 23% of the total variance within the data set, and combined they represent 46% of the total variance (Table 4.4).

The variables with the highest positive loadings in the third principal component (PC3) include (1) the catchment Melton Ruggedness Number (CMRN), (2) catchment median percent slope (CMDS), (3) slope of the delta plain (DESDP), and (4) catchment mean percent slope (CMNS); three of these variables are derived from catchment data (Figure 4.6; Table 4.3). Similarly, the delta perimeter length also has a relatively high correlation within PC3 (Table 4.3).

Table 4.4: A list of the principal components' interpreted characteristics, and their percent variance within the data set

| Principal Component | Interpreted Characteristic | Variance |
|---------------------|---|--------------------------------------|
| PC1 | Sediment characteristics (particle size) of the catchment | 23% |
| PC2 | Sediment characteristics (particle size) of the delta plain | 23% |
| PC3 | Topographic characteristics of the catchment and delta | 13% |
| PC4 | System extent | 10% |
| | | Total variance explained: 69% |

The majority of the highly correlated variables in PC3 related to slope either within the catchment or on the delta (Figure 4.6; Table 4.3). Therefore, the third principal component (PC3) is interpreted to capture the topographic characteristics within the catchment area *and* on the delta plain (Table 4.4). In total, PC3 represents 13% of the variance within dataset (Tables 4.4).

The last principal component – PC4 - includes the following four variables with largest loadings: (1) glacial lake contributions (GLC), (2) catchment area (CA), (3) delta abundance of major feeder channels, and (4) the delta length-width ratio (DLWR) (Figure 4.7; Table 4.3). In addition, the measured delta abundance of paleodistributary channels (DAPDC) and the delta perimeter length (DPL) variables were also strongly positively correlated (0.46 and 0.36, respectively) in PC4. The catchment area, delta perimeter length, and the abundance of feeder and paleodistributary channels are mostly size-related variables. Arguably, glacial lake contribution is also a size-related measure, because a system that is influenced by a glacial lake would receive inputs from a large area. PC4 was therefore interpreted to represent the areal extent of the delta *system*. PC4 represents 10% of the total variance (Table 4.4). Combined, the four components extracted from the PCA represent 69% of the total variance within the 31 variable dataset (Table 4.4).

4.2.4 K-means Clustering Analysis

For each delta, its scores on the four principal components (see Appendix E) were then entered into a K-means + Ward's clustering algorithm in order to group them; deltas with similar physical characteristics should group together. Recall that the *loadings* from the PCA that are listed in Figures 4.4 through 4.7 above refer to the relationship between the variables -

in this case the delta and catchment characteristics. However, the *scores* from the PCA refer to the similarity among the observations (i.e., samples, or in this case the deltas). The *scores* from the PCA are synthetic values that are plotted in n dimensions (or axes) depending on the number of components extracted from the PCA - in this case there are four axes, being that four components were extracted. Deltas that are more alike will have a similar set of *scores* and will be plotted relatively close together in the simulated, four-dimensional space. The K-means analysis identifies the clusters within the four-dimensional space and groups the points/deltas together.

The Ward's hierarchical clustering measurement was integrated with the K-means clustering algorithm in order "stabilize" the clustering results (Delamater et al., 2013). The K-means algorithm requires an initial "seed" or a starting location for the cluster analysis; this location is normally assigned randomly. However, with the Ward's measurement added to the clustering analysis, a standard seed location is set in order to obtain repeatable clustering results (Delamater et al., 2013). The appropriate number of clusters, or groups, to specify for the K-means clustering analysis was determined using the increment F statistic (Figure 4.8). This statistic is a measure of the amount of "fit" after assigning a certain number of clusters to the K-means + Ward's algorithm (Delamater et al., 2013). Peaks or local maxima in the incremental F value, as well as a particularly large $incF$ value, imply an optimal number of clusters (Gujarati, 1988). The scores from the PCA suggested that five clusters was the optimal number of clusters to specify in the clustering analysis (Figure 4.8).

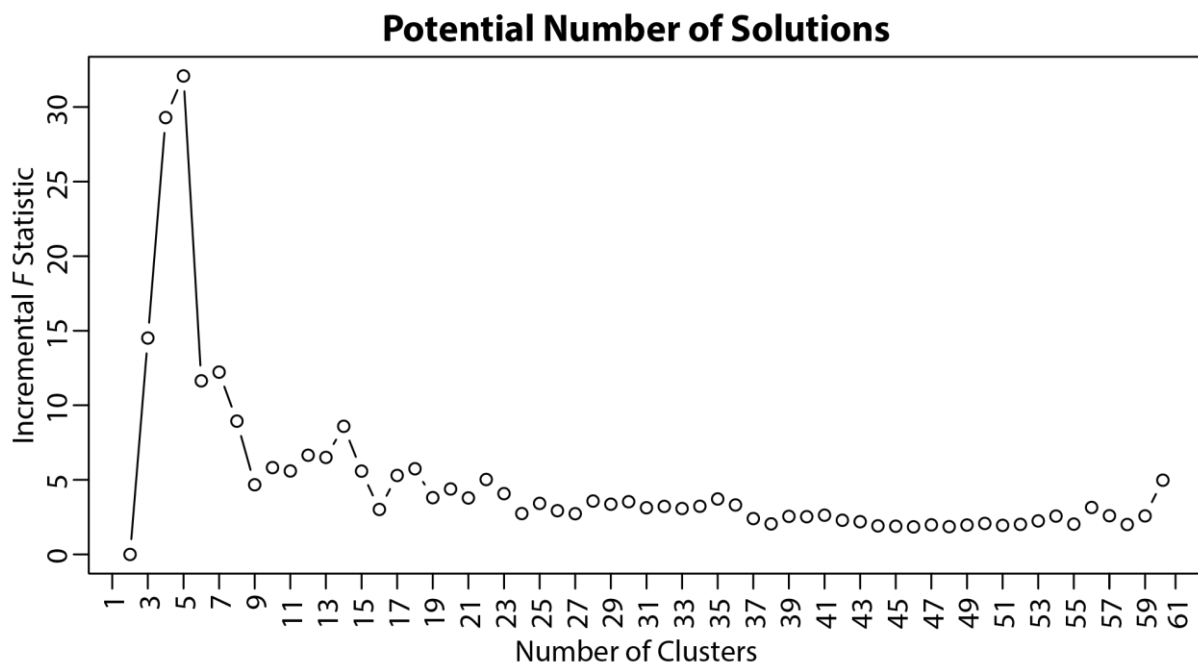


Figure 4.8: The goodness of "fit" for each number of clusters specified. Local peaks in the graph suggest potential numbers of clusters.

4.3 Results and Discussion

4.3.1 Delta and Catchment Sediment Characteristics

Results from the clustering analysis suggest that, based on their physical and locational characteristics, there are five primary groups of relict deltas in Lower Michigan. Each group has the following number of deltas: Group 1 = 22, Group 2 = 13 deltas, Group 3 = 16 deltas, Group 4 = 7 deltas, and Group 5 = 3 deltas (Figure 4.9). Deltas in Groups 1 and 2 are mostly located in the northern Lower Peninsula (Figure 4.9). Figure 4.10 illustrates the frequency and distribution of *scores* associated with each of the four components extracted from the PCA. Note the size of the *score* assigned to each delta within a specific dimension/component (i.e., PC1 - PC4) alludes to the amount of 'explanation' a particular component has on a delta.

Deltas in Groups 1 and 3 have large *scores* within the first dimension (PC1), which again describes the sediment characteristics within the catchments (Figure 4.10). Furthermore, deltas in Groups 1 and 2 have a similar distribution of *scores* within PC1 (Figure 4.10). The large positive and negative PC1 *scores* associated with Group 1 and 3 deltas suggest that the sediment catchment characteristics of the deltas are important in discriminating between these groups. Deltas in Groups 1 and 2 are located in northern Michigan where landforms are dominantly composed of sandy textured deposits (Figure 4.11). Conversely, deltas in Groups 3-5 are located in regions of southern Michigan where fine textured deposits (i.e., silts and clays) are more common (Figures 4.11). To summarize, deltas in Groups 1 and 2 have high amounts of sand within their catchment areas and low amounts of fine sediment (Figures 4.12 and 4.13;

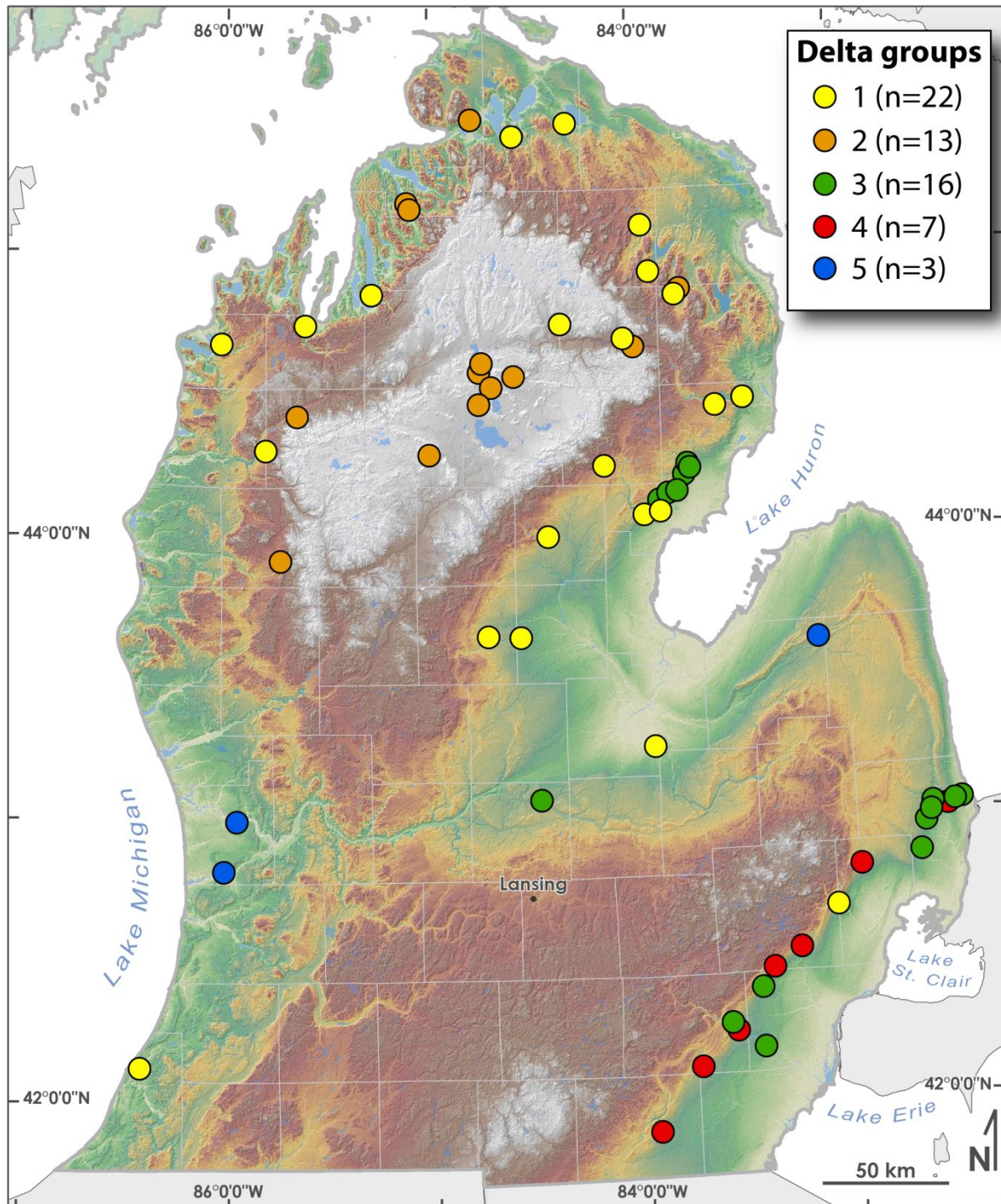


Figure 4.9: The distribution of the five groups of deltas, as identified by the K-means clustering analysis.

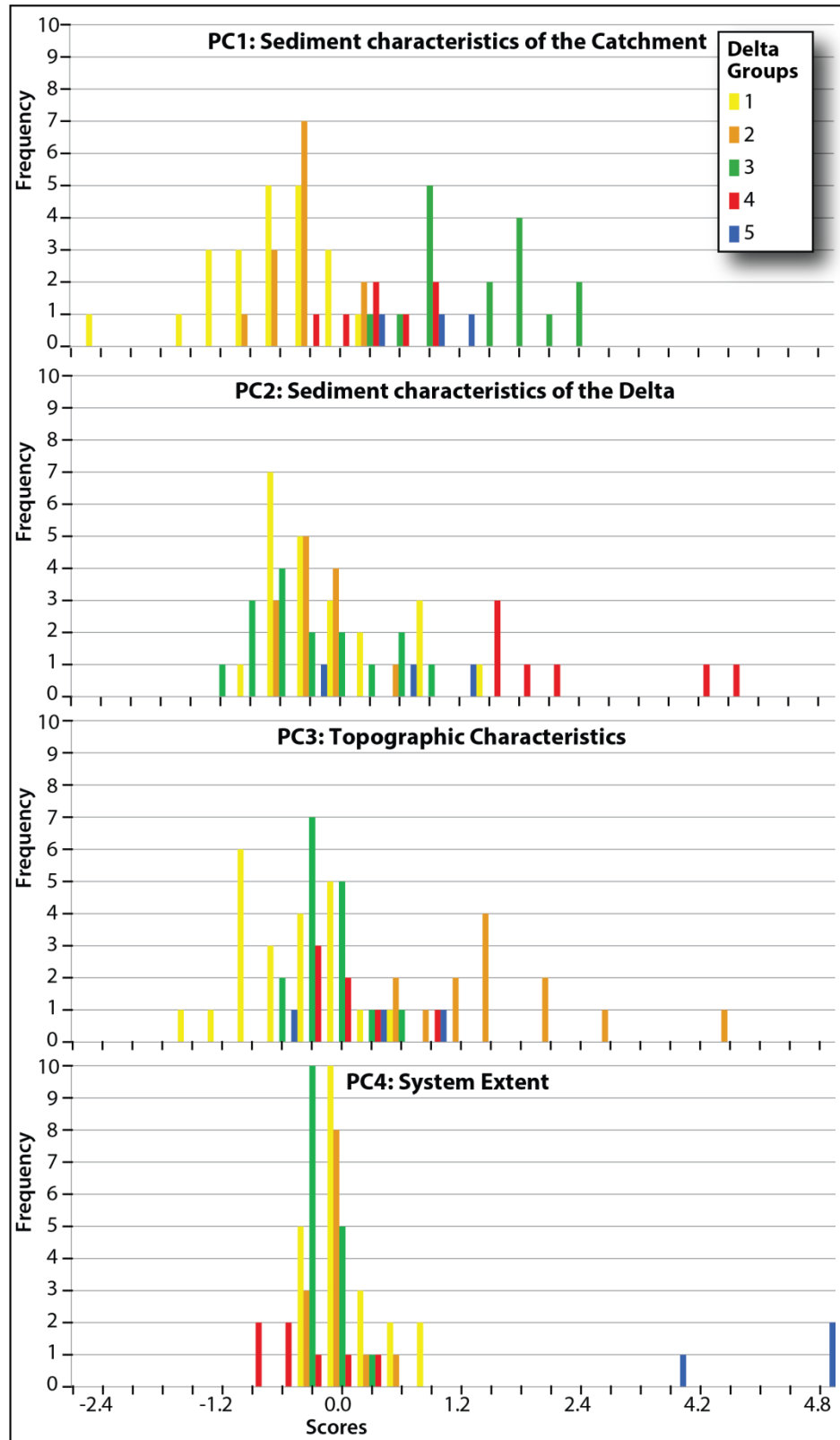


Figure 4.10: The frequency and distribution of PCA scores associated with each of the four components extracted from the PCA.

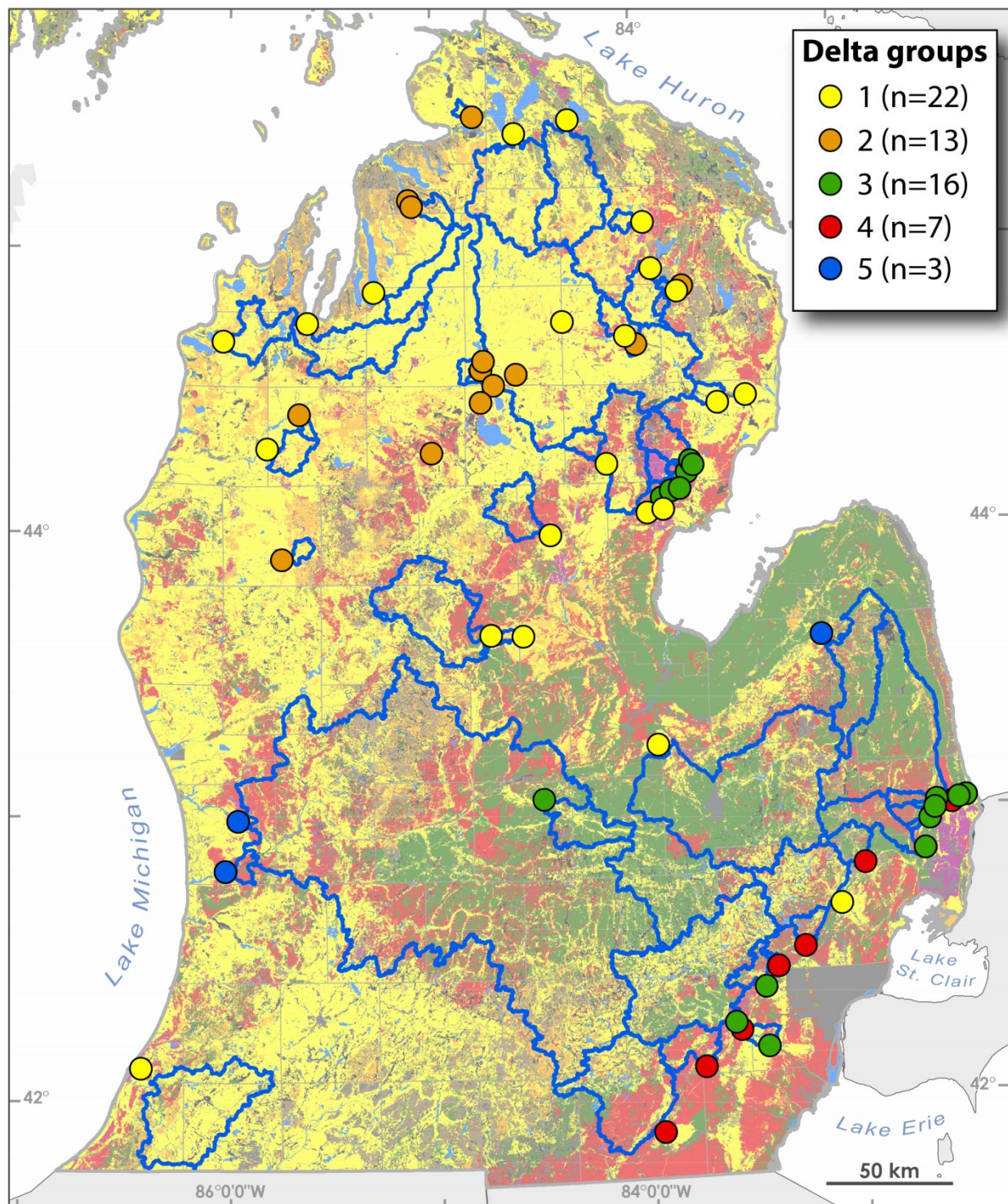


Figure 4.11: The distribution of the five groups of deltas and the extent of each delta's catchment area (outlined in blue), overlain onto a map of soil subsurface (C horizon) texture. Red and green colors represent fine textured soils and orange and yellow colors represent sandy textured soils.

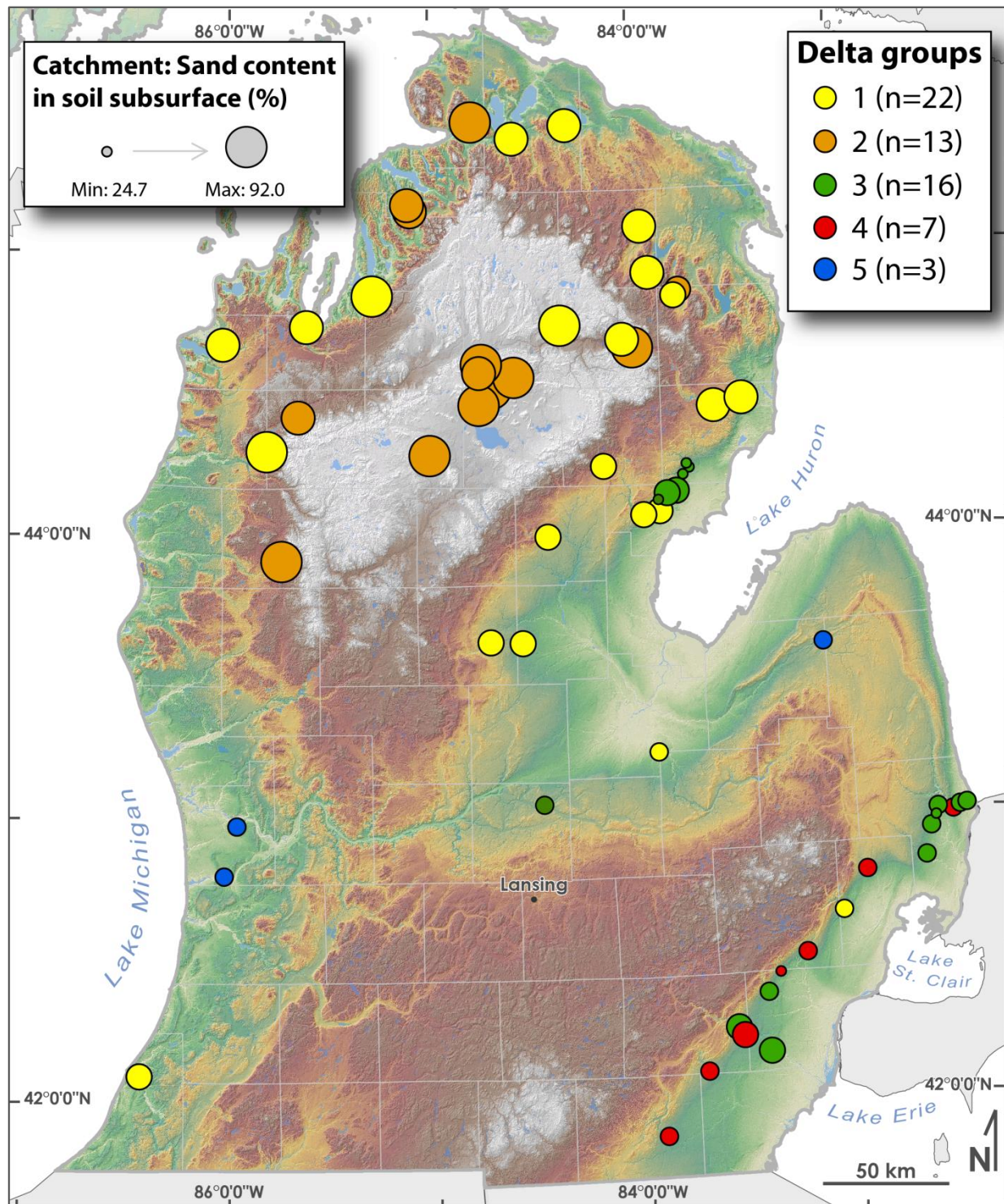


Figure 4.12: A graduated circle map illustrating sand content (%) in the subsurface horizon (C horizon) of soils within the delta catchment areas.

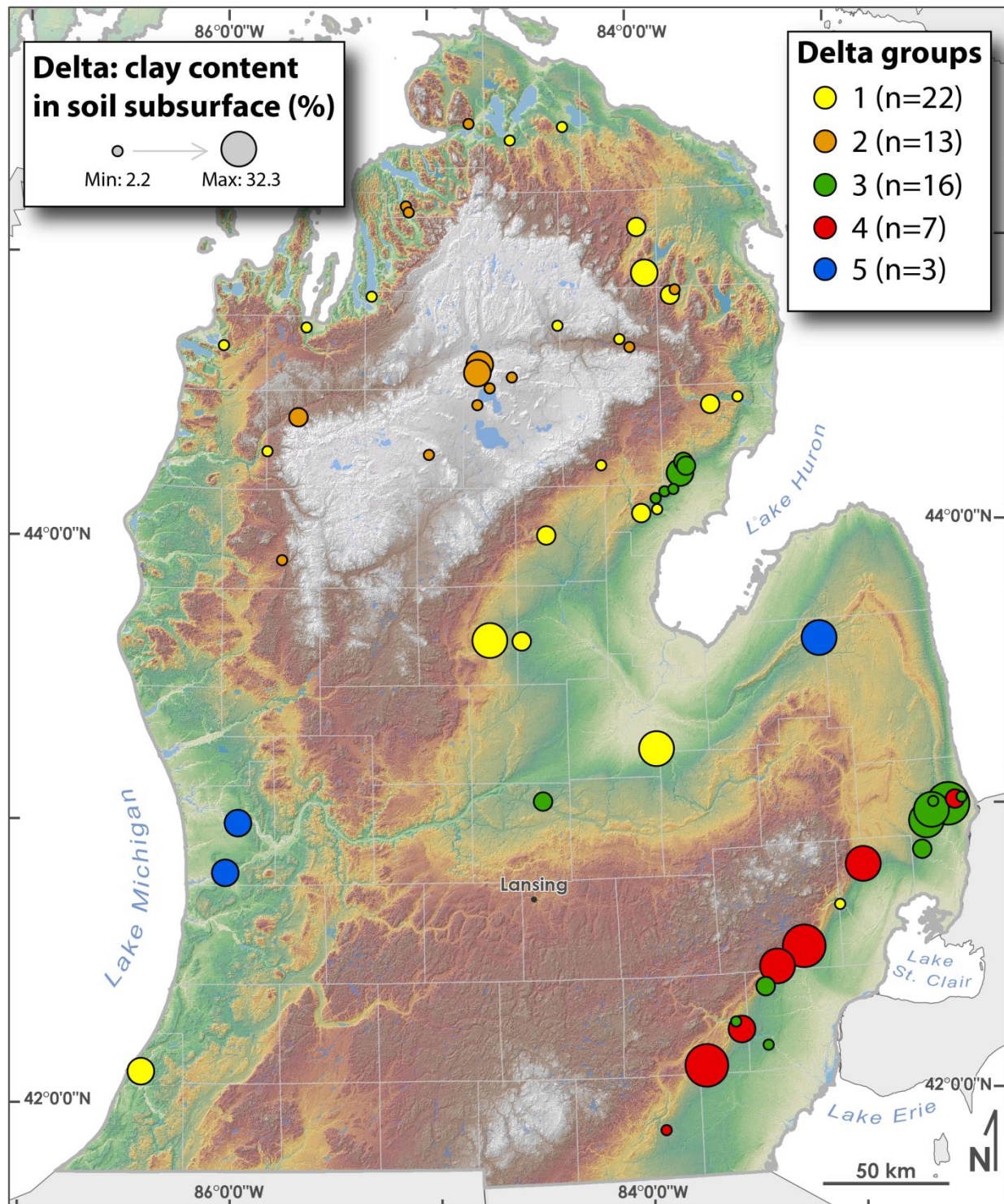


Figure 4.13: A graduated circle map illustrating clay content (%) in the subsurface horizon (C horizon) of soils within the delta plain extent.

Appendix F). Conversely, deltas in Groups 3-5 have relatively low amounts of sand in their catchments, and thus have fine-textured catchments (Figure 4.12). The *scores* from PC1 suggest that Group 1 and 3 are largely explained or categorized by the sediment characteristics within their catchments.

Deltas in Group 4 have particularly large *scores* within PC2, which describes the sediment characteristics within the deltas (Figure 4.10). The relatively large PC2 *scores* associated with Group 4 deltas suggest that this dimension is important in categorizing the Group 4 deltas. In addition to having a high amount of fine sediment within their catchments, deltas in Group 4 (except for the Raisin River delta, which is dominated by sandy textured sediment at depth) also have a high amount of fine sediment within their delta plain, and hence are within fine-textured systems overall (Figure 4.13; Appendix F). Conversely, deltas in Groups 1, 2, and 5 not only have a low amount of fine sediment within their catchments, but also within their delta plain, and are therefore part of sandy-textured systems (Figures 4.12 and 4.13; Appendix F). Lastly, deltas in Group 3 are unique in that they have fine-textured catchments but their delta plains are sandy (Figures 4.11 and 4.13; Appendix F).

Table 4.5 provides a summary of the relative amounts of sand content between the different delta groups within their catchment and delta areas. The variation in sediment characteristics between the delta groups is presumably related to sediment source in the deltas' respective catchments. The majority of the deltas in Groups 1 and 2 occur in landscapes that are dominated by sandy deposits, and hence they have sandy catchments. The likelihood for fine sediment to be deposited in those deltas is comparatively low, and hence, deltas in these two groups are sandy. Conversely, deltas in Groups 3, 4 and 5 are often located where

fine sediment is widespread throughout the catchment and there is high potential for entrainment of fine sediment by rivers, and its subsequent deposition within the delta and into the lake basin. Most of the Group 4 deltas have a high amount of fine sediment within their catchment and the deltas are composed of fine textured deposits (Figures 4.11 and 4.13; Table 4.5). However, many of the deltas in Groups 3 and 5 are *not* fine-textured but have a large amount of fine sediment within their catchments, possibly because there was enough time or sorting power to carry the fine sediment beyond the delta, resulting in a predominantly sandy textured delta (Figures 4.12 and 4.13; Table 4.5).

Table 4.5: A list of the different groups of relict deltas and a comparison of the relative amount of sand content and local topographic variation within their catchment and delta areas

| Delta Group | Catchment sand content | Delta sand content | Topographic variation |
|-------------|------------------------|--------------------|-----------------------|
| 1 | High | High | Moderate |
| 2 | High | High | High |
| 3 | Low | High | Low |
| 4 | Low | Low | Low |
| 5 | Low | High | Low |

4.3.2 Delta and Catchment Topographic Characteristics

Deltas in Group 2 have particularly large scores within PC3, which represents the degree of topographic variation within both the catchment area and delta plain (Figure 4.10). The relatively large PC3 scores associated with Group 2 deltas suggest that this dimension is important in categorizing the Group 2 deltas. Figure 4.14 is a graduated circle map illustrating the median slope (%) measured within each catchment. This map illustrates that many of the deltas in Group 2 have considerably more topographic variation within their catchments than do Group 1 deltas, even though both groups are primarily located in northern Michigan and are

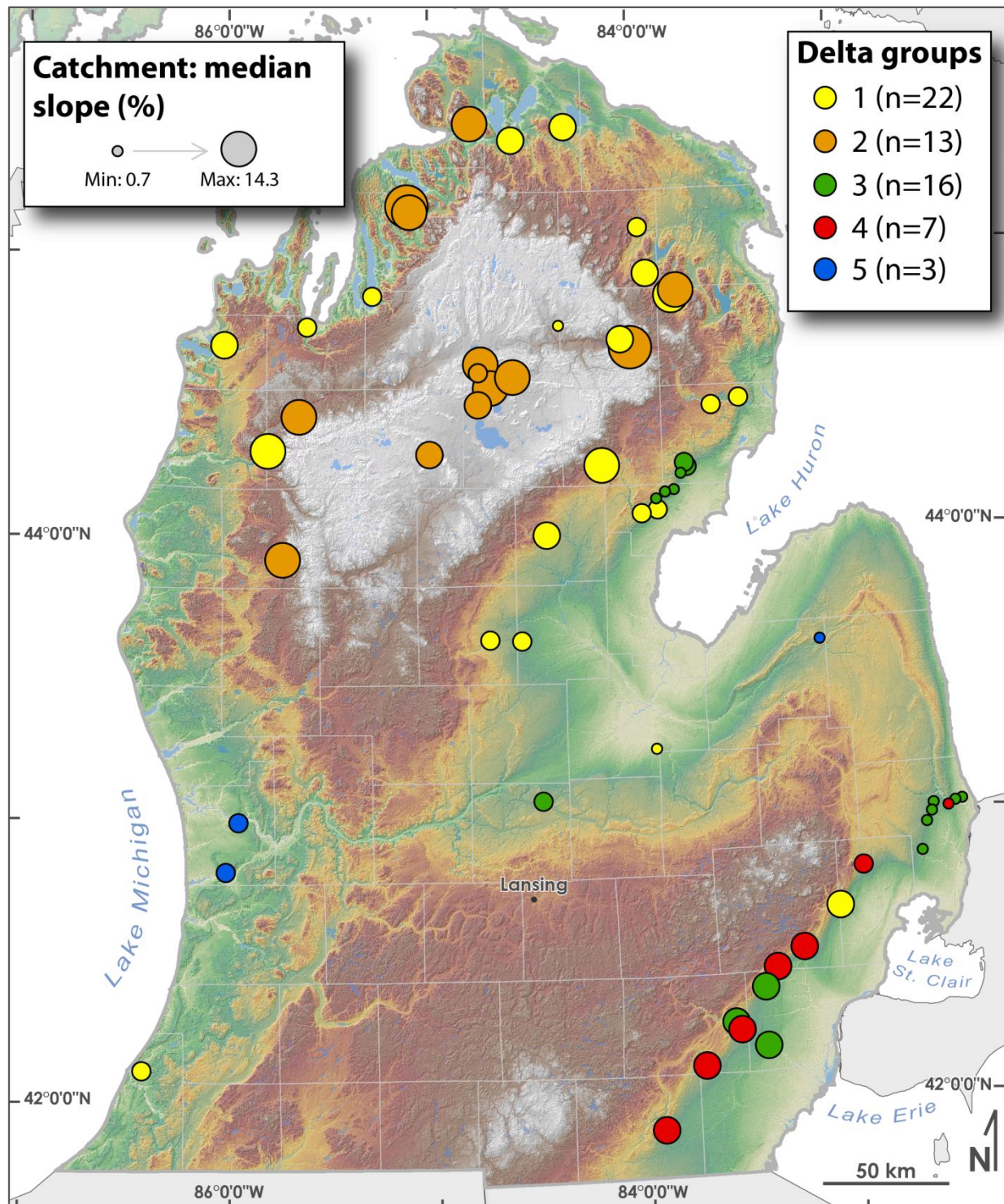


Figure 4.14: A graduated circle map illustrating the median percent slope within a 3 x 3 cell neighborhood, using a DEM, measured for delta catchment.

sandy (Figure 4.14; Table 4.5; Appendix F). Figure 4.14 also shows how the majority of the deltas in Groups 3-5 have similar, consistent, and low to moderate local relief within their catchments (Table 4.5).

The largest correlated variables in PC3 (listed from largest to smallest) are for (1) Melton Ruggedness Number, (2) median percent slope within the catchment, (3) slope of the delta plain, (4) mean percent slope within the catchment, and (5) delta perimeter length (Table 4.3). The delta perimeter length variable has a large negative correlation within PC3 (Table 4.3) and is interpreted to be related to the slope of the delta plain; the difference between the maximum and minimum elevation on a delta plain is often related to the size of the delta. However, three out of those four topographic variables refer to relief within the catchment area, and hence most of the topographic differences between the deltas allude to their catchments, not their deltas *per se*.

The topographic variation between the different groups of deltas is partly related to their geomorphic history. Many of the deltas in Group 2 are kame deltas associated with the sandy heads of outwash within the sandy High Plains region of north-central Lower Michigan. Several Group 2 deltas also formed at or near ice-contact slopes. The stagnant-ice surface and its associated ice-contact slopes collectively would have provided a relatively high relief catchment. Conversely, the majority of the deltas in Groups 1, 3, 4, and 5 often have catchments within interlobate regions and glacial spillway valleys, which range between high and lower relief landscapes.

4.3.3 Delta System Extent

Deltas in Group 5 have particularly large *scores* within PC4, which represents primarily the areal extent of the delta system as a whole; it incorporates both the catchment and delta areal extents (Figure 4.10). The relatively large PC4 *scores* associated with Group 5 deltas suggest that this measure is important in categorizing the Group 5 deltas. The score assigned to each delta in PC4 is largely determined by the following: (1) whether or not the delta had glacial lake contributions, (2) size of the catchment area, (3) abundance of major feeder channels, (4) abundance paleodistributary channels, (5) length-width ratio of the delta plain, and (6) perimeter length of the delta plain. Deltas with glacial lakes as their catchments would have had, assumedly, comparatively large catchments, perhaps larger than can be captured by the GIS. Each delta within Group 5 formed at the mouth of a major glacial spillway, has multiple paleodistributary channels, and has a large length-width ratio (i.e., they are elongate shaped) (Appendix F). Thus, the deltas in Group 5 were correctly assigned relatively large and similar *scores* in PC4 (Figure 4.10). Those feeder rivers that are associated with the majority of the deltas in Groups 1-4 are not known to have been connected to a major glacial lake outlet and also generally have a low length-width ratio (i.e., they are broad or cuspate shaped). This comparison suggests that much of the variation in delta size between the different groups is a function of catchment area, along with the number of feeder and paleodistributary channels (Appendix F).

The delta system extent that is captured in PC4 suggests that more extensive catchment areas lead to larger deltas (Appendix F). Figure 4.15 provides evidence that is slightly in support of this hypothesis. Furthermore, deltas with multiple feeder channels generally have larger

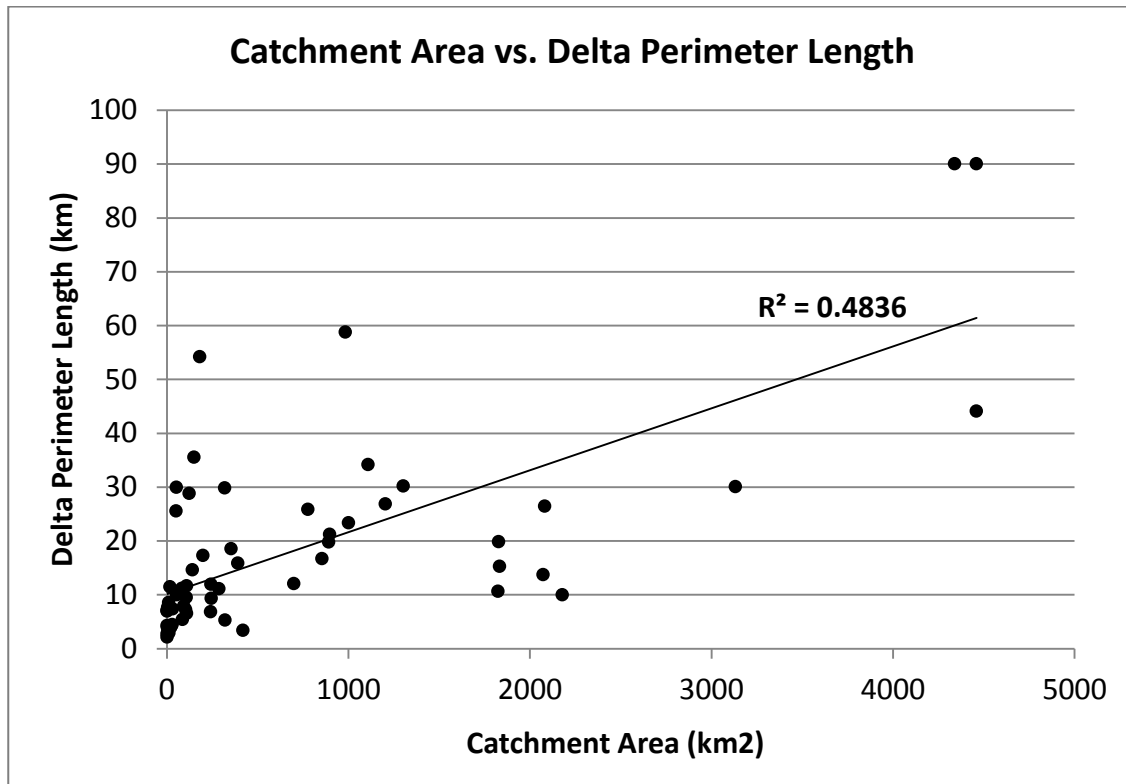


Figure 4.15: A graph that compares each delta's perimeter length (excluding those deltas in Group 5) to its measured catchment area.

catchments, and these rivers often emplace more deltaic sediment. Deltas with multiple feeder channels are likely to have more extensive catchments because the delta catchment includes an amalgamation of smaller watersheds, each of which contains a river that contributed sediment to the delta. Therefore, having multiple major feeder channels increases the extent of the delta catchment. The Sturgeon-Pigeon River and Slagle Fan deltas are two examples of deltas that are sourced by more than one major river and have particularly large catchments and delta plain extents.

Note, however that the catchment areas defined by the GIS for the deltas in Group 5 are not entirely accurate. Deltas in Group 5 were largely sourced from a major glacial lake and many of those landscapes that are presently delineated for the catchment were inundated by

water during delta construction. Hence, for this reason the “glacial lake contribution” was included as a variable in the overall data set. The extent of the catchment areas associated with Group 5 deltas were perhaps exceedingly underestimated with regard to water supply or overestimated in regard to terrestrial extent, which is the rationale for excluding them from Figure 4.15. That being said, the *scores* in PC4 did indeed capture the notion that the Group 5 deltas had a large contributing water source, which is akin to an extensive catchment. In summary, these data illustrate that more extensive deltas are often related to a large source of water and/or catchments (Figures 4.15; Appendix F).

4.4 Summary of Delta Group Analysis

This study numerically groups the relict, late-Pleistocene deltas in the Lower Peninsula of Michigan. Topographic data, used in conjunction with surface and subsurface textural data, enabled me to classify and group 61 relict deltas. For each delta and its modern catchment (watershed), 31 topographic and soil textural attributes were analyzed. Predominant morphologic variables from this data array were evaluated using PCA. The PCA identified four components that explained $\approx 69\%$ of the total variance. These components were interpreted to represent (1) the sediment characteristics of the catchments, (2) the sediment characteristics of the deltas, (3) topographic characteristics of both the deltas and the catchments, and (4) the delta system extent. An incremental *F* test of the PCA scores suggested five optimal clusters (or groups) of deltas. Subsequently, a K-means + Ward’s clustering algorithm was employed to assign the 61 deltas to five main groups. Group 1 deltas are located in northern Michigan, and are relatively large and sandy. Group 2 deltas are also sandy and also mainly located in northern Michigan, but are smaller and have higher relief catchments. Group 3 deltas are primarily

located in eastern and southern Michigan; they are relatively small deltas that have fine textured catchments but sandy deltas. Group 4 deltas are located in southeastern Michigan and have both fine textured catchments and deltas. There are only three Group 5 deltas, all of which are elongate, fluvial-type deltas that are located at the mouths of major meltwater spillways that carried the discharge from a proglacial lake.

4.5 Conclusions

Results from this study confirm that relict late-Pleistocene deltas – at least those in Lower Michigan - have unique topographic and sedimentologic characteristics that facilitate their morphologic grouping. At least five different, distinct types of deltas formed during the deglaciation of the Lower Peninsula, which further suggests that unique coastal and terrestrial conditions were contributing to delta formation. With additional research, these different types of deltas may be used as proxies for certain paleoshoreline and/or terrestrial conditions during their formative periods.

Using the data available in this dissertation, the section that follows describes and interprets the paleoenvironmental conditions associated with each delta group during their formative periods. Topographic and sedimentologic patterns suggest that the majority of Group 1 deltas are arcuate-shaped, sandy landforms, often with only one major feeder channel (Table 4.6). Catchments associated with these deltas include low to high relief landscapes that often encompass interlobate regions and ice-contact slopes that have extensive areas of sandy-textured deposits (Table 4.6). Group 1 deltas are interpreted as wave-dominated deltas (Galloway, 1975; Bhattacharya and Giosan, 2003; Janecke and Oaks, 2011) that form when large amounts of sand are rapidly deposited into a relatively large basin with strong wave

energy (Table 4.6). The Black River delta in northern Michigan is an example of a typical Group 1 delta (Figure 4.16).

Table 4.6: The common characteristics of the deltas within each of the five delta groups

| | Group 1 | Group 2 | Group 3 | Group 4 | Group 5 |
|---|----------------|----------------------------|-------------------------|-------------------------|-------------------------|
| Delta category | Wave-dominated | Wave-dominated, kame delta | Wave-dominated | Wave-dominated | Fluvial-dominated |
| Shape | Arcuate | Arcuate | Arcuate | Arcuate | Elongate |
| Delta most areally extensive sediment texture | Sand | Sand | Sand | Fine textured sediments | Sand |
| Catchment most areally extensive sediment texture | Sand | Sand | Fine textured sediments | Fine textured sediments | Fine textured sediments |
| Area of receiving basin | Large to small | Small | Large | Large | Small |
| Local-relief in catchment | Low to high | High | Moderate to high | Moderate to High | Moderate to High |
| Number of feeder channels | Single | Single | Single | Single | Single |
| Number of distributary channels | Single | Single | Single | Single | Multiple |
| Glacial lake contribution | No | No | No | No | Yes |

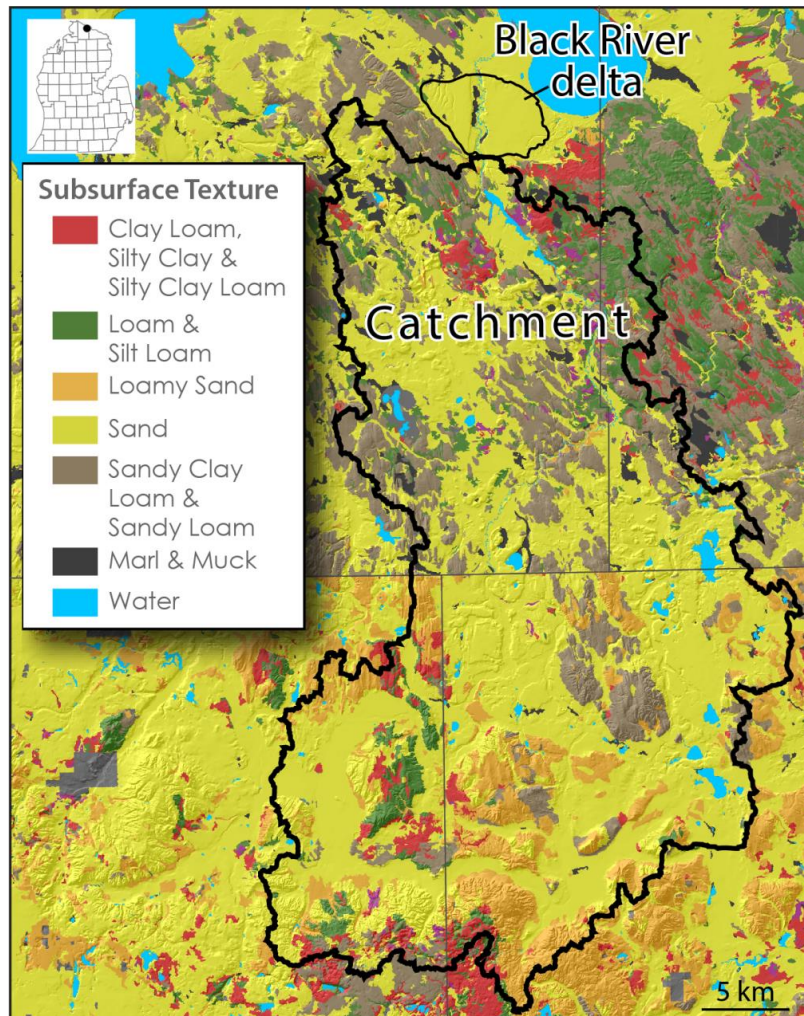


Figure 4.16: A map of the Black River delta and its catchment in northern Michigan, illustrating the typical sediment characteristics of a Group 1 delta and its

Similarly, Group 2 deltas are also mostly arcuate-shaped, sandy landforms, and often have only one major feeder channel (Table 4.6). These deltas, however, have smaller catchments with high local relief, and they were often sourced directly by melting ice. Group 2 deltas are interpreted as wave-dominated kame deltas that formed as large amounts of sand were debouched from a (likely) stagnant ice margin, into a relatively confined basin with powerful wave energy (Table 4.6). Seven of the 13 Group 2 deltas were likely sourced directly by melting ice. The remaining six that were presumably not directly emplaced from an ice margin have high relief catchments that promoted copious amounts of runoff, thereby contributing large amounts of sediment to the basin and its feeder streams. Several deltas within Groups 1 and 2 are also broadly shaped and have multiple major feeder channels (e.g., the Sturgeon-Pigeon River delta and the Slagle Fan delta); these deltas are interpreted to represent coalesced deltas. These deltas formed when multiple deltas formed in close proximity, and their deposits coalesced. Although not coalesced, the Higgins Lake Ridge and Coy Ridge deltas located in sandy High Plains region of north-central Lower Michigan are examples of typical Group 2 deltas (Figure 4.17).

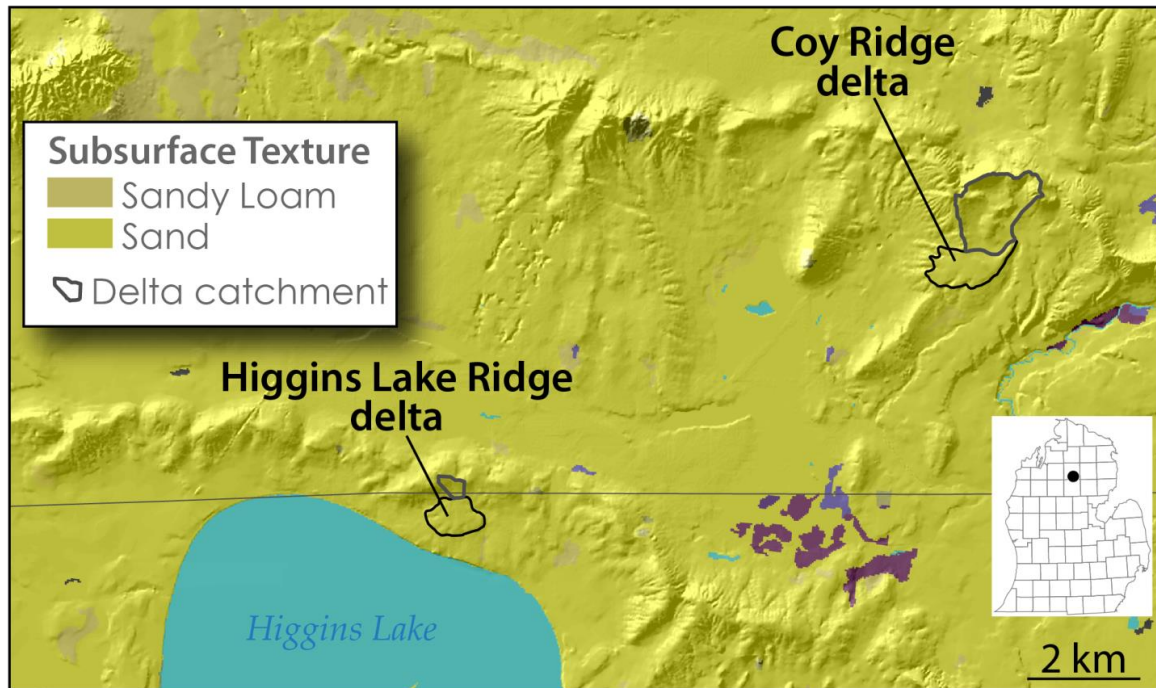


Figure 4.17: A map of the Higgins Lake Ridge and Coy Ridge deltas, along with their modern catchments, that illustrates the typical sediment characteristics Group 2 deltas. These are examples of kame deltas and thus the modern catchment area is much smaller than what would have been present while the deltas were forming.

Similar to Group 1 and 2 deltas, Group 3 deltas are mostly arcuate-shaped and sandy, and usually have only one major feeder channel (Table 4.6). The catchments associated with these deltas include moderate to high relief landscapes that often encompass interlobate regions and ice-contact slopes that are dominantly composed of fine-textured deposits. Group 3 deltas are interpreted as wave-dominated deltas that formed when large amounts of fine and coarse textured sediments were debouched into a relatively large basin (Table 4.6). These deltas likely formed over an extended period of time, or when there was an extensive area receiving water, enabling wave-sorting of the fine sediment beyond the delta, resulting in the preservation of mainly sandy-textured sediments within the delta proper. The Big Creek and Cedar Creek I deltas, near the northern limits of the Saginaw Lake plain region, are examples of typical Group 3 deltas (Figure 4.18).

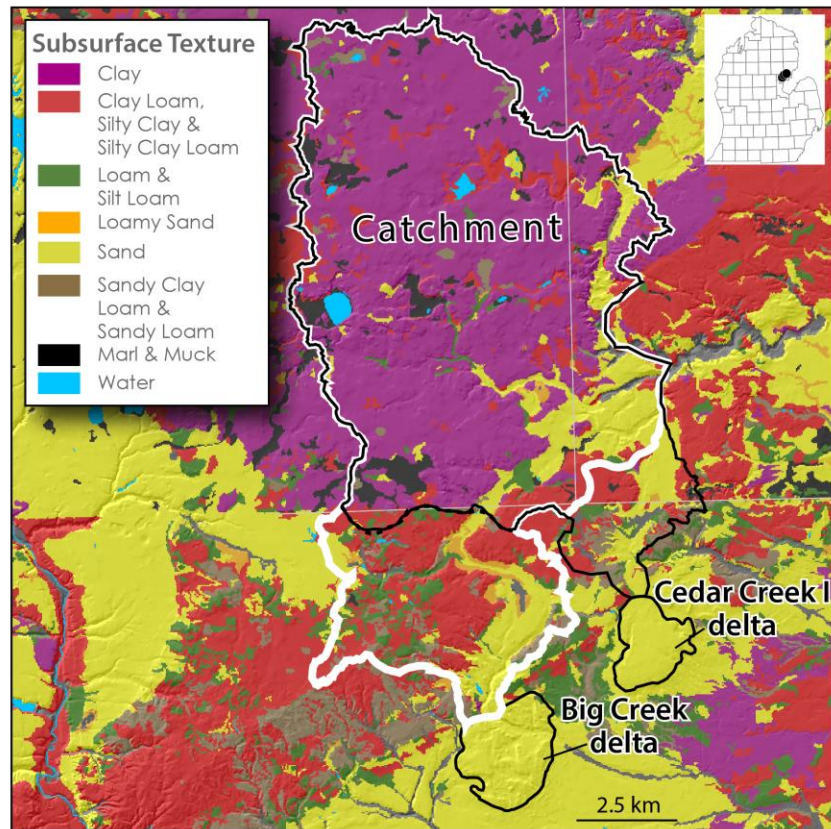


Figure 4.18: A map of the Big Creek and Cedar Creek I deltas, along with their catchments, and illustrating the typical sediment characteristics Group 3 deltas.

Similar to Group 3 deltas, Group 4 deltas are often arcuate-shaped and have one major feeder channel (Table 4.6). However, unlike the sandy Group 3 deltas, Group 4 deltas are mostly composed of fine textured deposits. The catchments associated with these deltas include moderate to high relief landscapes that often encompass interlobate regions that are also dominantly composed of fine-textured deposits. Group 4 deltas are interpreted as wave-dominated deltas that formed when large amounts of fine textured sediments were debouched into a relatively large basin with strong wave energy (Table 4.6). These deltas formed perhaps over a relatively short period of time, as they are relatively poorly sorted (Figure 4.19) or when there was a limited amount of sorting power available in the fluvial and coastal system to sort

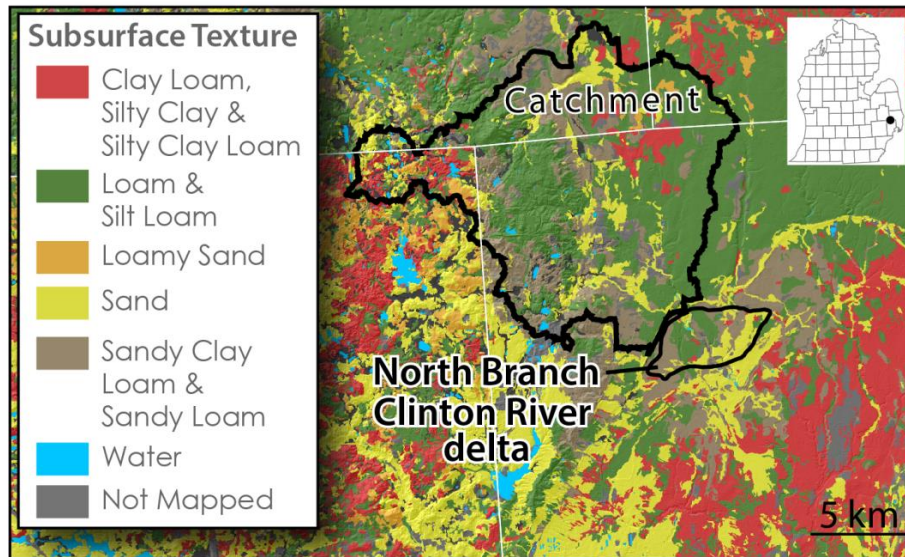


Figure 4.19: A map illustrating the North Branch Clinton River delta and its catchment, and illustrating the typical sediment characteristics of a Group 4 delta.

the majority of the fine textured sediments out of the delta sediments. Some Group 4 deltas may have also been influenced by higher succeeding lake levels which reworked the delta deposits and/or deposit a veneer of fine-textured sediment over the delta plain (Leverett and Taylor, 1915). The Saline River and North Branch Clinton River deltas located in southeast Lower Michigan are examples of typical Group 4 deltas (Figure 4.19).

Lastly, the three Group 5 deltas are all elongate-shaped, sandy landforms, with one large feeder channel and several, parallel or sub-parallel distributary channels. The three deltas in this group were all sourced from glacial lakes and are located at the mouths of spillways that carried the discharge from large proglacial lakes. Group 5 deltas are interpreted as fluvial-dominated deltas that form when water within a spillway is debouched into a relatively confined estuary (Table 4.6; Galloway, 1975). Fluvial processes dominate the construction of Group 5 deltas, due largely to the confined estuary in which they formed, implying that wave energy was limited or less influential during and after the construction of the delta.

Furthermore, Group 5 deltas may also be a product of unique inputs of water and sediment from the outflows from a glacial lake. The distributary channels that often form in these deltas could have resulted from the spillway having reduced water and sediment supply following periods of large, even catastrophic, sources of water and sediment. The Allendale and Cass River deltas, both located at the mouth of a major glacial lake spillway, are examples of typical Group 5 deltas (Figure 4.20).

Topographic and sedimentologic patterns suggest that wave-dominated deltas were the most common types of deltas formed during the late Pleistocene in the Lower Peninsula. The

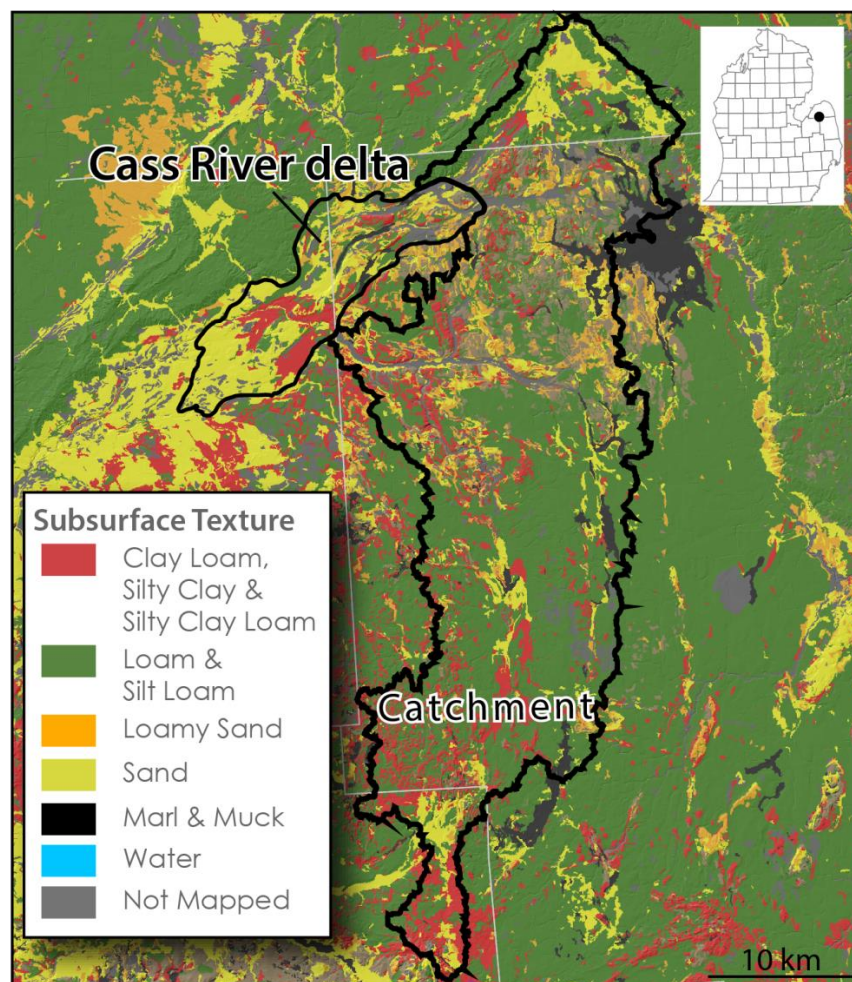


Figure 4.20: A map illustrating the Cass River delta and its catchment, and illustrating the typical sediment characteristics of a Group 5 delta.

wave-dominated deltas are often mapped on the east side of the Lower Peninsula, along the margins of relatively large glacial lake basins. These data emphasize strong, persistent and sustained wind and wave energies in the Great Lake region during the late Pleistocene and support the work of Krist and Schaetzl (2001) and Vader et al. (2012).

Chapter 5 – Conclusion

5. Summary

The late Pleistocene deglaciation of the Lower Peninsula of Michigan did not proceed as a steady retreat, but rather, was irregular and punctuated by a series of glacial retreats and readvances. The complicated series of stadial and interstadial glacial events that occurred here led to large fluxes of glacial meltwater associated with meltwater-rivers. Many of these rivers flowed into pro- and post-glacial lakes. The waxing and waning of the ice margin also created fluctuations in outlet locations, resulting in different lakes stages and phases within the Great Lakes' basins and on the interior uplands. Deltas were common features that formed in many of these proglacial lakes. Very few studies, however, have focused on these deltas. Instead, much of the research on the lakes and lacustrine systems of Michigan has focused on other features associated with the lake shorelines, e.g., beach ridges, meltwater spillways, wave-cut bluffs, and spits.

Several methods have been used to record paleo-water plane elevations from relict beach ridges, wave-cut bluffs, meltwater spillways, spits, and deltas. To date, methods for identifying the boundary between subaerial and subaqueous components of relict meltwater spillways and spits have not been established. Only the *range in elevations* of the lakes linked to relict meltwater spillways and spits, so far, have been quantifiable. As a result, they provide minimal information regarding paleolake-level elevation(s). Conversely, paleo-water plane elevation(s) can be estimated to a moderate to high degree of accuracy by using topographic information associated with features such as relict beach ridges, wave-cut bluffs, and deltas, although each provides a differing amount of uncertainty. For relict beach ridges, wave-cut

bluffs, and deltas, lake elevation is commonly associated with the contact between subaerial and subaqueous deposits, and this contact can be identified from either surface morphologies or internal sedimentology. The elevation at the boundary between subaerial and subaqueous deposits provides a reasonable estimate of lake level when the coastal featured formed. Researchers must be aware that paleolake-level reconstructions may differ, however, depending on the relict coastal feature(s) employed to interpret the elevation of the water plane. Likewise, the accuracy of the estimate varies as a function of the landform utilized as a lake level proxy.

Deltas are the product of a terrestrial fluvial system which ultimately flows into a lacustrine/marine system. They are, therefore, unique in their ability to infer both paleocoastal and paleoterrestrial conditions during their formative periods. Information about paleoterrestrial conditions within the catchment area (e.g., climate, discharge, sediment load, and landscape stability), as well as paleocoastal conditions within the lake (e.g., lake-level elevation, wave energy, wind direction, river mouth dynamics, basin subsidence, direction and intensity of longshore currents) are often recorded in the geometry, topography and sedimentological characteristics of relict deltas. Thus, deltas are potential proxies for a number of paleoenvironmental systems, but have, to date, been underutilized for this purpose. Future studies regarding the glacial history of the Great Lakes region may consider using relict deltas as proxies for water plane elevations, and to better understand the terrestrial and coastal conditions during their formative periods.

An extensive map of 61 relict Pleistocene deltas in the Lower Peninsula of Michigan is presented in this dissertation. This map, showing deltas that formed between ≈ 21.0 and 13.0

cal ka BP, will hopefully support future relict delta research in Michigan. Elevation data (10 m NED DEM), used in conjunction with surface and subsurface textural data (NRCS SSURGO county-level soil maps and water and oil/gas log data), facilitated this mapping effort. Twenty seven of the deltas that were mapped in this study had been acknowledged in previous works, whereas 34 deltas are unique to this research. Many of the deltaic systems and landforms mentioned in previous works consist of multiple or complex deltas that had formed over several lake *stages* and/or *phases*. Most of the deltas mapped in this study are associated with one or more of the major fluvial systems presently active in Lower Michigan; many of these rivers acted as meltwater conduits during the late Wisconsin (MIS 2). Most of the relict deltas studied here grade toward a known, ancestral Great Lakes' shoreline; however 16 deltas, many of which are kamic deltas, terminated into an unidentified and currently unknown or unstudied paleolake-level and/or lake stage. These latter types of deltas advocate for the existence of several pro- and postglacial lake-levels/stages that were overlooked in previous works, and thus, may spur further research on these lakes.

The relict deltas mapped in this dissertation were numerically grouped using principal components analysis and K-means clustering methods. Relict deltas with similar geomorphic and environmental components, and with comparable sediment textures and morphologic characteristics, were categorized together. The grouping analysis suggests that there are several – at least five - different, distinct types of deltas in Lower Michigan, suggesting that unique coastal and terrestrial conditions were contributing to the formation of these delta groups. With additional research, the different types of deltas may be used as proxies for certain paleoshoreline and/or terrestrial conditions during their formative periods.

To that end, the five groups of deltas mapped in this study are interpreted in represent the following paleoenvironmental conditions. The majority of Group 1 deltas are wave-dominated deltas that formed when large amounts of sandy textured sediments were rapidly deposited into a relatively large lake basin with strong wave energy. Group 1 deltas are mostly in the northern Lower Peninsula. All of Group 2 deltas are in northern Lower Michigan and most are wave-dominated kame deltas that formed as large amounts of sandy textured sediments were debouched from a stable (and likely stagnant) ice margin. Many of the Group 2 deltas are graded towards an unknown or unstudied paleolake. Group 3 deltas are located in both northern and southern Lower Michigan. The bulk of these deltas are wave-dominated that formed when large amounts of fine textured sediments were debouched into a relatively large lake basin with strong wave energies. These deltas are, however, sandy and thus, not fine-textured, even though fine textured sediments dominate their catchments. I believe that these deltas formed over an extended period of time, or when there is a sustained amount of water moving across the delta, facilitating the sorting of the fine sediment from the delta surface and transporting it beyond the delta proper. Thus, mainly sandy-textured sediments were preserved within these deltas. Similar to Group 3 deltas, the majority of Group 4 deltas are also wave-dominated and formed when large amounts of fine textured sediments were debouched into a relatively large lake with strong wave energy. However, unlike the Group 3 deltas, Group 4 deltas are mostly composed of fine textured deposits. Most of the Group 4 deltas are located in southeastern Michigan, and likely formed over a relatively short period of time, or when there was a limited amount of sorting power to winnow the fine textured sediments from the delta. Group 4 deltas may also result from situations in which a higher succeeding lake level reworks

the original delta deposits and/or deposits a veneer of fine-textured sediment over the delta plain. Group 5 deltas are fluvial-dominated deltas that formed when water within a spillway was debouched into a relatively confined estuary. Fluvial processes dominated the construction of Group 5 deltas, due to the confined system in which they formed, implying that wave energy was likely less influential during and after the construction of these deltas. Thus, Group 5 deltas have long, narrow bars and channels that resemble fluvial morphologies. Lastly, broadly shaped deltas that have multiple major feeder channels, mainly within Groups 1 and 2, are termed coalesced deltas in this study. They formed when multiple deltas were constructed in close proximity to each other, allowing their deposits to merge.

Detailed analysis of the internal structure of the deltas mapped in this study was beyond the scope of this dissertation. However, given that the majority of the deltas are dominated by coarse-grained, sandy texture sediments, which would have likely been deposited under homopycnal and hyperpycnal flow-conditions, the majority of the deltas in Lower Michigan likely have Gilbert-type sedimentologies.

Arcuate-shaped deltas are the most common type of delta in Lower Michigan; they are interpreted to have been largely influenced by strong waves during their formative periods. These deltas are often located on the eastern side of the Lower Peninsula, along the margins of relatively large lakes. The large numbers of arcuate deltas suggest that strong, persistent and sustained wind and wave energies were the norm in the Great Lakes region during the late Pleistocene (Krist and Schaetzl, 2001; Vader et al., 2012).

The new deltas identified in this study confirm that far more deltas formed in Lower Michigan, during deglaciation, than were previously known. It is my hope that the data

presented in this dissertation will promote further analysis of relict deltas in Michigan, with the goal of advancing our knowledge in the environmental conditions within which the deltas formed.

APPENDICES

APPENDIX A: Water and Oil/Gas Log Graphic Information

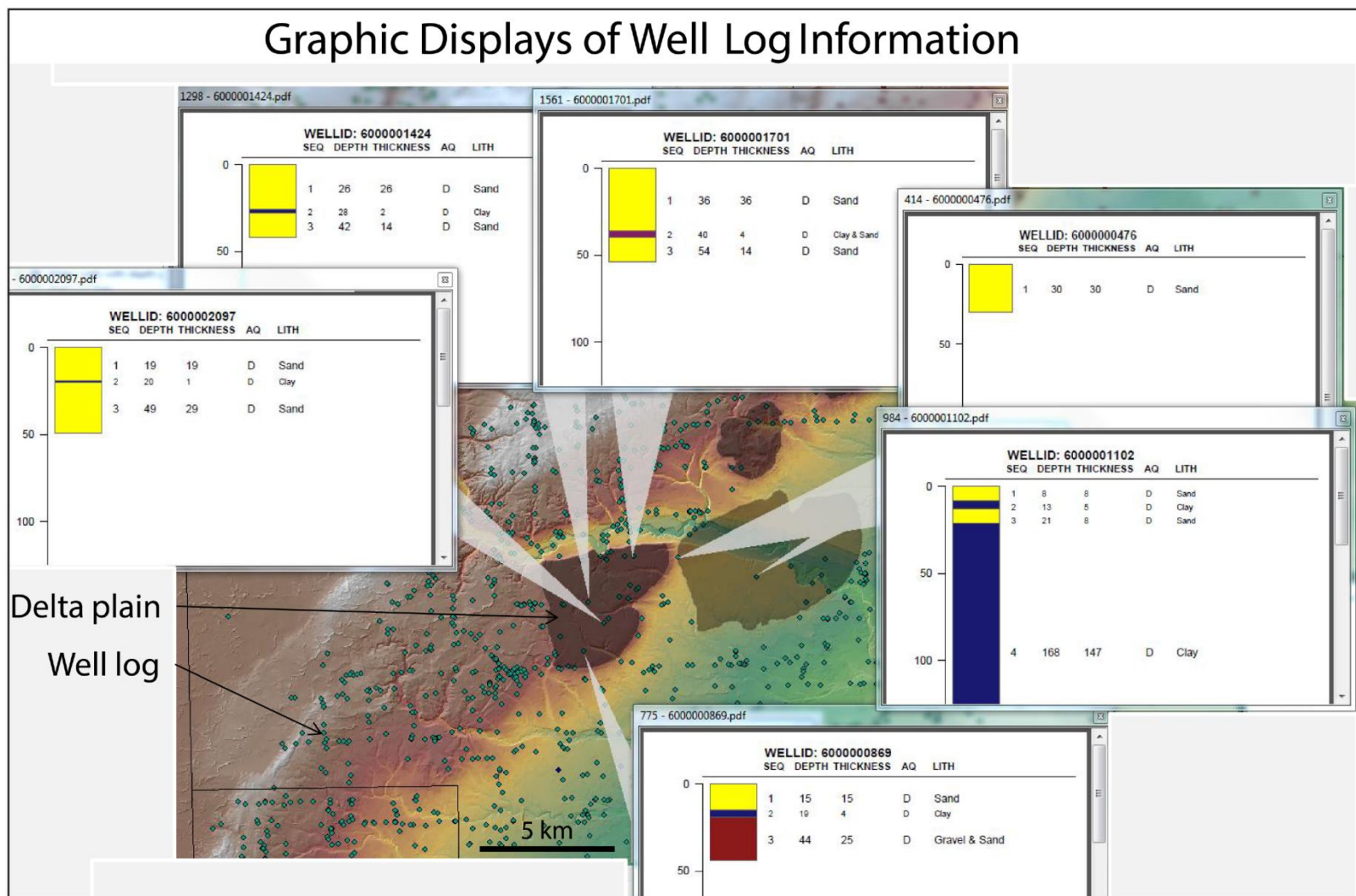


Figure A.1: Graphic display of well log information for a few wells located on a delta plain (delta plain shaded in black)

APPENDIX B: Profiles

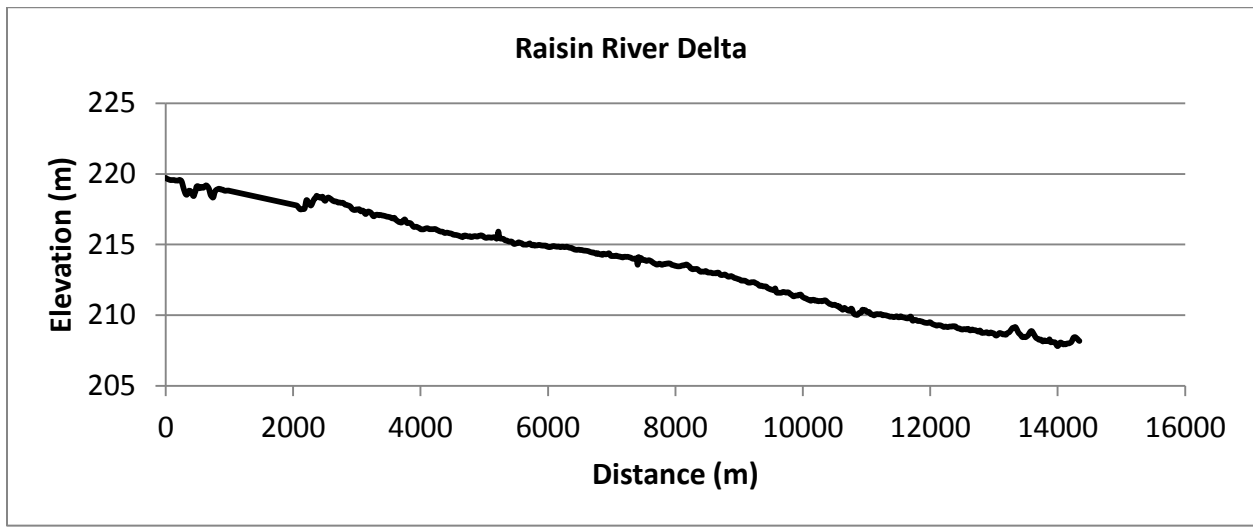


Figure B.1: Raisin River delta profile

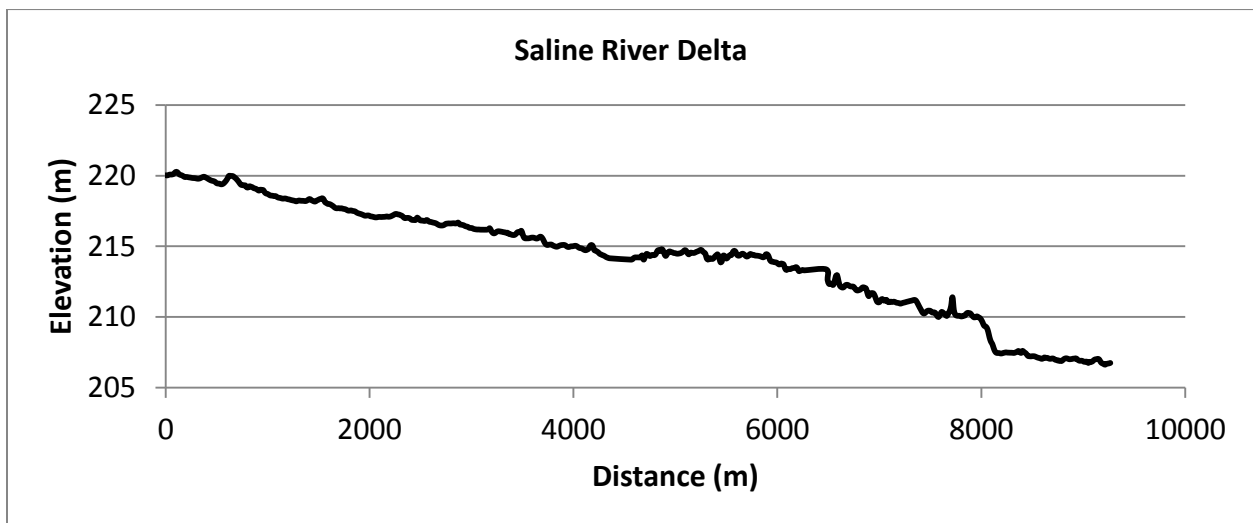


Figure B.2: Saline River delta profile

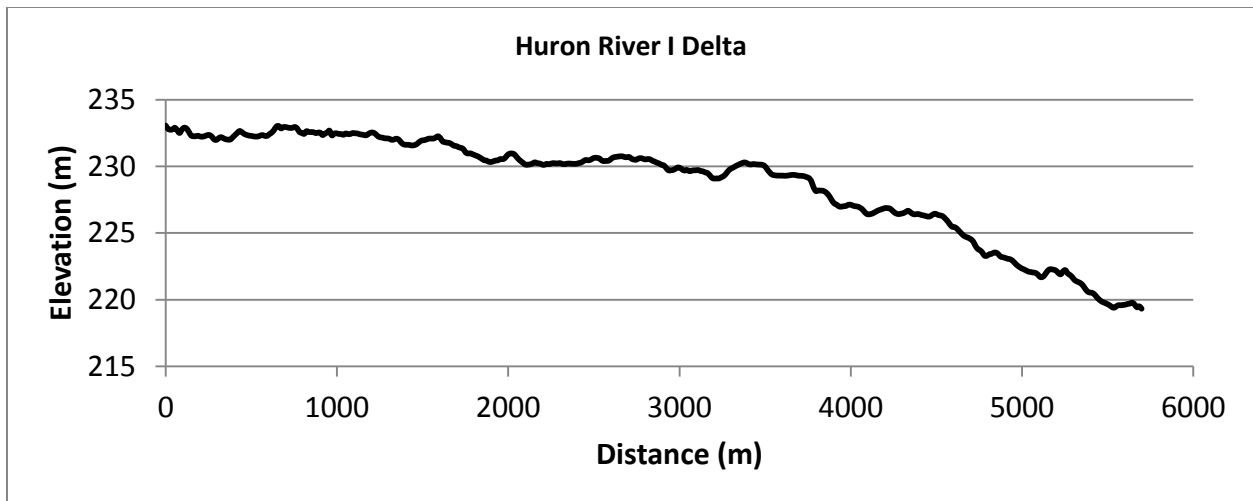


Figure B.3: Huron River I delta profile

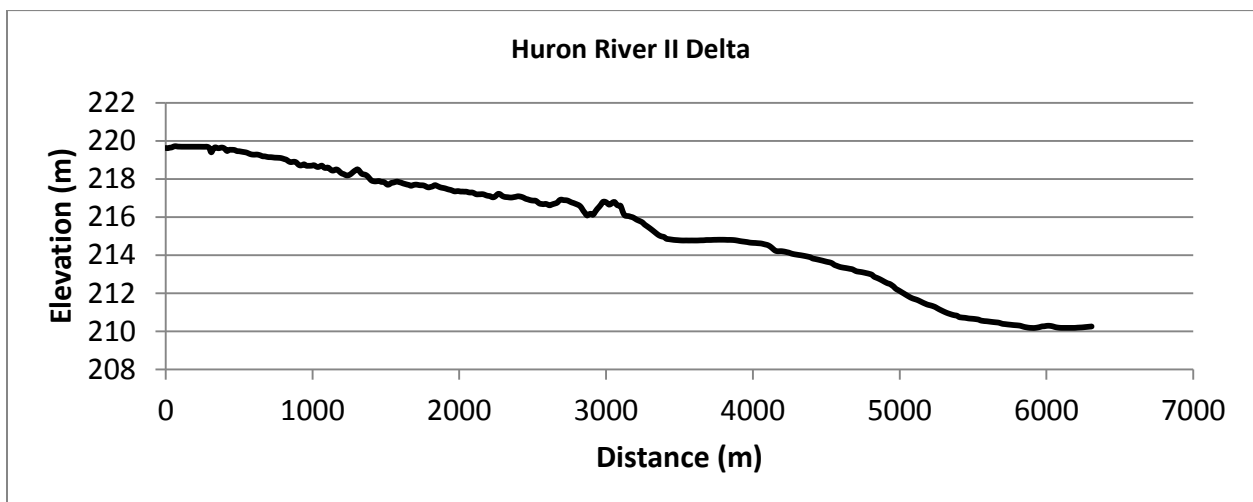


Figure B.4: Huron River II delta profile

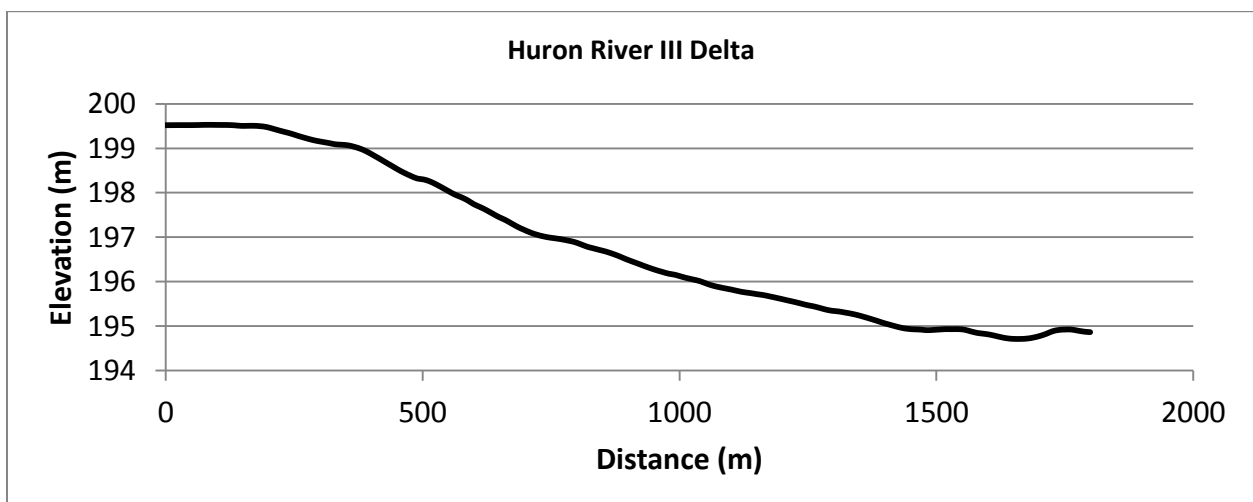


Figure B.5: Huron River III delta profile

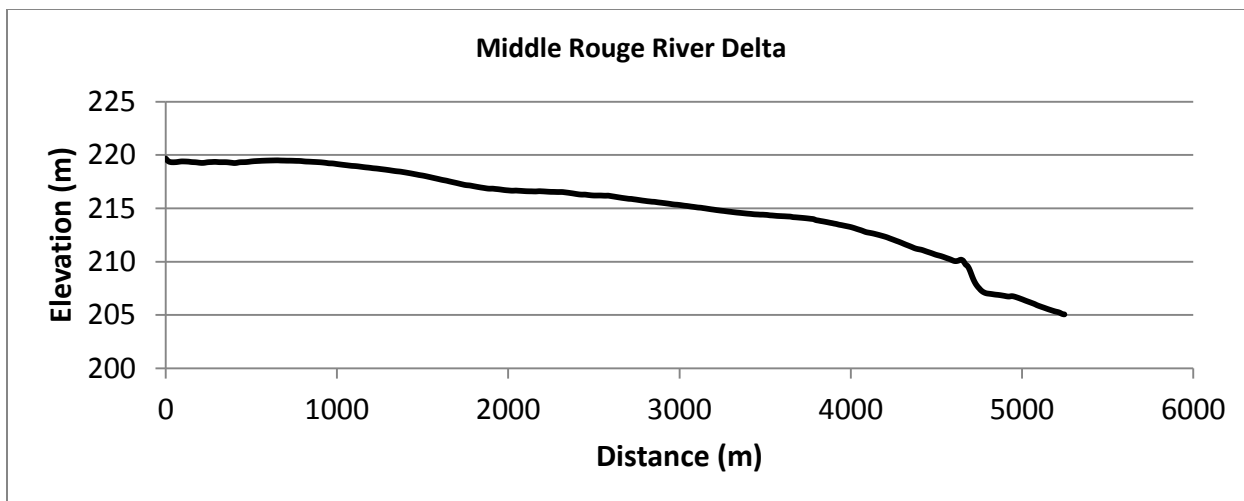


Figure B.6: Middle Rouge River delta profile

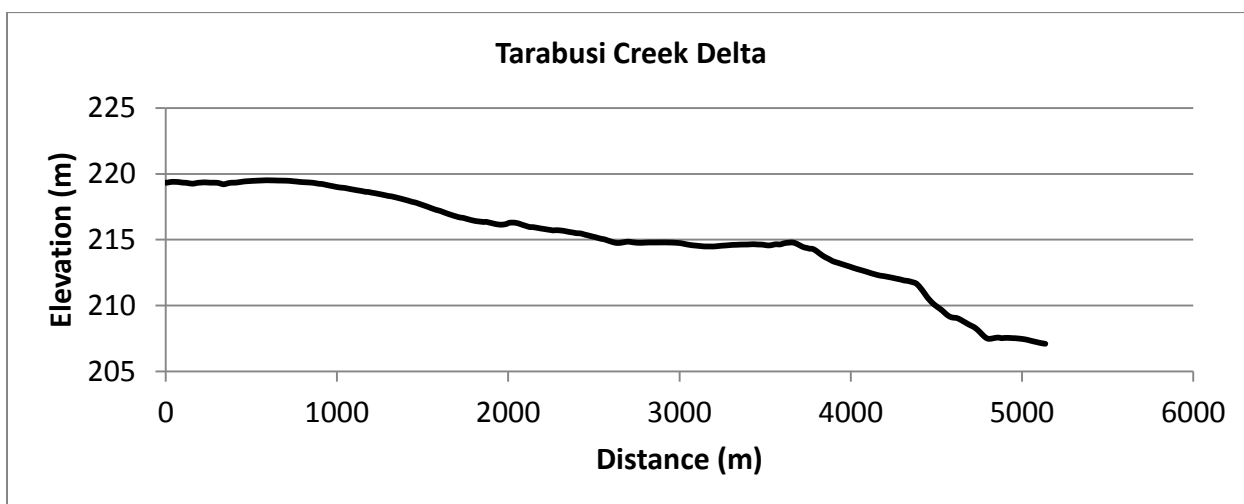


Figure B.7: Tarabusi Creek delta profile

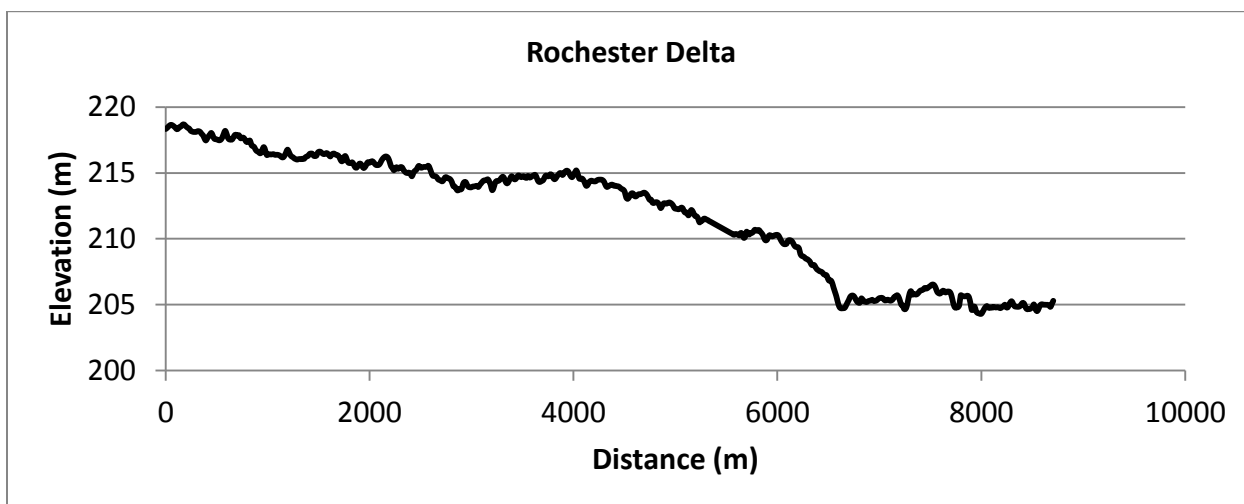


Figure B.8: Rochester delta profile

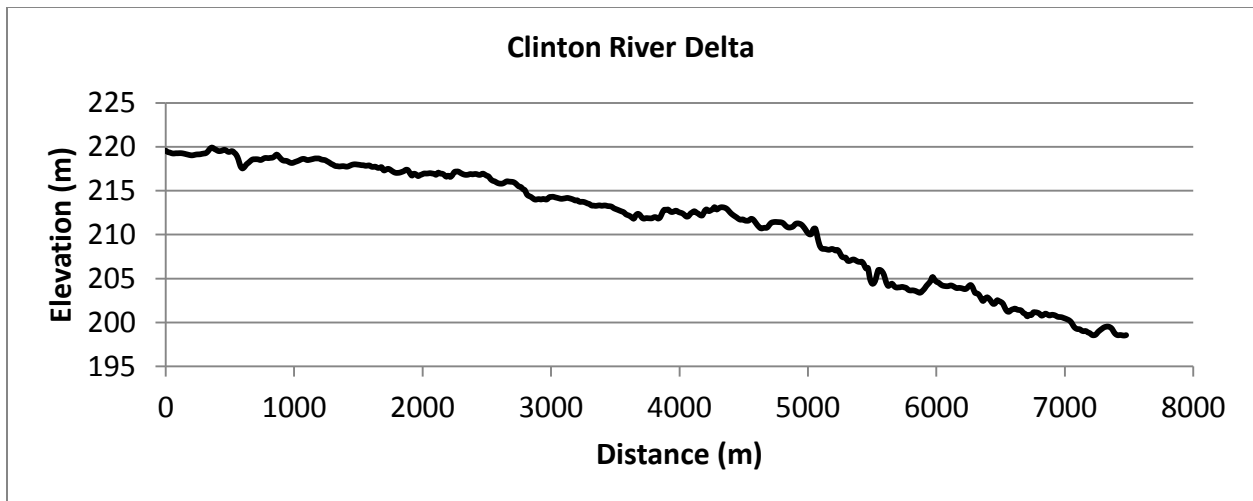


Figure B.9: Clinton River delta profile

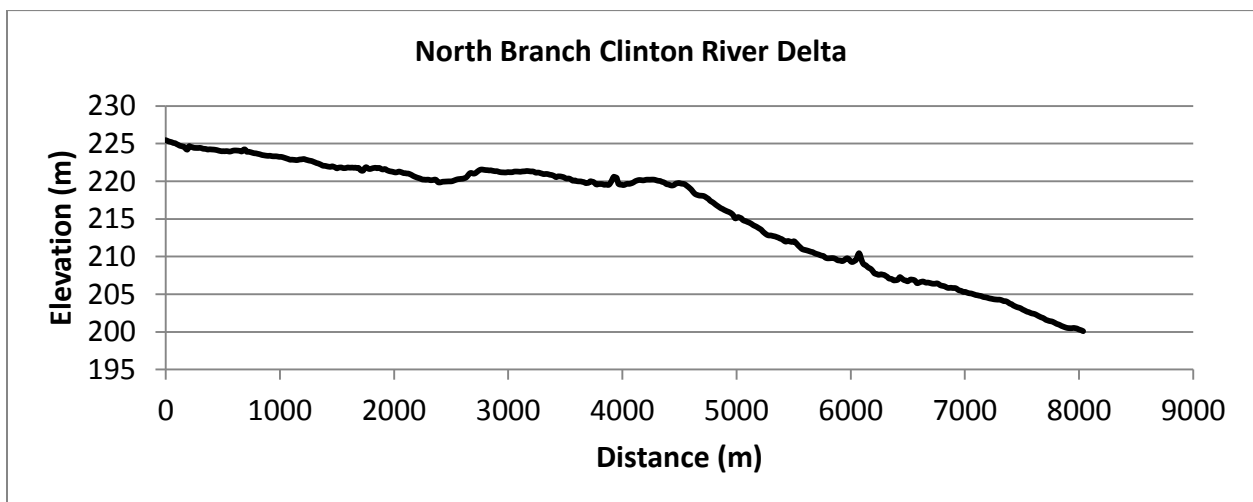


Figure B.10: North Branch Clinton River delta profile

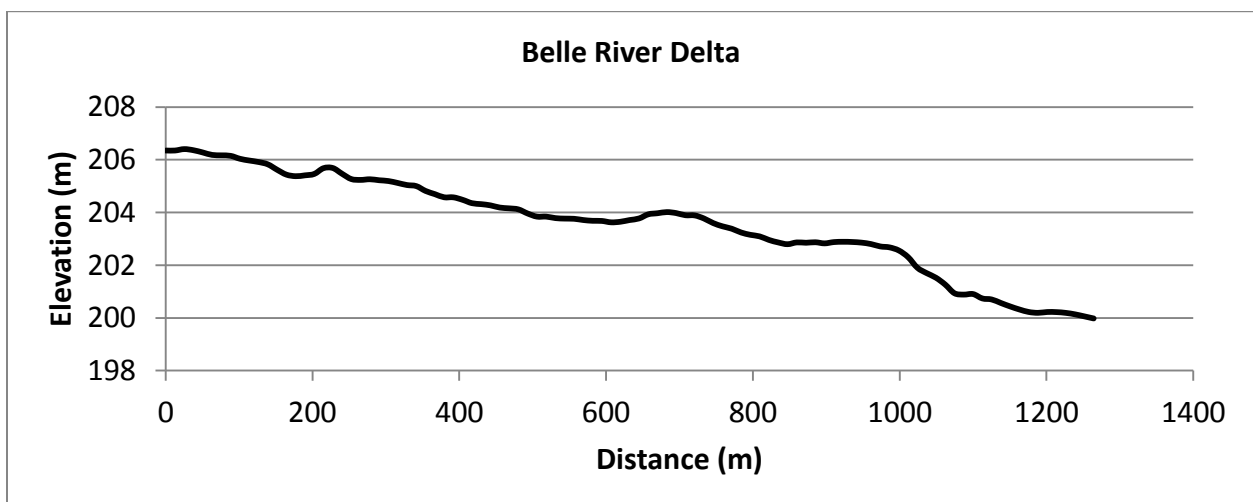


Figure B.11: Belle River delta profile

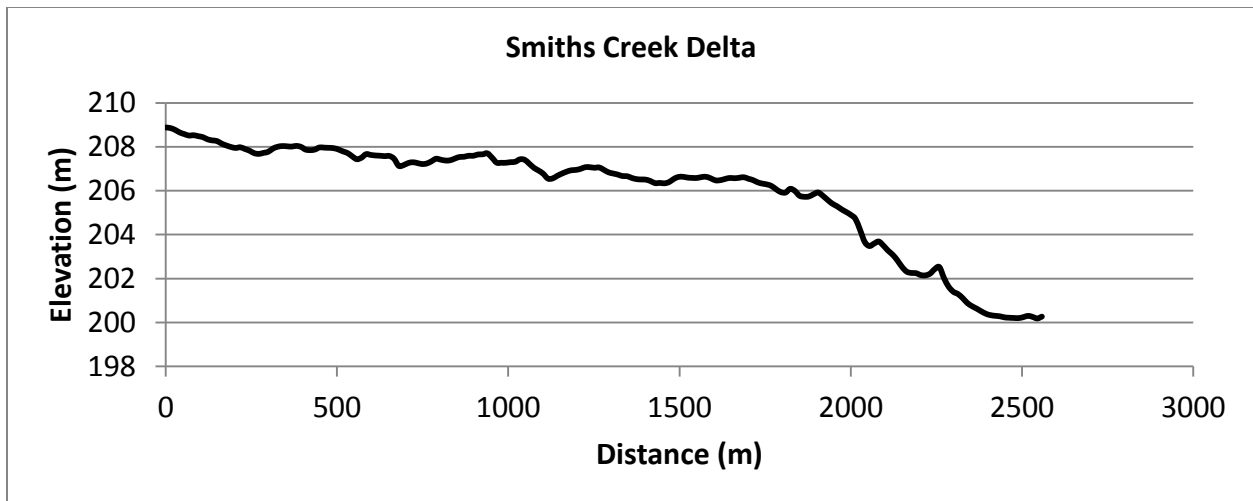


Figure B.12: Smiths Creek delta profile

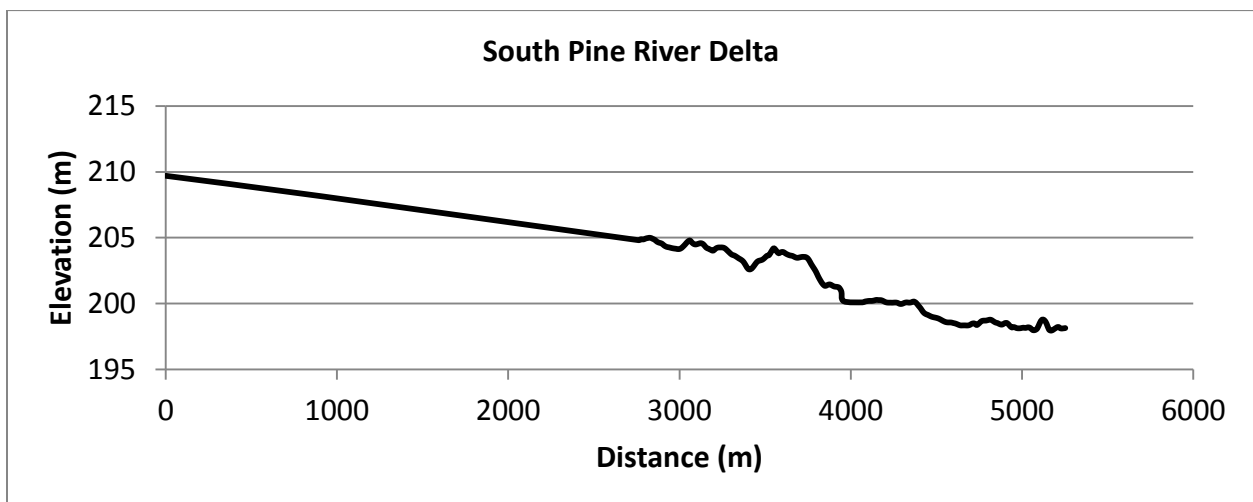


Figure B.13: South Pine River delta profile

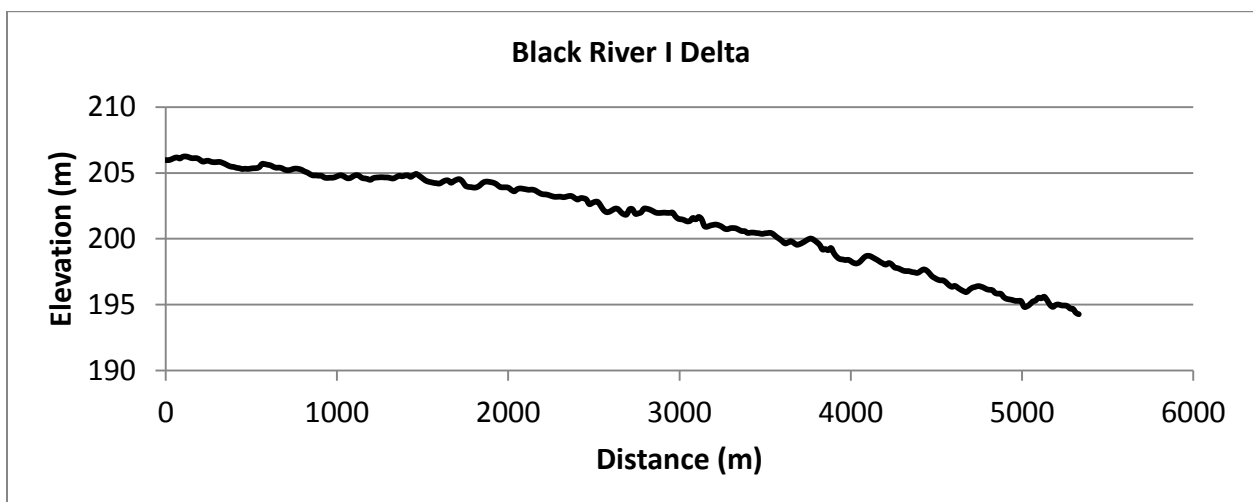


Figure B.14: Black River I delta profile

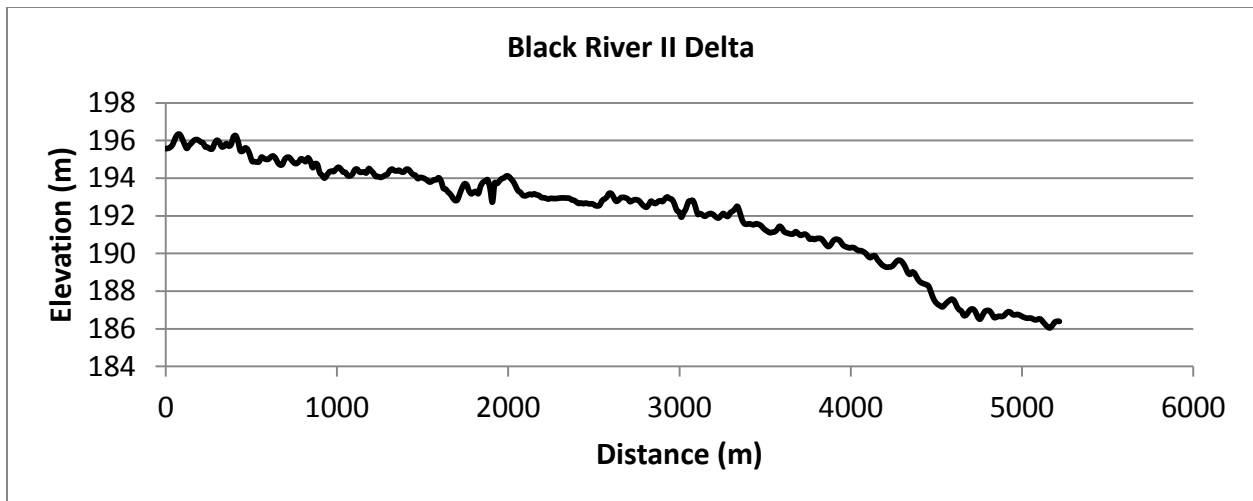


Figure B.15: Black River II delta profile

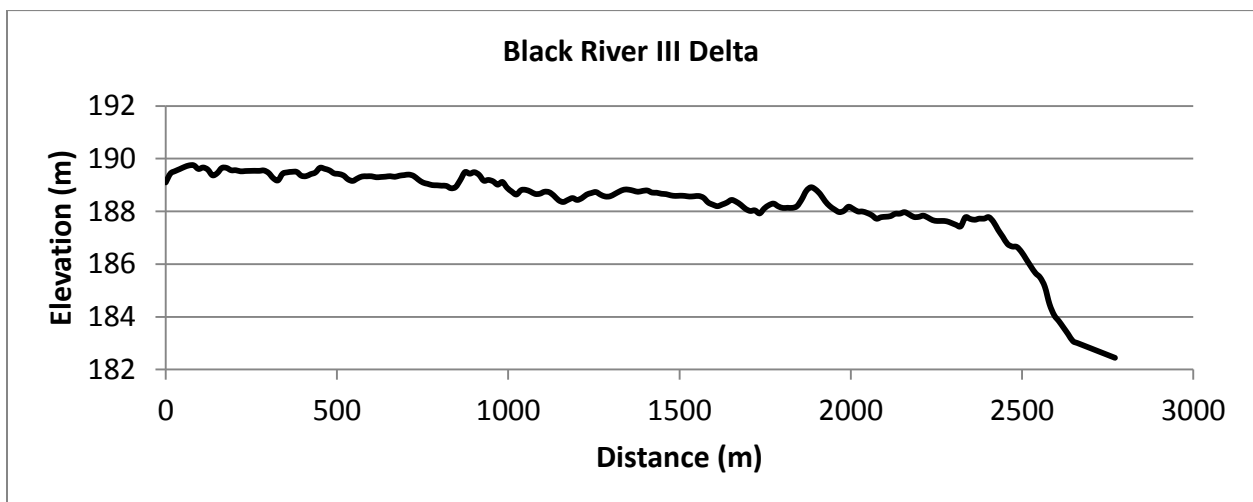


Figure B.16: Black River III delta profile

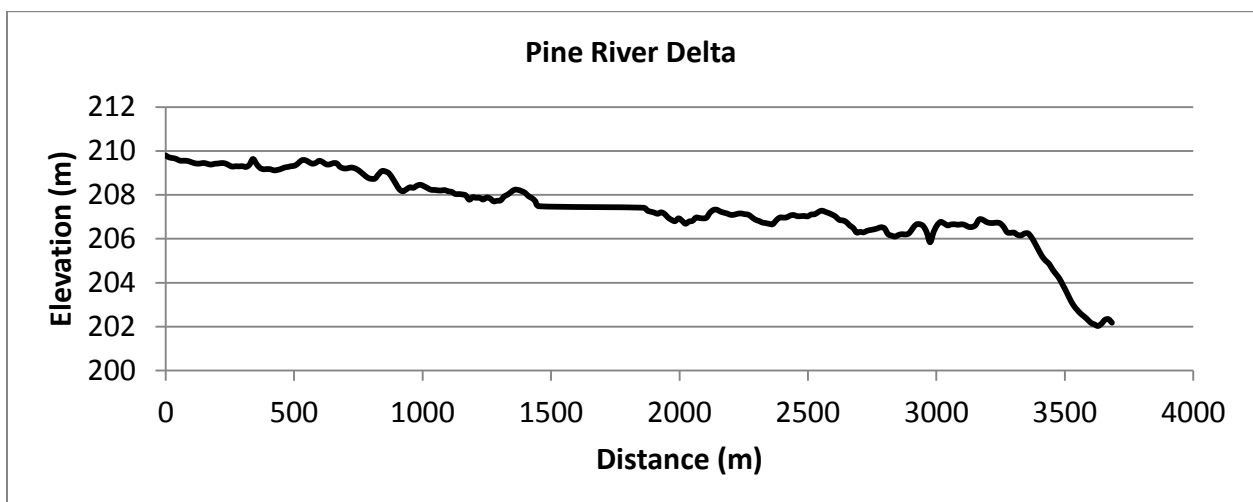


Figure B.17: Pine River delta profile

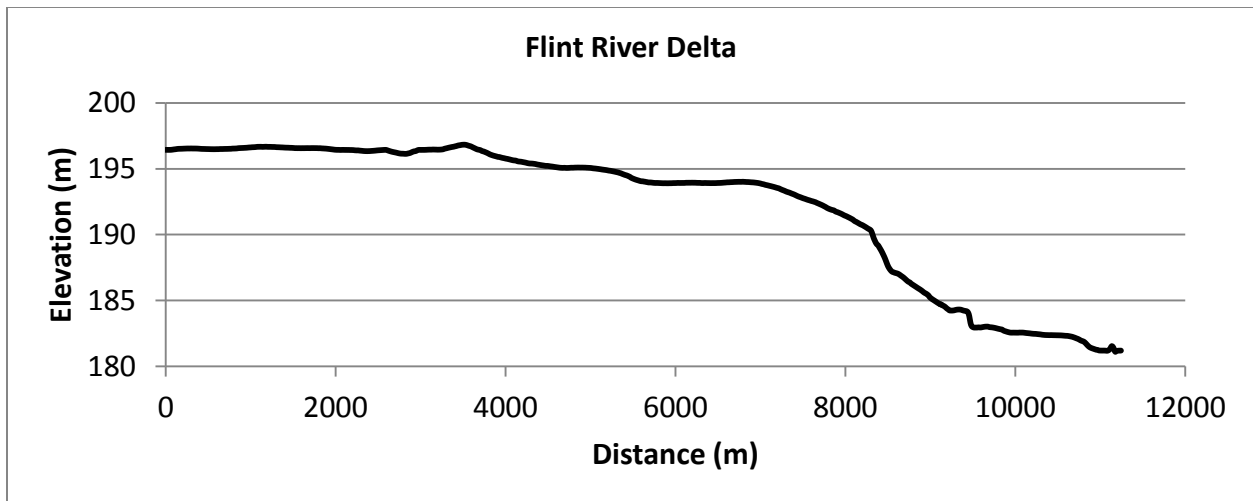


Figure B.18: Flint River delta profile

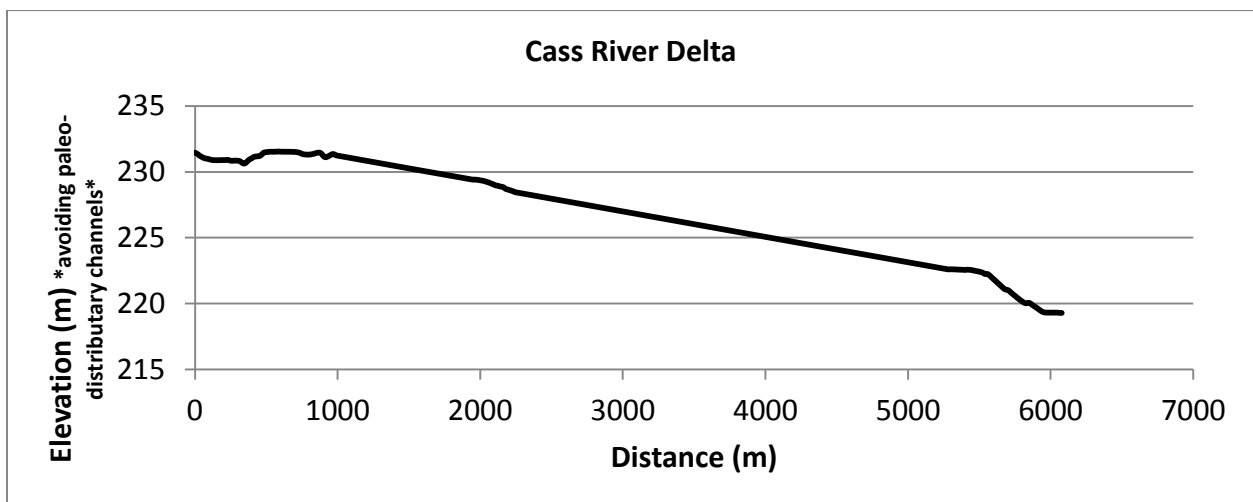


Figure B.19: Cass River delta profile

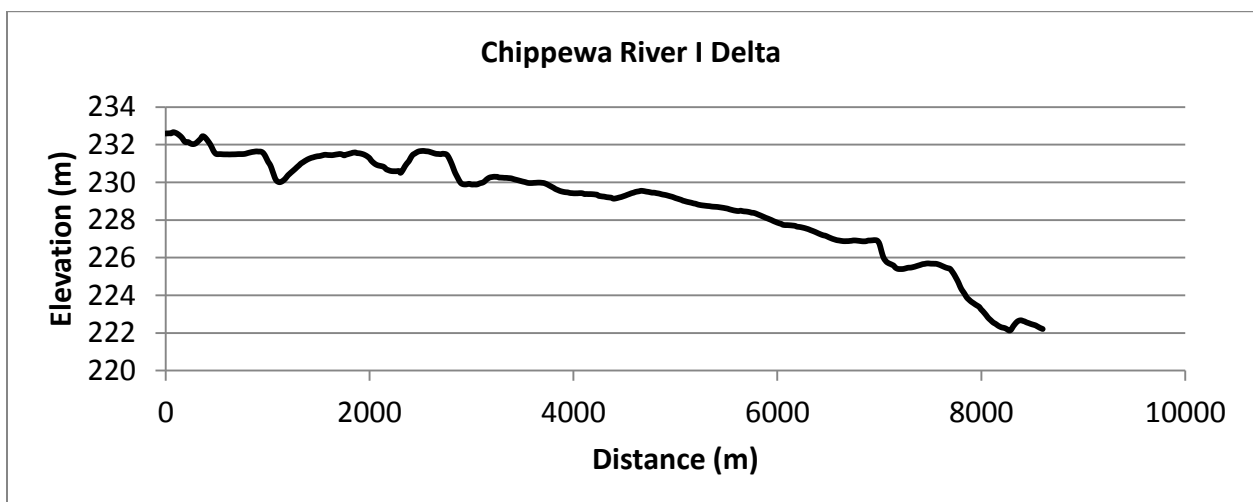


Figure B.20: Chippewa River I delta profile

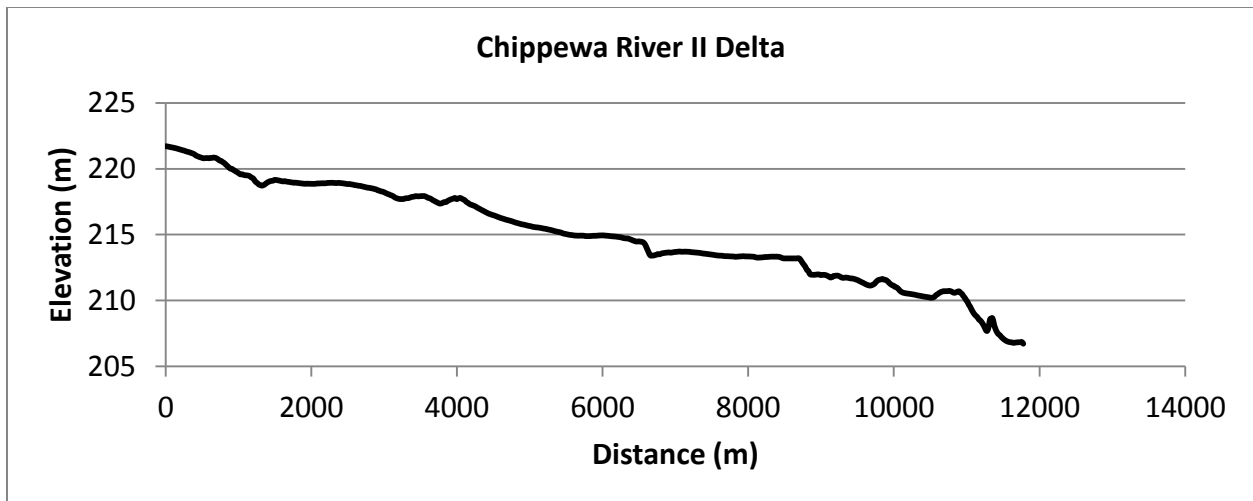


Figure B.21: Chippewa River II delta profile

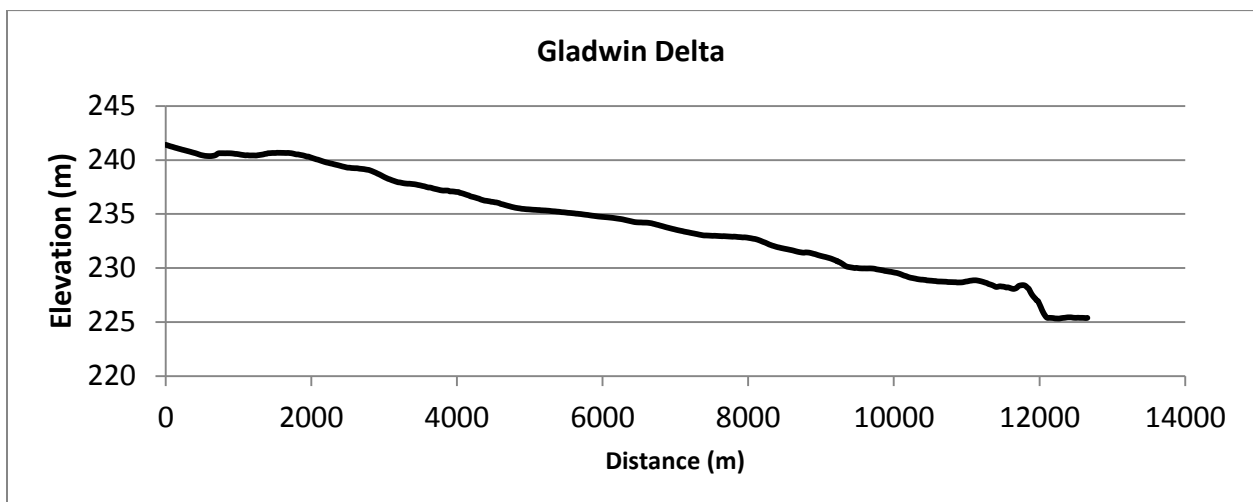


Figure B.22: Gladwin delta profile

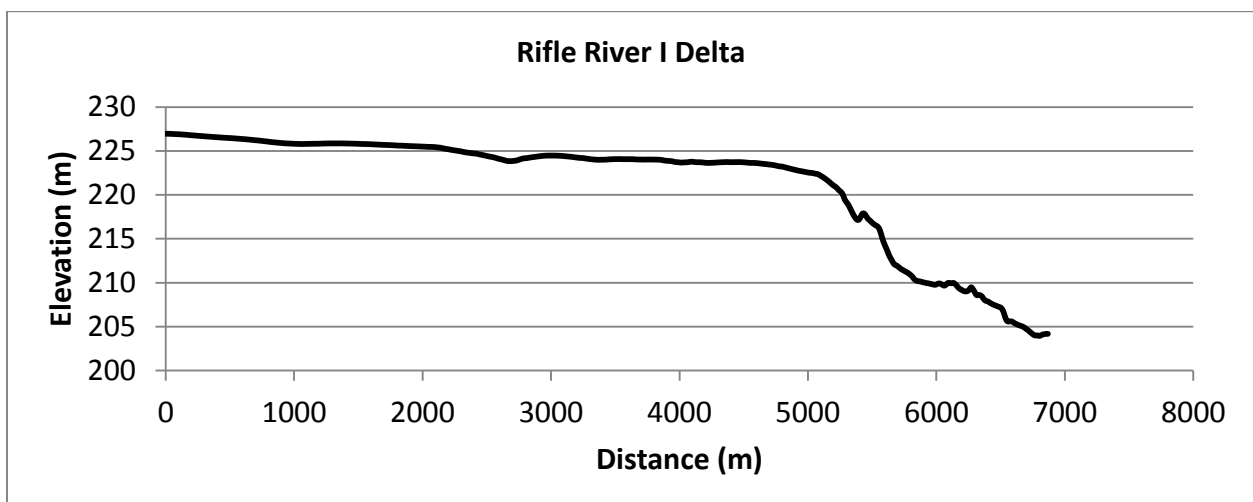


Figure B.23: Rifle River I delta profile

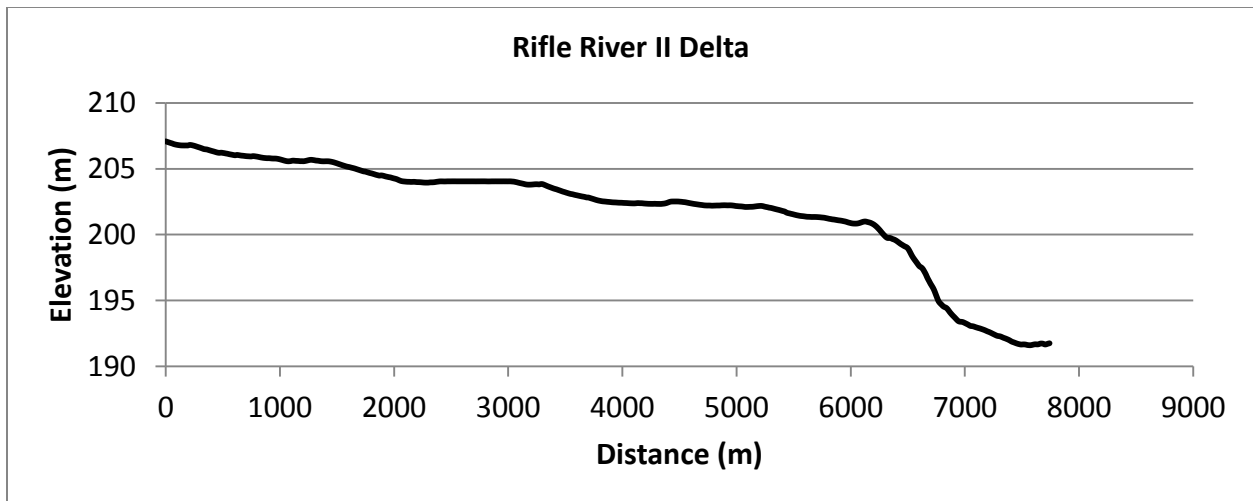


Figure B.24: Rifle River II delta profile

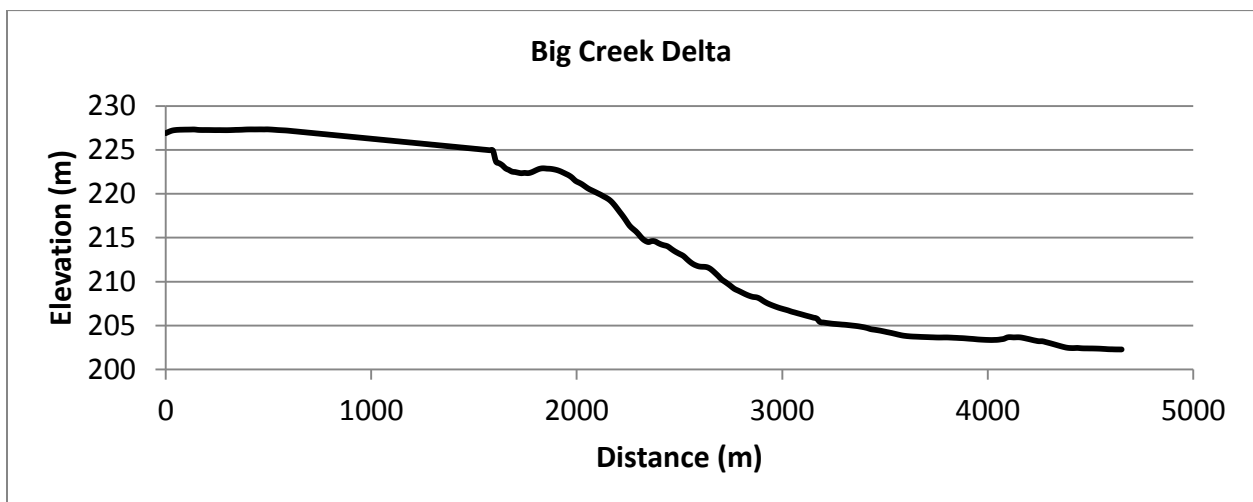


Figure B.25: Big Creek delta profile

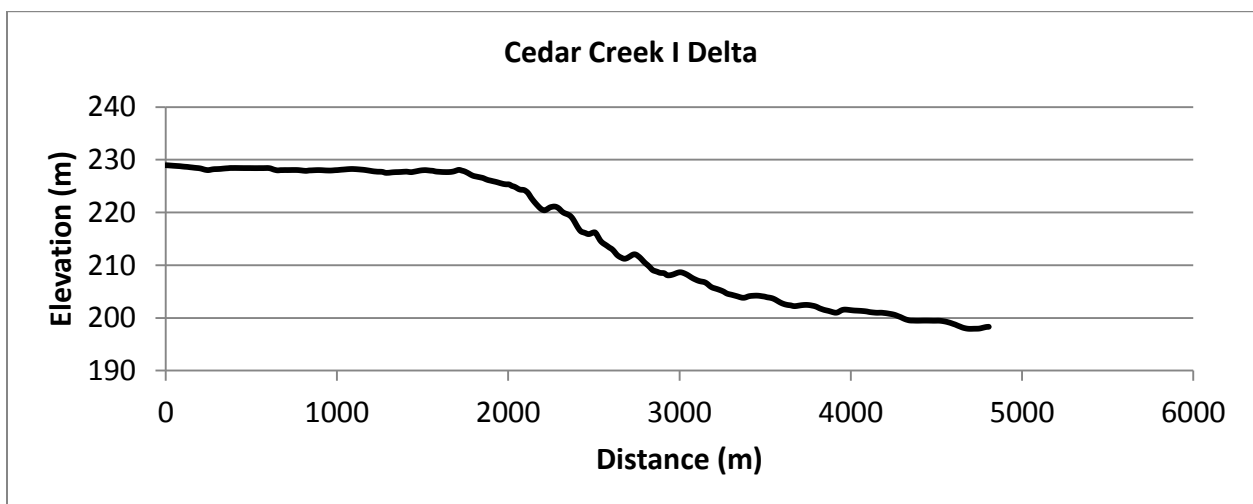


Figure B.26: Cedar Creek I delta profile

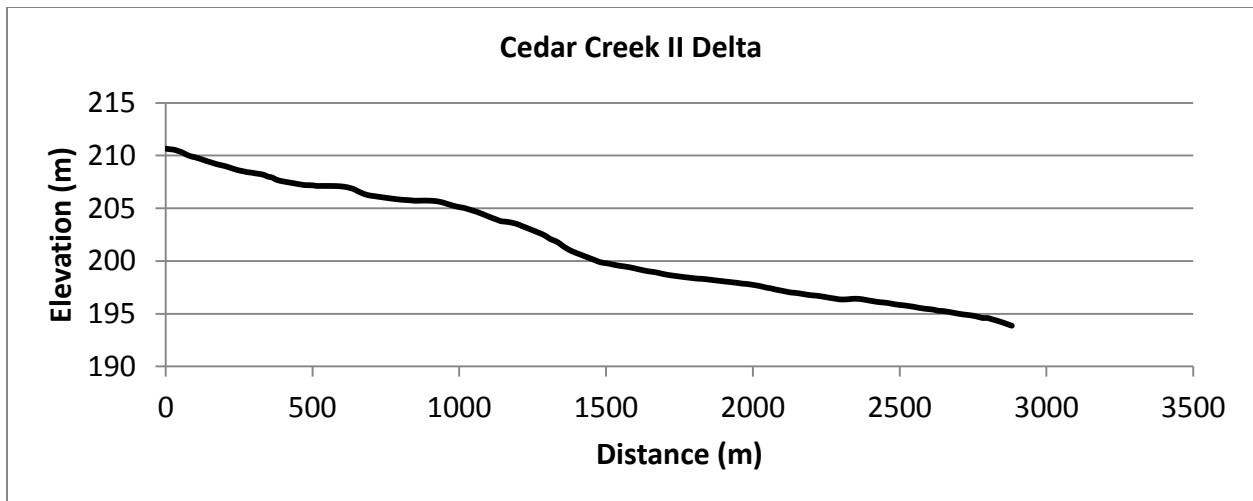


Figure B.27: Cedar Creek II delta profile

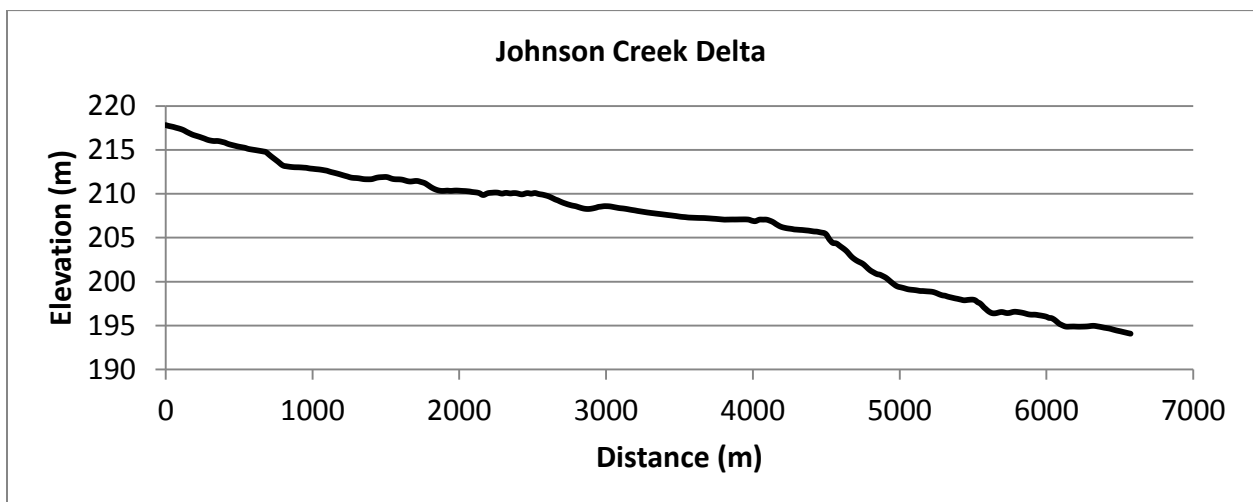


Figure B.28: Johnson Creek delta profile

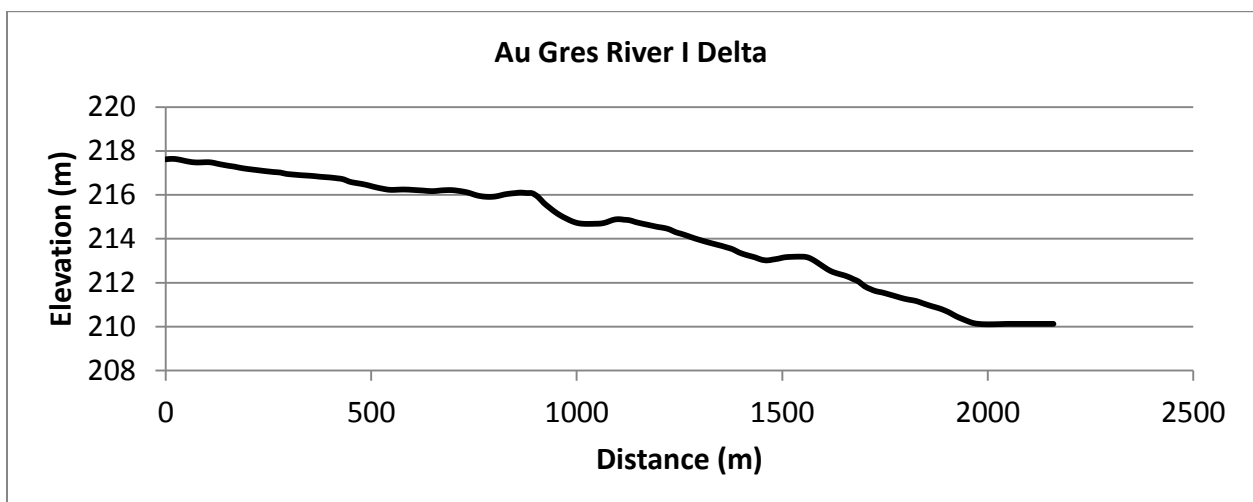


Figure B.29: Au Gres River I delta profile

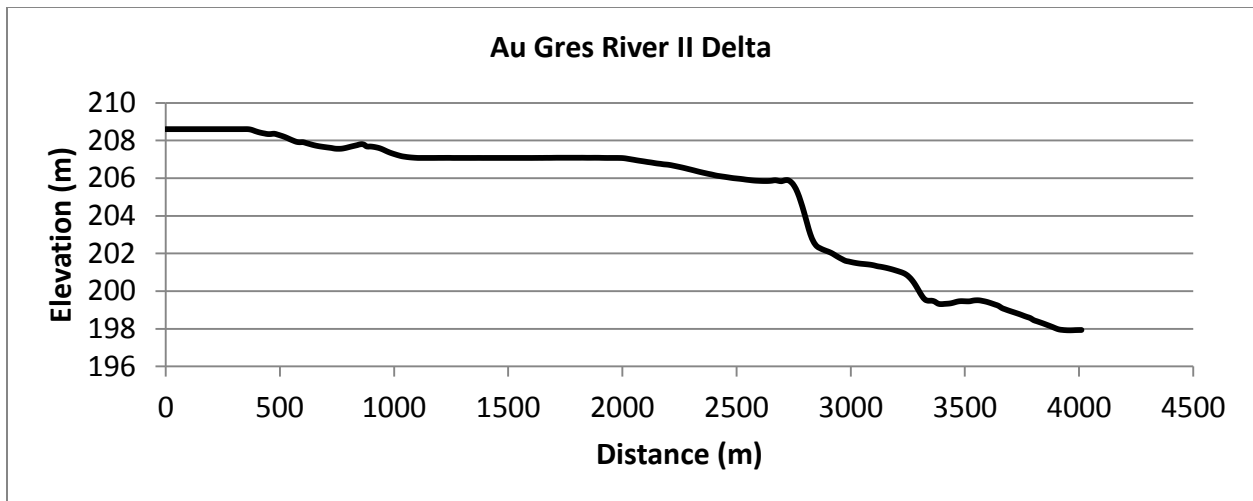


Figure B.30: Au Gres River II delta profile

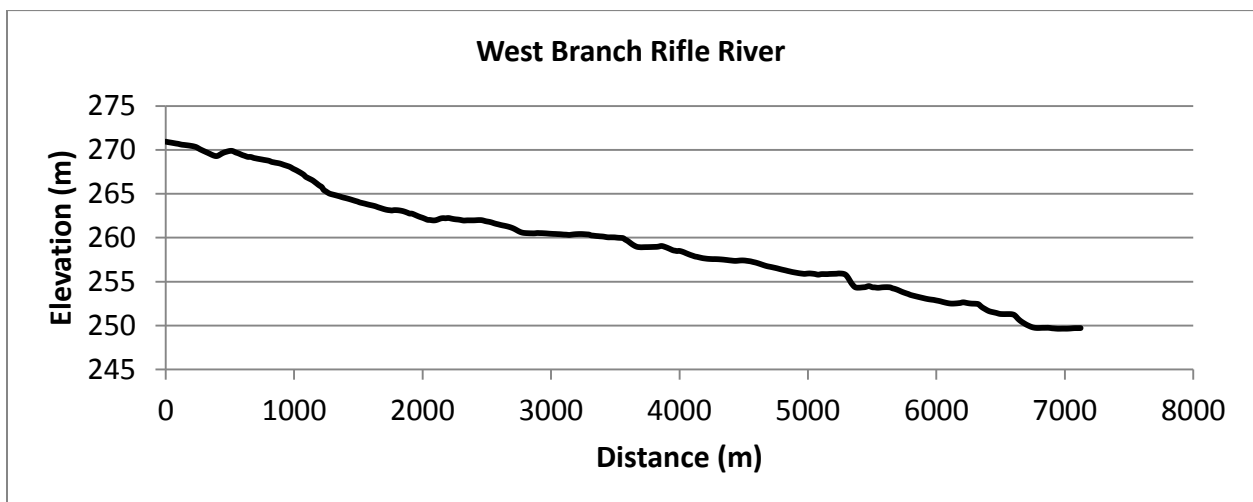


Figure B.31: West Branch Rifle delta profile

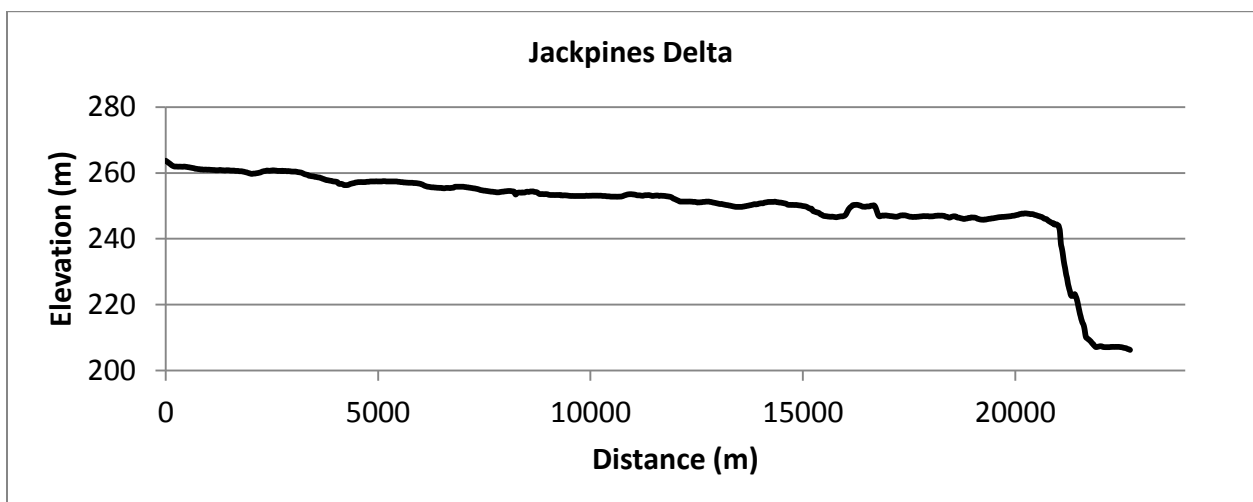


Figure B.32: Jackpines delta profile

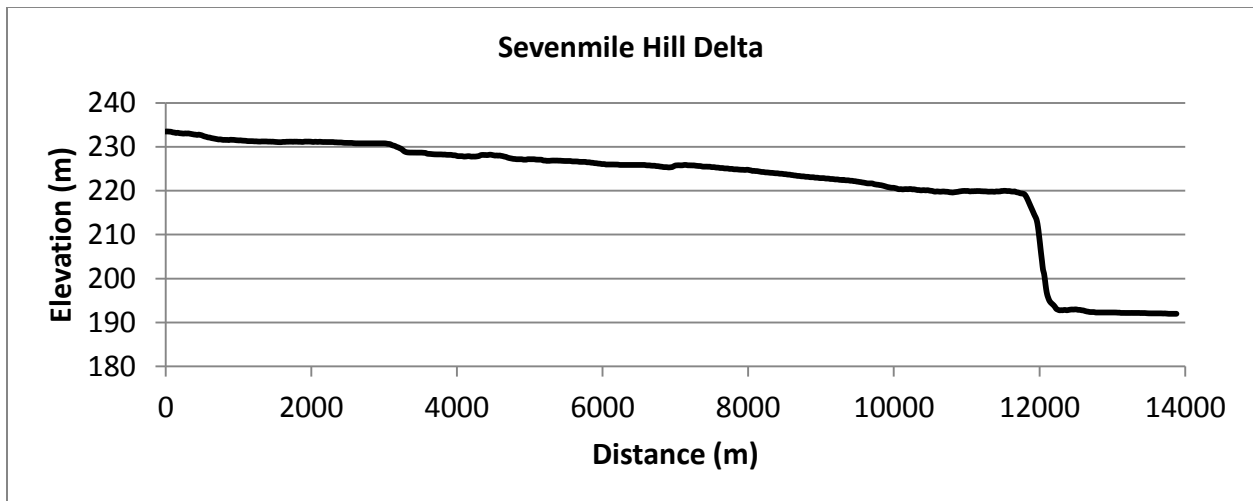


Figure B.33: Sevenmile Hill delta profile

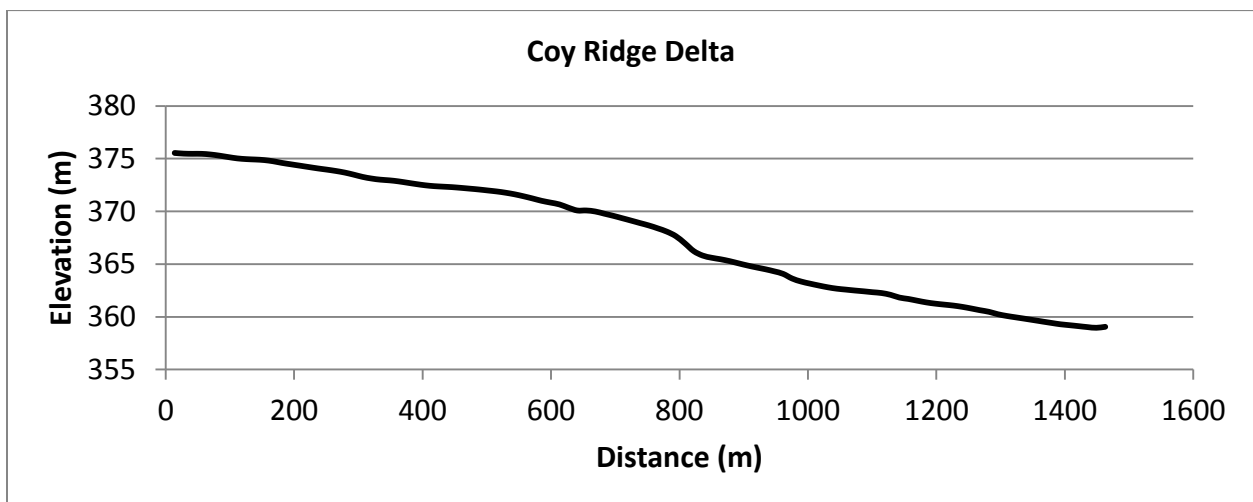


Figure B.34: Coy Ridge delta profile

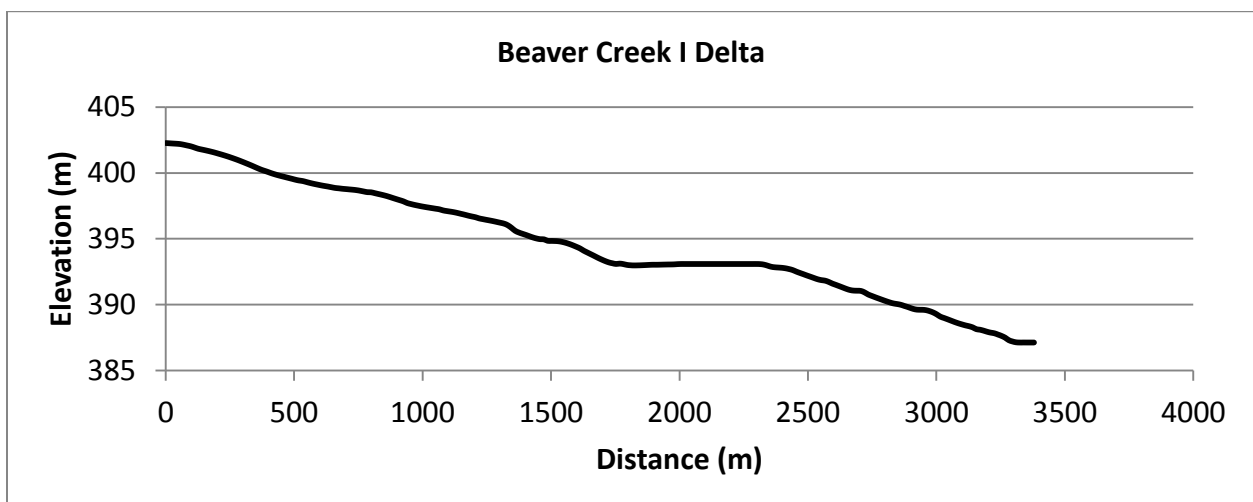


Figure B.35: Beaver Creek I delta profile

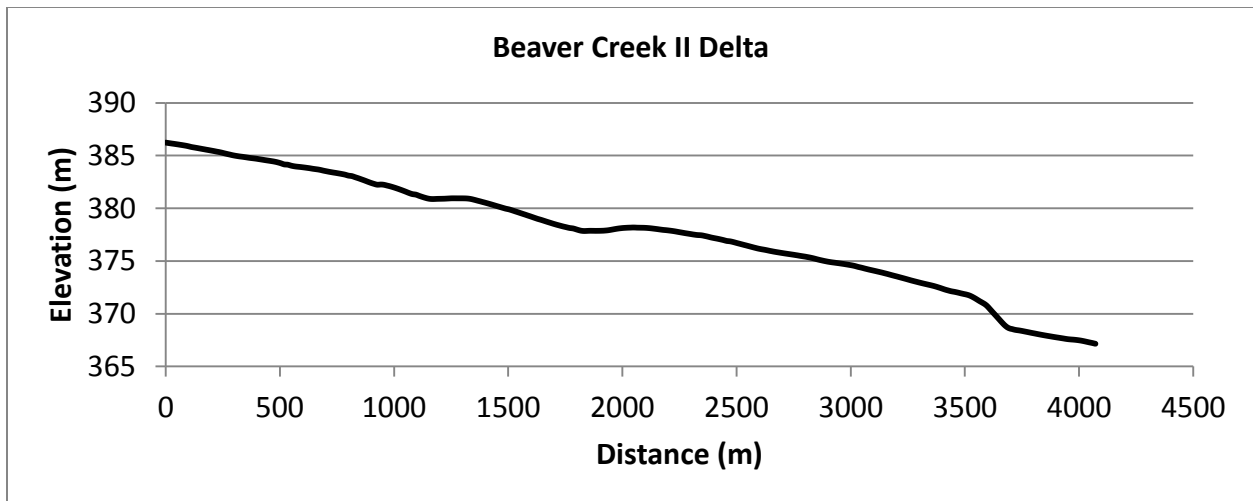


Figure B.36: Beaver Creek II delta profile

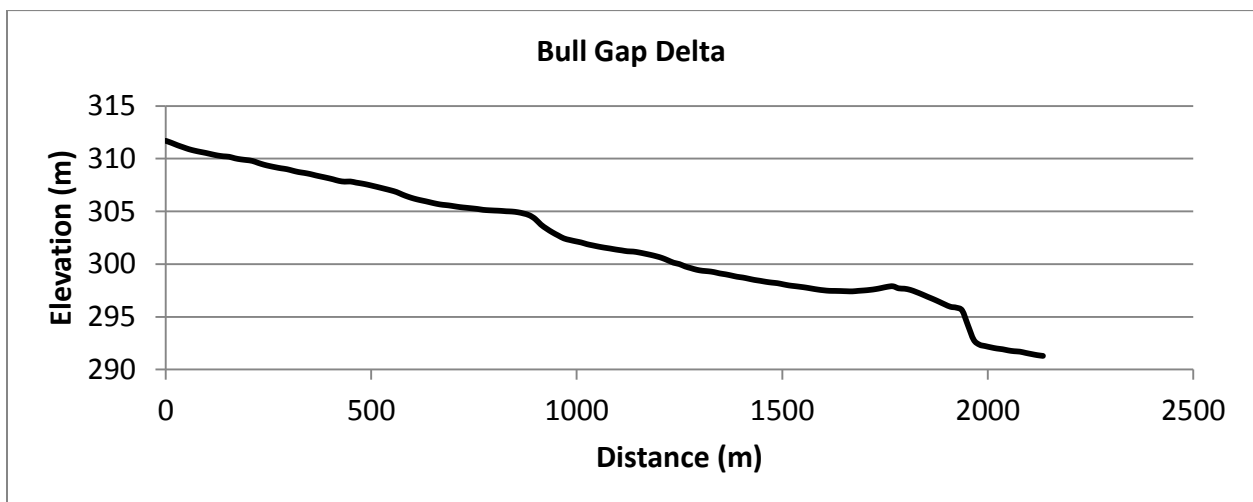


Figure B.37: Bull Gap delta profile

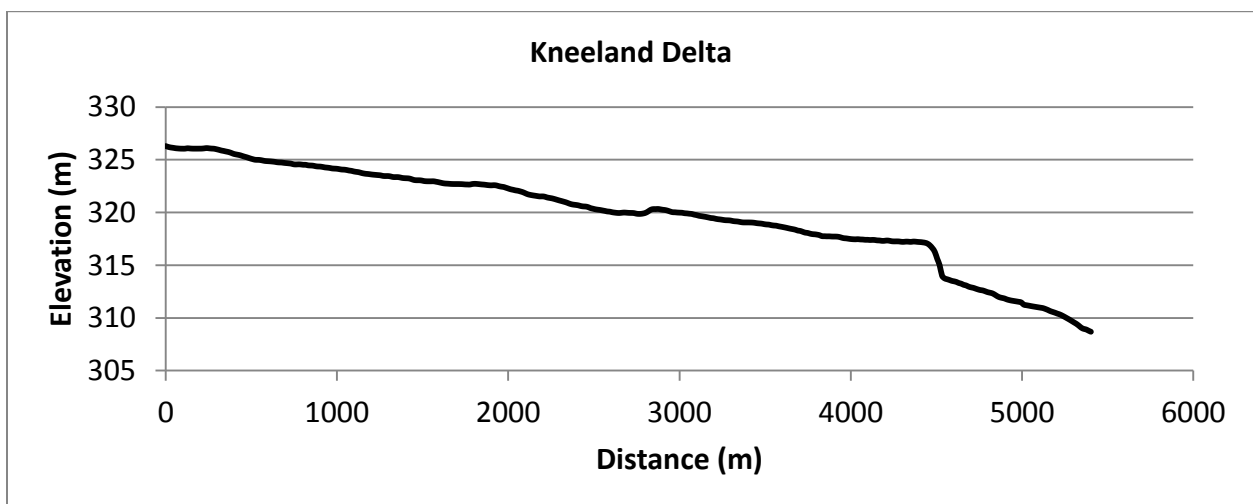


Figure B.38: Kneeland delta profile

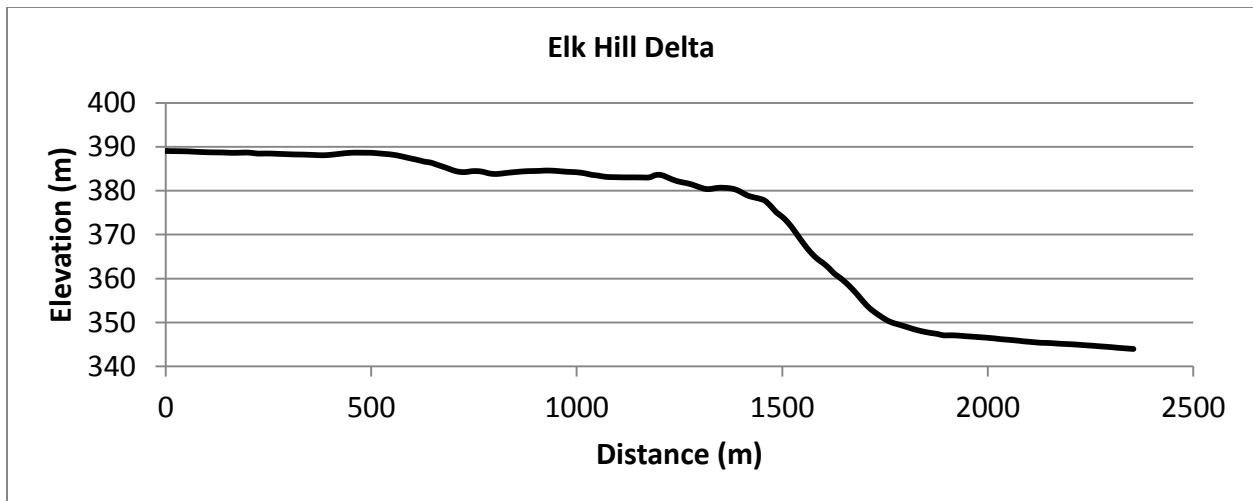


Figure B.39: Elk Hill delta profile

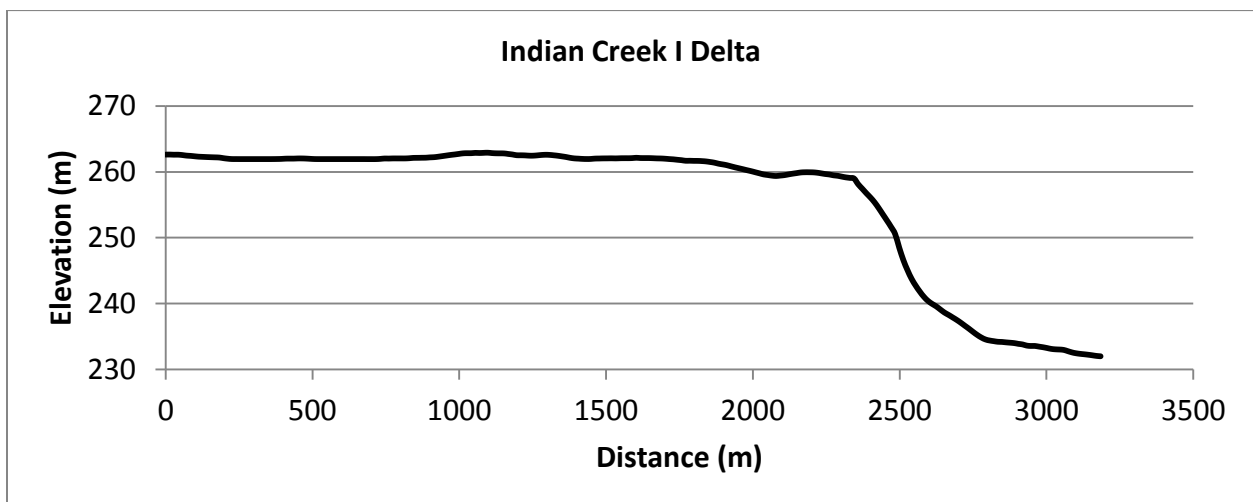


Figure B.40: Indian Creek I delta profile

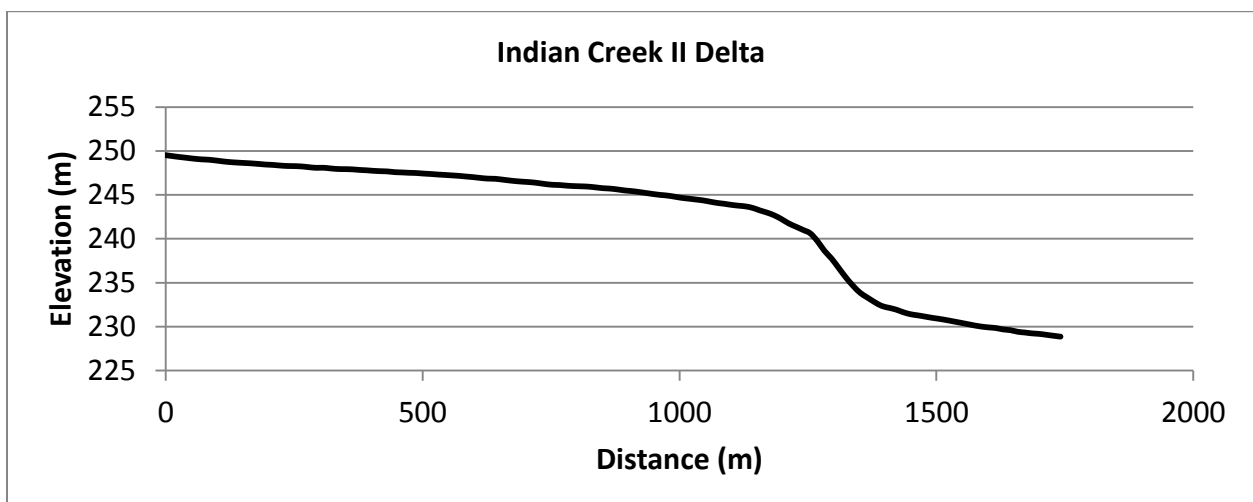


Figure B.41: Indian Creek II delta profile

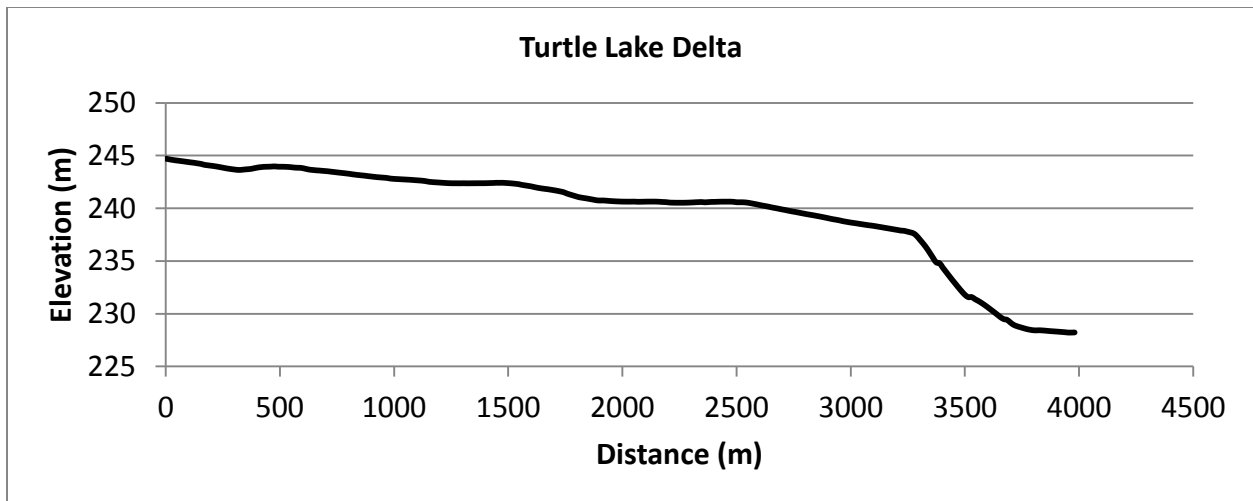


Figure B.42: Turtle Lake delta profile

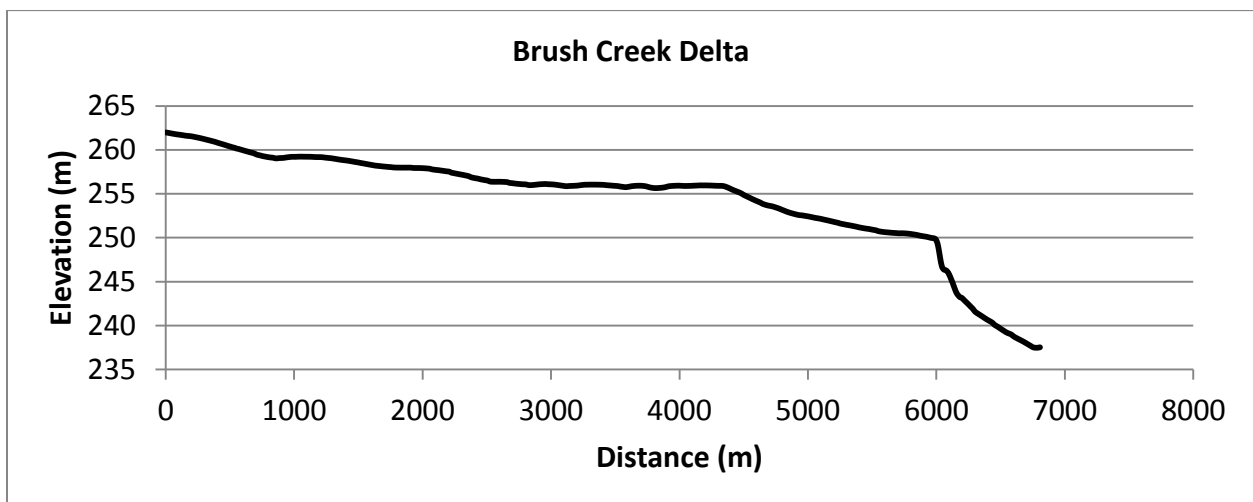


Figure B.43: Brush Creek delta profile

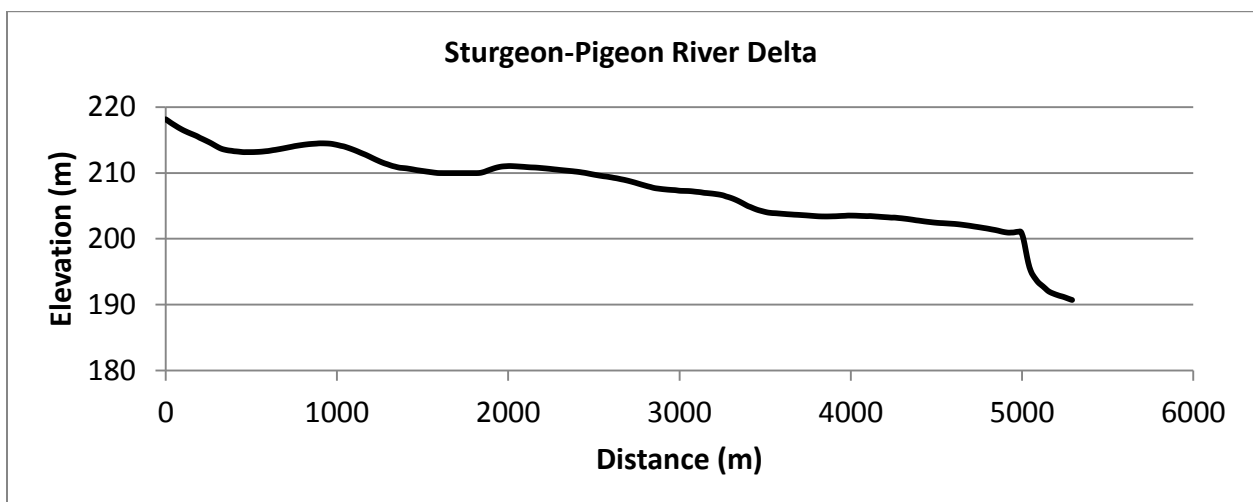


Figure B.44: Sturgeon-Pigeon River delta profile

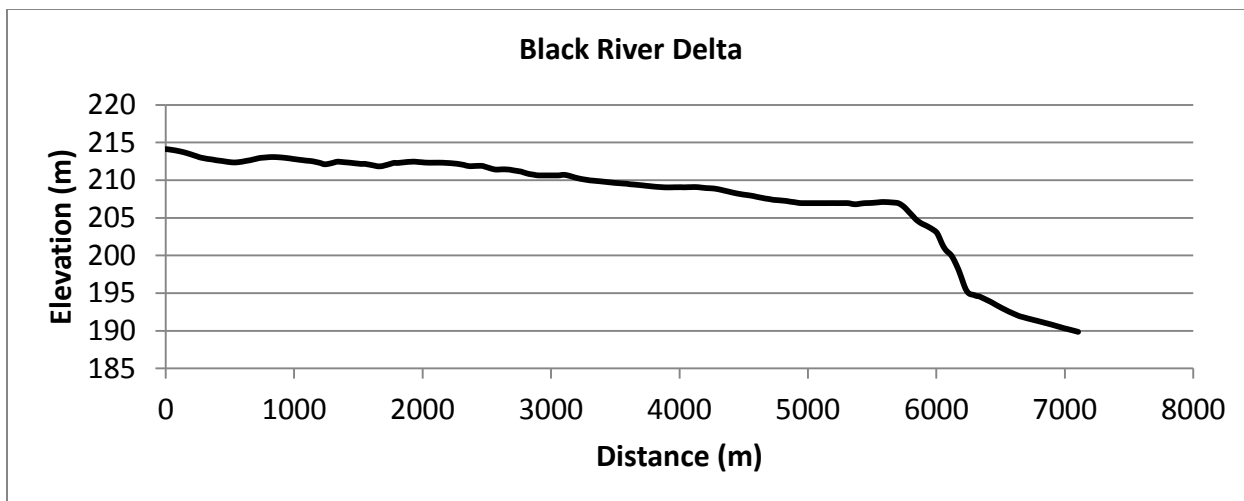


Figure B.45: Black River delta profile

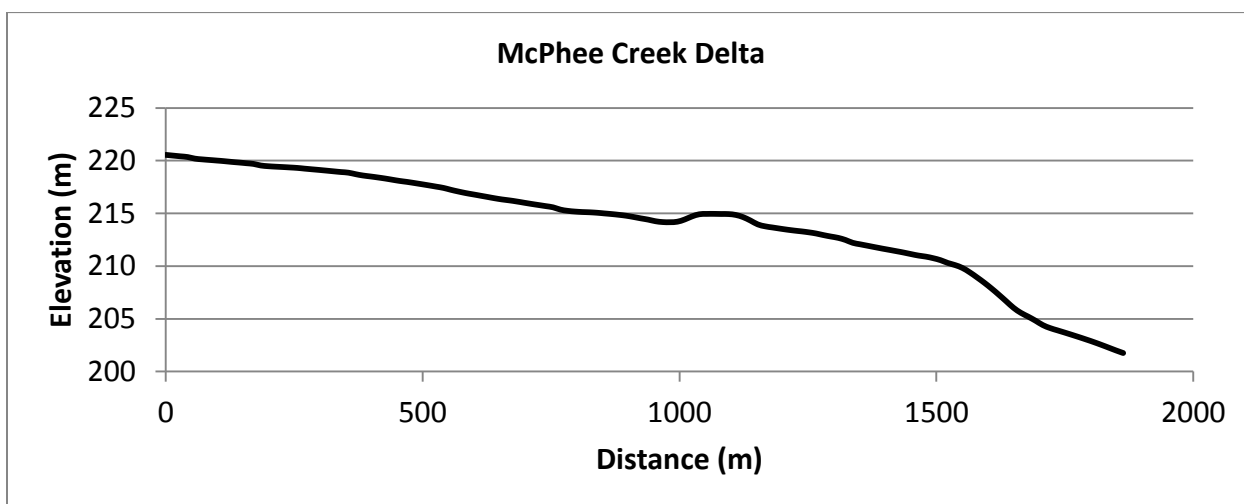


Figure B.46: McPhee Creek delta profile

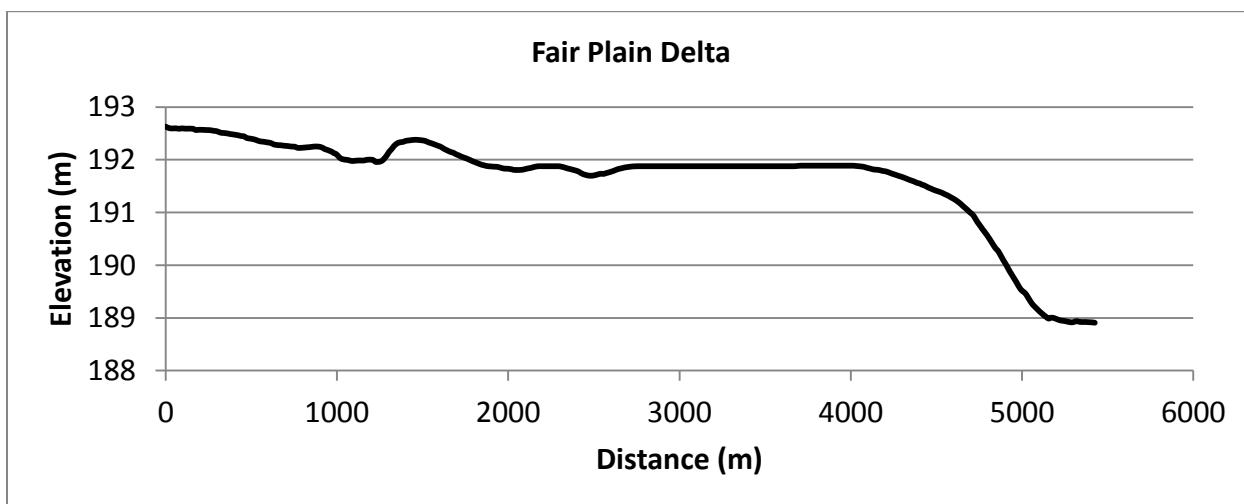


Figure B.47: Fair Plain delta profile

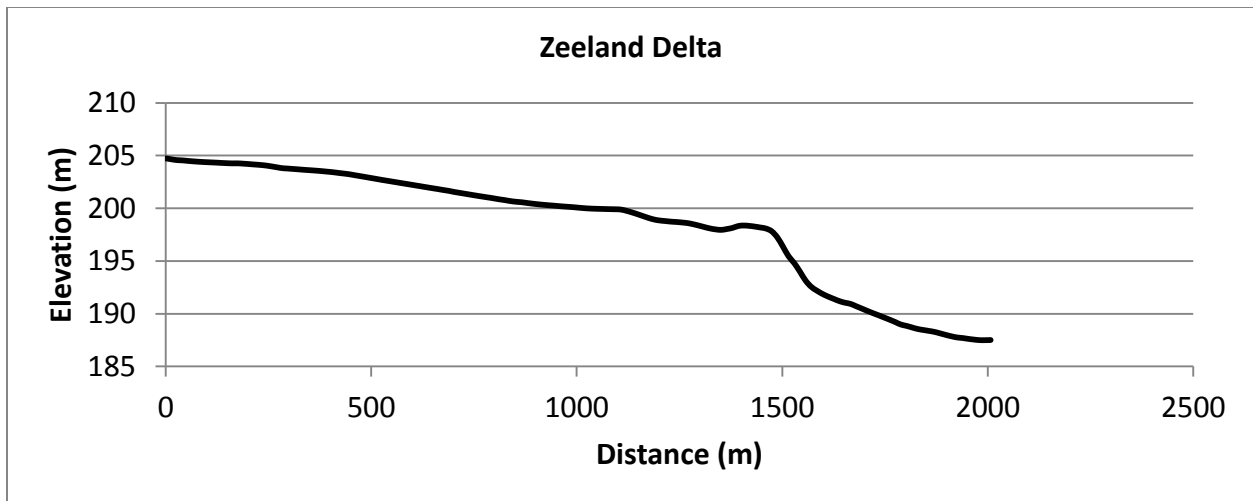


Figure B.48: Zeeland delta profile

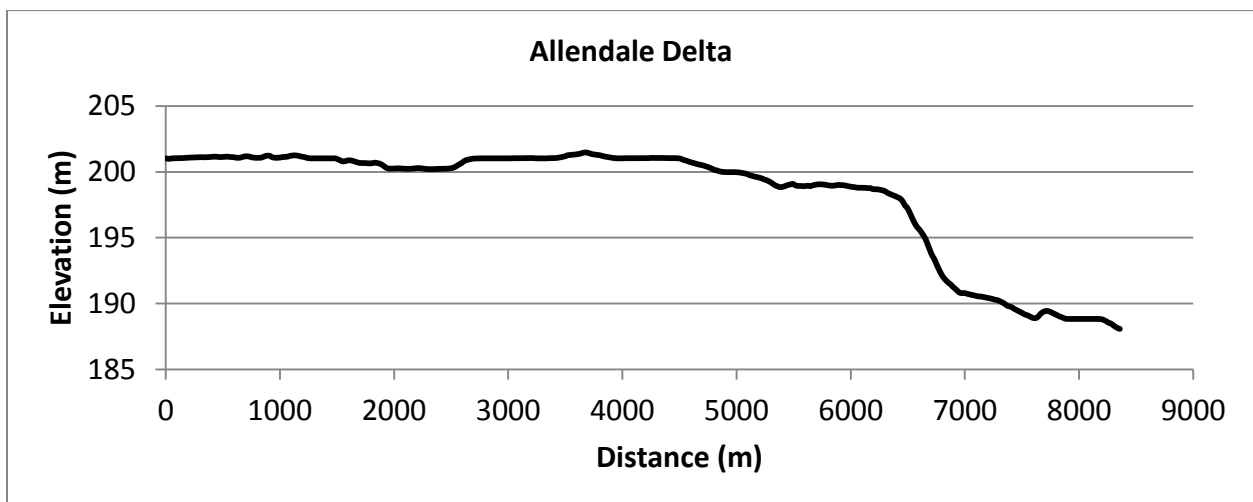


Figure B.49: Allendale delta profile

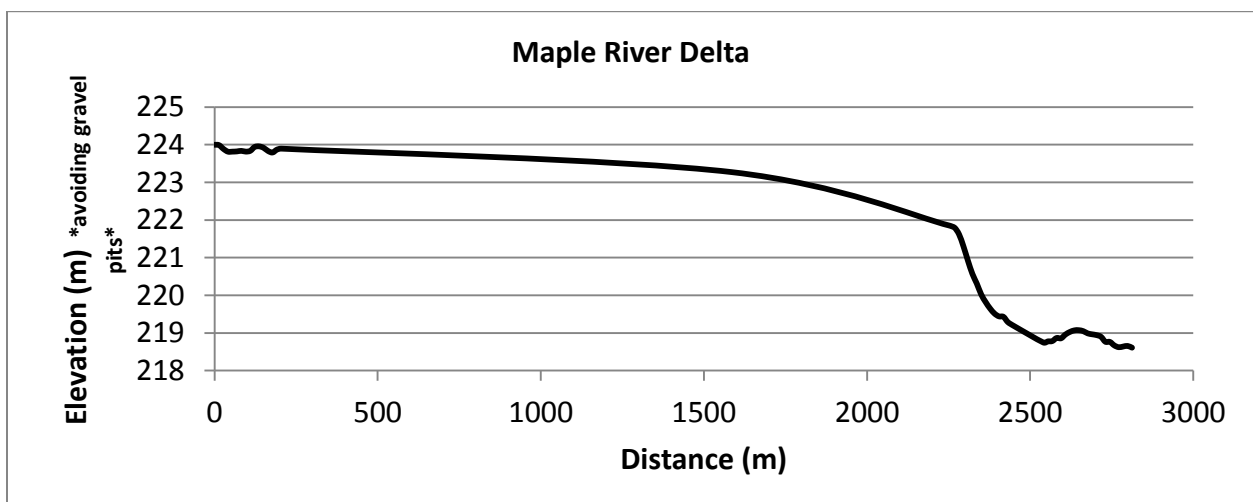


Figure B.50: Maple River delta profile

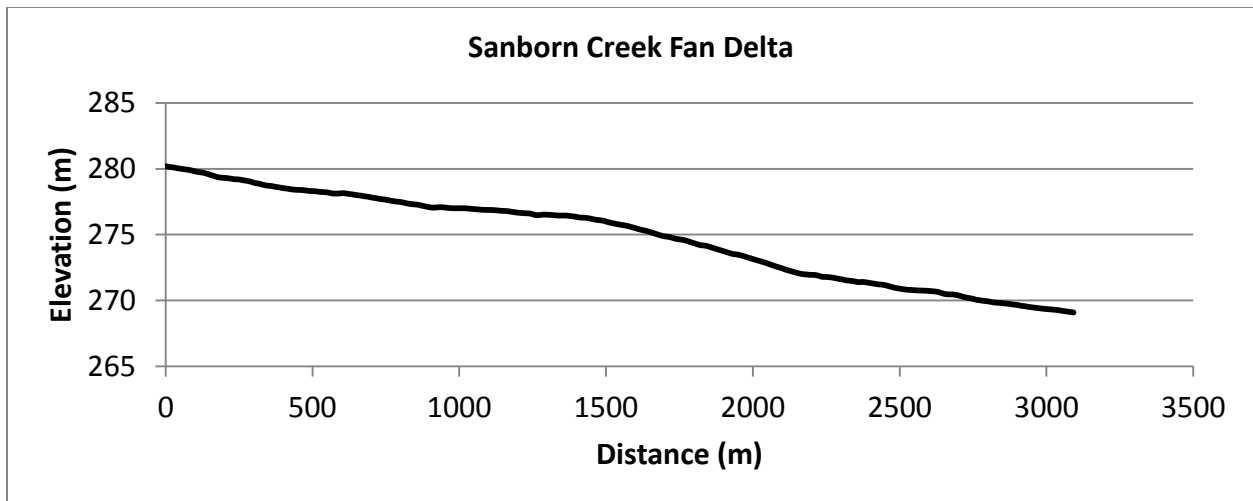


Figure B.51: Sanborn Creek Fan delta profile

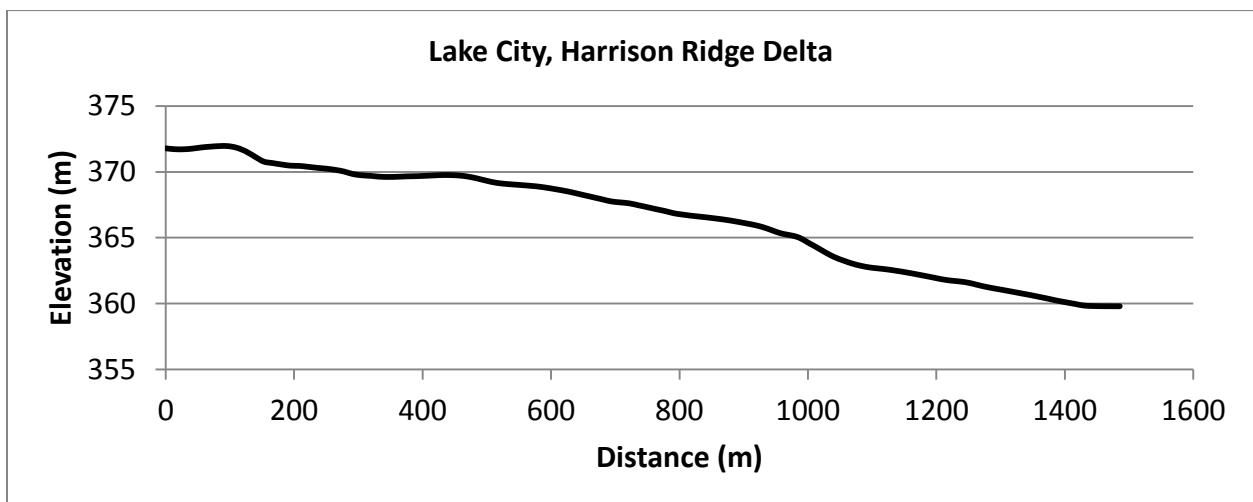


Figure B.52: Lake City, Harrison Ridge delta profile

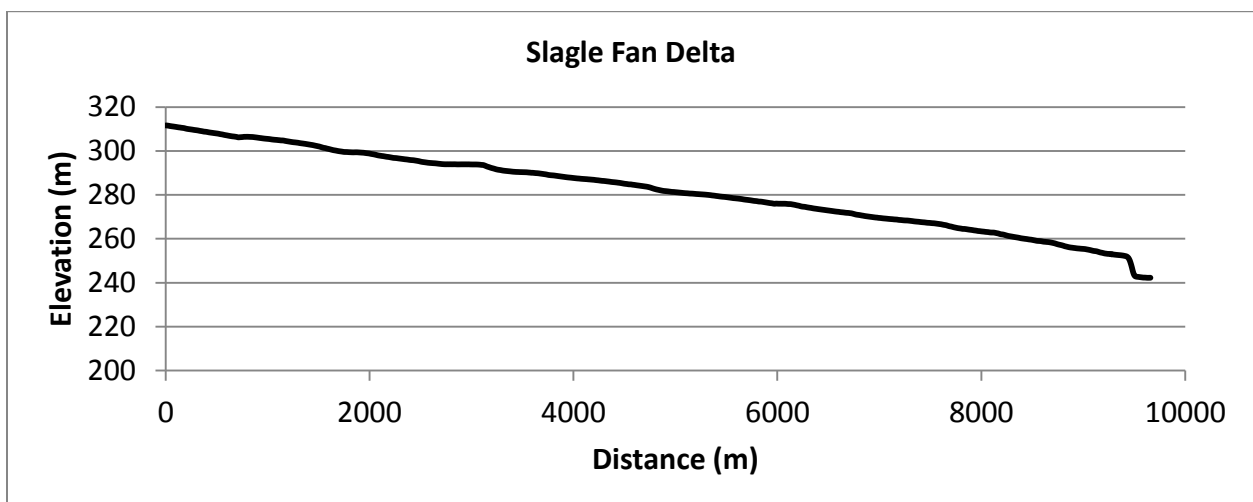


Figure B.53: Slagle Fan delta profile

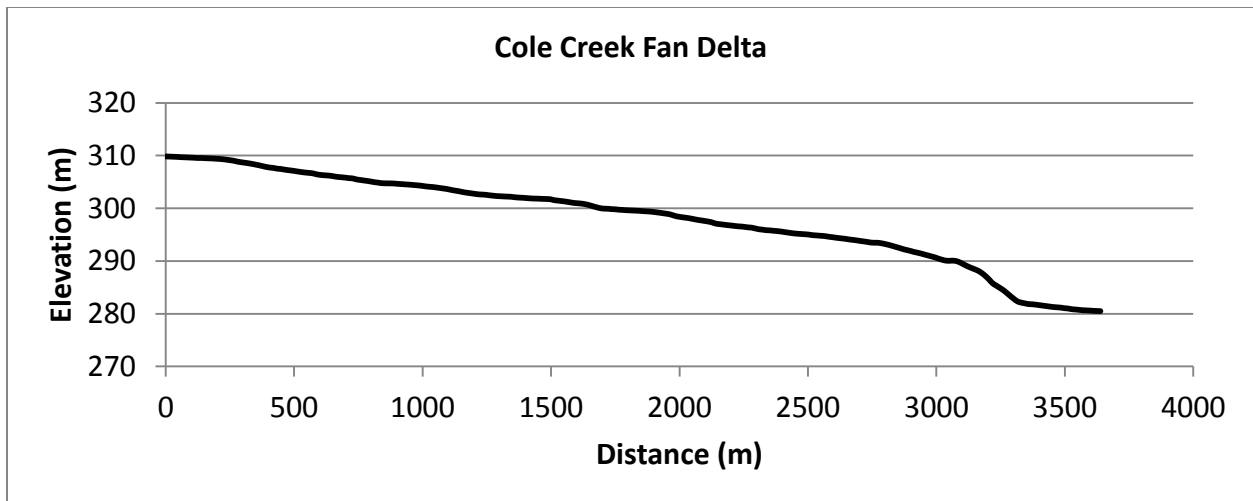


Figure B.54: Cole Creek Fan delta profile

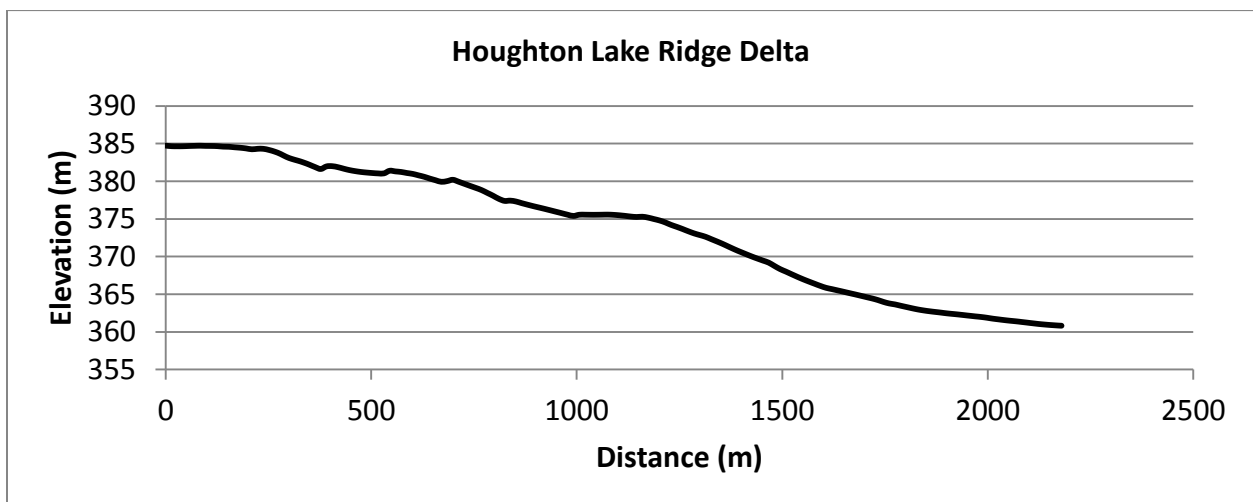


Figure B.55: Houghton Lake Ridge delta profile

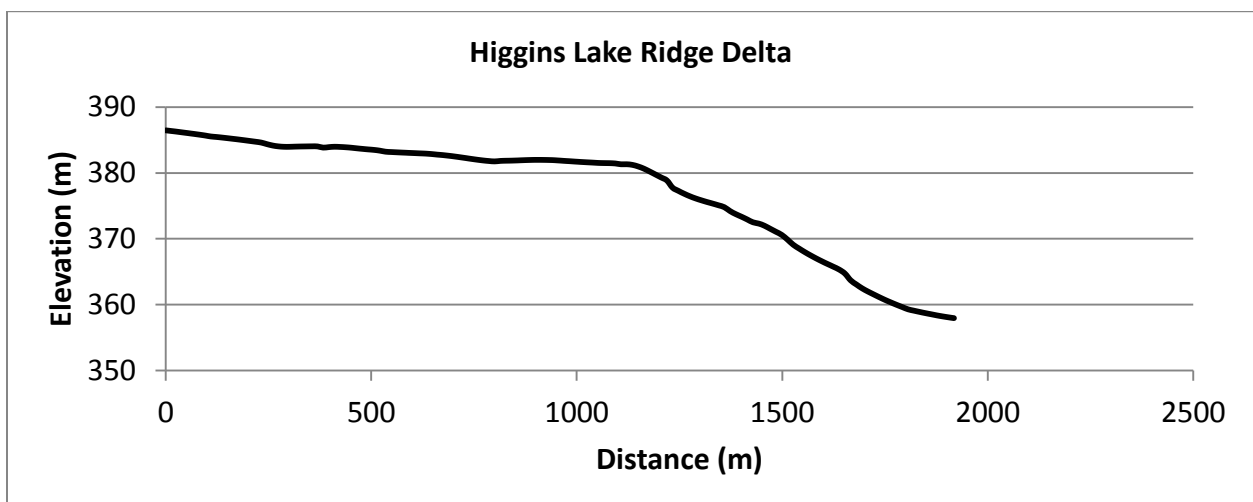


Figure B.56: Higgins Lake Ridge delta profile

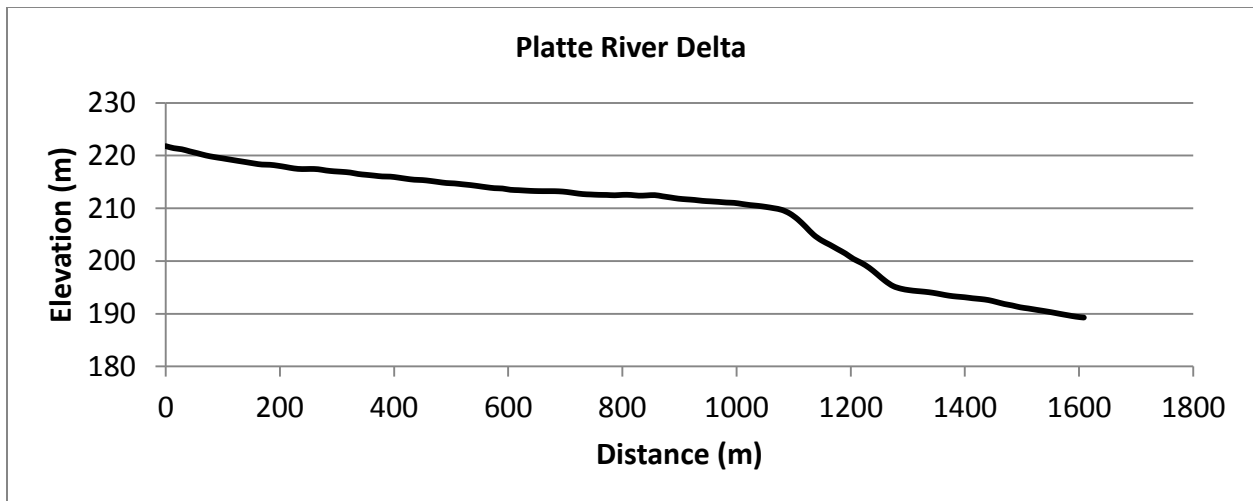


Figure B.57: Platte River delta profile

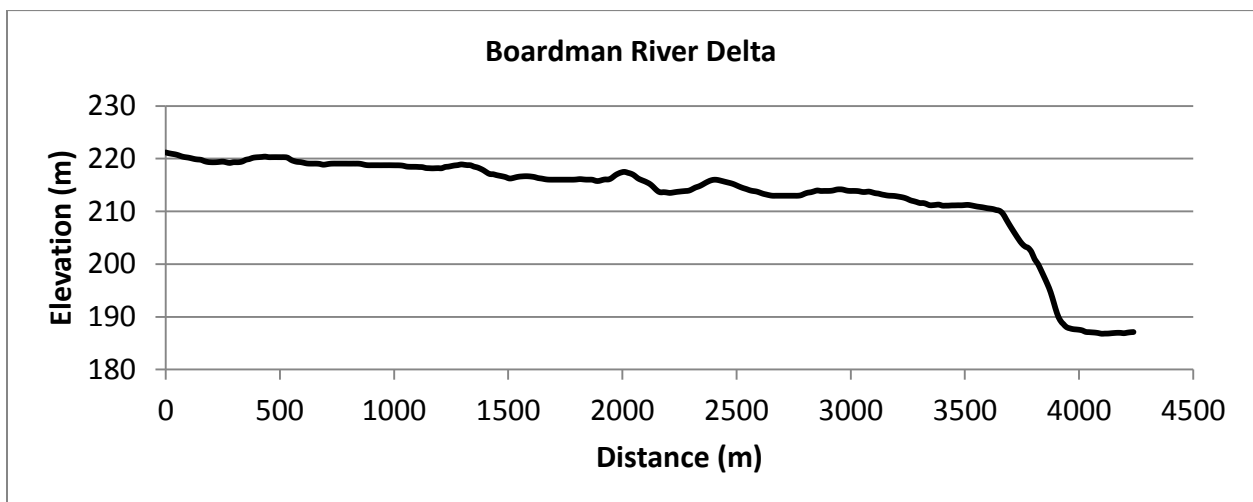


Figure B.58: Boardman River delta profile

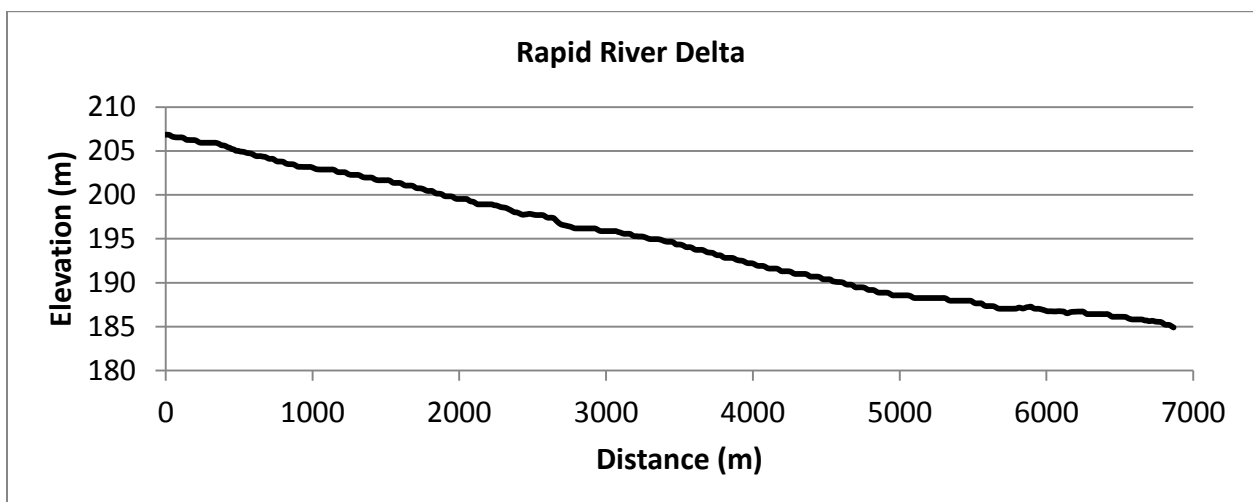


Figure B.59: Rapid River delta profile

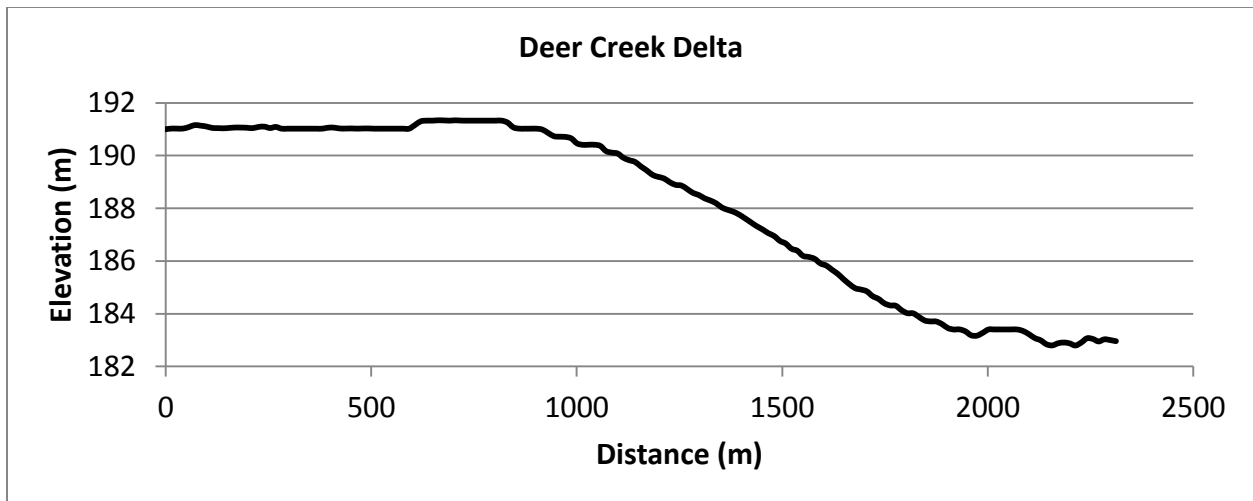


Figure B.60: Deer Creek delta profile

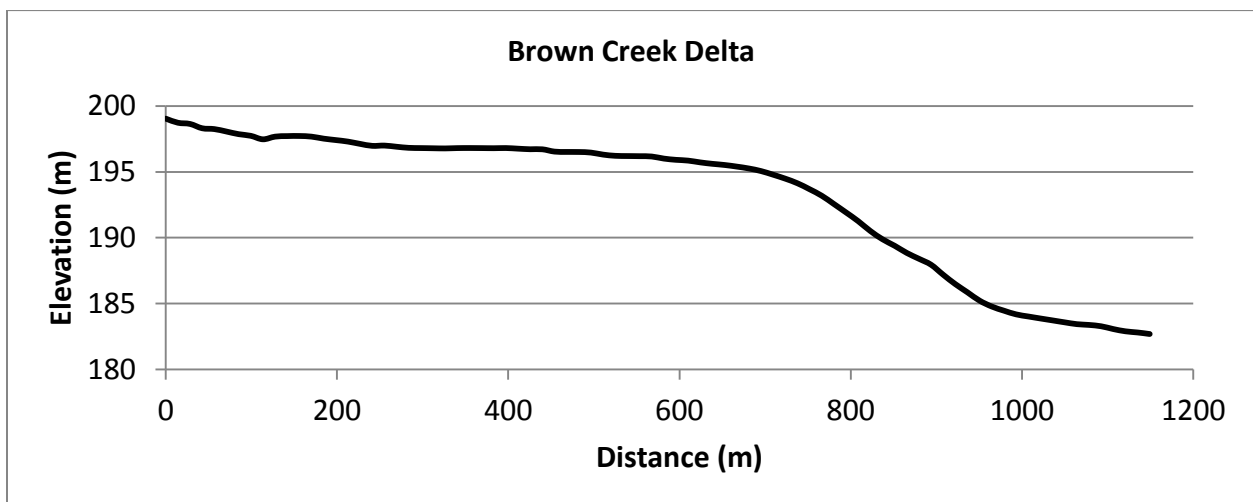


Figure B.61: Brown Creek delta profile

APPENDIX C: Delta Plain Extents and Modern Catchment Areas

(details on the methods used to delineate delta boundaries are outlined in Section 4 of the dissertation)

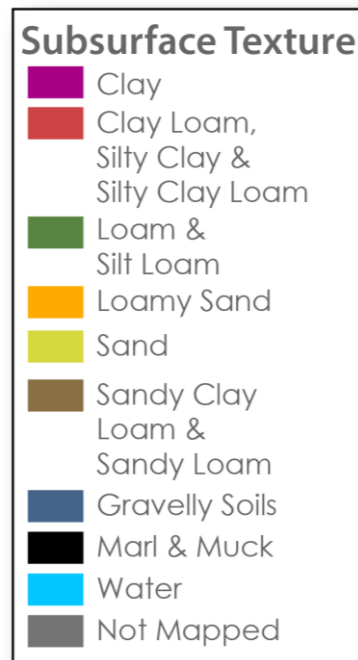


Figure C.1: Color symbology used to label the subsurface textural class's within each delta's catchment area.

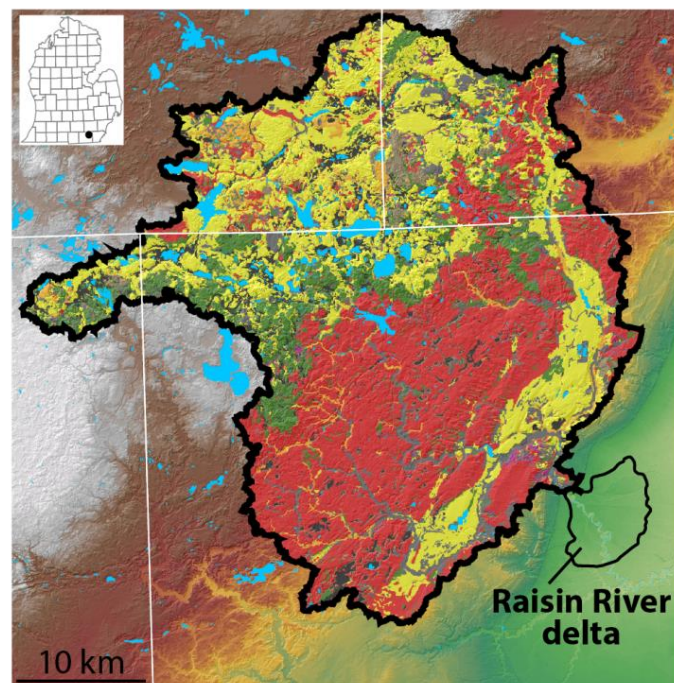


Figure C.2: Raisin River delta

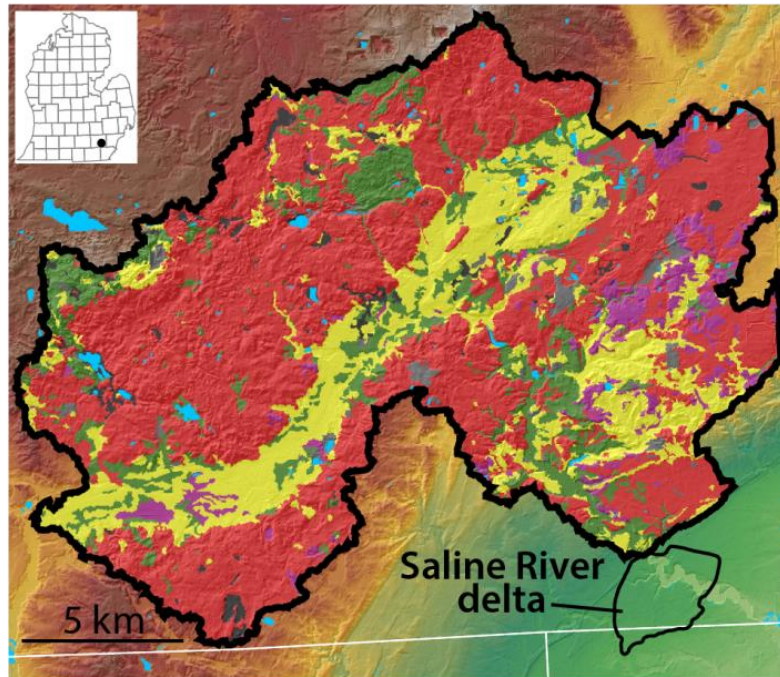


Figure C.3: Saline River delta

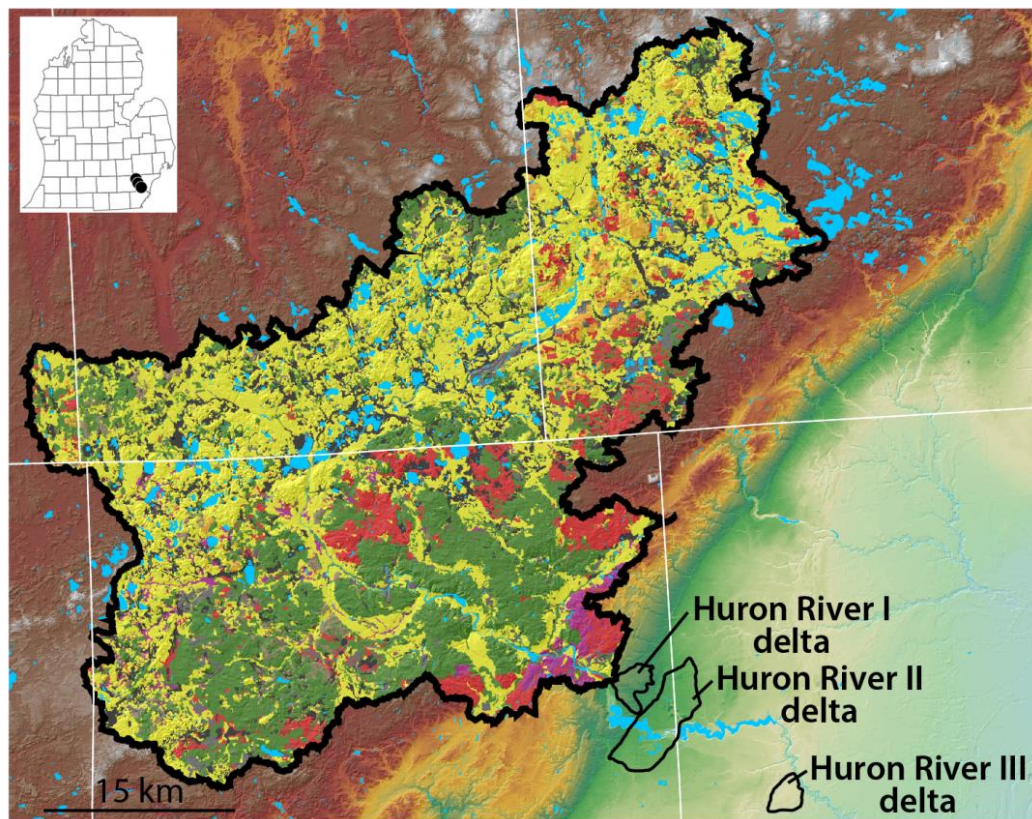


Figure C.4: Huron River I, II, and III deltas

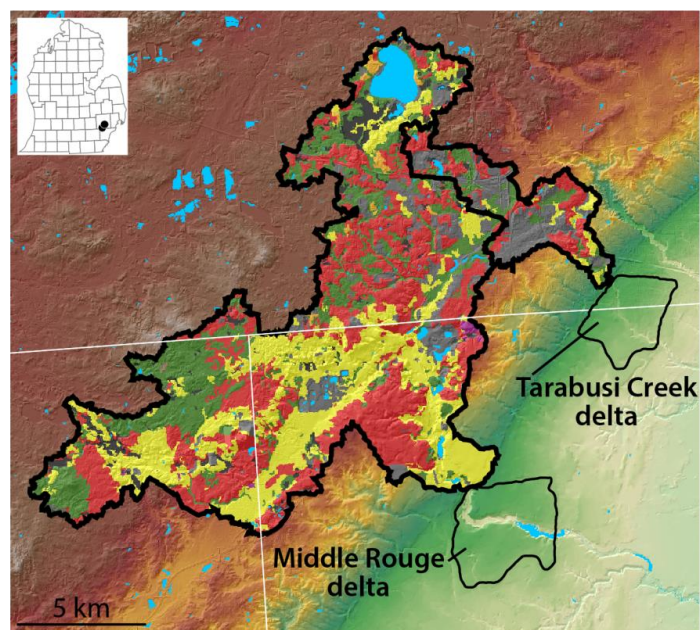


Figure C.5: Middle Rouge and Tarabusi Creek deltas

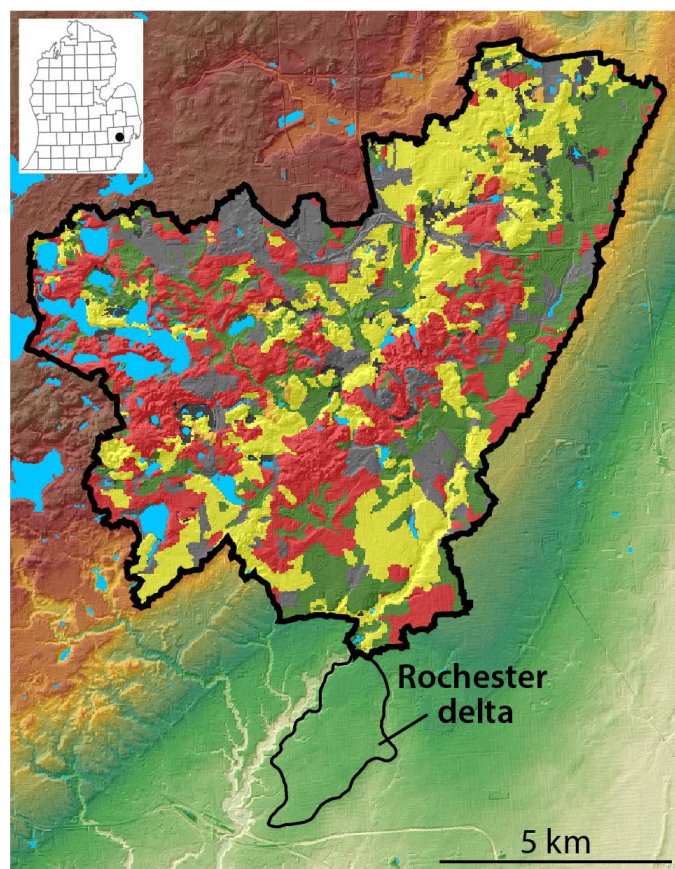


Figure C.6: Rochester delta

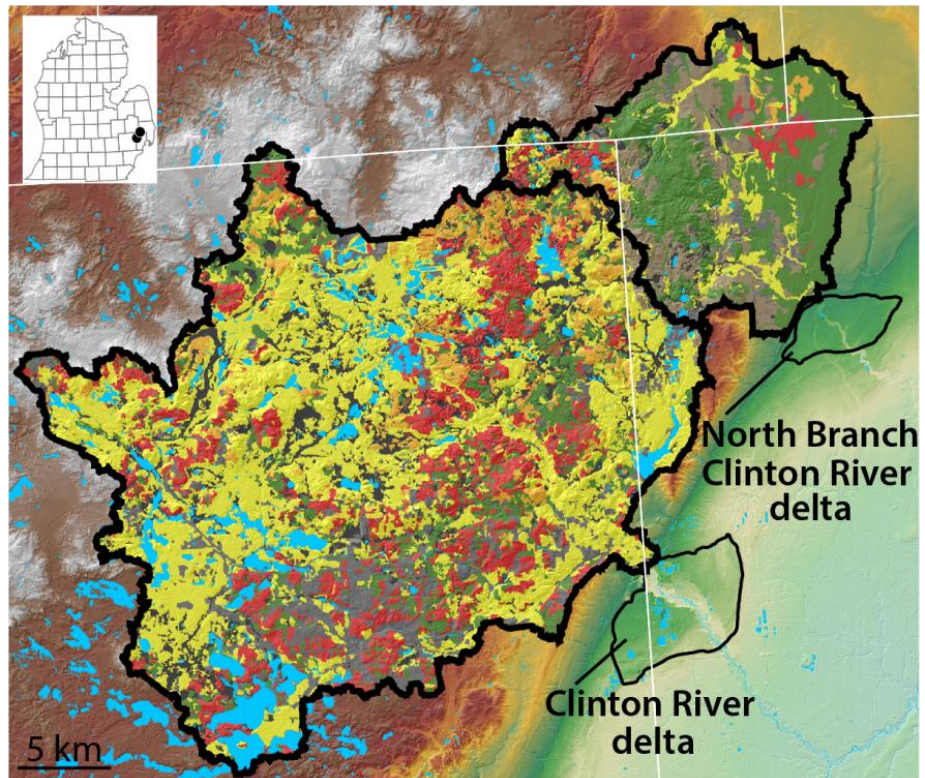


Figure C.7: Clinton River and North Branch Clinton River deltas

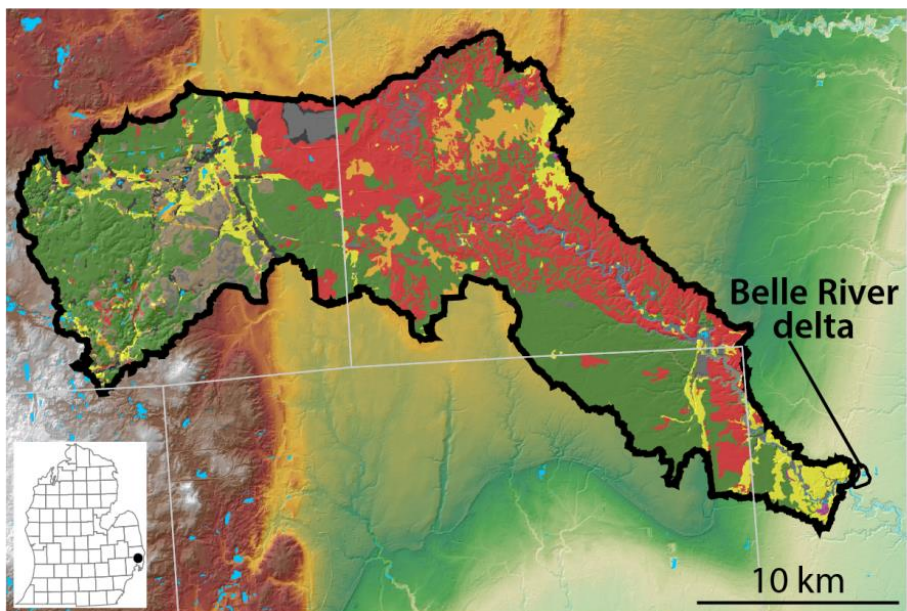


Figure C.8: Belle River delta

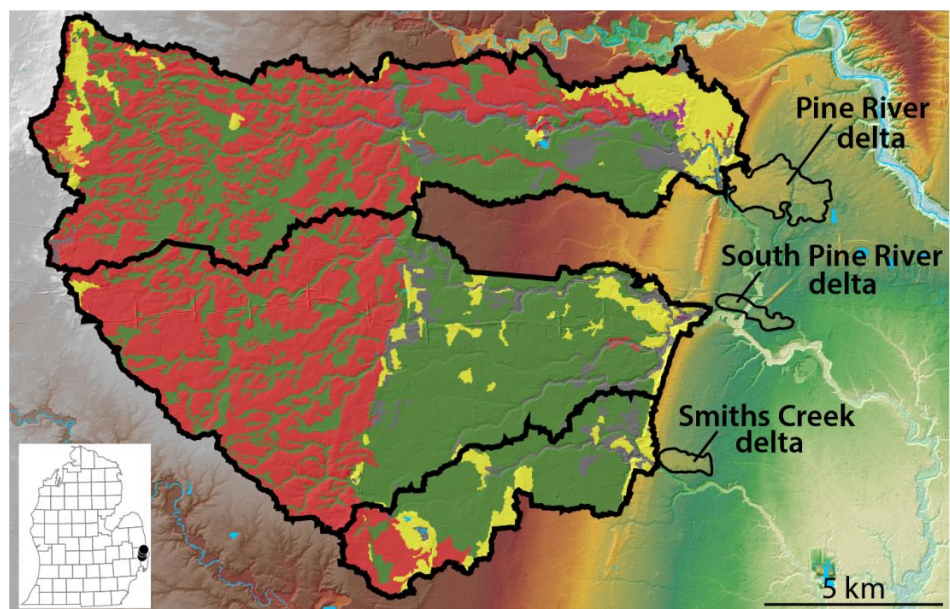


Figure C.9: Smith's Creek, South Pine River, and Pine River deltas

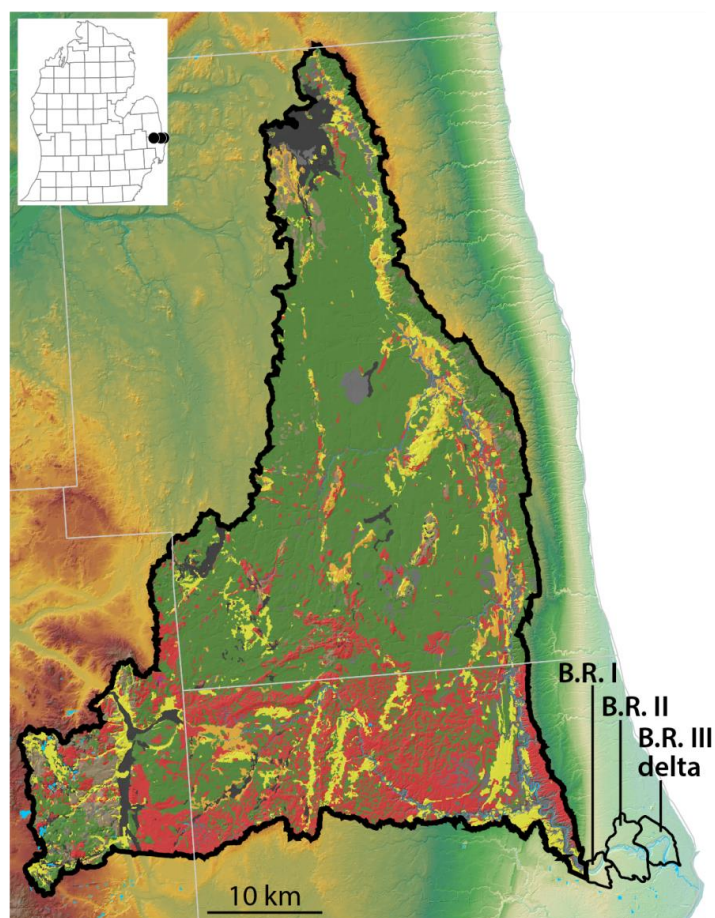


Figure C.10: Black River (B.R.) I, Black River II, and Black River III deltas

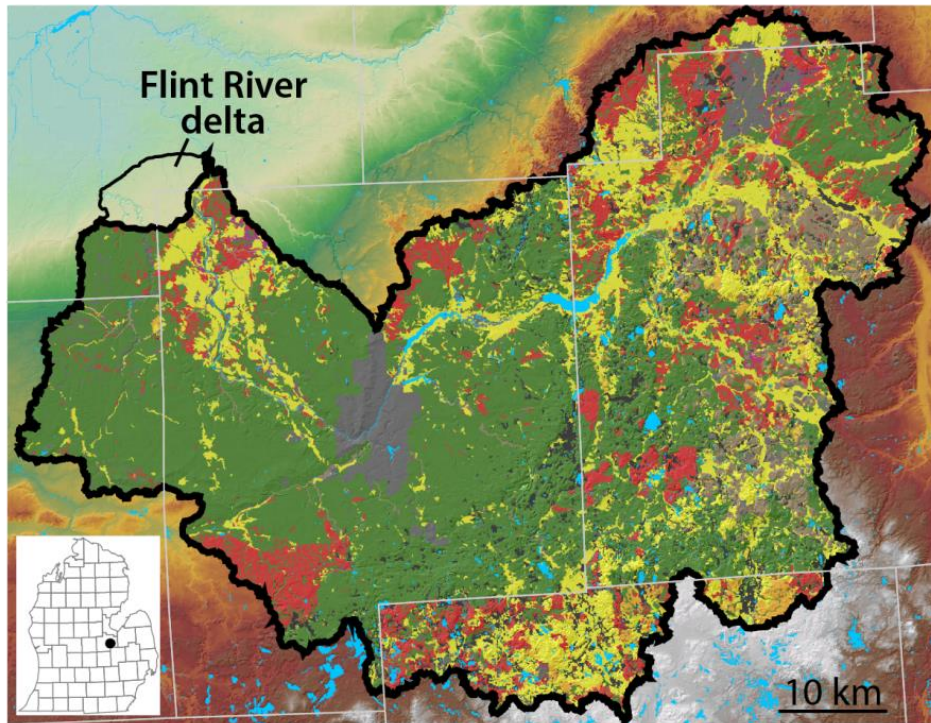


Figure C.11: Flint River delta

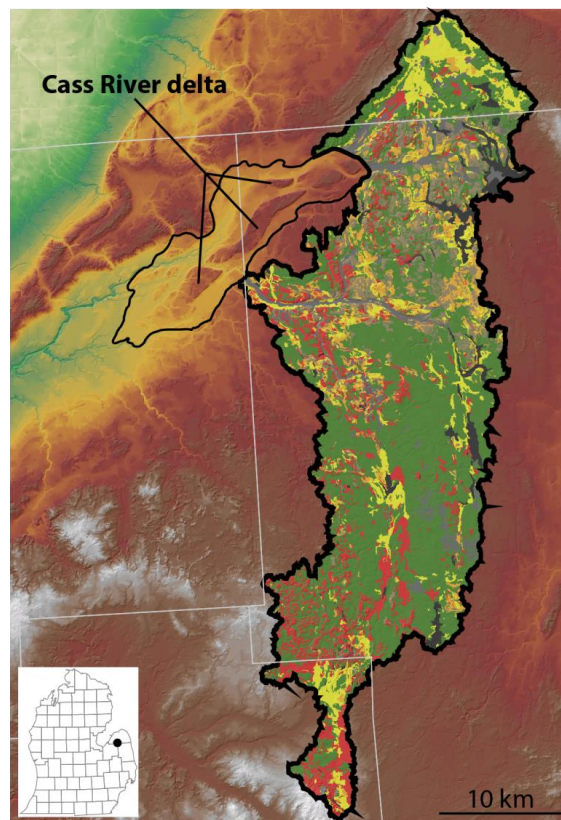


Figure C.12: Cass River delta

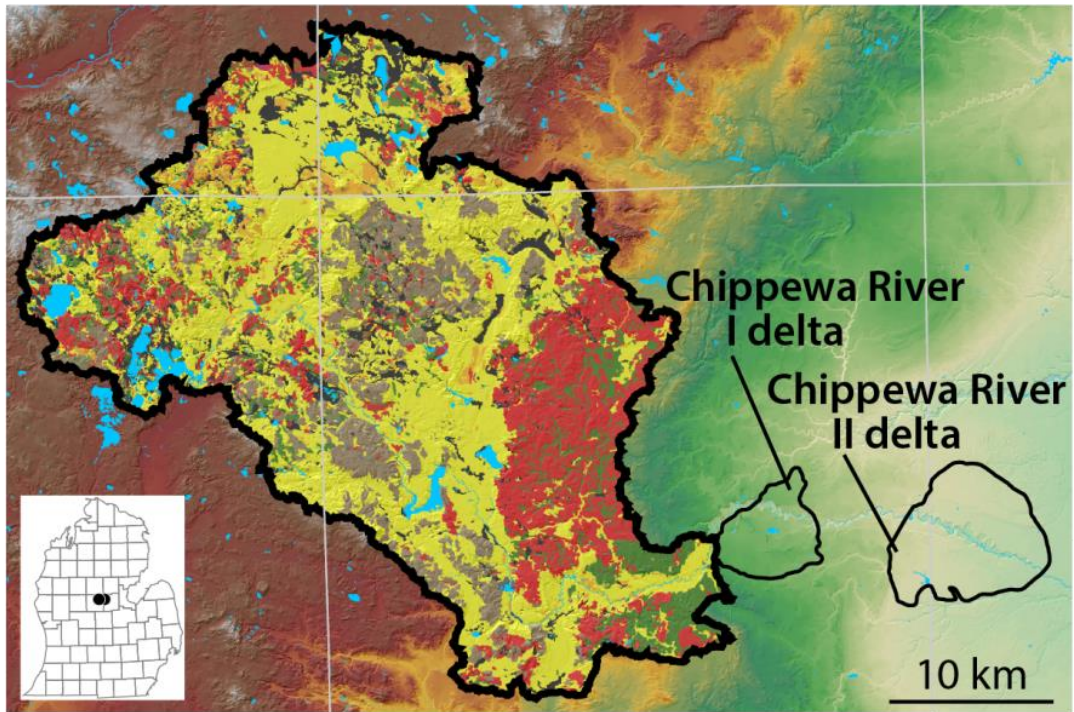


Figure C.13: Chippewa River I and Chippewa River II deltas

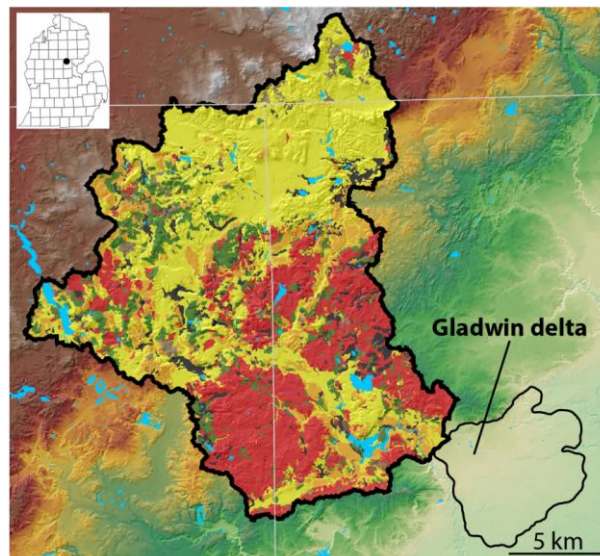


Figure C.14: Gladwin delta

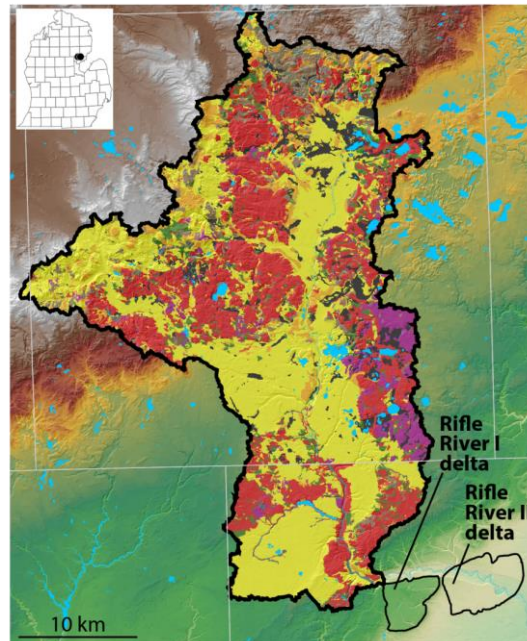


Figure C.15: Rifle River I and Rifle River II deltas

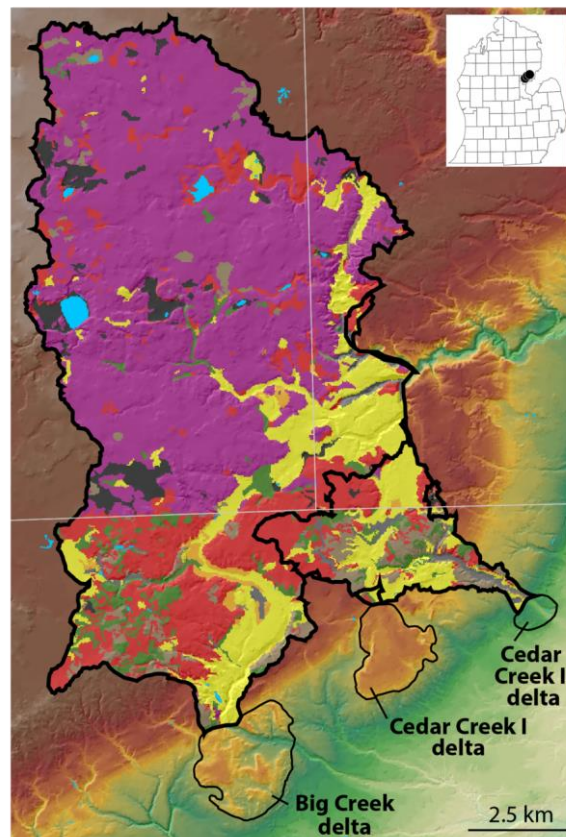


Figure C.16: Big Creek and Cedar Creek I and Cedar Creek II deltas

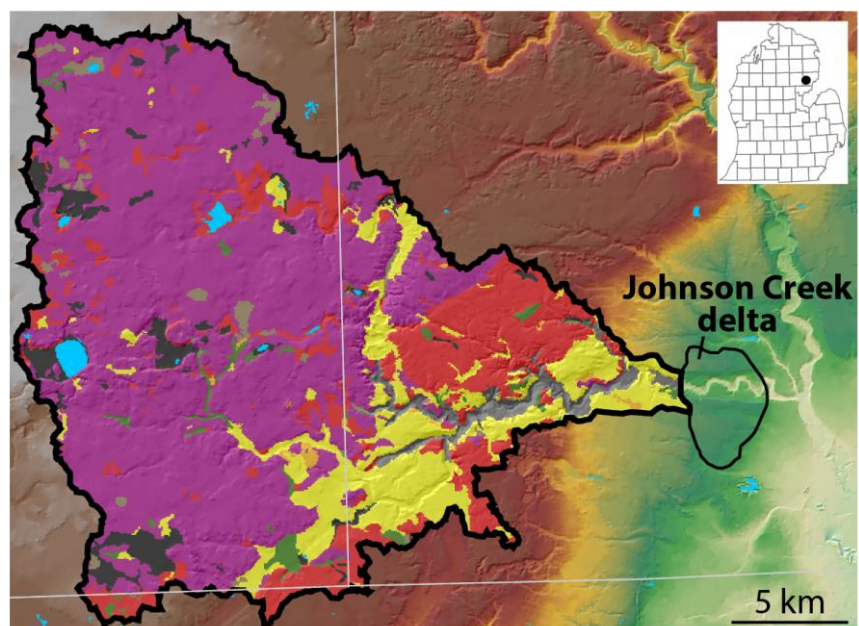


Figure C.17: Johnson Creek delta

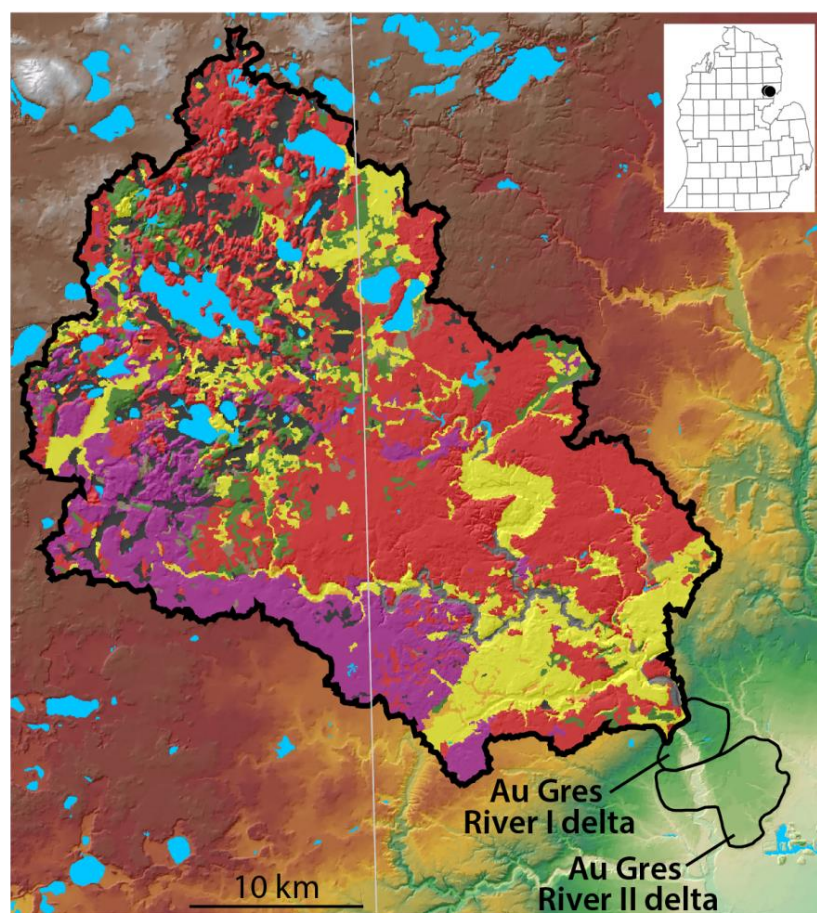


Figure C.18: Au Gres River I and Au Gres River II deltas

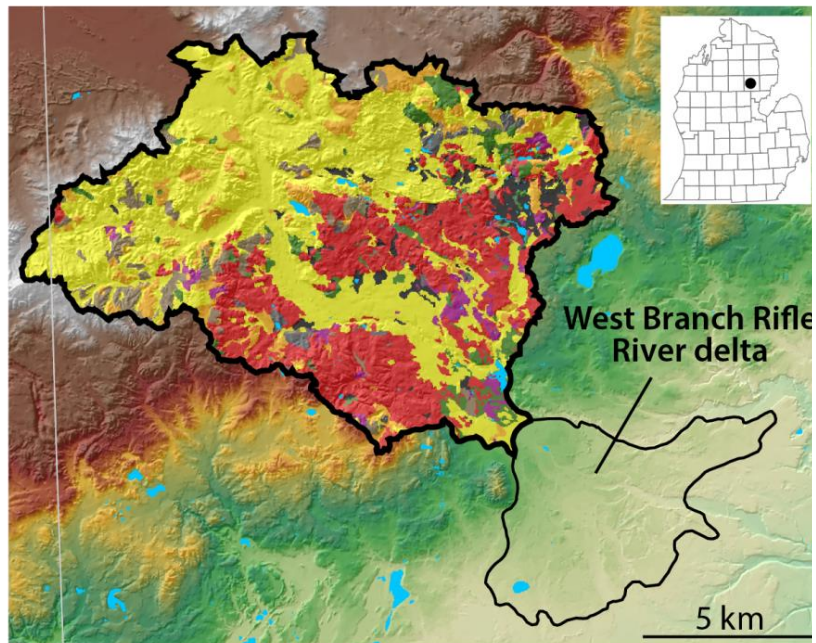


Figure C.19: West Branch Rifle River delta

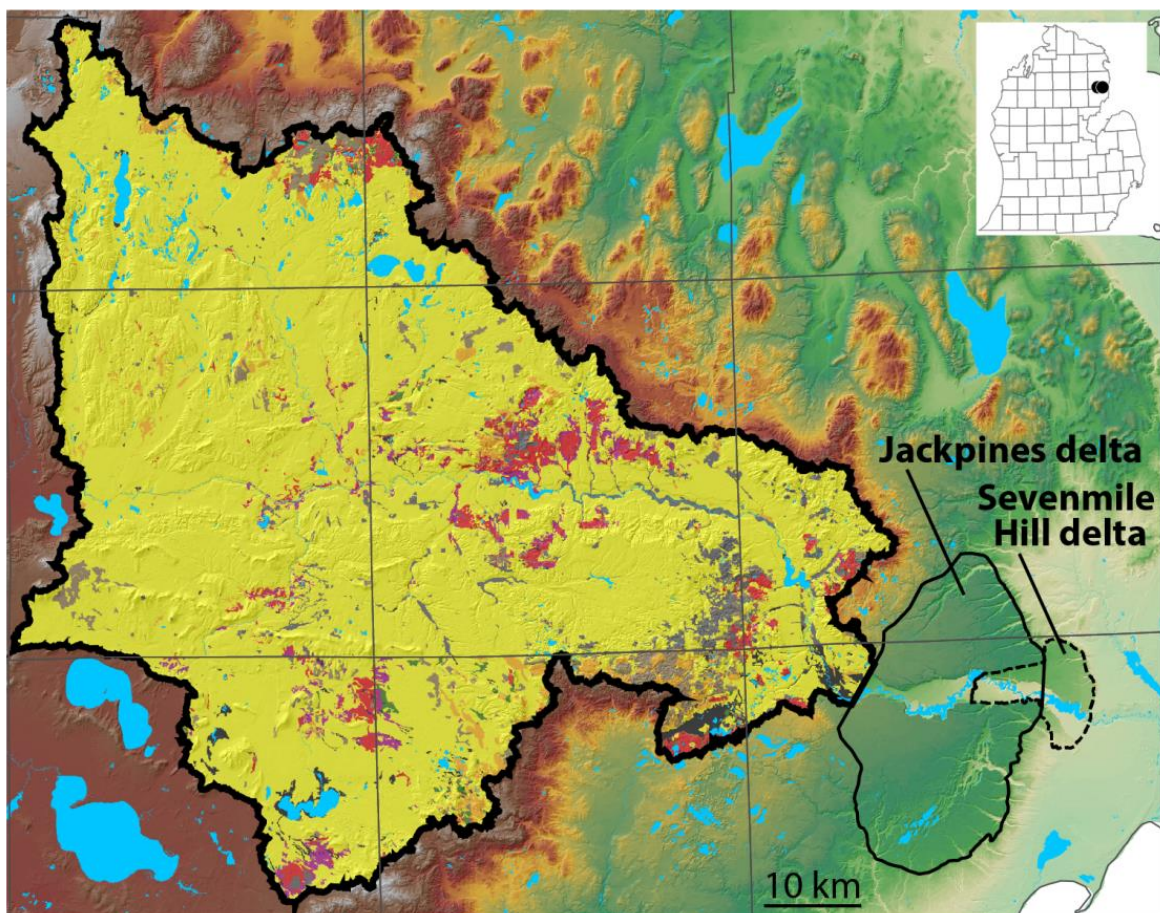


Figure C.20: Jackpines and Sevenmile Hill deltas

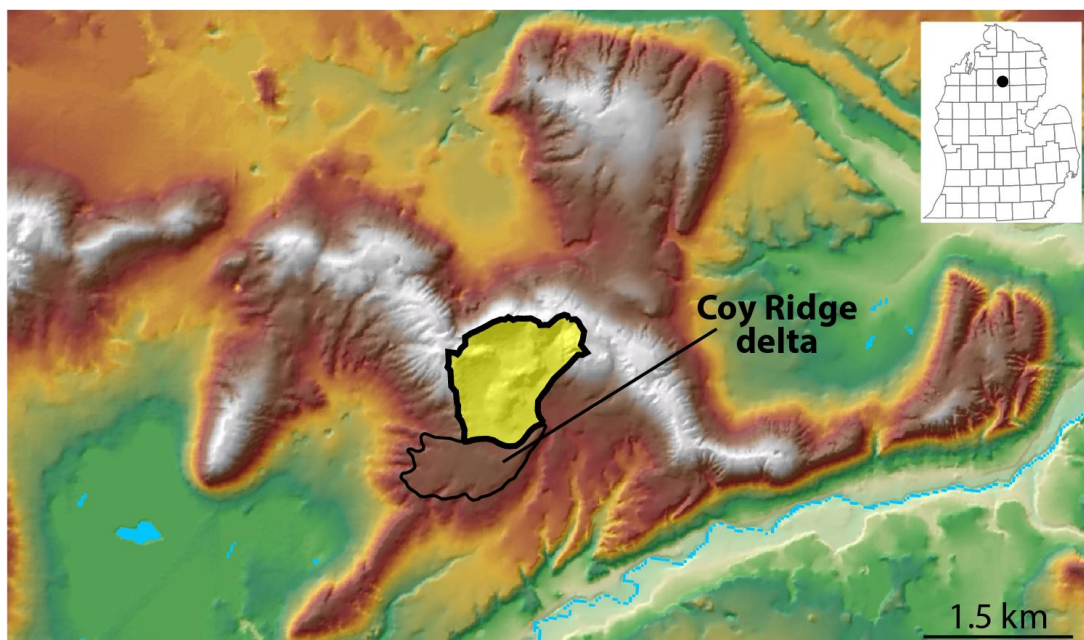


Figure C.21: Coy Ridge delta

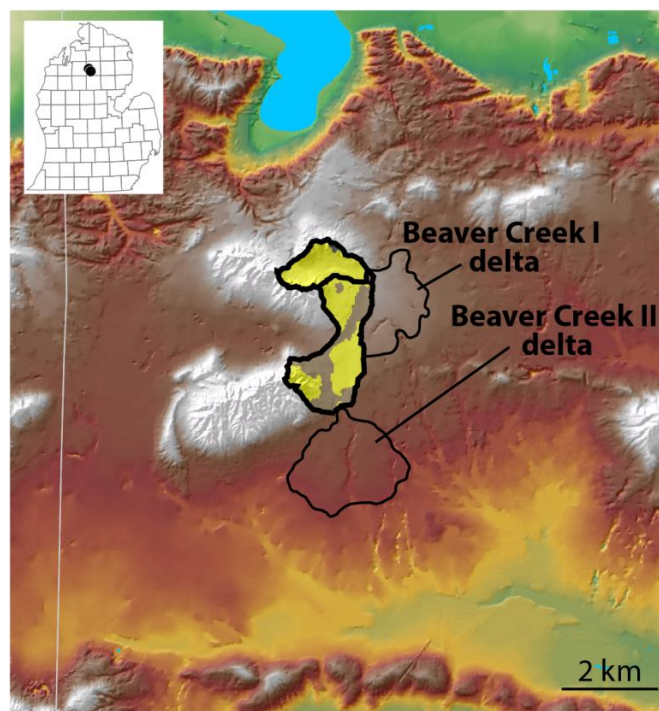


Figure C.22: Beaver Creek I and Beaver Creek II deltas

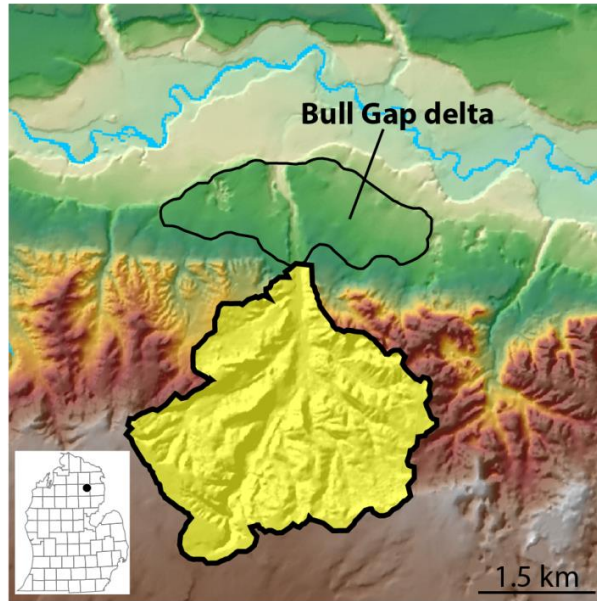


Figure C.23: Bull Gap delta

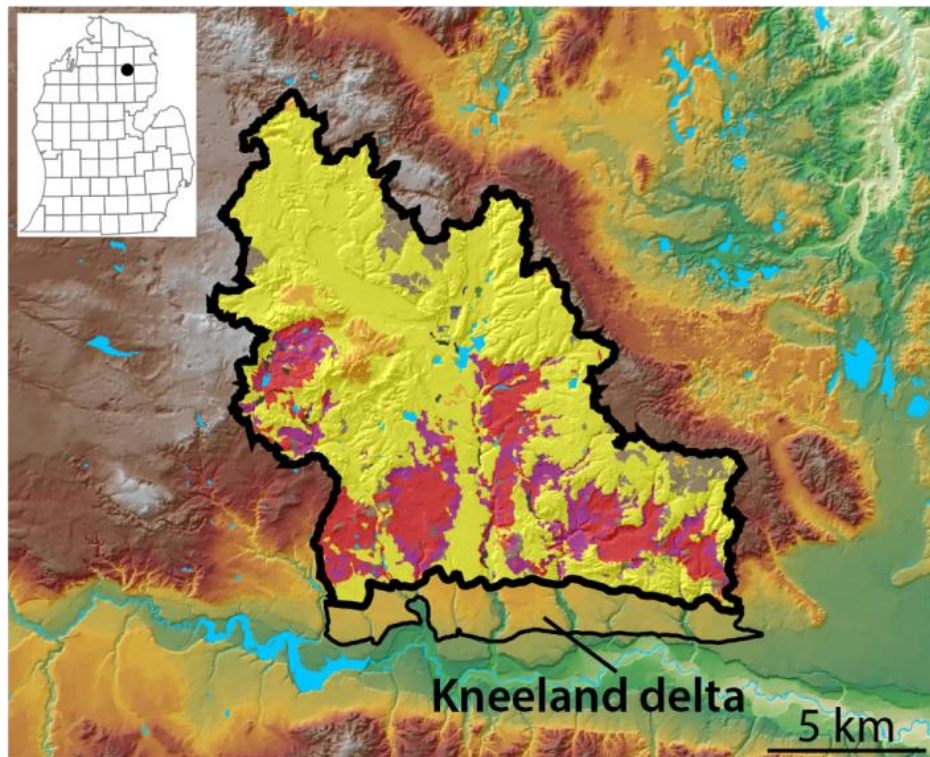


Figure C.24: Kneeland delta

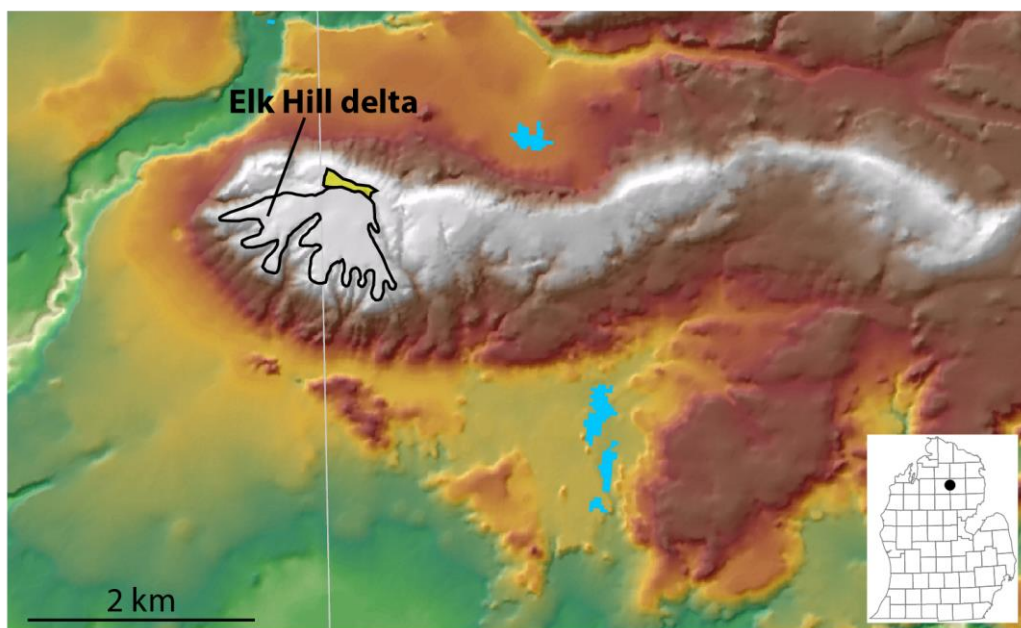


Figure C.25: Elk Hill delta

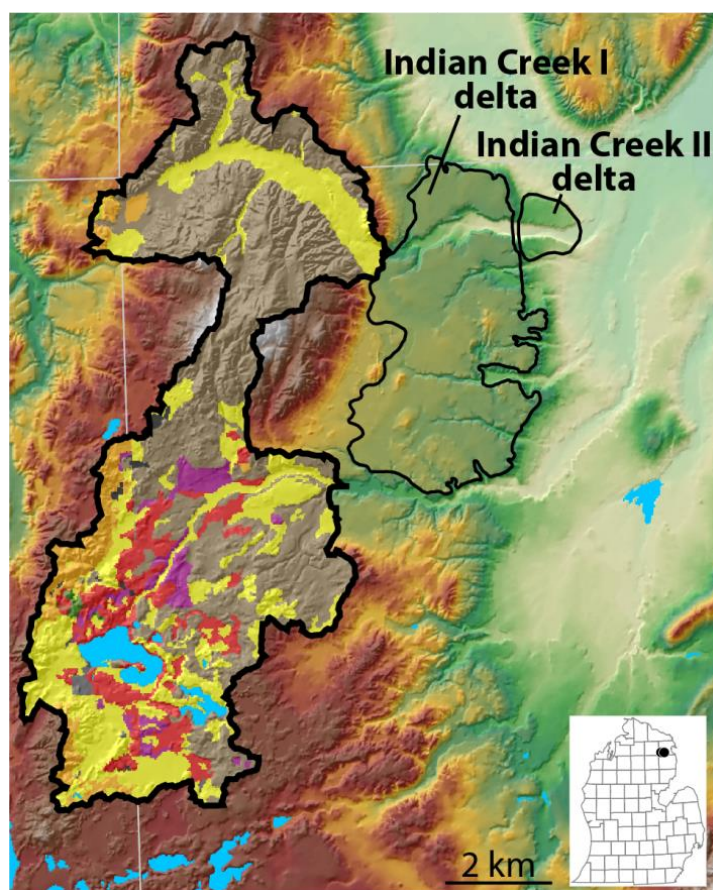


Figure C.26: Indian Creek I and Indian Creek II deltas

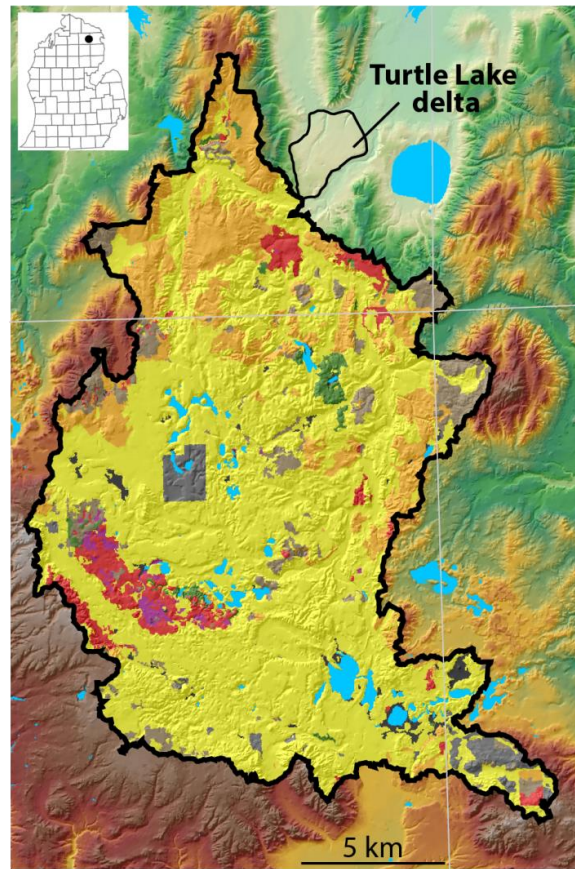


Figure C.27: Turtle Lake delta

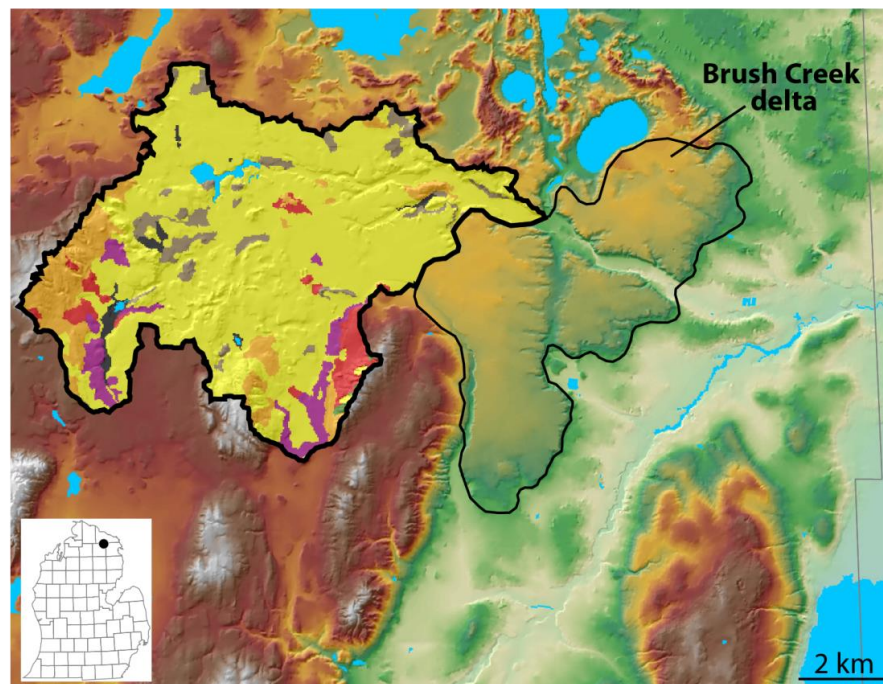


Figure C.28: Brush Creek delta

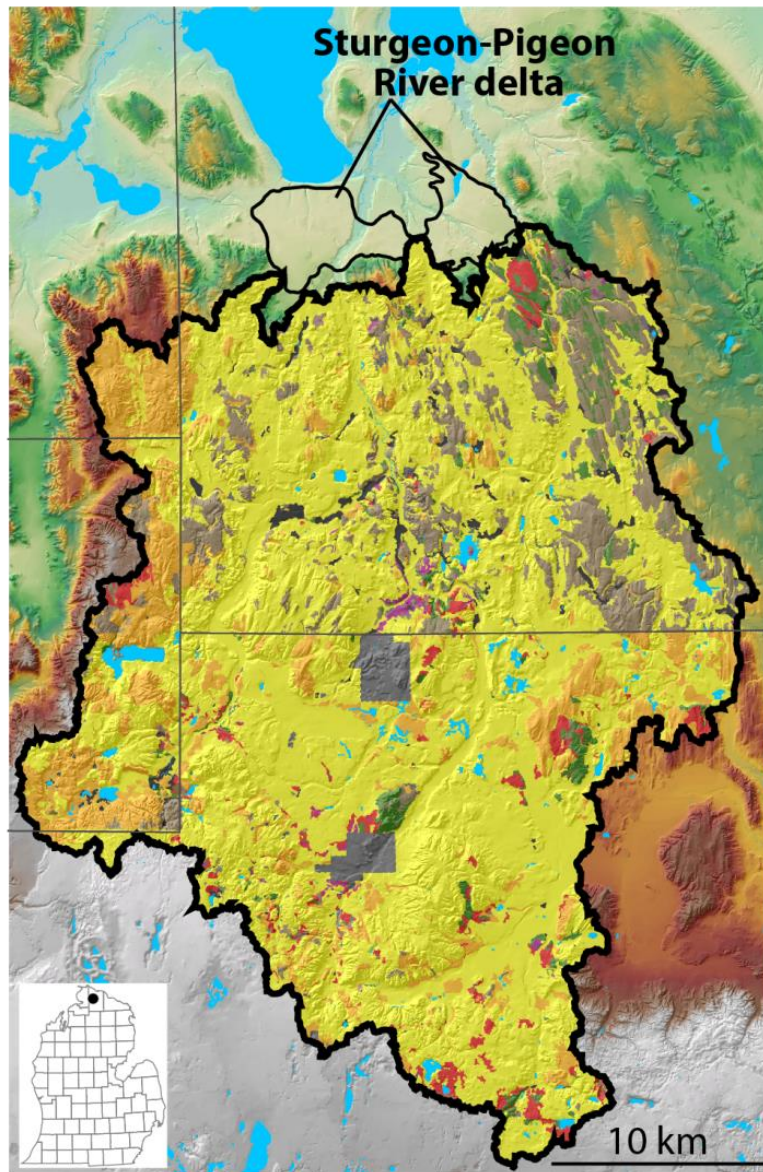


Figure C.29: Sturgeon-Pigeon River delta

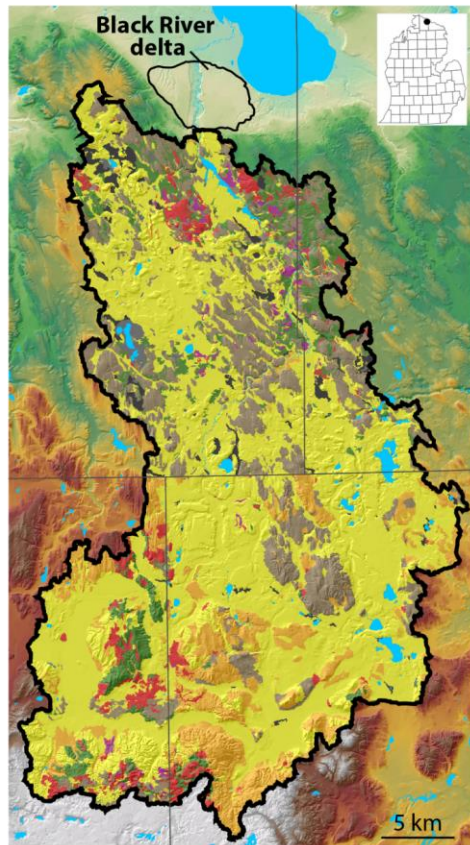


Figure C.30: Black River delta

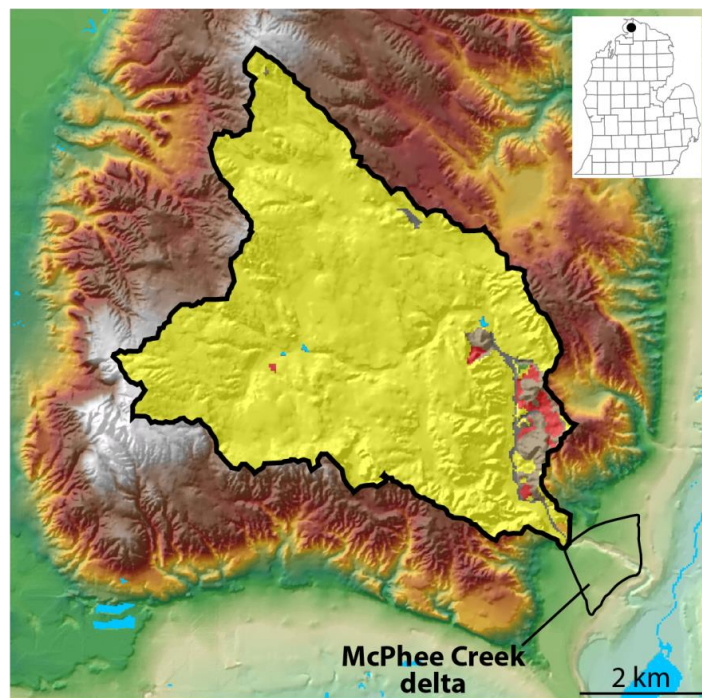


Figure C.31: McPhee Creek delta

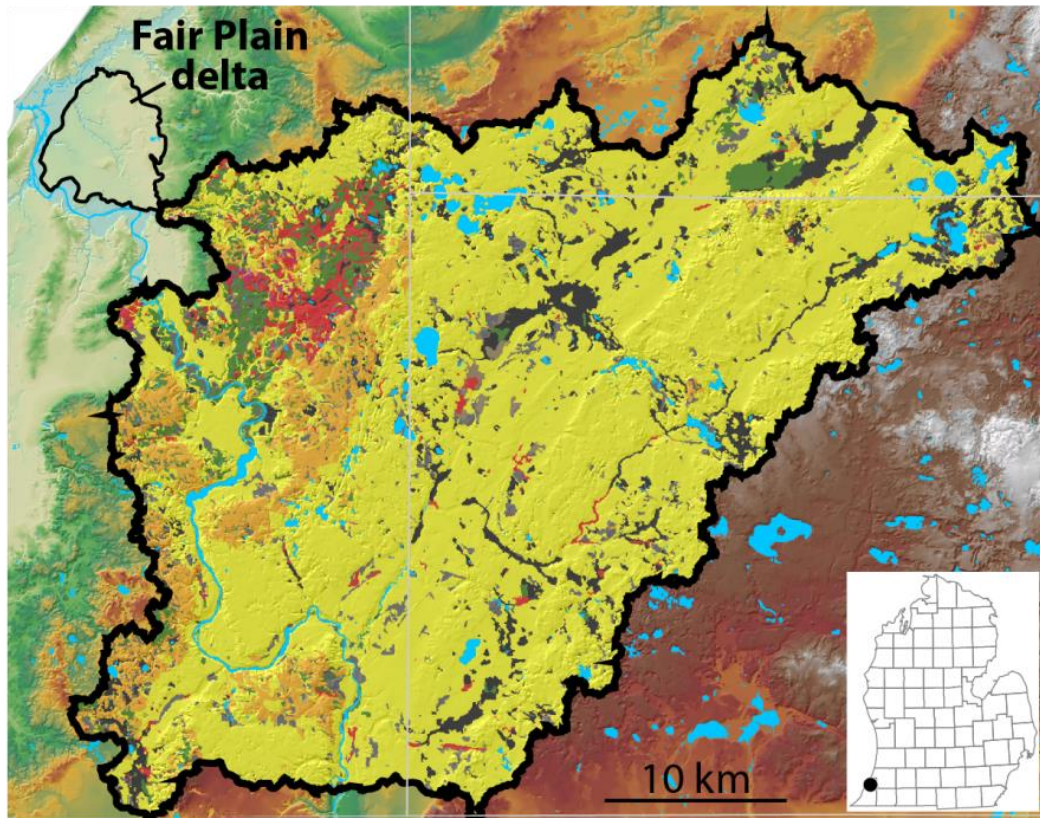


Figure C.32: Fair Plain delta

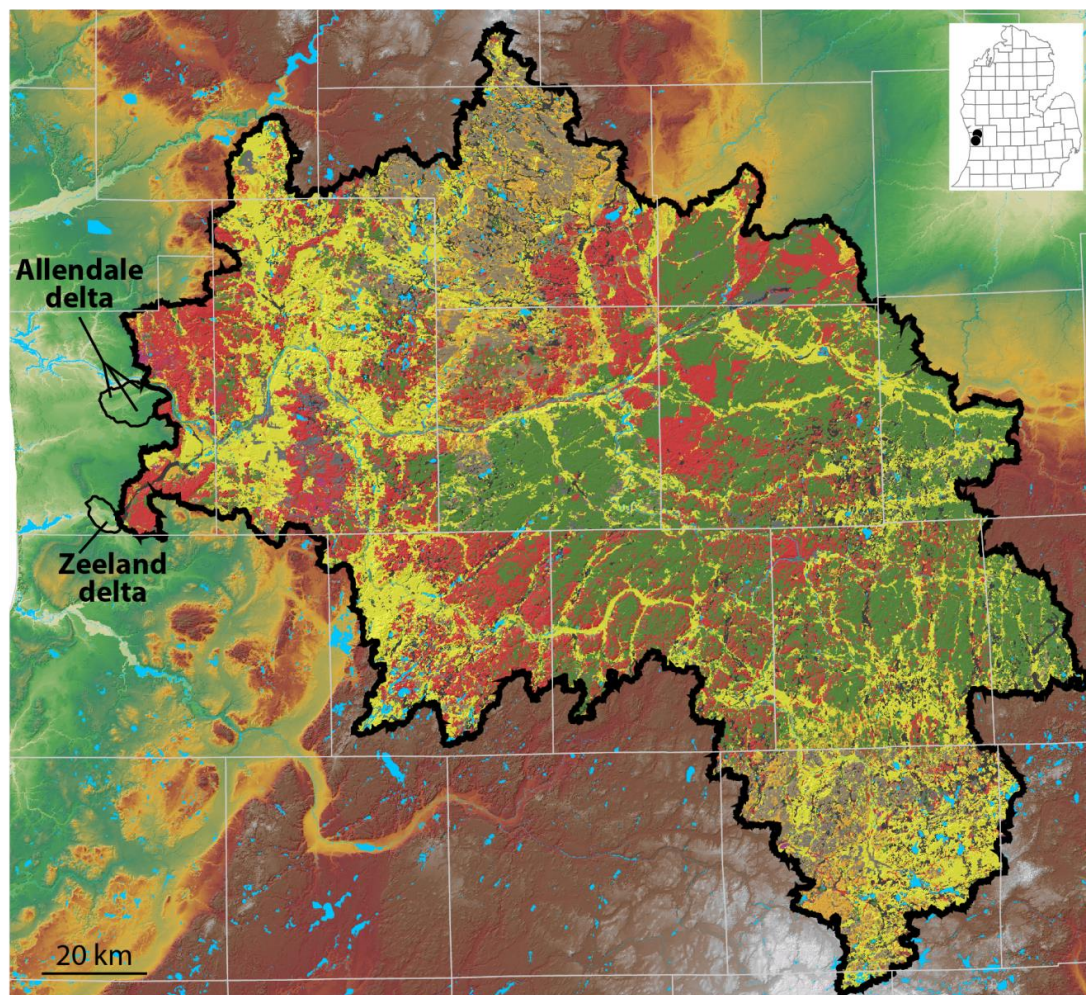


Figure C.33: Allendale and Zeeland deltas

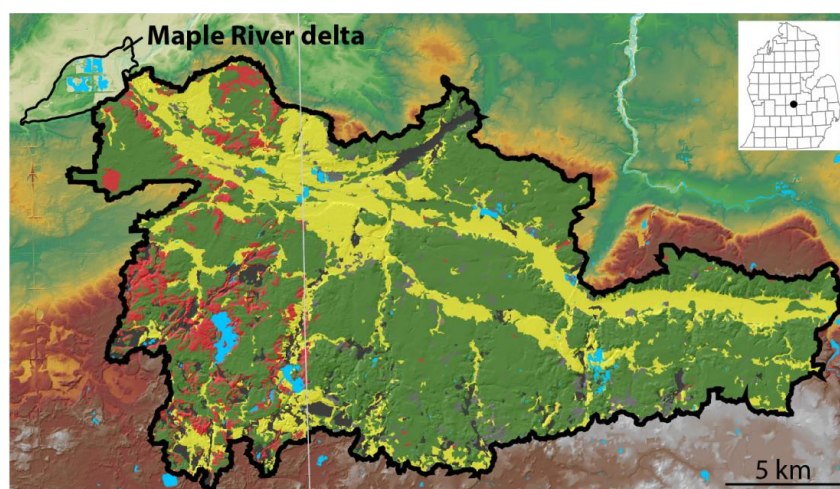


Figure C.34: Maple River delta (?). Leverett and Taylor (1915, pg. 256 and 257) emphatically states this feature is not a delta but “seems more like a kame”.

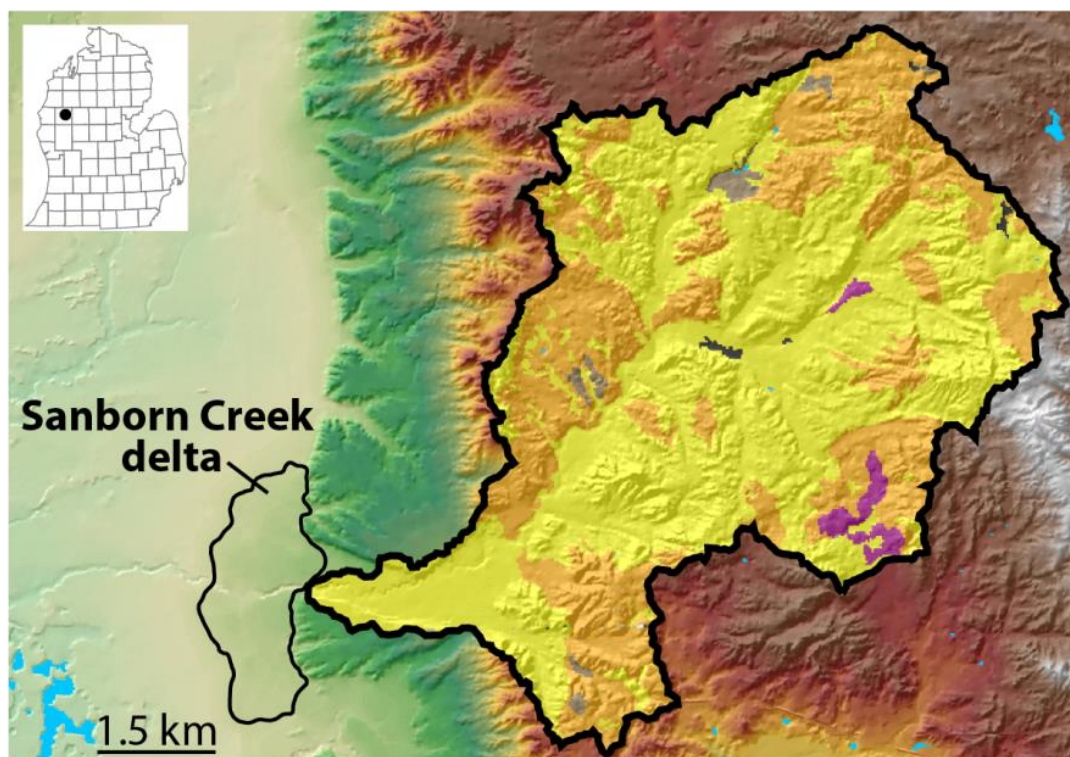


Figure C.35: Sanborn Creek delta

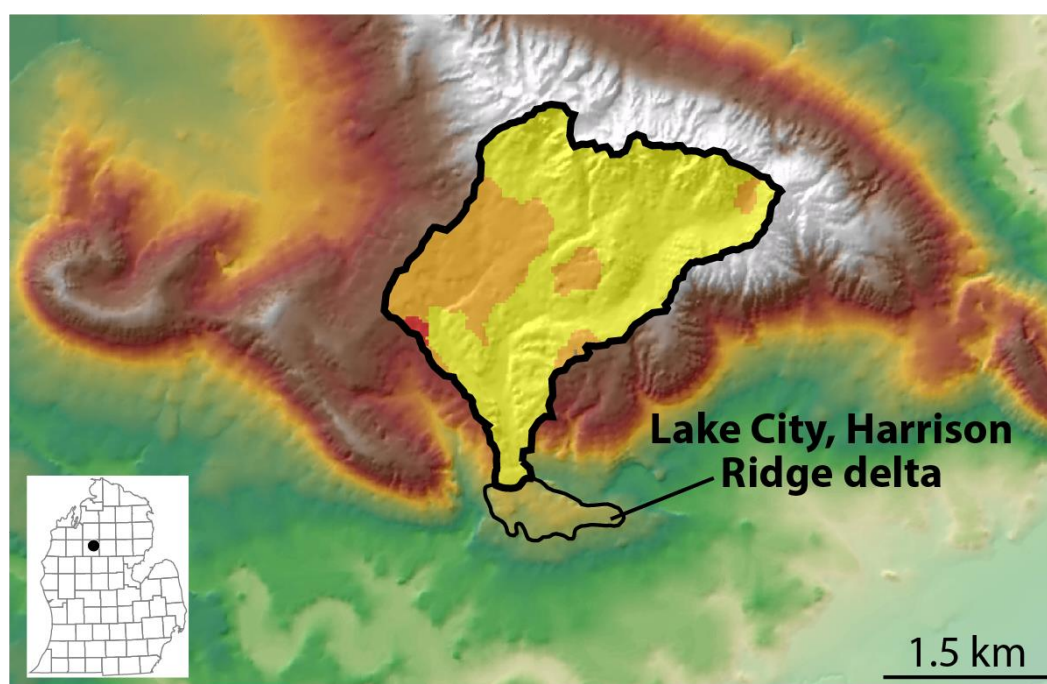


Figure C.36: Lake City, Harrison Ridge delta

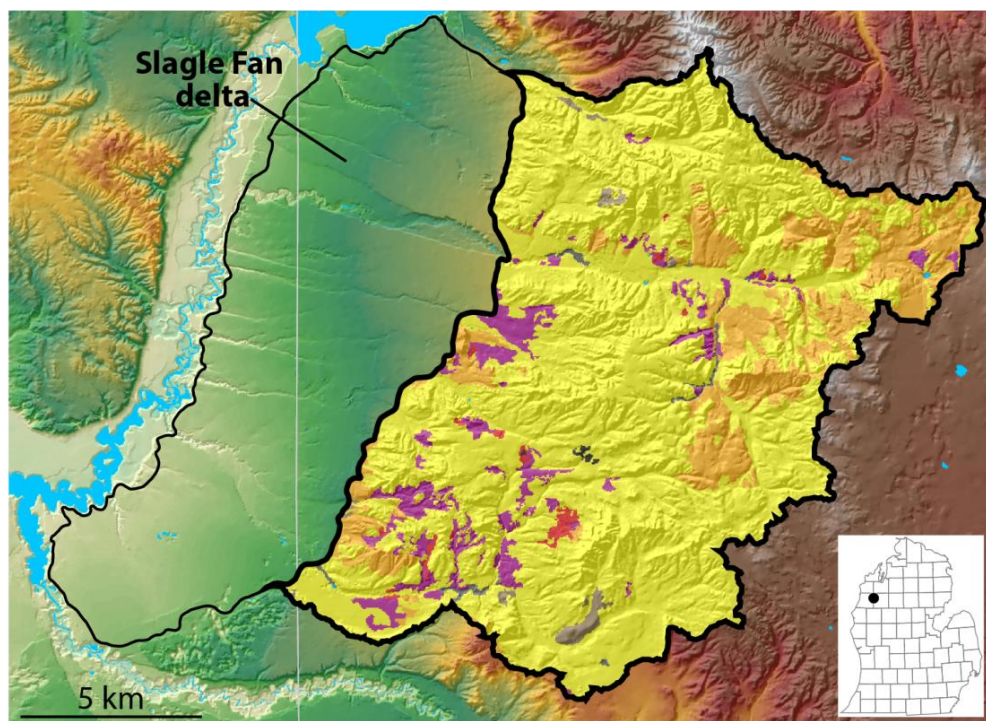


Figure C.37: Slagle Fan delta

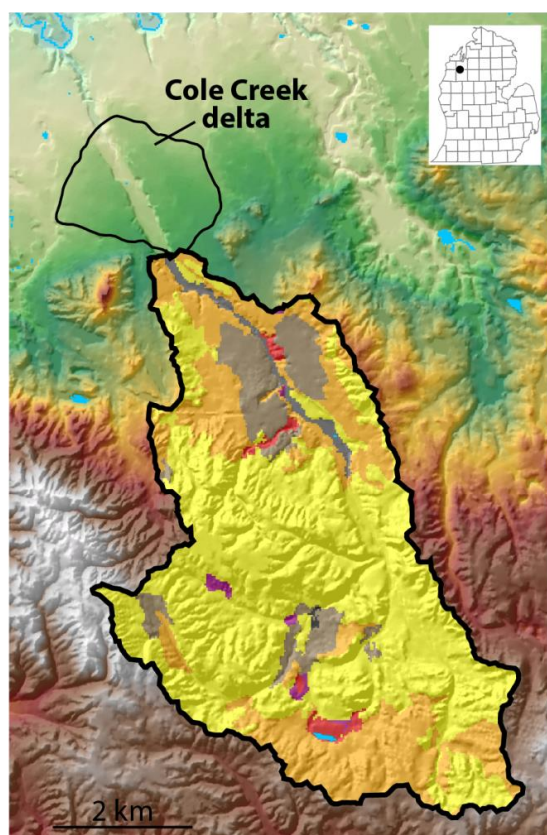


Figure C.38: Cole Creek delta

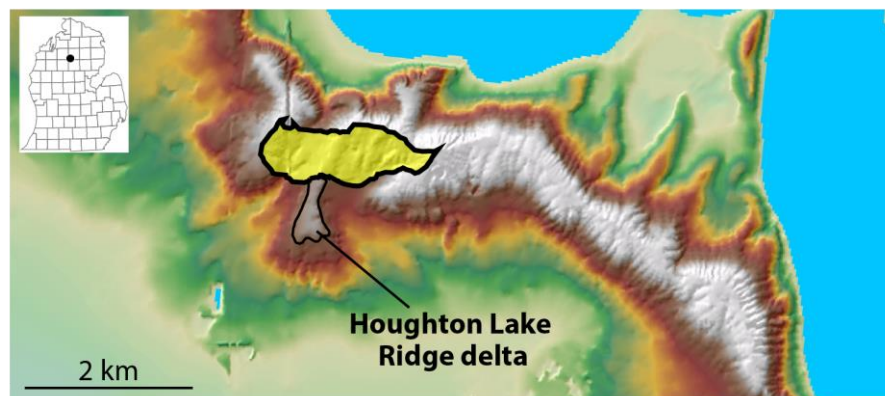


Figure C.39: Houghton Lake Ridge delta

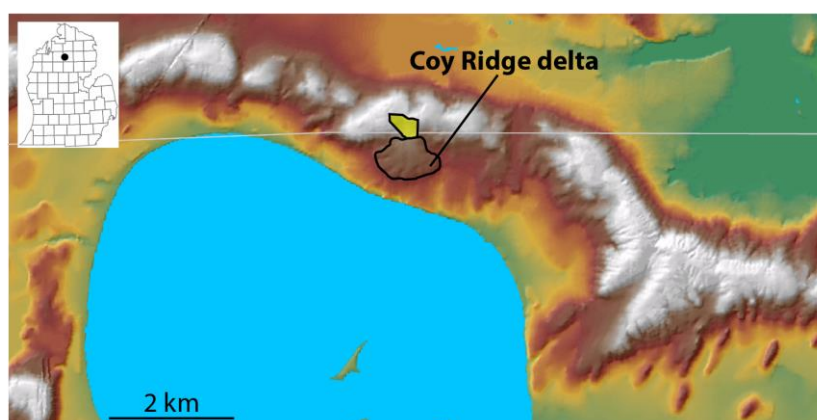


Figure C.40: Coy Ridge delta

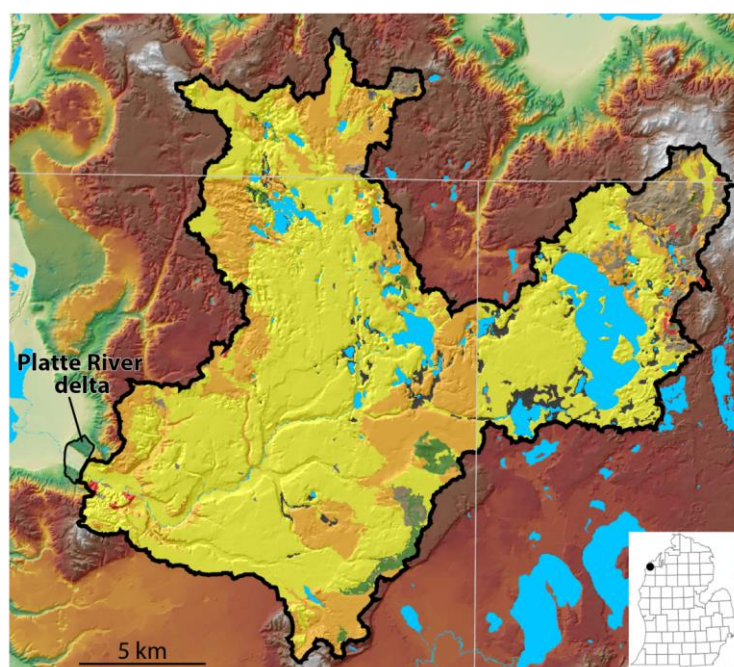


Figure C.41: Platte River delta

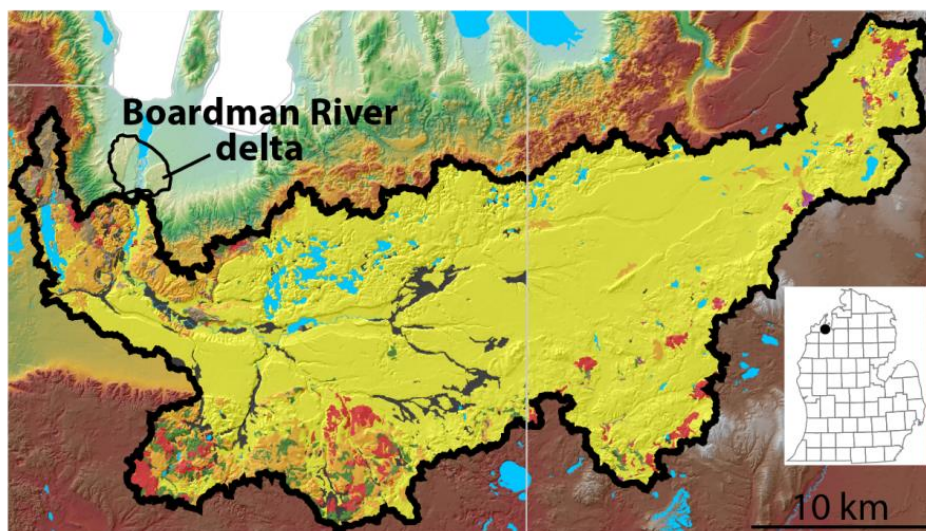


Figure C.42: Boardman River delta

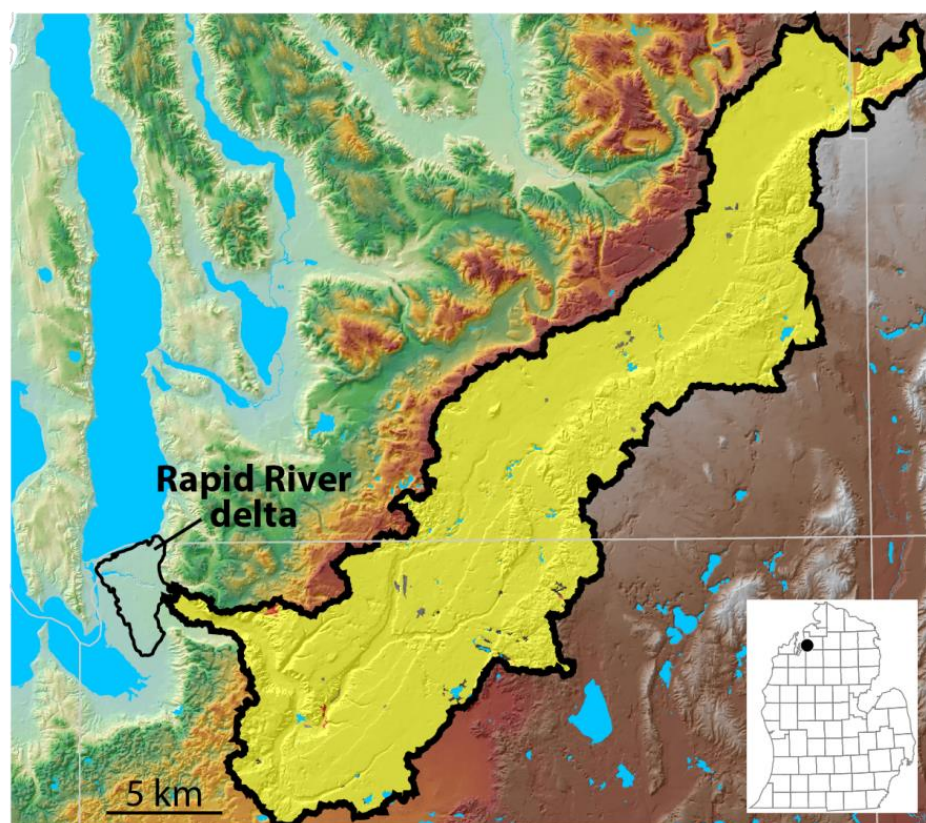


Figure C.43: Rapid River delta

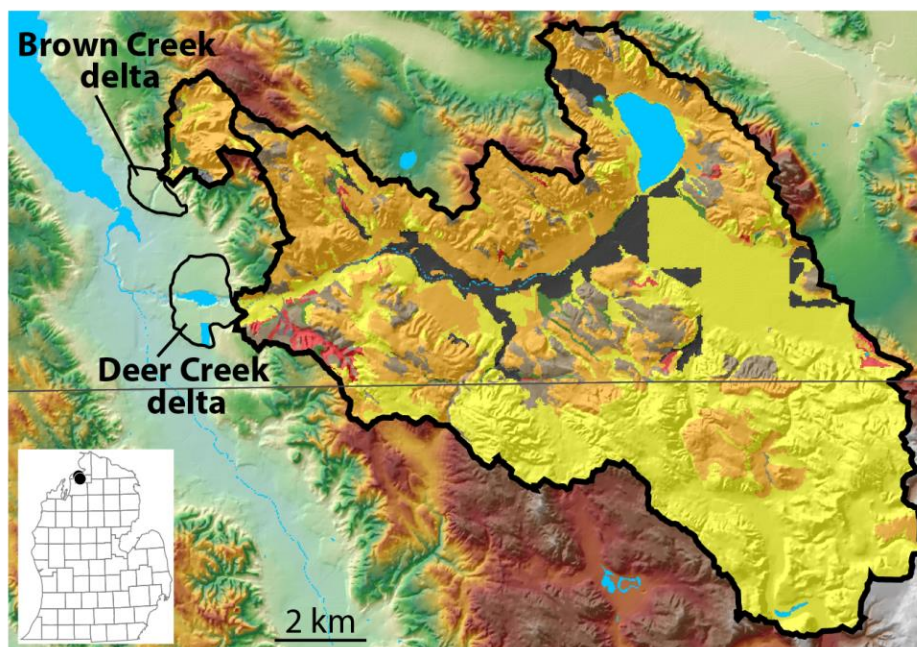


Figure C.44: Deer Creek and Brown Creek deltas

APPENDIX D: Raw Data - Delta and Catchment Characteristics

Table D.1: Raw Data – Delta Characteristics

| | | <i>Delta: Latitude (m)</i> | <i>Delta: Longitude (m)</i> | <i>Delta: Slope of the delta plain (%)</i> | <i>Delta: Max. elev. - Min. elev. (m)</i> | <i>Delta: Perimeter length (km)</i> | <i>Delta: Length / Width (m)</i> |
|-----------|-------------------------------------|--------------------------------|-------------------------------------|--|---|---|--|
| ID | Delta name | LAT | LONG | DESDP | DMMDP | DPL | DLWR |
| E-1 | Raisin River | 148457.67 | 671672.02 | 0.11 | 9.00 | 26.86 | 0.71 |
| E-2 | Saline River | 173908.93 | 687489.99 | 0.12 | 4.00 | 11.13 | 0.62 |
| E-3 | Huron River II | 191237.88 | 699034.69 | 0.24 | 8.00 | 13.76 | 0.73 |
| E-4 | Huron River I | 188231.32 | 701307.64 | 0.15 | 7.00 | 26.42 | 0.36 |
| E-5 | Huron River III | 182068.11 | 711863.23 | 0.4 | 2.00 | 10.00 | 0.69 |
| E-6 | Middle River Rouge | 205133.66 | 710657.68 | 0.41 | 10.00 | 14.63 | 0.71 |
| E-7 | Tarabusi Creek | 213073.69 | 715296.59 | 0.49 | 12.00 | 11.50 | 0.67 |
| E-8 | Rochester | 220997.21 | 725785.89 | 0.21 | 7.00 | 11.67 | 1.92 |
| E-9 | Clinton River | 237544.79 | 740005.20 | 0.25 | 15.00 | 25.89 | 0.57 |
| E-10 | North Branch Clinton River | 253488.15 | 749015.59 | 0.13 | 10.00 | 17.31 | 0.45 |
| E-11 | Belle River | 259210.78 | 772242.63 | 0.41 | 3.00 | 3.38 | 0.63 |
| E-12 | Smiths Creek | 270584.94 | 773957.57 | 0.21 | 4.00 | 3.98 | 1.00 |
| E-13 | South Pine River | 274714.97 | 775867.84 | 0.12 | 2.00 | 5.40 | 1.00 |
| E-14 | Black River I | 277113.73 | 782467.59 | 0.31 | 7.00 | 10.65 | 0.70 |
| E-15 | Black River II | 278969.88 | 785132.34 | 0.21 | 7.00 | 19.85 | 0.59 |
| E-16 | Black River III | 279710.79 | 787803.86 | 0.1 | 4.00 | 15.27 | 0.57 |
| E-17 | Pine River | 278061.64 | 776557.76 | 0.17 | 4.00 | 11.20 | 1.18 |
| H-1 | Flint River | 298618.63 | 667650.95 | 0.07 | 6.00 | 30.07 | 0.59 |
| H-2 | Cass River | 342400.45 | 731659.51 | 0.07 | 15.00 | 63.23 | 3.08 |

Table D.1 (cont'd)

| | | | | | | | |
|------|-------------------------|-----------|-----------|------|-------|-------|------|
| H-3 | Chippewa River I | 341195.30 | 602043.94 | 0.1 | 7.00 | 23.37 | 0.97 |
| H-4 | Chippewa River II | 340869.98 | 614603.31 | 0.12 | 10.00 | 34.19 | 0.80 |
| H-5 | Gladwin | 382521.68 | 624243.08 | 0.21 | 13.00 | 29.82 | 0.85 |
| H-6 | Rifle River I | 391314.82 | 661659.56 | 0.12 | 7.00 | 16.69 | 0.69 |
| H-7 | Rifle River II | 392886.79 | 667961.93 | 0.13 | 10.00 | 21.23 | 0.81 |
| H-8 | Big Creek | 397232.68 | 667305.21 | 0.27 | 7.00 | 9.49 | 0.78 |
| H-9 | Cedar Creek I | 399908.15 | 670787.15 | 0.31 | 5.00 | 7.93 | 0.88 |
| H-10 | Cedar Creek II | 400862.18 | 674321.56 | 1.18 | 4.00 | 2.94 | 0.65 |
| H-11 | Johnson Creek | 407284.64 | 676903.52 | 0.28 | 3.00 | 7.26 | 0.67 |
| H-12 | Au Gres River I | 411536.04 | 678247.50 | 0.34 | 7.00 | 6.86 | 0.63 |
| H-13 | Au Gres River II | 410028.08 | 679248.37 | 0.26 | 6.00 | 11.96 | 0.75 |
| H-14 | West Branch Rifle River | 410166.16 | 645923.16 | 0.24 | 15.00 | 28.82 | 0.60 |
| H-15 | Jackpines | 434322.43 | 688775.94 | 0.12 | 19.00 | 90.08 | 0.58 |
| H-16 | Sevenmile Hill | 437328.36 | 699554.05 | 0.2 | 13.00 | 44.12 | 0.41 |
| H-17 | Coy Ridge | 444709.26 | 610717.35 | 0.73 | 6.00 | 4.31 | 0.90 |
| H-18 | Beaver Creek I | 449786.60 | 598059.91 | 0.49 | 6.00 | 7.11 | 0.59 |
| H-19 | Beaver Creek II | 446431.73 | 597178.09 | 0.6 | 13.00 | 7.65 | 0.81 |
| H-20 | Bull Gap | 456670.68 | 657007.81 | 2.2 | 15.00 | 8.58 | 0.40 |
| H-21 | Kneeland | 459851.46 | 652996.57 | 0.32 | 14.00 | 35.53 | 0.17 |
| H-22 | Elk Hill | 465122.75 | 628763.03 | 0.59 | 5.00 | 6.94 | 0.62 |
| H-23 | Indian Creek I | 477254.02 | 672909.86 | 0.15 | 9.00 | 25.57 | 0.55 |
| H-24 | Indian Creek II | 479384.12 | 674774.04 | 0.88 | 8.00 | 4.04 | 0.85 |

Table D.1 (cont'd)

| | | | | | | | |
|------|---------------------------|-----------|-----------|------|-------|-------|------|
| H-25 | Turtle Lake | 485924.69 | 662843.76 | 0.32 | 9.00 | 9.35 | 1.51 |
| H-26 | Brush Creek | 504007.00 | 659676.87 | 0.24 | 4.00 | 29.98 | 0.52 |
| H-27 | Sturgeon-Pigeon River | 538006.88 | 609872.81 | 0.32 | 9.00 | 58.81 | 0.48 |
| H-28 | Black River | 543299.83 | 630447.12 | 0.23 | 7.00 | 19.79 | 0.59 |
| H-29 | McPhee Creek | 544503.47 | 593688.61 | 0.82 | 9.00 | 4.43 | 0.62 |
| M-1 | Fair Plain | 171683.47 | 464658.01 | 0.07 | 6.00 | 30.17 | 0.78 |
| M-2 | Zeeland | 249732.33 | 497872.30 | 0.45 | 9.00 | 19.68 | 1.82 |
| M-3 | Allendale | 269286.58 | 502883.85 | 0.09 | 8.00 | 33.67 | 1.57 |
| M-4 | Maple River | 277813.17 | 623015.34 | 0.1 | 2.00 | 15.86 | 0.39 |
| M-5 | Sanborn Creek | 372820.94 | 520242.34 | 0.46 | 6.00 | 10.00 | 0.45 |
| M-6 | Lake City, Harrison Ridge | 414221.96 | 578047.44 | 0.32 | 2.00 | 3.29 | 0.42 |
| M-7 | Slagle Fan | 415687.70 | 514505.59 | 0.83 | 54.00 | 54.20 | 0.40 |
| M-8 | Cole Creek | 429048.80 | 526748.97 | 1.25 | 21.00 | 7.36 | 0.71 |
| M-9 | Houghton Lake Ridge | 433800.92 | 597130.91 | 0.49 | 4.00 | 2.17 | 1.00 |
| M-10 | Higgins Lake Ridge | 440439.49 | 601986.08 | 1.49 | 10.00 | 2.75 | 0.63 |
| M-11 | Platte River | 457485.45 | 497419.82 | 0.89 | 10.00 | 5.28 | 0.54 |
| M-12 | Boardman River | 464421.23 | 529960.43 | 0.56 | 11.00 | 12.08 | 0.72 |
| M-13 | Rapid River | 476503.19 | 555499.43 | 0.36 | 11.00 | 18.53 | 0.61 |
| M-14 | Deer Creek | 509652.04 | 570123.53 | 0.64 | 10.00 | 6.55 | 0.77 |
| M-15 | Brown Creek | 512040.31 | 569021.12 | 1.08 | 10.00 | 3.98 | 0.49 |

Table D.1 (cont'd)

| | | <i>Delta: Abundance of major feeder channels</i> | <i>Delta: Abundance of paleodistri butary channels</i> | <i>Delta: Most areally extensive upper soil textural class</i> | <i>Delta: Most areally extensive subsurface textural class</i> | <i>Delta: Clay content in upper soil (%)</i> | <i>Delta: Sand content in upper soil (%)</i> |
|-----------|-------------------------------------|--|--|--|--|--|--|
| ID | Delta name | DAMFC | DAPDC | DDUPST | DDSUBST | DPCUPS | DPSUP S |
| E-1 | Raisin River | 1 | 2 | sandy loam | coarse sand | 10.30 | 51.85 |
| E-2 | Saline River | 1 | 1 | sandy loam | silty clay | 17.52 | 48.43 |
| E-3 | Huron River II | 1 | 1 | loamy sand | fine sand | 7.23 | 75.81 |
| E-4 | Huron River I | 1 | 1 | sandy loam | sand | 9.90 | 49.16 |
| E-5 | Huron River III | 1 | 1 | loamy fine sand | fine sand | 5.60 | 79.90 |
| E-6 | Middle River Rouge | 1 | 2 | loamy sand | fine sand | 6.78 | 65.66 |
| E-7 | Tarabusi Creek | 1 | 2 | sandy loam | very fine sand | 7.83 | 48.27 |
| E-8 | Rochester | 2 | 2 | loamy sand | clay loam | 11.90 | 25.82 |
| E-9 | Clinton River | 1 | 1 | loamy sand | coarse sand | 6.26 | 59.49 |
| E-10 | North Branch Clinton River | 1 | 2 | sandy loam | loam | 11.31 | 56.49 |
| E-11 | Belle River | 1 | 1 | loamy fine sand | fine sand | 3.80 | 65.55 |
| E-12 | Smiths Creek | 1 | 1 | fine sand | fine sand | 4.76 | 87.14 |
| E-13 | South Pine River | 1 | 1 | fine sand | fine sand | 17.42 | 57.50 |
| E-14 | Black River I | 1 | 1 | sand | clay | 5.73 | 54.82 |
| E-15 | Black River II | 1 | 1 | fine sand | very fine sand | 4.19 | 69.47 |
| E-16 | Black River III | 1 | 1 | fine sand | very fine sand | 3.91 | 63.40 |
| E-17 | Pine River | 1 | 1 | fine sand | very fine sand | 4.59 | 83.24 |

Table D.1 (cont'd)

| | | | | | | | |
|------|-------------------------|---|---|------------|-------------|------|-------|
| H-1 | Flint River | 2 | 2 | sand | sand | 7.19 | 77.75 |
| H-2 | Cass River | 2 | 2 | sandy loam | coarse sand | 8.22 | 52.77 |
| H-3 | Chippewa River I | 1 | 1 | sand | sand | 6.11 | 77.06 |
| H-4 | Chippewa River II | 1 | 2 | sand | sand | 4.57 | 81.74 |
| H-5 | Gladwin | 1 | 2 | loamy sand | sand | 4.79 | 80.36 |
| H-6 | Rifle River I | 1 | 1 | sand | sand | 3.34 | 89.52 |
| H-7 | Rifle River II | 1 | 1 | sand | sand | 3.13 | 77.37 |
| H-8 | Big Creek | 1 | 1 | sand | sand | 2.84 | 83.92 |
| H-9 | Cedar Creek I | 1 | 1 | sand | sand | 3.00 | 91.84 |
| H-10 | Cedar Creek II | 1 | 1 | sand | sand | 2.66 | 80.81 |
| H-11 | Johnson Creek | 1 | 1 | sand | sand | 2.93 | 82.04 |
| H-12 | Au Gres River I | 1 | 1 | sand | sand | 3.64 | 83.11 |
| H-13 | Au Gres River II | 1 | 1 | sand | sand | 3.27 | 87.94 |
| H-14 | West Branch Rifle River | 1 | 2 | sand | sand | 2.74 | 77.63 |
| H-15 | Jackpines | 1 | 1 | sand | sand | 2.77 | 80.06 |
| H-16 | Sevenmile Hill | 1 | 1 | sand | sand | 2.26 | 66.62 |
| H-17 | Coy Ridge | 1 | 1 | sand | sand | 3.00 | 92.00 |
| H-18 | BeaverCreek I | 1 | 1 | sand | sandy loam | 3.00 | 92.00 |
| H-19 | BeaverCreek II | 1 | 1 | sand | sand | 3.00 | 92.00 |
| H-20 | Bull Gap | 1 | 1 | sand | sand | 3.00 | 92.00 |
| H-21 | Kneeland | 2 | 2 | sand | sand | 3.04 | 88.95 |
| H-22 | Elk Hill | 1 | 1 | sand | sand | 2.69 | 82.46 |

Table D.1 (cont'd)

| | | | | | | | |
|------|---------------------------|---|---|------------|-------------|-------|-------|
| H-23 | Indian Creek I | 1 | 2 | sand | sand | 4.16 | 84.27 |
| H-24 | Indian Creek II | 1 | 1 | sand | sand | 2.56 | 69.23 |
| H-25 | Turtle Lake | 1 | 1 | sand | sand | 3.02 | 88.42 |
| H-26 | Brush Creek | 2 | 2 | sand | sand | 2.89 | 86.54 |
| H-27 | Sturgeon-Pigeon River | 2 | 2 | sand | sand | 2.87 | 83.73 |
| H-28 | Black River | 1 | 1 | sand | sand | 2.66 | 80.09 |
| H-29 | McPhee Creek | 1 | 1 | sand | sand | 3.64 | 88.36 |
| M-1 | Fair Plain | 2 | 2 | sandy loam | sand | 9.71 | 64.34 |
| M-2 | Zeeland | 2 | 2 | loamy sand | loamy sand | 11.14 | 57.56 |
| M-3 | Allendale | 2 | 2 | loamy sand | sand | 6.49 | 75.02 |
| M-4 | Maple River | 1 | 1 | loamy sand | coarse sand | 6.11 | 46.24 |
| M-5 | Sanborn Creek | 1 | 1 | sand | sand | 3.00 | 92.00 |
| M-6 | Lake City, Harrison Ridge | 1 | 1 | sand | sand | 3.00 | 92.00 |
| M-7 | Slagle Fan | 2 | 2 | sand | sand | 3.34 | 88.67 |
| M-8 | Cole Creek | 1 | 1 | sand | sand | 3.76 | 86.52 |
| M-9 | Houghton Lake Ridge | 1 | 1 | sand | sand | 3.00 | 92.00 |
| M-10 | Higgins Lake Ridge | 1 | 1 | sand | sand | 3.00 | 92.00 |
| M-11 | Platte River | 1 | 1 | sand | sand | 5.65 | 76.67 |
| M-12 | Boardman River | 1 | 1 | sand | sand | 2.79 | 76.27 |
| M-13 | Rapid River | 1 | 1 | sand | sand | 2.86 | 87.22 |
| M-14 | Deer Creek | 1 | 1 | sand | sand | 2.77 | 76.45 |

Table D.1 (cont'd)

| | | | | | | | |
|------|-------------|---|---|------|------|------|-------|
| M-15 | Brown Creek | 1 | 1 | sand | sand | 2.86 | 87.23 |
|------|-------------|---|---|------|------|------|-------|

Table D.1 (cont'd)

| | | <i>Delta: Silt content in upper soil (%)</i> | <i>Delta: Clay content in soil subsurface (%)</i> | <i>Delta: Sand content in soil subsurface (%)</i> | <i>Delta: Silt content in soil subsurface (%)</i> | <i>Delta: Most areally extensive Drainage Index value</i> | <i>Delta: Extent of gravelly soils across the delta (%)</i> |
|------|----------------------------|--|---|---|---|---|---|
| ID | Delta name | DPTUPS | DPCSUBS | DPSSUBS | DPTSUBS | DDDC | DGA |
| E-1 | Raisin River | 33.96 | 3.49 | 76.88 | 6.87 | 69 | 2.63 |
| E-2 | Saline River | 33.97 | 32.30 | 28.46 | 37.60 | 70 | 13.05 |
| E-3 | Huron River II | 16.94 | 3.36 | 90.99 | 5.50 | 37 | 23.35 |
| E-4 | Huron River I | 20.33 | 7.11 | 62.54 | 9.37 | 70 | 51.05 |
| E-5 | Huron River III | 11.11 | 2.99 | 88.67 | 4.95 | 69 | 0.00 |
| E-6 | Middle River Rouge | 15.93 | 4.42 | 76.93 | 7.02 | 37 | 17.58 |
| E-7 | Tarabusi Creek | 21.67 | 11.71 | 48.40 | 17.66 | 63 | 5.83 |
| E-8 | Rochester | 51.05 | 24.25 | 32.49 | 31.91 | 68 | 0.76 |
| E-9 | Clinton River | 13.92 | 2.87 | 73.13 | 5.19 | 41 | 47.28 |
| E-10 | North Branch Clinton River | 31.66 | 10.25 | 60.87 | 24.79 | 69 | 25.43 |
| E-11 | Belle River | 7.34 | 5.36 | 66.66 | 4.67 | 17 | 0.00 |
| E-12 | Smiths Creek | 6.65 | 14.58 | 71.95 | 7.93 | 39 | 0.00 |
| E-13 | South Pine River | 18.63 | 11.28 | 43.45 | 5.60 | 39 | 0.00 |
| E-14 | Black River I | 12.08 | 23.05 | 31.77 | 15.19 | 67 | 3.37 |
| E-15 | Black River II | 8.63 | 3.70 | 70.11 | 5.98 | 66 | 5.23 |

Table D.1 (cont'd)

| | | | | | | | |
|------|-------------------------|-------|-------|-------|-------|----|-------|
| E-16 | Black River III | 8.66 | 2.22 | 67.98 | 3.70 | 66 | 9.88 |
| E-17 | Pine River | 8.97 | 2.86 | 87.76 | 4.77 | 66 | 0.00 |
| H-1 | Flint River | 14.93 | 9.74 | 72.30 | 17.55 | 82 | 1.19 |
| H-2 | Cass River | 21.19 | 10.17 | 54.00 | 18.84 | 70 | 23.90 |
| H-3 | Chippewa River I | 13.81 | 11.31 | 69.91 | 15.75 | 66 | 13.74 |
| H-4 | Chippewa River II | 8.50 | 3.95 | 86.80 | 7.18 | 66 | 0.00 |
| H-5 | Gladwin | 9.28 | 3.64 | 86.96 | 6.87 | 82 | 34.06 |
| H-6 | Rifle River I | 5.36 | 3.72 | 90.19 | 5.99 | 14 | 0.00 |
| H-7 | Rifle River II | 5.75 | 2.99 | 88.07 | 4.95 | 14 | 0.15 |
| H-8 | Big Creek | 4.99 | 3.18 | 91.03 | 5.79 | 14 | 0.00 |
| H-9 | Cedar Creek I | 5.01 | 3.12 | 91.16 | 5.71 | 20 | 0.00 |
| H-10 | Cedar Creek II | 4.46 | 2.70 | 80.74 | 4.64 | 20 | 0.00 |
| H-11 | Johnson Creek | 4.86 | 5.91 | 77.26 | 8.55 | 51 | 0.00 |
| H-12 | Au Gres River I | 7.34 | 4.74 | 88.02 | 6.33 | 20 | 0.00 |
| H-13 | Au Gres River II | 6.17 | 4.69 | 88.90 | 5.66 | 66 | 0.00 |
| H-14 | West Branch Rifle River | 4.73 | 3.06 | 87.89 | 5.19 | 20 | 4.92 |
| H-15 | Jackpines | 4.80 | 3.63 | 81.98 | 5.31 | 14 | 0.00 |
| H-16 | Sevenmile Hill | 3.89 | 2.39 | 71.05 | 3.89 | 14 | 0.00 |
| H-17 | Coy Ridge | 5.00 | 3.00 | 92.00 | 5.00 | 28 | 0.00 |
| H-18 | BeaverCreek I | 5.00 | 8.53 | 88.73 | 26.33 | 37 | 0.00 |
| H-19 | BeaverCreek II | 5.00 | 6.35 | 75.75 | 17.91 | 28 | 0.00 |
| H-20 | Bull Gap | 5.00 | 3.00 | 92.00 | 5.00 | 14 | 0.00 |
| H-21 | Kneeland | 5.15 | 3.44 | 88.66 | 5.43 | 14 | 0.00 |

Table D.1 (cont'd)

| | | | | | | | |
|------|---------------------------|-------|------|-------|-------|----|-------|
| H-22 | Elk Hill | 4.48 | 2.69 | 82.46 | 4.48 | 28 | 0.00 |
| H-23 | Indian Creek I | 8.42 | 4.94 | 79.78 | 12.15 | 29 | 0.32 |
| H-24 | Indian Creek II | 4.45 | 2.29 | 70.14 | 3.81 | 28 | 0.00 |
| H-25 | Turtle Lake | 5.15 | 6.55 | 84.23 | 9.22 | 14 | 0.00 |
| H-26 | Brush Creek | 4.85 | 4.47 | 89.35 | 6.04 | 14 | 0.00 |
| H-27 | Sturgeon-Pigeon River | 4.84 | 3.13 | 88.63 | 5.42 | 14 | 0.36 |
| H-28 | Black River | 4.46 | 2.96 | 87.44 | 5.31 | 14 | 0.00 |
| H-29 | McPhee Creek | 6.52 | 2.99 | 90.51 | 5.01 | 20 | 1.18 |
| M-1 | Fair Plain | 24.95 | 7.03 | 80.52 | 10.98 | 43 | 38.91 |
| M-2 | Zeeland | 20.80 | 6.95 | 65.60 | 13.03 | 32 | 32.04 |
| M-3 | Allendale | 14.00 | 8.74 | 75.29 | 12.84 | 17 | 18.81 |
| M-4 | Maple River | 15.66 | 4.09 | 58.96 | 7.43 | 41 | 46.97 |
| M-5 | Sanborn Creek | 5.00 | 3.00 | 92.00 | 5.00 | 28 | 0.00 |
| M-6 | Lake City, Harrison Ridge | 5.00 | 3.00 | 92.00 | 5.00 | 28 | 0.00 |
| M-7 | Slagle Fan | 5.87 | 3.35 | 88.63 | 5.39 | 14 | 0.00 |
| M-8 | Cole Creek | 6.82 | 3.76 | 86.52 | 6.82 | 29 | 0.00 |
| M-9 | Houghton Lake Ridge | 5.00 | 3.00 | 92.00 | 5.00 | 28 | 0.00 |
| M-10 | Higgins Lake Ridge | 5.00 | 3.00 | 92.00 | 5.00 | 28 | 0.00 |
| M-11 | Platte River | 14.48 | 2.91 | 89.01 | 4.88 | 37 | 38.07 |
| M-12 | Boardman River | 4.96 | 2.64 | 77.02 | 4.57 | 29 | 2.37 |
| M-13 | Rapid River | 4.77 | 2.96 | 90.61 | 4.93 | 20 | 0.00 |
| M-14 | Deer Creek | 5.52 | 2.75 | 78.13 | 4.72 | 36 | 0.12 |
| M-15 | Brown Creek | 4.77 | 2.86 | 87.23 | 4.77 | 29 | 0.00 |

Table D.2: Raw Data - Catchment Characteristics

| | | <i>Delta: Glacial lake contributions</i> | <i>Catchment: Area (km²)</i> | <i>Catchment: Mean slope (%)</i> | <i>Catchment: Median slope (%)</i> | <i>Catchment: Melton basin ruggedness number</i> |
|-----------|-------------------------------------|--|---|--|--|--|
| ID | Delta name | GLC | CA | CMNS | CMDS | CMRN |
| E-1 | Raisin River | 0 | 1203.82 | 4.49 | 2.97 | 0.00 |
| E-2 | Saline River | 0 | 285.80 | 3.90 | 2.82 | 0.01 |
| E-3 | Huron River II | 0 | 2072.89 | 4.69 | 2.97 | 0.00 |
| E-4 | Huron River I | 0 | 2080.80 | 4.68 | 2.97 | 0.00 |
| E-5 | Huron River III | 0 | 2178.29 | 4.55 | 2.82 | 0.00 |
| E-6 | Middle River Rouge | 0 | 140.14 | 4.06 | 2.81 | 0.01 |
| E-7 | Tarabusi Creek | 0 | 17.25 | 4.67 | 3.21 | 0.02 |
| E-8 | Rochester | 0 | 107.73 | 4.44 | 2.94 | 0.01 |
| E-9 | Clinton River | 0 | 777.40 | 4.71 | 3.11 | 0.01 |
| E-10 | North Branch Clinton River | 0 | 197.69 | 3.50 | 1.91 | 0.01 |
| E-11 | Belle River | 0 | 418.47 | 2.05 | 1.10 | 0.01 |
| E-12 | Smiths Creek | 0 | 21.65 | 1.23 | 0.73 | 0.01 |
| E-13 | South Pine River | 0 | 86.31 | 1.48 | 0.87 | 0.01 |
| E-14 | Black River I | 0 | 1823.51 | 1.69 | 0.83 | 0.00 |
| E-15 | Black River II | 0 | 1827.56 | 1.70 | 0.83 | 0.00 |
| E-16 | Black River III | 0 | 1831.78 | 1.71 | 0.83 | 0.00 |
| E-17 | Pine River | 0 | 82.24 | 1.47 | 0.96 | 0.01 |
| H-1 | Flint River | 0 | 3131.75 | 2.82 | 1.40 | 0.00 |
| H-2 | Cass River | 1 | 768.46 | 1.53 | 0.85 | 0.00 |

Table D.2 (cont'd)

| | | | | | | |
|------|-------------------------|---|---------|-------|-------|------|
| H-3 | Chippewa River I | 0 | 999.63 | 3.53 | 2.08 | 0.01 |
| H-4 | Chippewa River II | 0 | 1108.69 | 3.36 | 1.89 | 0.01 |
| H-5 | Gladwin | 0 | 317.32 | 4.62 | 3.08 | 0.01 |
| H-6 | Rifle River I | 0 | 854.05 | 4.23 | 2.19 | 0.01 |
| H-7 | Rifle River II | 0 | 896.78 | 4.22 | 2.21 | 0.01 |
| H-8 | Big Creek | 0 | 107.04 | 2.10 | 1.20 | 0.01 |
| H-9 | Cedar Creek I | 0 | 93.04 | 1.98 | 1.12 | 0.01 |
| H-10 | Cedar Creek II | 0 | 11.86 | 2.40 | 1.34 | 0.01 |
| H-11 | Johnson Creek | 0 | 103.01 | 2.39 | 1.25 | 0.01 |
| H-12 | Au Gres River I | 0 | 240.76 | 3.39 | 1.66 | 0.01 |
| H-13 | Au Gres River II | 0 | 242.31 | 3.40 | 1.66 | 0.01 |
| H-14 | West Branch Rifle River | 0 | 121.86 | 6.76 | 5.14 | 0.02 |
| H-15 | Jackpines | 0 | 4339.89 | 4.06 | 1.91 | 0.00 |
| H-16 | Sevenmile Hill | 0 | 4459.98 | 4.03 | 1.86 | 0.00 |
| H-17 | Coy Ridge | 0 | 1.36 | 6.34 | 5.35 | 0.04 |
| H-18 | BeaverCreek I | 0 | 1.17 | 8.19 | 6.04 | 0.05 |
| H-19 | BeaverCreek II | 0 | 4.05 | 4.81 | 2.40 | 0.03 |
| H-20 | Bull Gap | 0 | 8.90 | 11.95 | 10.00 | 0.03 |
| H-21 | Kneeland | 0 | 148.62 | 5.30 | 3.28 | 0.01 |
| H-22 | Elk Hill | 0 | 0.04 | 1.42 | 0.79 | 0.02 |
| H-23 | Indian Creek I | 0 | 50.29 | 6.67 | 4.90 | 0.02 |
| H-24 | Indian Creek II | 0 | 19.62 | 8.24 | 6.47 | 0.03 |

Table D.2 (cont'd)

| | | | | | | |
|------|---------------------------|---|----------|-------|-------|------|
| H-25 | Turtle Lake | 0 | 243.93 | 6.25 | 4.40 | 0.01 |
| H-26 | Brush Creek | 0 | 52.23 | 2.94 | 1.52 | 0.01 |
| H-27 | Sturgeon-Pigeon River | 0 | 982.27 | 6.63 | 4.19 | 0.01 |
| H-28 | Black River | 0 | 891.90 | 4.87 | 2.61 | 0.01 |
| H-29 | McPhee Creek | 0 | 28.64 | 7.91 | 6.12 | 0.03 |
| M-1 | Fair Plain | 0 | 1301.32 | 3.27 | 1.65 | 0.00 |
| M-2 | Zeeland | 1 | 13598.94 | 3.36 | 1.97 | 0.00 |
| M-3 | Allendale | 1 | 13506.98 | 3.36 | 1.98 | 0.00 |
| M-4 | Maple River | 0 | 390.88 | 2.54 | 1.55 | 0.00 |
| M-5 | Sanborn Creek | 0 | 54.10 | 7.52 | 6.07 | 0.02 |
| M-6 | Lake City, Harrison Ridge | 0 | 5.62 | 5.54 | 4.29 | 0.04 |
| M-7 | Slagle Fan | 0 | 181.21 | 9.33 | 7.43 | 0.02 |
| M-8 | Cole Creek | 0 | 30.91 | 10.36 | 8.65 | 0.04 |
| M-9 | Houghton Lake Ridge | 0 | 1.02 | 5.28 | 4.61 | 0.05 |
| M-10 | Higgins Lake Ridge | 0 | 0.11 | 5.26 | 5.36 | 0.07 |
| M-11 | Platte River | 0 | 320.04 | 5.21 | 2.61 | 0.01 |
| M-12 | Boardman River | 0 | 699.18 | 4.72 | 2.40 | 0.01 |
| M-13 | Rapid River | 0 | 352.80 | 4.42 | 1.80 | 0.01 |
| M-14 | Deer Creek | 0 | 109.02 | 9.34 | 7.02 | 0.02 |
| M-15 | Brown Creek | 0 | 3.27 | 16.36 | 14.33 | 0.08 |

Table D.2 (cont'd)

| | | <i>Catchment: Most areally extensive upper soil textural class</i> | <i>Catchment: Most areally extensive subsurface soil textural class</i> | <i>Catchment: Clay content in upper soil (%)</i> | <i>Catchment: Sand content in upper soil (%)</i> |
|-----------|----------------------------|--|---|--|--|
| ID | Delta name | CDUPST | CDSUBST | CPCUPS | CPSUPS |
| E-1 | Raisin River | loamy sand | clay loam | 15.81 | 28.25 |
| E-2 | Saline River | silty clay loam | clay loam | 20.82 | 27.13 |
| E-3 | Huron River II | loamy sand | loam | 10.45 | 36.35 |
| E-4 | Huron River I | loamy sand | loam | 10.44 | 36.35 |
| E-5 | Huron River III | loamy sand | loam | 10.32 | 37.39 |
| E-6 | Middle River Rouge | loam | clay loam | 14.00 | 36.16 |
| E-7 | Tarabusi Creek | loam | sand | 9.37 | 28.30 |
| E-8 | Rochester | loam | clay loam | 10.56 | 40.96 |
| E-9 | Clinton River | loam | clay loam | 9.10 | 42.81 |
| E-10 | North Branch Clinton River | loam | loam | 12.82 | 40.84 |
| E-11 | Belle River | loam | loam | 14.64 | 34.79 |
| E-12 | Smiths Creek | loam | loam | 14.96 | 48.70 |
| E-13 | South Pine River | loam | loam | 14.16 | 35.66 |
| E-14 | Black River I | loam | loam | 12.90 | 41.30 |
| E-15 | Black River II | loam | loam | 12.89 | 41.27 |
| E-16 | Black River III | loam | loam | 12.88 | 41.26 |
| E-17 | Pine River | loamy sand | clay loam | 13.78 | 36.01 |
| H-1 | Flint River | loam | loam | 12.62 | 41.00 |
| H-2 | Cass River | loam | loam | 11.76 | 46.73 |
| H-3 | Chippewa River I | loamy sand | sand | 8.53 | 58.41 |
| H-4 | Chippewa River II | loamy sand | sand | 8.69 | 58.69 |

Table D.2 (cont'd)

| | | | | | |
|------|-------------------------|------------|------------|-------|-------|
| H-5 | Gladwin | sand | sand | 6.07 | 69.14 |
| H-6 | Rifle River I | sand | sand | 5.87 | 68.10 |
| H-7 | Rifle River II | sand | sand | 5.87 | 68.29 |
| H-8 | Big Creek | sandy loam | clay | 10.51 | 46.96 |
| H-9 | Cedar Creek I | sand | sand | 5.41 | 64.43 |
| H-10 | Cedar Creek II | sand | sand | 5.27 | 67.68 |
| H-11 | Johnson Creek | sandy loam | clay | 10.75 | 44.59 |
| H-12 | Au Gres River I | sandy loam | clay loam | 8.46 | 51.57 |
| H-13 | Au Gres River II | sandy loam | clay loam | 8.43 | 51.74 |
| H-14 | West Branch Rifle River | sand | sand | 5.65 | 72.18 |
| H-15 | Jackpines | sand | sand | 3.18 | 77.92 |
| H-16 | Sevenmile Hill | sand | sand | 3.16 | 77.79 |
| H-17 | Coy Ridge | sand | sand | 3.00 | 92.00 |
| H-18 | BeaverCreek I | sand | sand | 2.93 | 89.74 |
| H-19 | BeaverCreek II | sand | sand | 2.98 | 91.16 |
| H-20 | Bull Gap | sand | sand | 3.00 | 92.00 |
| H-21 | Kneeland | sand | sand | 4.62 | 78.60 |
| H-22 | Elk Hill | sand | sand | 3.00 | 92.00 |
| H-23 | Indian Creek I | sand | sandy loam | 4.11 | 77.51 |
| H-24 | Indian Creek II | sand | sandy loam | 3.92 | 85.79 |
| H-25 | Turtle Lake | sand | sand | 3.49 | 77.23 |
| H-26 | Brush Creek | sand | sand | 3.03 | 77.29 |

Table D.2 (cont'd)

| | | | | | |
|------|---------------------------|------------|------------|-------|-------|
| H-27 | Sturgeon-Pigeon River | loamy sand | sand | 4.58 | 72.13 |
| H-28 | Black River | sand | sand | 4.14 | 67.79 |
| H-29 | McPhee Creek | loamy sand | sand | 5.91 | 78.47 |
| M-1 | Fair Plain | loam | sand | 10.09 | 50.66 |
| M-2 | Zeeland | loam | loam | 10.73 | 49.27 |
| M-3 | Allendale | loam | loam | 10.71 | 49.32 |
| M-4 | Maple River | loam | loam | 12.15 | 41.23 |
| M-5 | Sanborn Creek | sand | sand | 4.17 | 87.70 |
| M-6 | Lake City, Harrison Ridge | sand | sand | 3.86 | 88.98 |
| M-7 | Slagle Fan | sand | sand | 3.67 | 89.10 |
| M-8 | Cole Creek | sand | sand | 4.48 | 84.23 |
| M-9 | Houghton Lake Ridge | sand | sand | 3.00 | 92.00 |
| M-10 | Higgins Lake Ridge | sand | sand | 3.00 | 92.00 |
| M-11 | Platte River | sand | sand | 3.49 | 79.63 |
| M-12 | Boardman River | sand | sand | 3.46 | 78.36 |
| M-13 | Rapid River | sand | sand | 3.00 | 88.98 |
| M-14 | Deer Creek | sand | sand | 4.39 | 69.19 |
| M-15 | Brown Creek | loamy sand | loamy sand | 5.33 | 74.23 |

Table D.2 (cont'd)

| | | <i>Catchment: Silt content in upper soil (%)</i> | <i>Catchment: Clay content in soil subsurface (%)</i> | <i>Catchment: Sand content in soil subsurface (%)</i> | <i>Catchment: Silt content in soil subsurface (%)</i> |
|-----------|-------------------|--|---|---|---|
| ID | Delta name | CPTUPS | CPCSUBS | CPSSUBS | CPTSUBS |
| E-1 | Raisin River | 42.57 | 15.64 | 43.02 | 20.85 |
| E-2 | Saline River | 46.70 | 23.12 | 39.85 | 28.83 |

Table D.2 (cont'd)

| | | | | | |
|------|----------------------------|-------|-------|-------|-------|
| E-3 | Huron River II | 35.42 | 9.35 | 53.58 | 16.18 |
| E-4 | Huron River I | 35.41 | 9.32 | 53.51 | 16.14 |
| E-5 | Huron River III | 34.75 | 9.16 | 54.37 | 15.81 |
| E-6 | Middle River Rouge | 35.32 | 16.27 | 44.88 | 22.39 |
| E-7 | Tarabusi Creek | 24.61 | 13.37 | 24.68 | 19.54 |
| E-8 | Rochester | 28.77 | 14.23 | 42.56 | 20.06 |
| E-9 | Clinton River | 23.70 | 8.68 | 47.98 | 12.34 |
| E-10 | North Branch Clinton River | 39.25 | 13.29 | 46.52 | 29.15 |
| E-11 | Belle River | 42.28 | 18.60 | 41.79 | 31.41 |
| E-12 | Smiths Creek | 33.83 | 16.30 | 44.42 | 30.76 |
| E-13 | South Pine River | 47.59 | 22.54 | 38.59 | 33.20 |
| E-14 | Black River I | 35.06 | 17.11 | 42.11 | 30.65 |
| E-15 | Black River II | 35.04 | 17.09 | 42.08 | 30.62 |
| E-16 | Black River III | 34.98 | 17.07 | 42.03 | 30.59 |
| E-17 | Pine River | 46.93 | 22.16 | 40.43 | 31.11 |
| H-1 | Flint River | 35.07 | 14.09 | 44.29 | 28.44 |
| H-2 | Cass River | 29.08 | 15.35 | 45.31 | 29.82 |
| H-3 | Chippewa River I | 17.95 | 12.91 | 60.85 | 15.51 |
| H-4 | Chippewa River II | 18.16 | 13.15 | 60.48 | 16.09 |
| H-5 | Gladwin | 13.58 | 12.88 | 61.40 | 17.91 |
| H-6 | Rifle River I | 13.71 | 14.64 | 58.40 | 18.30 |
| H-7 | Rifle River II | 13.72 | 14.58 | 58.46 | 18.44 |
| H-8 | Big Creek | 33.95 | 39.63 | 33.42 | 21.41 |
| H-9 | Cedar Creek I | 13.25 | 15.89 | 53.62 | 23.26 |

Table D.2 (cont'd)

| | | | | | |
|------|-------------------------|-------|-------|-------|-------|
| H-10 | Cedar Creek II | 12.80 | 14.92 | 54.47 | 23.37 |
| H-11 | Johnson Creek | 35.10 | 40.93 | 31.36 | 20.37 |
| H-12 | Au Gres River I | 21.27 | 25.15 | 35.95 | 24.04 |
| H-13 | Au Gres River II | 21.17 | 25.01 | 36.28 | 23.93 |
| H-14 | West Branch Rifle River | 12.75 | 13.25 | 64.39 | 16.73 |
| H-15 | Jackpines | 6.16 | 5.11 | 81.37 | 7.63 |
| H-16 | Sevenmile Hill | 6.11 | 5.04 | 81.22 | 7.54 |
| H-17 | Coy Ridge | 5.00 | 3.00 | 92.00 | 5.00 |
| H-18 | BeaverCreek I | 4.88 | 2.93 | 89.74 | 4.88 |
| H-19 | BeaverCreek II | 4.97 | 4.96 | 81.53 | 12.62 |
| H-20 | Bull Gap | 5.00 | 3.00 | 92.00 | 5.00 |
| H-21 | Kneeland | 12.59 | 12.60 | 70.65 | 15.13 |
| H-22 | Elk Hill | 5.00 | 3.00 | 92.00 | 5.00 |
| H-23 | Indian Creek I | 8.61 | 12.02 | 61.66 | 22.99 |
| H-24 | Indian Creek II | 7.34 | 7.51 | 67.54 | 22.37 |
| H-25 | Turtle Lake | 6.83 | 5.74 | 78.45 | 10.37 |
| H-26 | Brush Creek | 5.43 | 7.40 | 80.79 | 9.68 |
| H-27 | Sturgeon-Pigeon River | 9.83 | 5.35 | 79.03 | 11.22 |
| H-28 | Black River | 9.10 | 6.93 | 73.52 | 15.71 |
| H-29 | McPhee Creek | 12.28 | 3.58 | 89.28 | 6.07 |
| M-1 | Fair Plain | 25.86 | 3.68 | 62.18 | 6.76 |

Table D.2 (cont'd)

| | | | | | |
|------|---------------------------|-------|-------|-------|-------|
| M-2 | Zeeland | 28.11 | 13.82 | 49.67 | 23.44 |
| M-3 | Allendale | 28.04 | 13.76 | 49.72 | 23.40 |
| M-4 | Maple River | 35.87 | 13.81 | 49.47 | 27.72 |
| M-5 | Sanborn Creek | 7.86 | 4.87 | 86.88 | 7.97 |
| M-6 | Lake City, Harrison Ridge | 7.10 | 7.04 | 88.81 | 7.10 |
| M-7 | Slagle Fan | 6.70 | 6.67 | 85.53 | 7.24 |
| M-8 | Cole Creek | 9.55 | 5.13 | 83.51 | 9.62 |
| M-9 | Houghton Lake Ridge | 5.00 | 3.00 | 92.00 | 5.00 |
| M-10 | Higgins Lake Ridge | 5.00 | 3.00 | 92.00 | 5.00 |
| M-11 | Platte River | 7.17 | 4.11 | 77.88 | 8.37 |
| M-12 | Boardman River | 6.80 | 4.85 | 80.54 | 8.53 |
| M-13 | Rapid River | 5.08 | 3.03 | 91.01 | 5.07 |
| M-14 | Deer Creek | 9.49 | 4.91 | 77.58 | 10.17 |
| M-15 | Brown Creek | 11.17 | 6.32 | 77.30 | 13.30 |

APPENDIX E: PCA Scores and K-means Group Number

Table E.1: Raw data - PCA Scores and K-means Group Number

| Delta ID | PC1 | PC2 | PC3 | PC4 | K-means Group Number |
|-------------|-------|-------|-------|-------|----------------------|
| E-1 | 0.38 | 1.21 | -0.56 | -0.14 | 4 |
| E-2 | 0.72 | 3.85 | 0.75 | -1.05 | 4 |
| E-3 | 0.79 | 0.04 | -0.04 | 0.04 | 3 |
| E-4 | 0.06 | 1.21 | -0.46 | -0.36 | 4 |
| E-5 | 1.61 | -0.43 | 0.33 | -0.07 | 3 |
| E-6 | 0.69 | 0.47 | -0.21 | -0.08 | 3 |
| E-7 | -0.28 | 1.77 | -0.16 | -0.90 | 4 |
| E-8 | -0.43 | 3.45 | 0.26 | 0.18 | 4 |
| E-9 | -0.18 | 0.65 | -0.60 | -0.47 | 1 |
| E-10 | 0.07 | 2.06 | -0.42 | -0.65 | 4 |
| E-11 | 2.24 | -0.65 | 0.01 | -0.30 | 3 |
| E-12 | 1.79 | -0.32 | -0.10 | -0.40 | 3 |
| E-13 | 1.80 | 0.74 | -0.09 | -0.49 | 3 |
| E-14 | 0.87 | 1.36 | -0.24 | -0.86 | 4 |
| E-15 | 1.70 | -0.24 | -0.50 | -0.38 | 3 |
| E-16 | 1.79 | -0.30 | -0.54 | -0.41 | 3 |
| E-17 | 2.14 | -0.66 | -0.34 | -0.27 | 3 |
| H-1 | 0.04 | 0.76 | -1.03 | 0.46 | 1 |
| H-2 | 0.21 | 1.06 | -0.77 | 3.08 | 5 |
| H-3 | -0.49 | 0.62 | -0.59 | -0.43 | 1 |
| H-4 | -0.59 | -0.06 | -1.18 | -0.14 | 1 |
| H-5 | -0.77 | 0.12 | -0.88 | -0.13 | 1 |
| H-6 | -0.07 | -0.90 | -0.63 | -0.35 | 1 |
| H-7 | -0.16 | -0.80 | -0.72 | -0.28 | 1 |
| H-8 | 1.38 | -1.31 | -0.66 | -0.12 | 3 |
| H-9 | 0.23 | -1.10 | -0.75 | -0.41 | 3 |
| H-10 | 0.36 | -0.94 | 0.00 | -0.47 | 3 |
| H-11 | 1.38 | -0.86 | -0.56 | -0.44 | 3 |
| H-12 | 0.86 | -0.93 | -0.42 | -0.31 | 3 |
| H-13 | 0.83 | -0.81 | -0.55 | -0.40 | 3 |
| H-14 | -0.77 | -0.35 | -0.41 | -0.12 | 1 |
| H-15 | -1.52 | -0.60 | -1.76 | 0.12 | 1 |
| H-16 | -0.97 | -0.62 | -1.09 | -0.15 | 1 |
| H-17 | -0.50 | -0.61 | 1.20 | -0.20 | 2 |
| H-18 | -0.90 | 0.38 | 1.47 | -0.57 | 2 |
| H-19 | -0.78 | -0.13 | 0.52 | -0.41 | 2 |

Table E.1 (cont'd)

| Delta | | | | | |
|--------------|------------|------------|------------|------------|-----------------------------|
| ID | PC1 | PC2 | PC3 | PC4 | K-means Group Number |
| H-20 | -0.53 | -0.35 | 2.67 | -0.11 | 2 |
| H-21 | -1.17 | -0.48 | -1.02 | 0.15 | 1 |
| H-22 | -0.64 | -0.75 | -0.16 | -0.58 | 1 |
| H-23 | -0.59 | -0.13 | -0.23 | -0.23 | 1 |
| H-24 | 0.11 | -0.45 | 1.35 | -0.17 | 2 |
| H-25 | -0.48 | -0.54 | 0.27 | -0.03 | 1 |
| H-26 | -1.22 | -0.60 | -1.24 | 0.13 | 1 |
| H-27 | -1.47 | -0.34 | -0.97 | 0.58 | 1 |
| H-28 | -0.47 | -0.84 | -0.47 | -0.34 | 1 |
| H-29 | -0.43 | -0.44 | 1.29 | -0.19 | 2 |
| M-1 | -1.26 | 1.28 | -1.02 | 0.71 | 1 |
| M-2 | 0.93 | 0.34 | 0.65 | 4.55 | 5 |
| M-3 | 0.77 | -0.45 | 0.03 | 4.51 | 5 |
| M-4 | 0.74 | 0.58 | -0.51 | -0.34 | 3 |
| M-5 | -0.63 | -0.55 | 0.72 | -0.27 | 2 |
| M-6 | -0.45 | -0.70 | 0.59 | -0.49 | 2 |
| M-7 | -2.44 | 0.25 | -0.12 | 0.88 | 1 |
| M-8 | -0.68 | -0.08 | 1.97 | 0.06 | 2 |
| M-9 | -0.46 | -0.67 | 1.00 | -0.19 | 2 |
| M-10 | -0.41 | -0.53 | 1.97 | -0.21 | 2 |
| M-11 | -0.87 | -0.06 | 0.31 | -0.15 | 1 |
| M-12 | -0.73 | -0.52 | -0.06 | -0.20 | 1 |
| M-13 | -0.95 | -0.74 | -0.27 | -0.29 | 1 |
| M-14 | -0.51 | -0.27 | 1.08 | -0.20 | 2 |
| M-15 | 0.29 | -0.10 | 3.88 | 0.33 | 2 |

APPENDIX F: Physical Characteristics of the Groups of Deltas

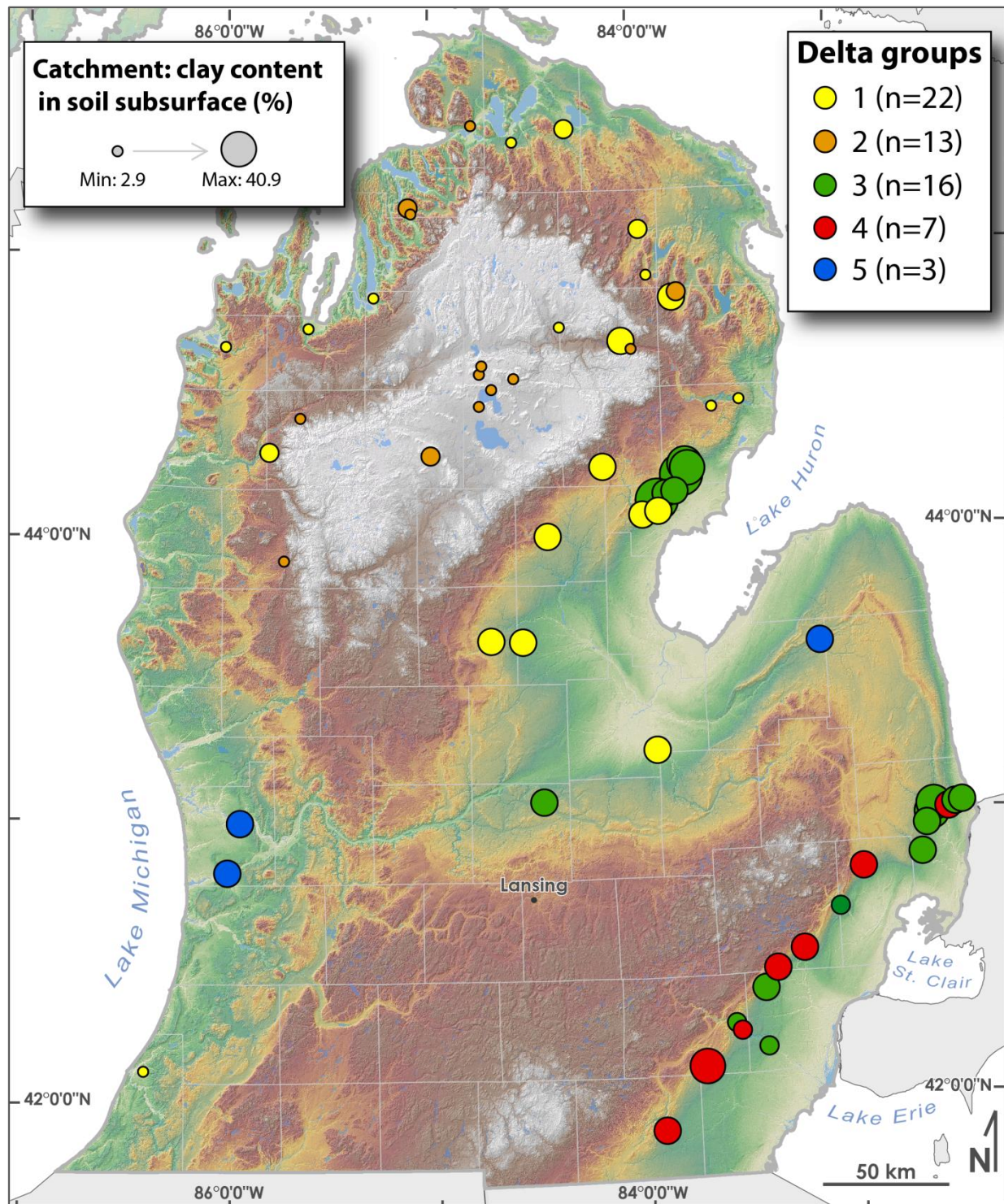


Figure F.1: A graduated circle map illustrating clay content (%) in the subsurface horizon (C horizon) of soils within the delta catchments.

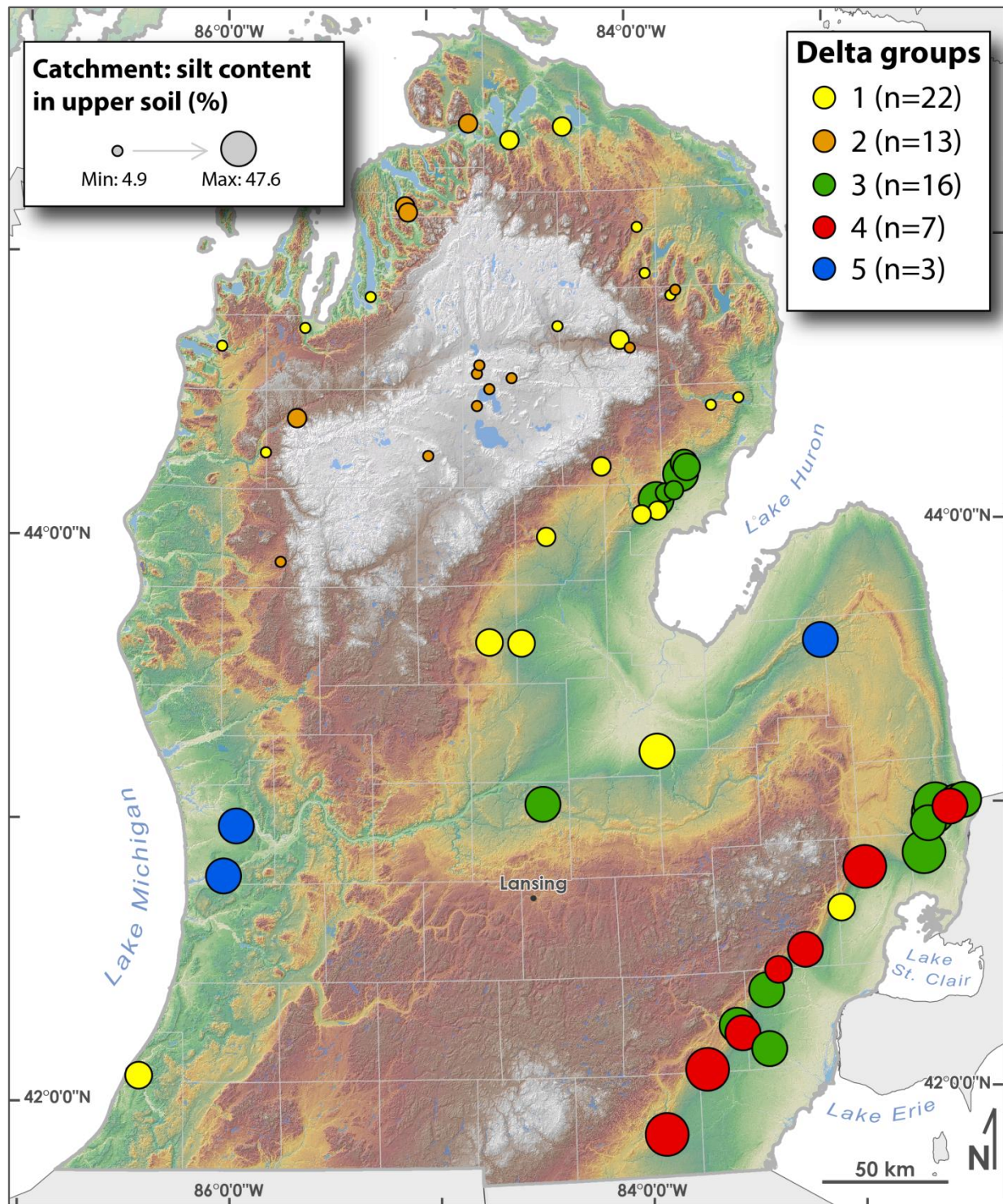


Figure F.2: A graduated circle map illustrating silt content (%) in the surface mineral horizon of soils within the delta catchments.

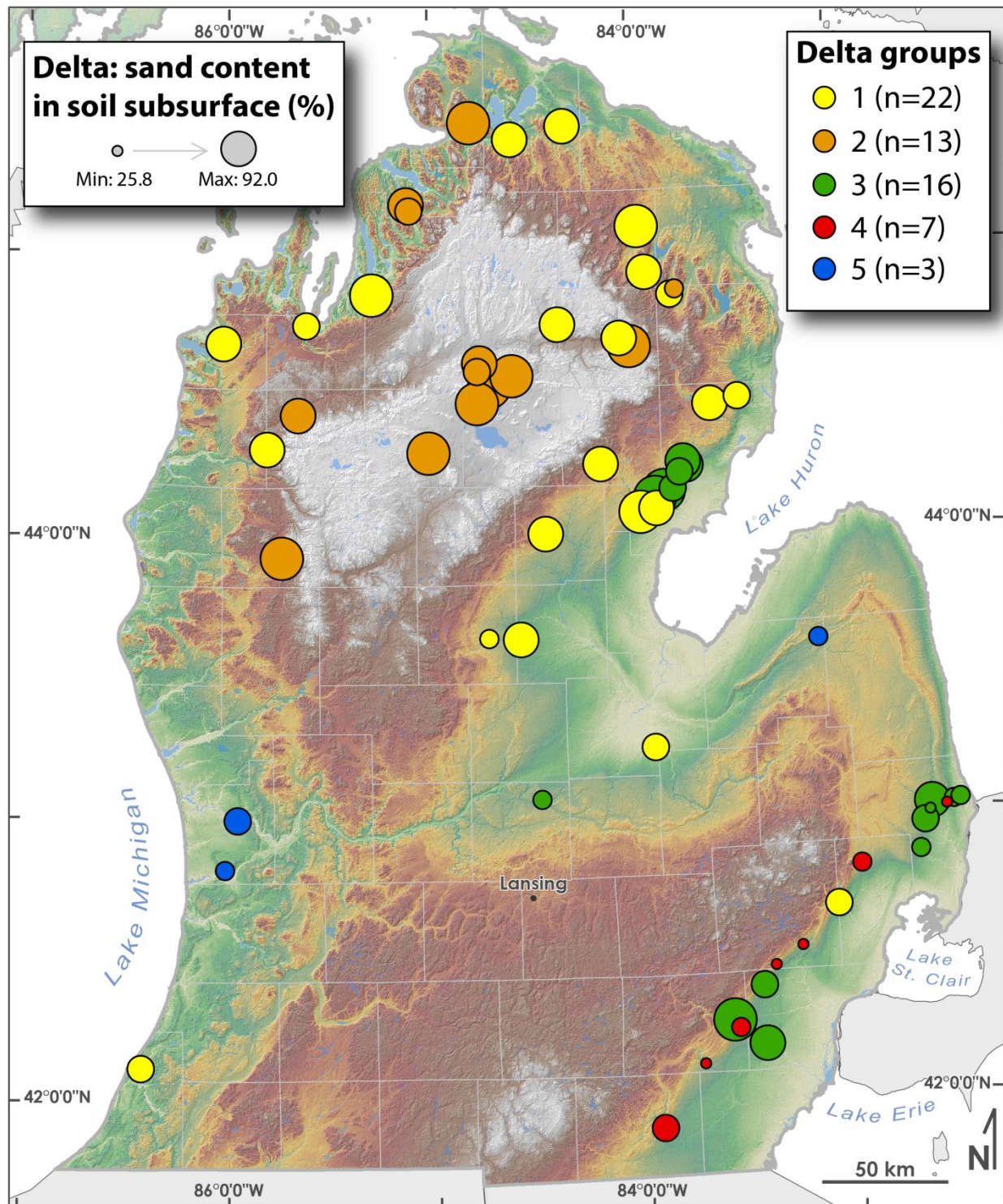


Figure F.3: A graduated circle map illustrating sand content (%) in the subsurface horizon (C horizon) of soils within the delta plains.

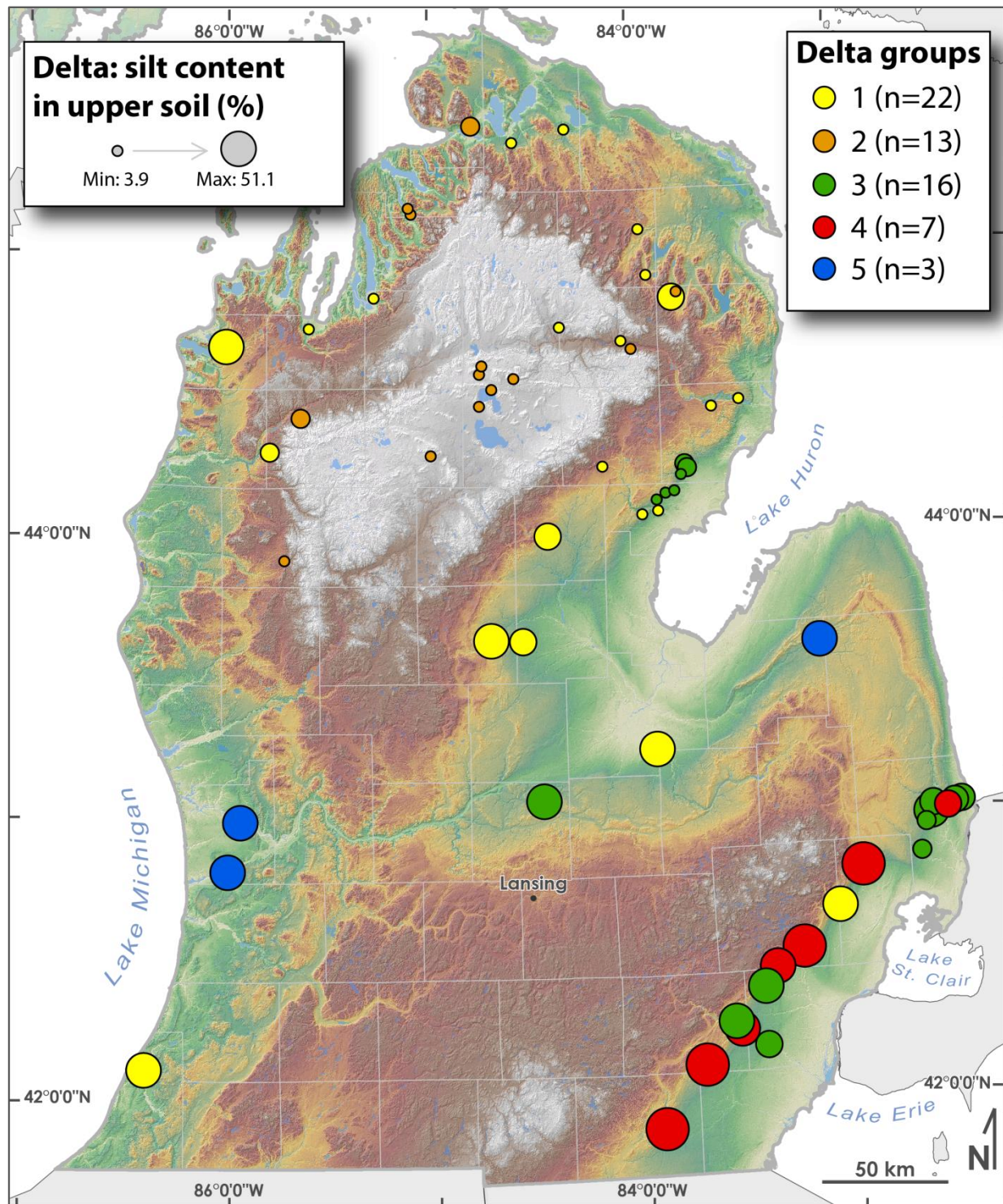


Figure F.4: A graduated circle map illustrating silt content (%) in the surface mineral horizon of soils within the delta plains.

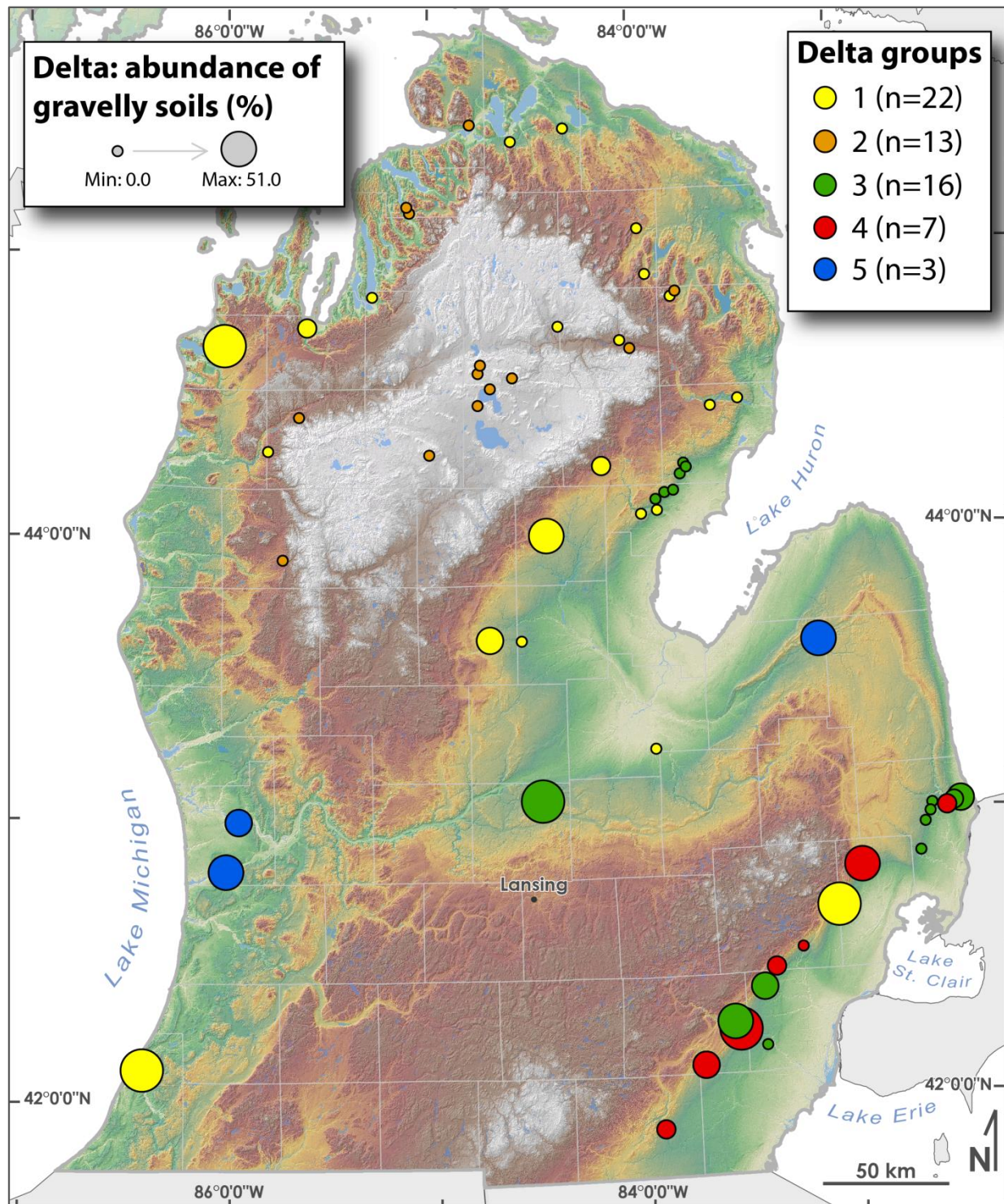


Figure F.5: A graduated circle map illustrating the percentage of gravelly soil parent materials within the delta plains.

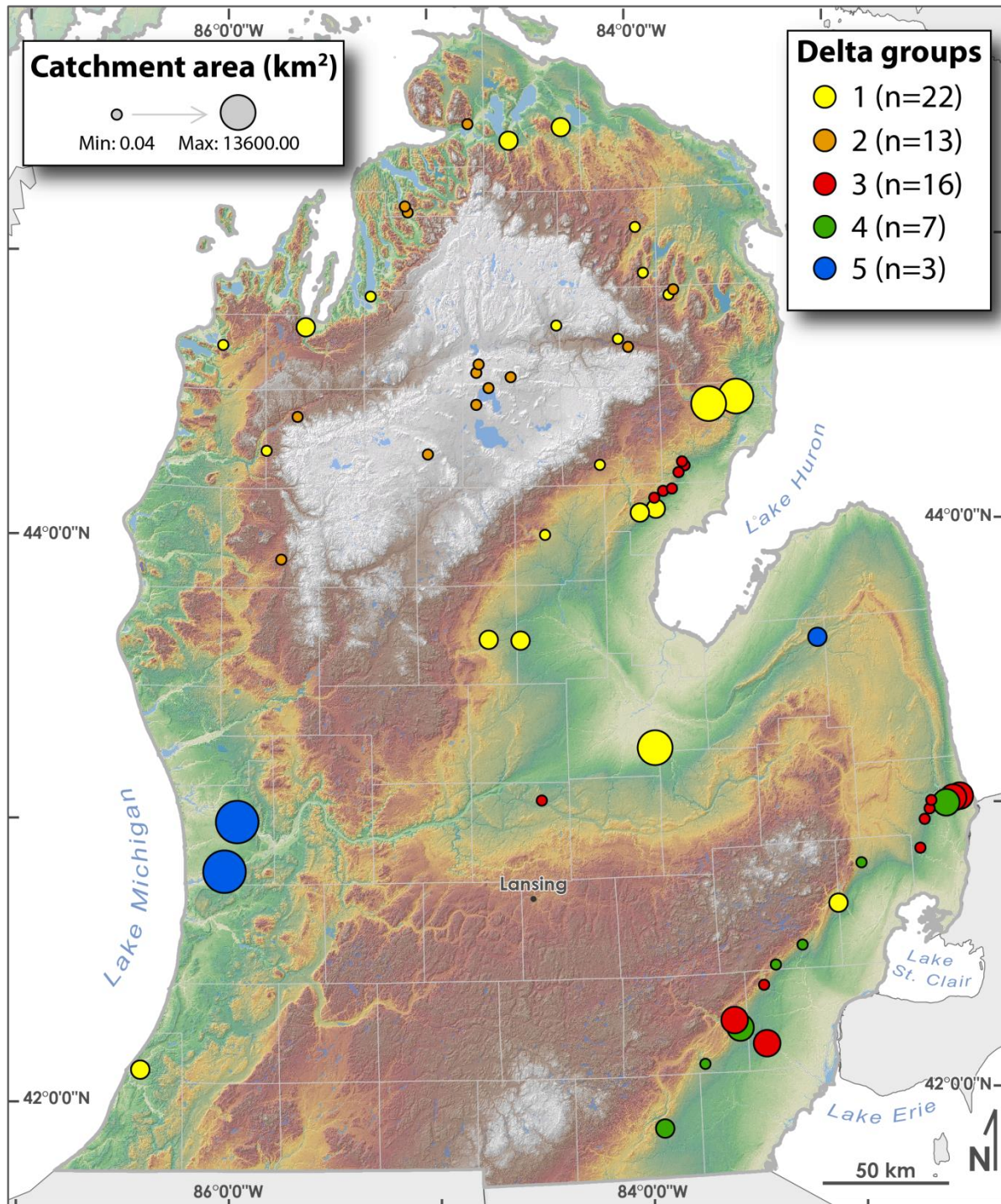


Figure F.6: A graduated circle map illustrating the different delta catchment areal extents.

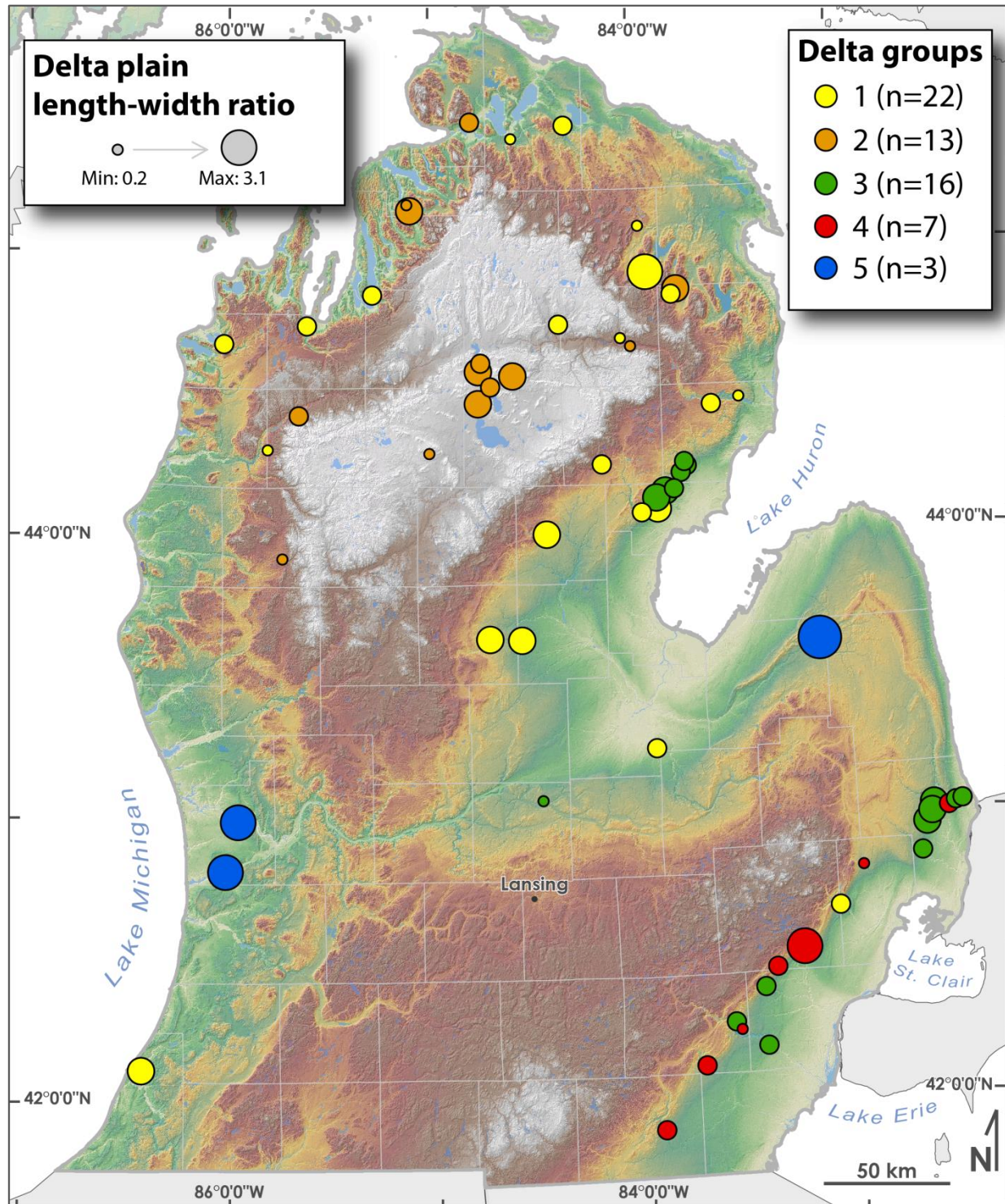


Figure F.7: A graduated circle map illustrating the different delta plain length-width ratios. Larger values indicate more elongate deltas whereas smaller values indicate wider, more fan-shaped deltas.

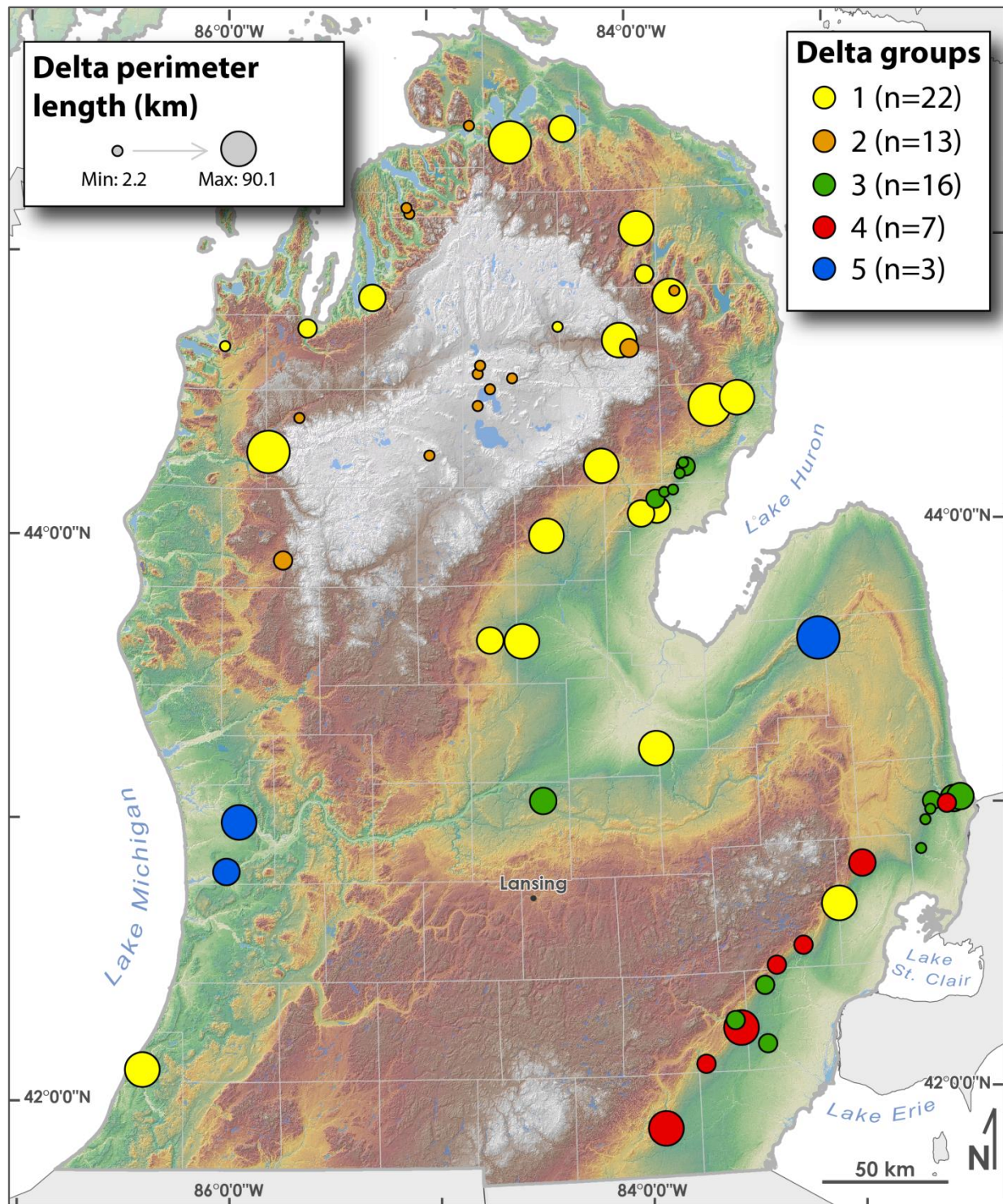


Figure F.8: A graduated circle map illustrating the different delta plain perimeter lengths.

REFERENCES

REFERENCES

- Abdi, H., and Williams, L.J. 2010. Principal component analysis. *WIREs Computational Statistics* 2:433-459.
- Antisari, L.V., Dell'Abate, M.T., Buscaroli, A., Gherardi, M., Nisini, L., and Vianello, G. 2010. Role of soil organic matter characteristics in a pedological survey: "Bosco Frattona" natural reserve (Site of Community Importance, Italy) case study. *Geoderma* 156:302–315.
- Arbogast A.F., Luehmann, M.D., Miller, B.A., Adams, K.M., Wernette, P.A., Waha, J.D., Oneil, G.A., Tang, Y., Boothroyd, J.J., Babcock, C.R., Hanson, P.R., Daly, T.A., and Young, A.R. 2015. Late-Pleistocene Paleowinds and Aeolian Sand Mobilization in North-Central Lower Michigan. *Aeolian Research* 16:109-116.
- Argyilan, E.P., Forman, S.L., Johnston, J.W., and Wilcox, D.A. 2005. Optically stimulated luminescence dating of late Holocene raised strandplain sequences adjacent to Lakes Michigan and Superior, Upper Peninsula, Michigan, USA. *Quaternary Research* 63:122–135.
- Argyilan, E.P., Forman, S.L., and Thompson, T.A. 2010. Variability of Lake Michigan water level during the past 1000 years reconstructed through optical dating of a coastal strandplain. *The Holocene* 20:723-731.
- Arrell, K.E., Fisher, P.F., Tate, N.J., and Bastin, L. 2007. A fuzzy c-means classification of elevation derivatives to extract the morphometric classification of landforms in Snowdonia, Wales. *Computers and Geosciences* 33:1366–1381.
- Asselen, S.V., and Seijmonsbergen, A.C. 2006. Expert-driven semi-automated geomorphological mapping for a mountainous area using a laser DTM. *Geomorphology* 78:309–320.
- Atwood, W.W. 1909. Glaciation of the Uinta and Wasatch Mountains. *U.S. Geological Survey Professional Paper* 61.
- Baedke, S.J., and Thompson, T.A. 2000. A 4,700-Year Record of Lake Level and Isostasy for Lake Michigan. *Journal of Great Lakes Research* 26:416–26.
- Baedke, S.J., Johnston, J.W. Thompson, T.A., and Wilcox, D. 2004. Reconstructing Paleo Lake Levels from Relict Shorelines along the Upper Great Lakes. *Aquatic Ecosystem Health and Management* 7:435-449.

- Baker, V.R. 1996. Megafloods and glaciation. In: *Late Glacial and Postglacial Environmental Changes*, Martini, I.P. (ed.). Oxford University Press, New York, pg. 123-148.
- Barnett, P.J. 1985. Glacial Retreat and Lake Levels, North Central Lake Erie basin, Ontario. In: *Quaternary Evolution of the Great Lakes*, Karrow, P.F, and Calkin, P.E. (eds.). *Geological Association of Canada Special Paper* 30:185-195.
- Barnett, P.J. 1992. Quaternary Geology of Ontario. In: *Geology of Ontario*, Thurston, P.C., Williams, H.R., Sutcliffe, R.H., and Stott, G.M. (eds.). *Ontario Geological Survey Special Volume* 4:1011-1088.
- Barnhardt, W.A., Gehrels, W.R., Belknap, D.F., and Kelley, J.T. 1995. Late Quaternary relative sea-level change in the western Gulf of Maine: Evidence for a migrating glacial forebulge. *Geology* 23:317–320.
- Barnhardt, W.A., Belknap, D.F., and Kelley, J.T. 1997. Stratigraphic Evolution of the Inner Continental Shelf in Response to Late Quaternary Relative Sea-Level Change, Northwestern Gulf of Maine. *Geological Society of America Bulletin* 5:612–630.
- Barrell, J. 1912. Criteria for the recognition of ancient delta deposits. *Geological Society of America Bulletin* 23:377–446.
- Bates, C.C. 1953. Rational Theory of Delta Formation. *Bulletin American Association of Petroleum Geologists* 37:2119-2161.
- Bay, J.W. 1937. Glacial-lake levels indicated by terraces of the Huron, Rouge, and Clinton River, Michigan. *Michigan Academy of Arts, Sciences, and Letters Papers* 22:411-419.
- Bay, J.W. 1938. Glacial history of the streams of southeastern Michigan. *Cranbrook Institution of Science Bulletin* 12, pg. 68 (map scale: 1:200,000).
- Bell, C.M. 2009. Quaternary lacustrine braid deltas on Lake General Carrera in southern Chile. *Andean Geology* 36:51-65.
- Bhattacharya, J.P., and Giosan, L. 2003. Wave-influenced deltas: geomorphological implications for facies reconstruction. *Sedimentology* 50:187–210.
- Bissell, H.J. 1963. Lake Bonneville: Geology of southern Utah Valley, Utah. *U.S. Geological Survey Professional Paper* 257-B:101-130.
- Blair, T.C. 1999. Sedimentology of gravelly Lake Lahontan highstand shoreline deposits, Churchill Butte, Nevada, USA. *Sedimentary Geology* 123:199-218.

- Bleuer, N.K., and Moore, M.C. 1972. Glacial stratigraphy of the Fort Wayne area and the draining of glacial Lake Maumee. *Proceedings of the Indiana Academy Sciences* 81:195-209.
- Blewett, W. 1991. Characteristics, correlations, and refinements of Leverett and Taylor's Port Huron moraine in Michigan. *East Lakes Geographer* 26:52-60.
- Blewett, W.L, Lusch, D.P., and Schaetzl, R.J. 2009. The Physical Landscape: A Glacial Legacy. In: *Michigan geography and geology*, Schaetzl, R.J., Darden, J.T., and Brandt, D. (eds.). Pearson Custom Publishing, Boston, MA. pg. 174-190.
- Blewett, W.L., Drzyzga, S.A., Sherrod, L., and Wang, H. 2014. Geomorphic Relations among Glacial Lake Algonquin and the Munising and Grand Marais Moraines in Eastern Upper Michigan, USA. *Geomorphology* 219:270-84.
- Bowman, D. 1990. Climatically triggered Gilbert-type lacustrine fan deltas, the Dead Sea área, Israel. In: Coarse-grained Deltas, Colella, A., and Prior, D.B. (eds.). *International Association Sedimentologists, Special Publication* 10: 273-280.
- Breda, A., Mellere, D., Andmassari, F. 2007. Facies and processes in a Gilbert-delta filled incised valley (Pliocene of Ventimiglia, NW Italy). *Sedimentary Geology* 200:31-55.
- Breda, A., Mellere, D., Massari, F., and Asioli, A. 2009. Vertically stacked Gilbert type deltas of Ventimiglia (NW Italy): the Pliocene record of an overfilled Messinian incised valley. *Sedimentary Geology* 219:58-76.
- Breckenridge, A. 2013. An analysis of the late glacial lake levels within the western Lake Superior basin based on digital elevation models. *Quaternary Research* 80:383-395.
- Bretz, J.H. 1951. Causes of the Glacial Lake Stages in Saginaw Basin, Michigan. *The Journal of Geology* 59:244-258.
- Bretz, J.H. 1953. Glacial Grand River, Michigan. *Papers of the Michigan Academy of Sciences Arts and Letters* 38:359-382.
- Bretz, J.H. 1955. Geology of the Chicago region, Part II-The Pleistocene. *Illinois State Geological Survey Bulletin* 65.
- Bretz, J.H. 1964. Correlation of glacial lake stages in the Huron-Erie and Michigan basins. *Journal of Geology* 74:62-77.

- Broecker, W.S., Kennett, J., Flower, B., Teller, J., Trumbore, S., Bonani, G., and Wolfli, W. 1989. Routing of meltwater from the Laurentide Ice Sheet during the Younger Dryas cold episode. *Nature* 341:318–321.
- Burgis, W.A. 1977. Late-Wisconsin history of northeastern Lower Michigan. Ph.D. dissertation, University of Michigan, Ann Arbor.
- Burgis, W.A. 1981. Late-Wisconsinan History of Northeastern Lower Michigan. Guidebook, 30th Midwest Friends of the Pleistocene field trip. University of Michigan, Ann Arbor.
- Caldwell, R.L., and Edmonds, D.A. 2014. The effects of sediment properties on deltaic processes and morphologies: A numerical modeling study. *Journal of Geophysical Research: Earth Surface* 119:961–982.
- Calkin, P.E. 1970. Strand lines and chronology of the glacial Great Lakes in northwestern New York. *Ohio Journal of Science* 70:78-96.
- Calkin, P.E., and Feenstra, B.H. 1985. Evolution of the Erie-basin Great Lakes. In: Quaternary Evolution of the Great Lakes, Karrow, P.F, and Calkin, P.E. (eds.). *Geological Association of Canada Special Paper* 30:150–170.
- CERC. 1984. Shore Protection Manual. Coastal Engineering Research Center, Waterway Experiment Station, US Army Corps of Engineers.
- Chamberlin, T.C. 1909. Diastrophism as the ultimate basis of correlation. *Journal of Geology* 17:685-693.
- Chidsey, T.C., Jr. 2002. Geological and Petrophysical Characterization of the Ferron Sandstone for 3-D simulation of a fluvial-deltaic reservoir — final report: U.S. Department of Energy, pg. 2-17.
- Chorley, R.J. , Dunn, A.J., and Beckinsale, R.P. 1964. The history of the study of landforms, volume 1. Geomorphology before Davis. London, Methuen.
- Chrastowski, M.J., and Thompson, T.A. 1992. Late Wisconsinan and Holocene coastal evolution of the southern shore of Lake Michigan. In: *Quaternary Coasts of the United States: Marine and Lacustrine Systems*, Fletcher, C.H., and Wehmiller, J.F. (eds.). *Society for Sedimentary Geology Special Publication* 48, pg. 397-413.
- Chrastowski, M.J., and Thompson, T.A. 1994. Late Wisconsinan and Holocene geologic history of the Illinois-Indiana coast of Lake Michigan. *Journal of Great Lakes Research* 20:9-26.

- Clague, J.J., Luternauer, J.L., Pullan, S.E., and Hunter, J.A. 1991. Postglacial deltaic sediments, southern Fraser River delta, British Columbia. *Canadian Journal of Earth Sciences* 28:1386-1393
- Clark, J.A., Hendriks M., Timmermans T.J., Struck C., Hilverda, K.J. 1994. Glacial isostatic deformation of the Great Lakes region. *Geological Society of America Bulletin* 106:19–31.
- Clark, P., Marshall, S.J., Clarke, G.K.C., Hostetler, S.W., Licciardi, J.M., and Teller, J.T. 2001. Freshwater forcing of abrupt climate change during the last glaciation. *Science* 13:283–287.
- Clayton, L., Attig, J.W. and Mickelson, D.M. 2001. Effects of late Pleistocene permafrost on the landscape of Wisconsin, USA. *Boreas* 30:173 - 188.
- Clayton, L., Attig, J. W., Ham, N.R., Johnson, M.D., Jennings, C.E., and Syverson, K.M. 2008. Ice-walled-lake plains: Implications for the origin of hummocky glacial topography in middle North America. *Geomorphology* 97:237-248.
- Coleman, A.P. 1901. Marine and freshwater beaches of Ontario. *Bulletin of the Geological Society of America* 12:129-46.
- Coleman, J.M., and Wright, L.D. 1975. Modern river deltas: Variability of processes and sand bodies. In: *Deltas: Models for Exploration*, Broussard, M.L. (ed.). Houston Geological Society, Houston, TX, pg. 99-149.
- Coleman, J.M. 1981. Deltas: Processes of Deposition and Models for Exploration. Burgess Publishing Co., Minneapolis, MN.
- Coleman, J.M., Roberts, H.H., and Stone, G.W. 1998. Mississippi River delta: an overview. *Journal of Coastal Research* 14:698–716.
- Collela, A. and Prior, D.B. 1990. Coarse-grained deltas. *International Association of Sedimentologists Special Publication*, 10, pg. 357.
- Colman, S.M., Clark, J.A., Clayton, L., Hansel, A.K., and Larsen, C.E. 1994. Deglaciation, lake levels, and meltwater discharge in the Lake Michigan basin. *Quaternary Science Reviews* 13:879-90.
- Currey, D.R., and Oviatt, C.G. 1985. Durations, average rates, and probable causes of Lake Bonneville expansion, stillstands, and contractions during the last deep-lake cycle, 32,000 to 10,000 years ago. In: *Problems of and prospects for predicting Great Salt Lake levels*, Kay, P.A., and Diaz, H.F. (eds.). *Proceedings of a National Oceanic and*

- Atmospheric Administration (NOAA) Conference*, University of Utah, Salt Lake City, pg. 9–24.
- Curry, B., and Petras, J. 2011. Chronological Framework for the Deglaciation of the Lake Michigan Lobe of the Laurentide Ice Sheet from Ice-Walled Lake Deposits. *Journal of Quaternary Science* 26:402–10.
- Davidson-Arnott, R.G.D., and Conliffe Reid, H.E. 1994. Sedimentary Processes and the Evolution of the Distal Bayside of Long Point, Lake Erie. *Canadian Journal of Earth Sciences* 31:1461–73.
- Deane, R.E. 1950. Pleistocene geology of the Lake Simcoe district, Ontario. Geological Survey of Canada Memoir 256. Ottawa: Canada Department of Mines and Technical Surveys.
- Delamater, P.L., Shortridge, A.M., and Messina, J.P. 2013. Regional Health Care Planning: A Methodology to Cluster Facilities Using Community Utilization Patterns. *BMC health services research* 13:333.
- Delcourt, P.A., Petty, W.H., and Delcourt, H.R. 1996. Late-Holocene formation of Lake Michigan beach ridges correlated with a 70-yr oscillation in global climate. *Quaternary Research* 45:321–326.
- Di Achille, G., and Hynek, B.M. 2010. Deltas and valley networks on Mars: Implications for a global hydrosphere. In: *Lakes on Mars*, Cabrol, N.A., Grin, E.A. (Eds.). Elsevier, pg. 223–248.
- Dietz, R.S., and Menard, H.W. 1951. Origin of abrupt change in slope at continental shelf margin. *American Association of Petroleum Geologists Bulletin* 35:1994-2016.
- Dott, E.R., and Mickelson, D. 1995. Lake Michigan Water Levels and the Development of Holocene Beach-Ridge Complexes at Two Rivers , Wisconsin : Stratigraphic , Geomorphic, and Radiocarbon Evidence. *Geological Society of America Bulletin* 107:286–296.
- Dreimanis, A. 1966. Lake Arkona-Whittlesey and Post-Warren Radiocarbon Dates from “Ridgetown Island” in Southwestern Ontario. *The Ohio Journal of Science* 66: 582-586.
- Dreimanis, A. 1977. Late Wisconsin glacial retreat in the Great Lakes region, North America. *Annals New York Academy of Science* 288:70-89.
- Drzyzga, S.A. 2007. Relict Shoreline Features at Cockburn Island, Ontario. *Journal of Paleolimnology* 37:411–17.

- Drzyzga, S.A., Shortridge, A.M., and Schaetzl, R.J. 2012. Mapping the Stages of Glacial Lake Algonquin in Northern Michigan, USA, and Nearby Ontario, Canada, Using an Isostatic Rebound Model. *Journal of Paleolimnology* 47:357-371.
- Eschman, D.F., and Karrow, P.F. 1985. Huron basin glacial lakes: a review. In: *Quaternary Evolution of the Great Lakes*, Karrow, P.F. and Calkin, P.E. (eds.). *Geological Association of Canada Special Paper* 30:79-93.
- Eilertsen, R.S., Corner, G.D., Aasheim, O., and Hansen, L. 2011. Facies Characteristics and Architecture Related to Palaeodepth of Holocene Fjord-Delta Sediments. *Sedimentology* 58:1784–1809.
- ESRI (Environmental Systems Resource Institute). 2014. ArcMap 10.1. ESRI, Redlands, California.
- Evans, J.E., and Clark, A. 2011. Re-interpreting Great Lakes shorelines as components of wave-influenced deltas: An example from the Portage River delta (Lake Erie). *Journal of Great Lakes Research* 37:64–77.
- Evans, O.F. 1942. The origin of spits, bars, and related structures. *Journal of Geology* 50:846–865.
- Evenson, E.B. 1973. Late Pleistocene Shorelines and Stratigraphic Relations in the Lake Michigan Basin. *Geological Society of America Bulletin* 84:2281–98.
- Farrand, W.R., and Eschman, D.F. 1974. Glaciation of the southern peninsula of Michigan: a review. *Michigan Academician* 7:31-56.
- Farrand, W.R., and Bell, D.L. 1982. The Quaternary Geology of Michigan. Ann Arbor, MI: University of Michigan Press.
- Feth, J.H. 1955. Sedimentary features in the Lake Bonneville Group in the East Shore Area near Ogden, Utah. *Utah Geological Society Guidebook* 10:45-69.
- Fisher, T.G., Smith, D.G., and Andrews, J.T. 2002. Preboreal oscillation caused by a glacial Lake Agassiz flood. *Quaternary Science Reviews* 21:873–878.
- Fisher, T.G. 2003. Chronology of glacial Lake Agassiz meltwater routed to the Gulf of Mexico. *Quaternary Research* 59:271–276.
- Fisher, T.G. 2005. Strandline Analysis in the Southern Basin of Glacial Lake Agassiz, Minnesota and North and South Dakota, USA. *Geological Society of America Bulletin* 117:1481-1496.

- Fisher, T.G. 2007. Abandonment chronology of glacial Lake Agassiz's Northwestern outlet. *Palaeogeography, Palaeoclimatology, Palaeoecology* 246:31-44.
- Fisher, W.L. 1969. Facies characterization of Gulf Coast Basin delta systems, with some Holocene analogues. *Gulf Coast Association of Geological Societies* 19:239–261.
- Forsyth, J.L. 1959. The beach ridges of northern Ohio. Ohio Department of Natural Resources Division of Geological Survey Information Circular 25.
- Fraser, G.S., Thompson, T.A., Kvale, E.P., Carlson, C.P., Fishbaugh, D.A., Graver, B.L., Holbrook, J., Kairo, S., Kohler, C.S., Malone, A.E., Moore, C.H., Rachmanto, B., and Rhoades, L. 1991. Sediments and sedimentary structures of a barred, nontidal coastline, southern shore of Lake Michigan. *Journal of Coastal Research* 7:1113-1124.
- Friedman, G.M., and Sanders, J.E. 1978. Principles of Sedimentology. Wiley, New York
- Fullerton, D.S. 1980. Preliminary correlation of Post-Erie interstadial events (16000-10000 radiocarbon years before present), central and eastern Great Lakes region and Hudson, Champlain, and St. Lawrence lowlands, United States and Canada. *U.S. Geological Survey Professional Paper* 1089.
- Futyma, R.P. 1981. The northern limits of glacial Lake Algonquin in Upper Michigan. *Quaternary Research* 15:291–310.
- Galloway, W.E. 1975. Process framework for describing the morphologic and stratigraphic evolution of deltaic depositional systems. In: *Deltas: Models for Exploration*, Broussard, M.L. (ed.). Houston Geological Society, Houston, TX, pg. 87-98.
- Galloway, W.E. and Hobday, D.K. 1996. Terrigenous Clastic Depositional Systems. Springer-Verlag, Heidelberg, pg. 489.
- Gao, J., and Liu, Y. 2001. Applications of Remote Sensing, GIS and GPS in Glaciology: A Review. *Progress in Physical Geography* 25:520–40.
- Gesch, D., Oimoen, M., Greenlee, S., Nelson, C., Steuck, M., and Tyler, D. 2002. The national elevation dataset. *Photogrammetric Engineering and Remote Sensing* 68:5–11.
- Gilbert, G.K. 1885. The topographic features of lake shores. *U.S. Geological Survey Annual Report* 5, pg. 69-123.
- Gilbert, G.K. 1890. Deltas. U.S. Geological Survey Monograph 1, pg. 153-167.

- Gilbert, G.K. 1898. Recent earth movements in the Great Lakes region. United States geological survey 18th annual report, Part 2, pg. 601–647.
- Gobo, K., Ghinassi, M., and Nemec, W. 2014. Reciprocal Changes In Foreset To Bottomset Facies In A Gilbert-Type Delta: Response To Short-Term Changes In Base Level. *Journal of Sedimentary Research* 84:1079–95.
- Goldthwait, J.W. 1908. A reconstruction of the water planes of the extinct glacial lakes in the Lake Michigan basin. *Journal of Geology* 16:459-476.
- Goldthwait, R.P. 1958. Wisconsin-age forests in Western Ohio, part 1-age and glacial events. *Ohio Journal of Science* 58:209-219.
- Grimley, D.A. 2000. Glacial and nonglacial sediment contributions to Wisconsin Episode loess in the central United States. *Geological Society of America Bulletin* 112:1475-1495.
- Gujarati, D.N. 1988. Basic Economics. New York, NY, McGraw-Hill.
- Hansel, A.K, and Mickelson, D.M. 1988. A Reevaluation of the Timing and Causes of High Lake Phases in the Lake Michigan Basin. *Quaternary Research* 29:113–28.
- Hansel, A.K., Mickelson, D.M., Schneider, A.F., and Larsen, C.E. 1985. Late Wisconsin and Holocene history of the Lake Michigan basin. In: *Quaternary Evolution of the Great Lakes*, Karrow, P.F, and Calkin, P.E. (eds.). *Geological Association of Canada Special Paper* 30:39-53.
- Haslett, S.K. 2000. Coastal Systems. Routledge, London and New York.
- Holcombe, T.L., Taylor, L.A., Reid, D.F., Warren, J.S., Vincent, P.A., and Herdendorf, C.E. 2003. Revised Lake Erie postglacial lake level history based on new detailed bathymetry. *Journal of Great Lakes Research* 29:681–704.
- Holmes, A. 1965. Principles of physical geology, 2nd ed. London, Thomas Nelson and Sons, pg. 1288.
- Hori, K., and Saito, Y. 2007. Classification, architecture, and evolution of large-river Deltas. In: *Large Rivers: Geomorphology and Management*, Gupta, A. (ed.). Chichester, U.K., Wiley, pg. 75–96.
- Hough, J.L. 1958. Geology of the Great Lakes. University Illinois Press, Urbana, IL.
- Hough, J.L. 1963. The prehistoric Great Lakes of North America. *American Scientist* 51:84–109.

- Hough, J.L. 1966. Correlation of glacial lake stages in the Huron-Erie and Michigan basins. *Journal of Geology* 74:62–77.
- Howard, J.L. 2010. Late Pleistocene glaciolacustrine sedimentation and paleogeography of southeastern Michigan, USA. *Sedimentary Geology* 223:126-142.
- Hunt, C.B., Varnes, J.D., and Thomas, H.E. 1953. Lake Bonneville geology of northern Utah Valley, Utah. *U.S. Geological Survey Professional Paper* 257-A.
- Jain, A.K. 2010. Data clustering: 50 years beyond K-means. *Pattern Recognition Letters* 31:651-666.
- Janecke, S.U., and Oaks, R.Q. 2011. Reinterpreted history of latest Pleistocene Lake Bonneville: Geologic setting of threshold failure, Bonneville flood, deltas of the Bear River, and outlets for two Provo shorelines, southeastern Idaho, USA. *The Geological Society of America Field Guide* 21:195-222.
- Jervey, M.T. 1988. Quantitative geological modeling of siliciclastic rock sequences and their seismic expression. In: *Sea-level changes—an integrated approach*, Wilgus, C.K., Hastings, B.S., Kendall, C.G., Posamentier, H.W., Ross, C.A., and VanWagoner, J.C. (eds.). *Special Publication of the Society of Economic Paleontologists and Mineralogists* 42, pg. 47-69.
- Jewell, P.W. 2007. Morphology and paleoclimatic significance of Pleistocene Lake Bonneville spits. *Quaternary Research* 68:421-430.
- Johnson, W.H. 1990. Ice-wedge casts and relict patterned ground in central Illinois and their environmental significance. *Quaternary Research* 33:51-72
- Johnston, J.W., Thompson, T.A., and Baedke, S.J. 2007. Systematic pattern of beach-ridge development and preservation: Conceptual model and evidence for ground penetrating radar. In: *Stratigraphic Analyses Using GPR*, Baker, G.S., and Jol, H.M. (eds.). *The Geological Society of America Special Paper* 432:47-58.
- Johnston, J.W., Thompson, T.A., and Wilcox, D.A. 2014. Palaeohydrographic reconstructions from strandplains of beach ridges in the Laurentian Great Lakes. *Geological Society, London, Special Publications* 388: 213-228.
- Jolliffe, I.T. 2002. Principal Components Analysis. Springer and Verlag, New York, pg. 502.
- Kagan, A., and Shepp, L.A. 1998. Why the variance? *Statistics & Probability Letters* 38:329-333.

- Kaiser, H.F. 1958. The varimax criterion for analytic rotation in factor analysis. *Psychometrika* 23:187-200.
- Kaiser, K.F. 1994. Two Creeks interstadial dated through dendrochronology and AMS. *Quaternary Research* 42:288–298.
- Karrow, P.F., Anderson, T.W., Clarke, A.H., Delorme, L.D., and Sreenivasa, M.R. 1975. Stratigraphy, paleontology, and age of Lake Algonquin sediments in southwestern Ontario, Canada. *Quaternary Research* 5:49-87.
- Karrow, P.F. 1984. Quaternary stratigraphy and history, Great Lakes-St. Lawrence region. In: *Quaternary Stratigraphy of Canada-A Canadian Contribution to IGCP Project 24, Geological Survey Canada Paper* 84-10, pg. 137-153.
- Karrow, P.F., and Calkin, P. 1985. Quaternary Evolution of the Great Lakes. *Geological Association of Canada Special Paper* 30.
- Karrow, P.F. 1986. Valley terraces and Huron basin water levels, southwestern Ontario. *Geological Society of America Bulletin* 97:1089-1097.
- Karrow, P.F., Dreimanis, A., and Barnett, P.J. 2000. A Proposed Diachronic Revision of Late Quaternary Time-Stratigraphic Classification in the Eastern and Northern Great Lakes Area. *Quaternary Research* 54:1-12.
- Kehew, A.E. 1982. Catastrophic flood hypothesis for the origin of the Souris spillway, Saskatchewan and North Dakota. *Geological Society of America Bulletin* 93:1051-1058.
- Kehew, A.E, and Lord, M.L. 1986. Origin and large-scale erosional features of glacial-lake spillways in the northern Great Plains. *Geological Society of America Bulletin* 97:162-177.
- Kehew, A.E, and Lord, M.L. 1987. Glacial-lake outbursts along the mid-continent margins of the Laurentide Ice Sheet. In: *Catastrophic Flood*, Mayer, L., and Nash, D. (eds.). Allen and Unwin, Boston, pg. 95-120.
- Kehew, A.E. 1993. Glacial-Lake Outburst Erosion of the Grand Valley, Michigan, and Its Impacts on Glacial Lakes in the Lake Michigan Basin. *Quaternary Research* 39:36–44.
- Kehew, A.E., Esch, J.M., Kozlowski, A.L., and Ewald, S.K. 2012. Glacial landsystems and dynamics of the Saginaw Lobe of the Laurentide Ice Sheet, Michigan, USA. *Quaternary International* 260:21-31.

- Kenyon, P.M., and Turcotte, D.L. 1985. Morphology of a delta prograding by bulk sediment transport. *Geological Society of America Bulletin* 96:1457-1465.
- Kincare, K., and Larson, G.J. 2009. Evolution of the Great Lakes. In: *Michigan geography and geology*, Schaetzl, R.J., Darden, J.T., and Brandt, D. (eds.). Pearson Custom Publishing, Boston, MA. pg. 174–190.
- Kincare, K.A. 2007. Response of the St. Joseph River to lake level changes during the last 12,000 years in the Lake Michigan basin. *Journal of Paleolimnology* 37 (3), 383-394.
- Komar, P.D. 1973. Computer models of delta growth due to sediment input from rivers and longshore transport. *Geological Society of America Bulletin* 84:2217-2226.
- Kor, P.S., Cowell, D.W., Karrow, P.F., and Kristjansson, F.R. 2012. The Cabot Head Archipelago: evidence of glacial Lake Algonquin on the Northern Bruce Peninsula, Ontario. *Canadian Journal of Earth Sciences* 49: 576-589.
- Kozlowski, A.L., Kehew, A.E., and Bird, B.C. 2005. Outburst flood origin of the Central Kalamazoo River Valley, Michigan, USA. *Quaternary Science Reviews* 24:2354–2374.
- Krist, F., and Schaetzl, R.J. 2001. Paleowind (11,000 BP) directions derived from lake spits in northern Michigan. *Geomorphology* 38:1-18.
- Larsen, C.E. 1987. Geological History of Glacial Lake Algonquin and the Upper Great Lakes. *United States Geological Survey Bulletin* 1801.
- Larsen, C.E. 1994. Beach Ridges as Monitors of Isostatic Uplift in the Upper Great Lakes. *Journal of Great Lakes Research* 20:108–34.
- Larson, G.J., Lowell, T.V., and Ostrom, N.E. 1994. Evidence for the Two Creeks interstate in the Lake Huron basin. *Canadian Journal of Earth Sciences* 31:793-797.
- Larson, G.J., and Schaetzl, R.J. 2001. Origin and Evolution of the Great Lakes. *Journal of Great Lakes Research* 27:518–46.
- Larson, G.J., and Kincare, K. 2009. Late Quaternary history of the eastern midcontinent region, USA. In: *Michigan Geography and Geology*, Schaetzl, R., Darden, J., and Brandt, D. (eds.). Custom Publishing, New York, pg. 69–90.
- Larson, G.J. 2011. Ice-Margin Fluctuations at the End of the Wisconsin Episode, Michigan, USA. In: *Quaternary Glaciations – Extent and Chronology: A Closer Look*, Ehlers, J., Gibbard, P.L., and, Hughes, P.D. (eds.). *Developments in Quaternary Science* 15, pg. 489-497.

- Lawson, A.C. 1891. Sketch of the coastal topography of the north side of Lake Superior with special reference to the abandoned strands of Lake Warren (the greatest of the late Quaternary lakes of North America). In: *The geological and natural history survey of Minnesota, the twentieth annual report for the year 1891*, Winchell, N.H. (ed.). *The Geological and Natural History Survey*, Minnesota, Minneapolis, pg. 183–289.
- LeBlanc, R.J. 1975. Significant studies of modern and ancient deltaic sediments. In: *Deltas, Models for Exploration*, Broussard, M.L. (ed.). *Houston Geological Society*, Houston, pg. 13-85.
- LeBlanc, R.J. 1976a. Modern Deltas. *American Association of Petroleum Geologists*, Reprint No. 18.
- LeBlanc, R.J. 1976b. Ancient Deltas. *American Association of Petroleum Geologists*, Reprint No. 19.
- Lemons, D.R., and Chan, M.A. 1999. Facies architecture and sequence stratigraphy of fine-grained lacustrine deltas, Bonneville basin, northern Utah and southern Idaho. *American Association of Petroleum Geologists Bulletin* 83:635-665.
- Leverett, F. 1897. The Pleistocene features and deposits of the Chicago area. *Chicago Academy of Sciences Geology and Natural History Bulletin* 2.
- Leverett, F., and Taylor, F.B. 1915. The Pleistocene of Indiana and Michigan and the history of the Great Lakes. U.S. Geological Survey Monograph 53.
- Lewis, C.F.M., and Anderson, T.W. 1992. Stable isotope (O and C) and pollen trends in Lake Erie, evidence for locally induced climatic reversal of Younger Dryas age in the Great Lakes basin. *Climate Dynamics* 6:241–250.
- Lewis, C.F.M., Moore, T.C., Rae, D.K., Dettman, D.L., Smith, A.M., and Mayer, L.A. 1994. Lakes of the Huron Basin: Their record of runoff from the Laurentide ice sheet. *Quaternary Science Reviews* 13:891–922.
- Lewis, C.F.M., Blasco, S.M., and Gareau, P.L. 2005. Glacial isostatic adjustment of the Laurentian Great Lakes Basin: Using the empirical record of strandline deformation for reconstruction of early Holocene Paleo-lakes and discovery of a hydrologically closed phase. *Géographie physique et Quaternaire* 59:187–210.
- Lewis, C.F.M., Karrow, P.F., Blasco, S.M., McCarthy, F.M.G., King, J.W., Moore, T.C.M., and Rea, D.K. 2008. Evolution of Lakes in the Huron Basin: Deglaciation to Present. *Aquatic Ecosystem Health & Management* 11:127–36.

- Lewis, C.F.M., Rea, D.K., Hubeny, J.B., Thompson, T.A., Blasco, S.M., King, J.W., Reddin, M., and Moore Jr., T.C. 2010. Using geological history of the Laurentian Great Lakes to better understand their future. *Aquatic Ecosystem Health and Management Society* 13:118-126.
- Lichter, J. 1995. Lake Michigan beach-ridge and dune development, lake level, and variability in regional water balance. *Quaternary Research* 44:181-189.
- Lichter, J. 1997. AMS radiocarbon dating of Lake Michigan beach ridge and dune development. *Quaternary Research* 48:137-140.
- Lichter, J. 1998. Rates of weathering and chemical depletion in soils across a chronosequence of Lake Michigan sand dunes. *Geoderma* 85:255-282.
- Lord, M.L. 1991. Depositional record of a glacial-lake outburst: Glacial Lake, Souris, North Dakota. *Geological Society of America Bulletin* 103:290-299.
- Luehmann, M.D., Schaetzl, R.J., Lusch, D.P., Larson, G.J., Kincare, K.A, and Arbogast, A.F. 2013. Distribution and characteristics of late Wisconsin Deltas in Southern Michigan, USA. *National meeting of the Geological Society of America, Denver, CO*: Poster presentation.
- Luehmann, M.D. 2015. Late Pleistocene deltas in the Lower Peninsula of Michigan, USA. *North-Central Regional meeting of the Geological Society of America, Madison, WI*: Presentation talk.
- Lusch, D.P., Stanley, K.E., Schaetzl, R.J., Kendall, A.D., van Dam, R.L., Nielsen, A., Blumer, B.E., Hobbs, T.C., Archer, J.K., Holmstadt, J.L.F., and May, C.L. 2009. Characterization and Mapping of Patterned Ground in the Saginaw Lowlands, Michigan: Possible Evidence for Late-Wisconsin Permafrost. *Annals of the Association of American Geographers* 99:445-466.
- Lyell, C. 1832. Principles of geology, being an attempt to explain the former changes of the Earth's surface, by reference to causes now in operation. London, John Murray 2.
- Mangold, N., and Ansan, V. 2006. Detailed Study of an Hydrological System of Valleys, a Delta and Lakes in the Southwest Thaumasia Region, Mars. *Icarus* 180:75–87.
- Margold, M., Jansson, K.N., Kleman, J., Stroeve, A.P. ,and Clague, J.J. 2013. Retreat pattern of the Cordilleran Ice Sheet in central British Columbia at the end of the last glaciation reconstructed from glacial meltwater landforms. *Boreas* 42:830–847

- Martin, H.M. 1955. Map of the surface formations of the southern peninsula of Michigan: Michigan Department of Conservation, Geological Survey Division Publication 49, Part 1, scale 1:500,000.
- McPherson, J.G., Shanmugam, G., and Moiola, R.J. 1987. Fan Deltas and braid deltas; varieties of coarse-grained deltas. *Geological Society of America Bulletin* 99:331-340.
- Melton, M.A. 1965. The geomorphic and palaeoclimatic significance of alluvial deposits in Southern Arizona. *Journal of Geology* 73:1-38.
- Miall, A.D. 1976. Facies Models 4. Deltas. *Geoscience Canada* 3:215-227.
- Miall, A.D. 1984. Deltas. In: *Facies Models*, Walker, R.G (ed.). *Geosciences Canada*, Reprint Series 1, pg. 105-117.
- Mickelson, D.M., Clayton, L., Fullerton, D.D., and Borns Jr., H.W. 1982. The Late Wisconsin glacial record of the Laurentide Ice Sheet in the United States. In: *Late Quaternary Environments of the United States, Volume 1. The Late Pleistocene*, University Minnesota Press, Minneapolis, MN, pg. 3-37.
- Miller, A.A. 1939. Attainable standards of accuracy in the determination of preglacial sea levels by physiographic methods. *Journal of Geomorphology* 2:95-115.
- Miller, D.A., and White, R.A. 1998. A Conterminous United States Multi-Layer Soil Characteristics Data Set for Regional Climate and Hydrology Modeling. *Earth Interactions* 2.
- Milligan, M.R., and Chan, M.A. 1998. Coarse-grained Gilbert deltas; facies, sequence stratigraphy and relationships to Pleistocene climate at the eastern margin of Lake Bonneville, northern Utah. In: *Relative Role of Eustasy, Climate, and Tectonism in Continental Rocks*, Shanley, K.W., and McCabe, P.J. (eds.). *Society of Sedimentary Geology, Special Publication* 59: 177–189.
- Milligan, M.R., and Lemons, D.R. 1998. A sequence stratigraphic overview of sandy and gravelly lacustrine deltas deposited along the eastern margin of late Pleistocene lake Bonneville, northern Utah and southern Idaho. In: *Modern and Ancient Lake Systems*, Pitman, J.K., and Carroll, A.R. (eds.). *Utah Geological Association Guidebook* 26:105-129.
- Monaghan, G.W., and Hansel, A.K. 1990. Evidence for the Intre-Glenwood (Mackinaw) Low-Water Phase of Glacial Lake Chicago. *Canadian Journal of Earth Sciences* 27:1236–41.
- Morgan, R.P.C. 1971. Rainfall of west Malaysia: a preliminary regionalization using principal components analysis. *Area* 3:222–227.

- Mörner, N.A., and Dreimanis, A. 1973. The Erie interstade. *Geological Society of America Memoir* 136:107–134.
- Nelson, S. T., Wood, M. J., Mayo, A. L., Tingey, D. G., and Eggett, D. 2005. Shoreline Tufa and Tufaglomerate from Pleistocene Lake Bonneville, Utah, USA: stable isotopic and mineralogical records of lake conditions, processes, and climate. *Journal of Quaternary Science* 20:3–19.
- Nishizawa, S., Currey, D.R., Brunelle, A., and Sack, D. 2013. Bonneville Basin Shoreline Records of Large Lake Intervals during Marine Isotope Stage 3 and the Last Glacial Maximum. *Palaeogeography, Palaeoclimatology, Palaeoecology* 386:374–91.
- Oldale, R.N., Wommack, L.E., and Whitney, A.B. 1983, Evidence of a postglacial low relative sea-level stand on the drowned delta of the Merrimack River, western Gulf of Maine. *Quaternary Research* 33:325–336.
- Olson, J.S. 1958a. Lake Michigan dune development: Wind-velocity profiles. *Journal of Geology* 66:254–263.
- Olson, J.S. 1958b. Lake Michigan dune development: Plants as agents and tools in geomorphology. *Journal of Geology* 66:345–351.
- Orton, G.J. 1988. A spectrum of middle Ordovician fan and braidplain deltaic sequences, North Wales: a consequence of varying fluvial input. In: *Fan Deltas: Sedimentology and Tectonic Settings*, Nemec, W., and Steel, R.J. (eds.), pg. 23–49.
- Orton, G.J., and Reading, H.G. 1993. Variability of deltaic processes in terms of sediment supply, with particular emphasis on grain size. *Sedimentology* 40:475–512.
- Oviatt, C.G., Madsen, D.B., and Schmitt, D.N. 2003. Late Pleistocene and early Holocene rivers and wetlands in the Bonneville basin of western North America. *Quaternary Research* 60:200–210.
- Petty, W.H., Delcourt, P.A., and Delcourt, H.R. 1996. Holocene Lake-Level Fluctuations and Beach-Ridge Development along the Northern Shore of Lake Michigan, USA. *Journal of Paleolimnology* 15:147–69.
- Phillips, R.T.J., and Desloges, J.R. 2014. Alluvial Floodplain Classification by Multivariate Clustering and Discriminant Analysis for Low-Relief Glacially Conditioned River Catchments. *Earth Surface Processes and Landforms* 40:756–770.
- R Core Team. 2014. R: A language and environment for statistical computing. R Foundation for Statistical Computing, Vienna, Austria. URL <http://www.R-project.org/>.

- Ritter, D.F., Kochel, R.C., and Miller, J.R. 2006. Process Geomorphology 4th edition. Long Grove, IL, Waveland Press.
- Rovey, C.W.II, and Borucki, M.K. 1994. Bluff evolution and long-term recession rates, southwestern Lake Michigan. *Environmental Geology* 23:256-263.
- Russel, R.J. 1967. River and Delta Morphology. Baton Rouge, Louisiana State University Press.
- Saha, K., Wells, N.A., and Munro-Stasiuk, M. 2011. An object-oriented approach to automated landform mapping: A case study of drumlins. *Computers and Geosciences* 37:1324–1336.
- Schaetzl, R.J. 2001. Late Pleistocene Ice Flow Directions and the Age of Glacial Landscapes in Northern Lower Michigan. *Physical Geography* 22:28-41.
- Schaetzl, R.J., Drzyzga, S.A., Weisenborn, B.N., Kincare, K.A., Lepczyk, X.C., Shein, K.A., Dowd, C.M., and Linker, J. 2002. Measurement, Correlation, and Mapping of Glacial Lake Algonquin Shorelines in Northern Michigan. *Annals of the Association of American Geographers* 92:399-415.
- Schaetzl, R.J. 2008. The Distribution of Silty Soils in the Grayling Fingers Region of Michigan: Evidence for Loess Deposition onto Frozen Ground. *Geomorphology* 102:287-296.
- Schaetzl, R.J., Krist, F.J.Jr., Stanley, K.E., and Hupy, C.M. 2009. The Natural Soil Drainage Index: An ordinal estimate of long-term, soil wetness. *Physical Geography* 30: 383–409.
- Schaetzl, R.J., Yansa, C.H, and Luehmann, M.D. 2013a. Paleobotanical and Environmental Implications of a Buried Forest Bed in Northern Lower Michigan, USA. *Canadian Journal of Earth Sciences* 50:483–493.
- Schaetzl, R.J., Enander, H., Luehmann, M.D., Lusch, D.P., Fish, C., Bigsby, M., Steigmeyer, M., Guasco, J., Forgacs, C., and Pollyea, A. 2013b. Mapping the Physiography of Michigan with GIS. *Physical Geography* 34:1-38.
- Schaetzl R.J., Krist, F.J., Luehmann, M.D., Lewis, C.M., and Michalek, M.J. Spits formed in Glacial Lake Algonquin indicate strong easterly winds in the Great Lakes regions in the late Pleistocene. *Journal of Paleolimnology*: under review.
- Scherzer, W.H. 1916. Detroit Folio. Geologic atlas of the United States. U.S. Geological Survey Folio, 205.

- Schneider, A.F., and Need, E.A. 1985. Lake Milwaukee: an “early” proglacial lake in the Lake Michigan basin. In: *Quaternary Evolution of the Great Lakes*, Karrow, P.F, and Calkin, P.E. (eds.). *Geological Association of Canada Special Paper* 30:55-62.
- Schofield, I., Jewell, P., Chan, M., Currey, D., and Gregory, M. 2004. Shoreline development, longshore transport, and surface wave dynamics, Pleistocene Lake Bonneville, Utah. *Earth Surface Processes and Landforms* 29:675–1690.
- Scott, W.E., McCoy, W.D., Shroba, R.R., and Rubin, M. 1983. Reinterpretation of the exposed record of the last two cycles of Lake Bonneville, western U.S. *Quaternary Research* 20:261–285.
- Scruton, P.C. 1960. Delta building and the deltaic sequence. In: *Recent sediments, northwest Gulf of Mexico*, Shepard, F.P., Phleger, F.B., and Van Andel, T.H. (eds.). *American Association of Petroleum Geologists*, pg. 82-102.
- Shipp, R.C., Belknap, D.F., and Kelley, J.T. 1991. Seismicstratigraphic and geomorphic evidence for a post-glacial sea-level lowstand in the northern Gulf of Maine. *Journal of Coastal Research* 7:341–364.
- Shirley, M.L., and Ragsdale, J.A. 1966. Deltas in their geologic framework. Houston Geological Society, Houston, Texas.
- Shlens, J. 2014. A tutorial on principal component analysis. *arXiv preprint arXiv: 1404.1100*.
- Smith, D.G. 1991. Lacustrine deltas. *Canadian Geographer* 35: 311-316.
- Smith, D.G. and Jol, H.M. 1992. Ground penetrating radar investigation of a Lake Bonneville delta, Provo level, Brigham City, Utah. *Geological Society of America, Geology* 20:1083-1086.
- Smith, D.G., and Jol, H.M. 1997. Radar Structure of a Gilbert-Type Delta, Peyto Lake , Banff National Park, Canada. *Sedimentary Geology* 113:195–209.
- Sohn, Y.K., Kim, S.B., Hwang, I.G., Bahk, J.J., Choe, M.Y., and Chough, S.K. 1997. Characteristics and depositional processes of large-scale gravelly Gilbert-type foresets in the Miocene Doumsan fan delta, Pohang basin, SE Korea. *Journal of Sedimentary Research* 67:130–141.
- Spencer, J.W. 1891. Deformation of the Algonquin beach, and birth of Lake Huron. *American Journal of Science* 41:12-21.
- Suess, H.E. 1954. U.S. Geological Survey radiocarbon dates 1. *Science* 120:467-473.

- Suter, J.R. 1994. Deltaic coasts. In: *Coastal Evolution: Late Quaternary shoreline morphodynamics*, Carter, R.W.G., and Woodroffe, C.D. (eds.). Cambridge University Press, New York, NY.
- Tardy, S.W. 2005. Soil survey of Roscommon County, Michigan. US department of agriculture. Natural Resources Conservation Service, Washington, DC.
- Taylor, F.B. 1892. The highest old shoreline on Mackinac Island. *American Journal of Science* 63:210-218.
- Teller, J.T. 1987. Proglacial lakes and the southern margin of the Laurentide Ice Sheet. In: *North America and Adjacent Oceans during the Last Deglaciation*, Ruddiman, W.F., Wright Jr. H.E. (eds.). *Geological Survey of America, Decade of North American Geology* K-3, pg. 39-69.
- Teller, J.T. 2002. Formation of large beaches in an area of rapid differential isostatic rebound: the three outlet control of Lake Agassiz—reply to the comment by P.F. Karrow. *Quaternary Science Reviews* 21:2119-2122.
- Teller, J.T., and Leverington, D.W. 2004. Glacial Lake Agassiz: a 5000-year history of change and its relationship to the isotopic record of Greenland. *Geological Society of America Bulletin* 116:700-714.
- Teller, J.T., Boyd, M. Yang, Z., Kor, P.S.G., and Fard, A.M. 2005. Alternative routing of Lake Agassiz overflow during the Younger Dryas: new dates, paleotopography, and a re-evaluation. *Quaternary Science Reviews* 24:1890-1905.
- Thompson, T.A. 1988a. Sedimentology and stratigraphy as tools in interpreting the evolution of wetland areas in the Indian Dunes National Lakeshore. In: *Interdisciplinary Approaches to Freshwater Wetlands Research*, Wilcox, D.A. (ed.). National Park Service Monograph, pg. 25-36.
- Thompson, T.A., Fraser, G.S., and Olyphant, G. 1988b. Establishing the altitude and age of past lake levels in the Great Lakes. *Geological Society of America Abstracts with Programs* 20:392.
- Thompson, T.A. 1992. Beach-ridge development and lake-level variation in southern Lake Michigan. *Sedimentary Geology* 80:305-318.
- Thompson, T.A., and Baedke, S.J. 1995. Beach-ridge development in Lake Michigan: shoreline behavior in response to quasi-periodic lake-level events. *Marine Geology* 129:163-174.

- Thompson, T.A., and Baedke, S.J. 1997. Strandplain evidence for late Holocene lake-level variations in Lake Michigan. *Geological Society of America Bulletin* 109:666–682.
- Totten, S.M. 1985. Chronology and nature of the Pleistocene beaches and wave-cut cliffs and terraces, northeastern Ohio. In: *Quaternary Evolution of the Great Lakes*, Karrow, P.F, and Calkin, P.E. (eds.). *Geological Association of Canada Special Paper* 30:171-184.
- Vader, M.J., Zeman, B.K., Schaetzl, R.J., Anderson, K.L., Walquist, R.W., Freiburger, K.M., Emmendorfer, J.A., and Wang, H. 2012. Proxy Evidence for Easterly Winds in Glacial Lake Algonquin, from the Black River Delta in Northern Lower Michigan. *Physical Geography* 33:252-268.
- Walker, H.J. 1998. Arctic Deltas. *Journal of Coastal Research* 14:718–38.
- Winters, H.A., Rieck, R.L, and Kapp, R.O. 1986. Significance and Ages of Mid-Wisconsin Organic Deposits in Southern Michigan. *Physical Geography* 7:292–305.
- Woodroffe, C.D. and Saito, Y. 2011. River-Dominated Coasts. In: *Treatise on Estuarine and Coastal Science*, Wolanski, E. and McLusky, D.S. (eds.). Waltham, Academic Press, Vol 3, pg. 117–135.
- Wright, L.D., and Coleman, J.M. 1973. Variations in morphology of major river deltas as functions of ocean wave and river discharge regimes. *American Association of Petroleum Geologists Bulletin* 57:370-398.
- Wright, L.D., and Coleman, J.M. 1974. Mississippi River mouth processes: effluent dynamics and morphologic development. *The Journal of Geology* 82:751-778.
- Wright, L.D. 1977. Sediment transport and deposition at river mouths: a synthesis. *Geological Society of America Bulletin* 88:857-868.
- Wright, L.D. 1985. River deltas. In: *Coastal Sedimentary Environments*, Davis, R.A. (ed.). Springer Verlag, NY, pg. 1-76.